
THE UNIVERSITY *of* EDINBURGH

# Analysis of the structural response of tall buildings under multifloor and travelling fires

Panagiotis Kotsovinos


Doctor of Philosophy

The University of Edinburgh

2013

# Declaration

I declare that this thesis has been composed solely by myself and that it has not been submitted, either in whole or in part, in any previous application for a degree. Except where otherwise acknowledged, the work presented is entirely my own.

Panagiotis Kotsovinos

May 2013

# Abstract

The last decades have seen a surge in the construction of tall buildings all over the world. Due to their, often, innovative and complex layouts, tall buildings can pose unique challenges to architects and engineers. Previous tall building failures raised significant concerns on the applicability of prescriptive fire design for these structures. The use of structural fire engineering can enhance the safety of a tall building under fire by strengthening any vulnerable areas in the structure and at the same time reduce the costs of fire protection by removing it when unnecessary.

Commercial finite element and specialist structural fire engineering software have their advantages and disadvantages. In this thesis, the object-oriented and open-source finite element software OpenSees is presented along with its development with structural fire capabilities by the author and other researchers at the University of Edinburgh. Specifically, new pattern, element, section and material classes have been introduced. All the developed code follows the object-oriented paradigm and is consistent with the ethos of the existing framework. Verification and validation studies of the developed code are also presented. Several procedures including that for dynamic analysis of structures in fire for the collapse assessment of structures are discussed. The development

of OpenSees with structural fire capabilities allows the collaboration of engineers across geographical boundaries and disciplines using a community tool.

In this work, the behaviour of tall buildings under different fire scenarios has been modelled using the developed OpenSees code. Firstly, the collapse mechanisms of generic tall buildings are investigated, namely the strong and weak floor mechanisms are demonstrated, and criteria are established on when each of these mechanisms occurs. The parametric study performed demonstrated that the weak floor collapse is less probable for generic composite buildings however this type of failure can become easier to appear as the number of floors in fire increase. The effect of vertically travelling fires on these mechanisms is also examined. The results of the study show that slower travelling rates delay or avoid the global failure of a tall building compared to quicker travelling rates allowing for the time required for steel members to regain their strength during cooling to ambient temperature. However, it was seen that higher tensile membrane forces were observed in the floors as the travelling rates increased which could result in possible connection failure.

Most of the research and design codes, such as Eurocode, typically assume a uniform thermal environment across the floor area of a structure when defining the design fire. However, in reality fires are more likely to travel in large enclosures, hence there is a need to understand how tall buildings behave under more realistic fire conditions such as travelling fires. A methodology for defining the thermal environment of large enclosures using travelling fires has been recently developed at the University of Edinburgh. Taking into account OpenSees' programmable architecture and its recent inclusion with heat transfer capabilities by other researchers, there was a collaborative effort in order to understand

the thermal and structural response of a generic composite tall building under horizontally travelling fires. The findings of the study showed that larger travelling fire sizes produce quicker heating to the steel beams while smaller fire sizes produce higher peak temperatures in the concrete slab. The structural analysis also demonstrated that travelling fires produced higher midspan deflections in comparison to Eurocode parametric fires and higher plastic deformations which is an indication of higher damage.

Further work focused on looking at the behaviour of tall buildings under the combined scenario of horizontally and vertically travelling fires. The results of the study showed that the travelling fires produce lower maximum compressive and tensile membrane forces in the composite floor compared to the Eurocode parametric fires for the building examined and thus in a multifloor scenario the columns are pulling-in less after large deflections develop in the floor. More specifically, the short-hot fire produced the most demanding response. This suggests that in long floors where uniform heating is really impossible, the time of failure predicted by parametric fires in a multifloor scenario can be more onerous.

The outcomes of this work can aid designers when considering the structural fire response of tall buildings in a performance based design context. It was demonstrated that multifloor fires could be a threat for tall buildings, and thus this possibility should be considered in design. The use of more realistic fire definition for large enclosures, such as travelling fires, should also be considered. The travelling fire methodology can provide an enhanced level of confidence for the safety of a building since it can represent a range of similar fires to those that may occur in a real fire scenario.

# Publications

The following output has been produced as a result of this research:

**Journal papers**

Kotsovinos P, Usmani AS (2012) WTC Towers and lessons learnt on the progressive collapse of tall buildings. Fire Technology Journal (Special issue on WTC collapse), 1-25.

Kotsovinos P, Jiang YQ, Usmani AS (2013) Effect of vertically travelling fires on the collapse of tall buildings. Invited paper in special issue on fire engineering of International Journal of High Rise Buildings, Vol.2, No.1.

Jiang YQ, Kotsovinos P, Usmani AS, Rein G, Stern-Gottfried J (2013) Numerical investigation of thermal responses of a composite structure in horizontally travelling fires using OpenSees. Journal of Procedia Engineering (to appear)

Jiang J, Jiang L, Kotsovinos P, Zhang J, Usmani AS, McKenna F, Li GQ (2013) OpenSees Software Architecture for the analysis of structures in fire, Journal of Computing in Civil Engineering (in press)

**Conference papers**

Jiang YQ, Kotsovinos P, Usmani AS, Rein G, Stern-Gottfried J (2012) Numerical investigation of thermal responses of a composite structure in horizontally travelling fires using OpenSees. In: Ninth Asia-Oceania Symposium on Fire Science and Technology, State Key Laboratory of Fire Science, University of Science & Technology of China, 17-20 October, Hefei, China.

Kotsovinos P, Usmani AS (2011) Stability of Steel Structures subject to Fire using OpenSees. In: Proceedings of the Thirteenth International Conference on Civil, Structural and Environmental Engineering Computing 6-9 September, Chania, Crete, Greece.

Kotsovinos P, Usmani A (2011) Fire resistance of steel trusses with OpenSeeS. In: Proceedings of International Conference Applications of Structural Fire Engineering 29-30 April, Prague, Czech Republic

Kotsovinos P, Usmani A (2011) Modelling the response of trusses in fire. In: Proceedings of ACME Conference 5-6 April, Herriot Watt University, UK

Jiang J, Usmani AS, Zhang J, Kotsovinos P (2011) Numerical analysis of structures in fire using OpenSees. Proceedings of International Conference on Applications of Structural Fire Engineering, Prague, 319-323.

Usmani AS, Zhang J, Jiang J, Jiang YQ, Kotsovinos P (2010) Using OpenSees for structures in fire. Proceedings of 6th International Conference on Structures in Fire, Michigan, 1089-1094.

Zhang J, Usmani AS, Jiang J, Jiang YQ, Kotsovinos P, May I (2011) Development and application of OpenSees for a RC frame in fire. Proceedings of the 19th

UK Conference of the Association for Computational Mechanics in Engineering, Edinburgh, 233-236.

Zhang J, Usmani AS, Jiang J, Jiang YQ, Kotsovinos P, May I (2011) Using OpenSees for an RC frame in fire. Proceedings of International Conference on Applications of Structural Fire Engineering, Prague, 122-126.

**Other professional presentations**

Kotsovinos P - World Trade Centre Towers and lessons learnt on progressive collapse of tall buildings, Panel presentantion, Young Researchers Conference (YRC), Institution of Structural Engineers (IStructE), 15 March 2012.

Kotsovinos P - Structural fire engineering for tall buildings, The Lloyd's Register Educational Trust (LRET) Technical Leadership Seminar, 27 June 2012.

Kotsovinos P - Tall building behaviour under travelling fires, Institution of Civil Engineers(ICE) Annual General Meeting, Poster Presentation, Royal Society of Edinburgh (RSE), 5 November 2012.

# Acknowledgements

First of all, I would like to acknowledge the support and expert guidance of my supervisor, Prof Asif Usmani. I was honoured to have him as a supervisor. I would also like to thank my second supervisor Dr Pankaj. Dr. Guillermo Rein, although not formally one of my supervisors, has provided valuable help and suggestions during this work and I would like to thank him for that. Prof. Luke Bisby is also appreciated for inviting me to participate in the LRET Technical Leadership Seminar, it was truly an unforgetable experience (LRET is also aknowledged for financially supporting my presence in the seminar). Prof Jose Torero has provided input for one of the publications of this thesis and he is much appreciated for this.

A very big thank you goes to my friend and collaborator, Yaqiang Jiang, that we did together some of the work presented in this thesis. I am very glad to meet and make Yaqiang my friend during my PhD.

I would like to thank other OpenSees Group members that I have worked with such as, Jian Zhang, Liming Jiang, Jian Jiang, Praveen Kamath, Payam Khazaeinejad as well as the other members of the Fire Group for fruitful discussions. Dr Frank McKenna and the OpenSees team at UC,Berkeley are also appreciated for providing guidance whenever asked to.

Outside of the Fire Group members, I would also like to thank other PhD students from IIE for interesting discussions. In particular, Iraklis and Dominic thank you for the time we spent together inside and outside of the office!

I would also like to thank my partner in residence for providing her kind support during all these years. Finally, I would like to thank my family, my parents and brother, for supporting me through difficult times and who are always there for me despite our physical distance. I really owe to them more than I could ever thank them for.

# Contents

# List of Tables

# List of Figures

# List of Notations

**Alphabetic symbols**

| | |
|---|---|
| $a$ | Rate of heating |
| $r$ | Distance from the centre of a fire |
| $u$ | Displacement |
| $q_f$ | Fire load density |
| $s$ | Speed |
| $t$ | Time |
| $t_b$ | Burning time |
| $t_t$ | Total time |
| $A$ | Area |
| $A_f$ | Floor area |
| $C$ | Damping matrix |
| $E$ | Young modulus |
| $F$ | Force |
| $H$ | Height |
| $I$ | Moment of inertia |
| $K$ | Stiffness matrix |
| $M$ | Mass matrix |
| $L$ | Length |
| $L_f$ | Length of fire |
| $\dot{Q}$ | Heat release rate |
| $\dot{Q}''$ | Heat release rate per unit area |
| $S$ | Stiffness |
| $T$ | Temperature |
| $T_0$ | Temperature at time equal to 0 seconds |
| $T_{max}$ | Maximum temperature |

**Greek letters**

| | |
|---|---|
| $\delta$ | Deformation |
| $\epsilon_{mechanical}$ | Mechanical strain |
| $\epsilon_{thermal}$ | Thermal strain |
| $\epsilon_{total}$ | Total strain |
| $\sigma$ | Stress |
| $\Delta$t | Time increment |
| $\Delta$T | Temperature increment |

# Chapter 1

# Introduction

## 1.1 Background

The last decades have seen tectonic shifts in the construction of tall and supertall buildings due to the rapid increase of population around the world and economic and technological advancements. In addition, there is an increasing desire by architects and engineers to design more innovative, complex and large structures, for reasons that have to do with the significant political, social and economic consequences [1, 2] that these structures can have in the cities that they are built in. This rally of continuous innovation is realised by visionary architects and engineers with the assistance of performance based engineering in order to achieve an optimum balance of integral design components such as safety, economics and sustainability. However, this situation is not uniform for all the disciplines involved in the building sector. Fire engineering is often applied in a prescriptive context even for innovative and complex structures such as tall buildings.

The tragic events of the 9/11 disaster, raised significant concerns on the collapse of tall buildings in fire that challenged the traditional thinking of an adequate and conservative prescriptive fire safety design framework. Despite these concerns, the design of tall buildings under fire conditions is still mainly done in many parts of the world in a prescriptive manner. While other loads that may affect tall buildings, such as earthquakes and wind, are treated by engineers in a performance based design context by considering the response of a building under a variety of reasonable worst case different scenarios in a parametric way, fire design is carried out in a codified way that has its origins on concepts derived more than 100 years ago [3]. This approach can be typically deemed conservative since fire induced structural failures may be notable in some cases (WTC Towers, Windsor Tower, Delft University Building) but rather rare. However, recent years have brought big innovations in architectural design and the development of new construction materials, which are often designed in accordance to all the environmental standards but are highly combustible. Hence, questions are posed on a possible *unsafe* prescriptive design since prescriptive code regulations were developed for structures with other characteristics and thus have limited applicability to modern innovative infrastructure. The use of performance based engineering for the structural fire design of tall buildings and other complex structures is a more rational approach and consistent with the design practice in other engineering disciplines. This has started gaining more acceptance by engineers and regulatory authorities in order to demonstrate safety for these types of structures. Moreover, this design procedure can allow architects to realise their creative ideas without any constraints set by a list of predefined rules that can be overcome by achieving the same goals with alternative means.

This quantification of structural performance in fire can spot possible weaknesses

in a structure that can be enhanced by strengthening the key elements as well as possible locations of overdesign where fire protection can be removed. However, in order for performance based structural fire engineering to be used in practice effectively, *realistic* fire conditions must be taken into account. This need for realistic fire conditions has not been investigated in detail in the past. Very few studies have examined more complex thermal conditions with notable example the failure investigation of the WTC towers, carried out by NIST. On the contrary, many researchers focused on developing very detailed and complex structural models while at the same time the thermal input considered was often very simplistic. This kind of approach, although useful, has little relevance to practical applications where the uncertainty in design may primarily originate from the definition of the thermal environment. Hence, a greater cooperation between fire safety engineers and structural fire engineers is required in order to characterise the thermal environment of buildings with large enclosures.

The recent advances in computer hardware have made it possible to examine relatively quickly different computational models varying several parameters in order to understand structural behaviour in fire and its sensitivities that would be impossible to undertake through experiments which would be cost prohibitive to perform for each building and under different parameters. However, it should be noted that computational models have to be firstly verified against results from experimental tests before these models can be used in design. There are generally two different categories of software for finite element modelling, commercial finite element codes and specialist structural fire engineering software. However, other communities such the fire safety engineering community (OpenFoam, FDS) or earthquake engineering community have also adopted a third category of software,

that of an open-source community code that is continuously under development by many people all around the globe.

The work of researchers and the assumptions of their models are usually not very widely accessible and thus are not open to thorough criticism. An open-source community code can provide the platform for exchanging and communicating of ideas between researchers from different disciplines across geographical boundaries and can also allow for quicker implementation of research codes in commercial software and in practise. Moreover, this type of community code can have more sustainability compared to research codes that are solely dependent on their original developers.

## 1.2 Aim and objectives

This work will study the collapse mechanisms of tall buildings and their behaviour under multifloor and travelling fires within an object-oriented and open-source framework (OpenSees). More specifically, the objectives of the present thesis are to;

- Extend the object-oriented and open-source finite element framework OpenSees so it can be used for structural fire modelling and develop efficient procedures to model the collapse of structures in fire.

- Examine the collapse mechanisms of generic tall buildings in fire and the way these mechanisms occur by conducting a series of parametric studies.

- Understand the behaviour of tall building under horizontally and vertically travelling fires separately and in combined scenarios.

## 1.3 Organisation of the thesis

The organisation of this thesis is described here.

**Chapter 2** presents a literature review of recent research and state of the practise in the structural fire engineering field related to this thesis.

**Chapter 3** presents a review of the architecture and capabilities of the OpenSees finite element framework along with the classes developed by the author and colleagues to facilitate structural fire modelling.

**Chapter 4** examines the collapse mechanisms of generic composite tall buildings in fire under simultaneous multifloor and vertically travelling fires.

**Chapter 5** investigates the thermal as well as structural response of a generic composite tall building under horizontally travelling fires.

**Chapter 6** uses the methodology of horizontally travelling fires as shown in Chapter 5 in a combined scenario with vertically travelling fires similarly to Chapter 4 for a generic composite building.

**Chapter 7** presents the summary points from this work as well as possible future areas of research.

# Chapter 2

# Review of current structures in fire context

## 2.1 Introduction

The increase of complexity and innovation in architectural design and construction technology has been accompanied with challenges that have not been thought or faced before to that extent. One of these challenges is the fire protection of tall and complex buildings and has led to the development of Performance Based Fire Engineering (PBFE) which adopts similar philosophy to Performance Based Structural Engineering (PBSE). In the performance based fire engineering of tall buildings, structural fire engineering is a critical part of the fire design, considering the long evacuation times in these structures and the difficulties in containing the fire both inside the structure and externally.

Performance Based Fire Engineering design process typically involves the following stages;

1. Determination of fire design scenarios (fire risk assessment)
2. Selection of suitable design fires based on the fire risk assessment of the first stage
3. Determination of temperature evolution in structural members over time (Heat transfer)
4. Examination of the mechanical response of structural members using the data from the third stage (If required)

This work is applying a performance based fire engineering methodology in order to examine the behaviour of modern tall buildings under uniform and non-uniform multifloor fires. This chapter firstly examines the way fire is developed including both in rooms (for postflashover fires) and in open large compartments (for localised and travelling fires) and provides a definition of fire severity. The way structures respond under fire and the definition of structural failure are also discussed. Then the behaviour of structural materials is presented, with emphasis on steel and concrete, under elevated temperatures and subsequent cooling. Later, the performance based design context of tall and unusual buildings in fire is reviewed. The chapter finishes with a discussion of gaps in knowledge in structural fire research based on the review that was carried out, and the significance of this work.

## 2.2 Fire dynamics in structures

### 2.2.1 Fire development

Typically a fire starts in a single room or compartment of a building. A lot of the understanding that exists today on the development and growth of fires arises mainly from experiments conducted on rooms of the order of 100 $m^3$ [4]. These room fires have three distinctive phases as seen in Figure 2.1 ; the growth or pre-flashover stage, the fully developed or post-flashover fire and the decay period [4, 5]. In the growth stage, the average temperature of the compartment is typically low (thus this stage is not so important in terms of structural behaviour) and the fire size is increasing and spreading. This stage is very important for life safety purposes as it can affect the means of escape of occupants. The transition to the fully developed stage occurs once a sudden ignition of the whole compartment occurs, also known as flashover. This stage is very critical in terms of structural behaviour as gas temperatures can exceed $1200^0C$. At this stage fire spread to neighbouring compartments and adjacent buildings is also possible [4]. The third stage, is the decay period when the temperature of the fire cools down to ambient temperature. This stage, although neglected in the past, plays also a major role in structural behaviour of buidings especially in the context of repairing fire damaged structures.

It should be noted that Thomas and Heselden [6, 7] and Harmathy [8, 9] identified two distinct regimes of fire behaviour, namely ventilation-controlled and fuel-controlled fires. In fuel-controlled fires, fire growth is predominantly limited by the availability and characteristics of the fuel, while in ventilation-controlled fires, fire growth is predominantly limited by available oxygen. Previous experiments

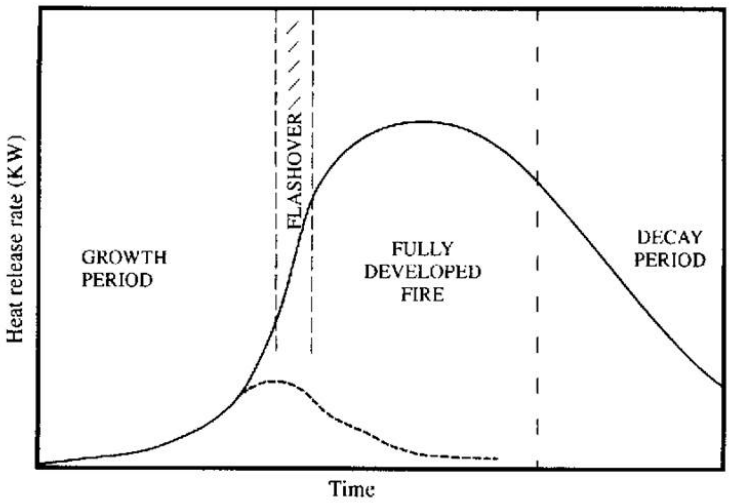


**Figure 2.1:** A typical compartment fire

have shown that ventilation-controlled fires are more severe for typical room fires compared to fuel-controlled fires [4, 10]. Thus most of the design codes [11] assume the worst case design scenario as a ventilation-controlled fire. However, for fires in large compartments, it has been argued by some researchers [12, 13] that fuel controlled fires may provide a more onerous response. The concept of travelling fires [14] presented later in Section 2.2.3.2 for large compartments is based on the characteristics of fuel-controlled fires.

In order to get full representation of the fire growth in a compartment, the use of zone modelling or CFD analysis can give approximate results by dividing a compartment into many elemental volumes and by solving the fundamental equations governing the transfer of mass, momentum, and energy. However, such analyses are time-intensive and thus design fires have been introduced into codes in order to predict the compartment temperatures. Design fires can be categorised into three categories, 1) postflashover, 2) localised and 3) travelling fires. It should be mentioned that travelling fires are also localised fires but travel through the

floor plate area of a structure. In the postflashover fires, the thermal environment is given in gas temperature versus time curves while in localised fires it is typically heat release rate versus time. For travelling fires, in their simple form proposed recently [14, 15, 16], a temperature versus time definition is currently used.

### 2.2.2 Postflashover fires

These fires are the ones that are most typically found in buildings. Commonly they have been named as Parametric fires. Important work for determining the characteristics of these fires was done by several researchers and most predominantly by Pettersson *et al.* [10], Babrauskas and Williamson [17], Magnusson and Thelandersson [18] among others. Eurocode 1 [11] has introduced these fires as natural fires by extending Pettersson's *et al.* [10] model. The definition of these fires is based on physics and thus takes into account various factors such as the compartment size, fuel load, ventilation conditions and the thermal properties of compartment boundaries that affect the thermal environment. In the postflashover fires, a critical stage that is sometimes neglected, is the decay phase. A critical assumption in the parametric fires is that fire burns uniformly in a compartment. This assumption can be considered relatively valid for rooms or small compartments although it has been found that even for small compartments large spatial temperature gradients can occur, as evidenced recently in the Cardington and Dalmarnock experiments [19, 20]. Eurocode 1 [11] suggests some limiting boundaries such as: the height of the compartment (less than 4m); the floor area (less than $500\text{m}^2$); the thermal inertia of compartment linings should be between $100 \sim 2200\ \text{J/m}^2\cdot\text{s}^{-1}\cdot\text{K}$; and that the opening factor should be in the range of 0.02

$\sim$ 0.20 $m^{-1}$. However, UK Annex B allows its use in the design of all types of structures.

### 2.2.3 Localised and travelling fires

These fires are applicable to compartments that fall outside the limits previously defined for the postflashover fires e.g. tall buildings, atria, car parks, metros and airports.

#### 2.2.3.1 Localised fires

Localised fires are seen in compartments when the conditions do not allow for flashover to occur. Flashover may not occur because a building is sprinklered or the compartment is very large (airports, shopping malls etc). A localised fire can also produce a demanding structural response and has to be investigated in case a post-flashover fire is not feasible.

Eurocode 1 (Annex C) provides two different models for considering the effects of a localised fire that are dependant on the flame length. These two models represent the cases of a) open-air fires and smaller fires that do not affect the ceiling level and b) fires that reach the level of the ceiling. These models are limited to fires with diameters (D) $\leq$ 10m and rate of heat release (Q) $\leq$ 50 MW. More details and the formulas can be found in Annex C. These Eurocode models are based on Hasemi [21] after validation with several fire tests as discussed by Schleich *et al.* [22]. Another localised fire model is the Alpert ceiling jet model [23] which is also used in this thesis for the far-field definition of travelling fires.

#### 2.2.3.2 Travelling fires

As discussed before, for large enclosures such as those found in tall buildings, flashover may not occur and thus temperatures may not be uniform in the floor area. Experiments as well as real world fires have demonstrated that fire may travel across the floor plate area of a structure. This movement of fire can have any origin and occur in different ways (such as corner fires or ring fires). Recently, researchers at the University of Edinburgh [24] have proposed a methodology as a means of simple input to structural analysis that maintains the travelling nature of the fire. According to this methodology, as the fire travels across the floor, the thermal environment can be divided into two horizontal regions, namely, "near field" and "far field" as seen in Figure 2.2. This approximation can be considered adequate in order to represent the basic characteristics of a real travelling fire [24]. More details about the travelling fire methodology are given in Chapter 5 where the thermal and structural response of a generic composite tall building are examined.

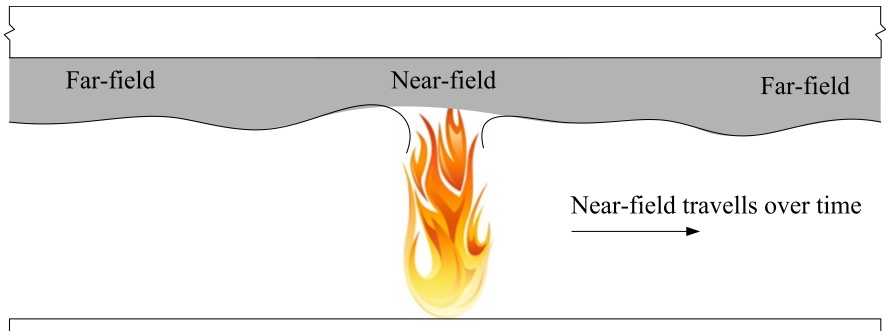


**Figure 2.2:** Illustration of a travelling fire with near field and far fields

### 2.2.4 Definition of fire severity

#### 2.2.4.1 The standard fire curve

The typical procedure of defining fire severity is by testing a sample under the *standard* fire in a furnace. The standard fire has its origins in the late $19_{th}$ century and was conceived as the worst possible fire. As Gales *et al* noted recently, the earliest references of such test can be found in New York during the late $1800s$ [3] where the city's fire codes were allowing floors made of building materials that are known to be problematic in fire to be used if they "pass" (deflection is less than 1.4% of the span) the *standard* fire test. Changes were made to the *standard* fire curve over the years, but these were minimal and the concept remains almost the same until today. It is common to express the curve mathematically as seen below.

$$T = T_0 + 345log(0.133t + 1) \tag{2.1}$$

Where $T$ and $T_0$ are the temperatures at time $t$ and 0 respectively.

#### 2.2.4.2 Ingberg's Equal Area Concept

Ingberg in the 1920s was one of the first researchers to try to relate the standard fire to real fire conditions. Consequently, he proposed the equal area hypothesis that was arguing that if the area under a temperature-time curve is equal to that of standard fire then the severity is also equal as seen in Figure 2.3 [4]. Inberg also developed a table relating fire load and fire severity as seen in Table 2.1.

Although it is important that he recognised the limitations of the standard fire, the method does not have any scientific merit [4].

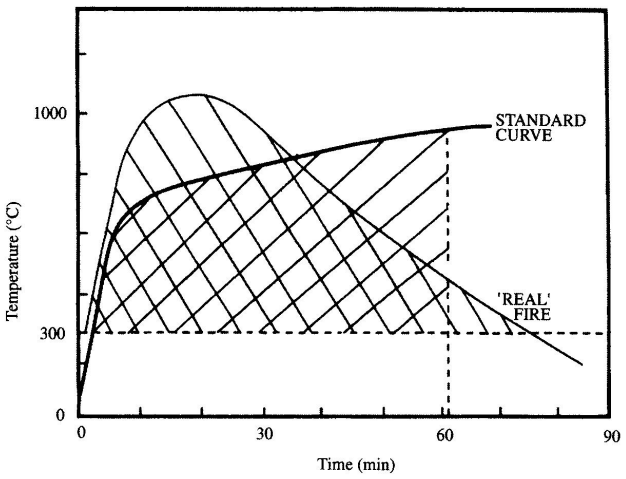


**Figure 2.3:** Ingberg's Concept of Equal Area

| **Combustible content**[a] | **Fuel Load**[a,b] | **Standard Fire duration** |
|---|---|---|
| **kg/m2** | **lb/ft2** | **MJ/m2** | **hours** |
| 49 | 10 | 900 | 1 |
| 73 | 15 | 1340 | 1.5 |
| 98 | 20 | 1800 | 2 |
| 146 | 30 | 2690 | 3 |
| 195 | 40 | 3590 | 4.5 |
| 244 | 50 | 4490 | 6 |
| 293 | 60 | 5390 | 7.5 |

[a] Calculated on the basis of floor area.

[b] Heat of combustion of wood taken as 18.4 kJ/g.a

**Table 2.1:** Ingberg's fuel load-fire-severity relationship

#### 2.2.4.3 Maximum Temperature Concept and Time Equivalent Formulas

Another concept that relates a *real* fire to a *standard* fire is the maximum temperature concept. This concept was proposed by Law [25] and other researchers, and compares the maximum temperature reached in a compartment after burnout in a protected member in order to define the equivalent time of fire severity [5]. Hence, some time equivalent formulae have also been put forward by researchers and codes [26, 27] that are applicable only to protected steelwork and concrete members [5].

#### 2.2.4.4 Minimum Load Capacity Concept

The minimum load capacity concept is based on the principle that a material has a well defined minimum load capacity. Thus it is not suitable for materials like wood where charring can continue to affect the capacity of the material even during the decay period of a fire [5]. According to this concept the fire severity is defined as the time that would result in an equivalent load bearing capacity of a standard fire. It should also be noted that although the load capacity is decreasing constantly during a standard fire, during a real fire the load capacity is expected to increase during the cooling period [5] as seen in Figure 2.4.

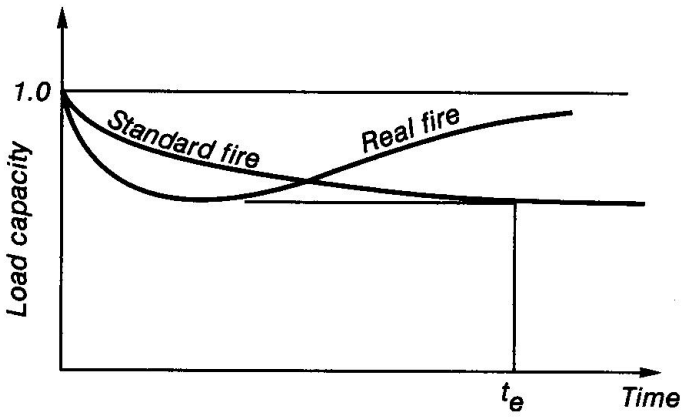


**Figure 2.4:** Minimum Load Capacity Concept

## 2.3 Structural behaviour and material properties in fire

### 2.3.1 Structural behaviour

Thermal expansion and its geometric effects play the key role in the behaviour of structures in fire. The fundamental relationship that governs the behaviour of structures under fire [28] is shown in Eq. 2.2

$$\epsilon_{total} = \epsilon_{mechanical} + \epsilon_{thermal} \tag{2.2}$$

It should be noted that, the stress state in a structural member depends only on the mechanical strains ($\sigma = f(\epsilon_{mechanical})$) while its deformations depend on the total strains($\delta = f(\epsilon_{total})$).

A lot of the knowledge in structural fire engineering comes from the large scale

tests carried out at Cardington [28, 29, 30, 31] in the 1990s where several fire tests were conducted on a multi-storey composite steel framed structure. One of the main outcomes from the tests was that redundant composite steel-concrete frame structures possess reserves of strength since the building maintained its stability during the whole duration of the fire despite most beams having be left unprotected and floor plates experiencing large deflections. Deflections in fire come mainly from thermal strains less so from mechanical strains therefore large deflections do not imply damage as they may do at ambient temperatures [28]. The large deflections in the composite floor also enabled a tensile membrane action in the concrete slab [30].

The beneficial effects of redundancy were also observed previously in the accidental fire on Broadgate Phase 8 in London where limited permanent damage was observed [32] even though the 14 storey composite structure was still under construction and thus only partially protected. Cardington experiments also showed that isolated models of single elements do not represent the real behaviour of structures and thus global models are required to represent the actual stiffness and restraint from surrounding structure [31]. The experiments also demonstrated that despite common belief, the structural behaviour in fire is dominated by thermal expansion and bowing rather than material degradation [28, 29, 30].

The Broadgate phase 8 fire and the Cardington test demonstrated the limitations of the standard fire resistance tests. This was also recognised by certain researchers in the 1980*s*. For example, Arup's engineer Margaret Law after contributing to the fire engineering design of the Pompidou Centre in Paris, as well as other buildings, criticised the standard fire test for being unrealistic. Her criticism was based on the fact that the fire growth and duration do not represent

the actual fire dynamics and that the end conditions of the specimen cannot represent the actual restraint, continuity and load redistribution [33].

Due to the limitations of the standard fire resistance tests as described above, and their use in prescriptive design, the discipline of structural fire engineering was born. In a performance based design the structural behaviour in fire can be quantified by treating fire as a load. Such a procedure can determine which parts of a structure are possibly overdesigned (and may not need additional fire protection) or other parts that need further strengthening and/or fire protection. This design approach can also include possible uncertainties in the definition of thermal environment by incorporating a risk based approach [34, 35, 36].

#### 2.3.1.1 Definition of structural 'failure'

There are no widely accepted criteria for defining structural failure in a performance based context. It should be mentioned that a fire safety failure (ie spread of fire) does not imply that a structural failure will also occur. A structural failure can be said to occur when the structure is not able to sustain a certain load [37].

Traditional ambient design is based on limiting maximum displacements. Similar concepts have also been introduced in codes for fire situations based on experiments of isolated elements in furnaces where *runaway* failure occurred. For example BS476 (part 20) defines failure when a maximum displacement of $L/20$ is reached in a beam or the rate of deflection is higher than $L^2/9000d$ (Where $L$ is the clear length of the beam). While these definitions can be used conservately in a design context, there is no evidence that they really represent failure of large and redundant structures. Usmani and Rotter [37] criticised using only deflection

limits to define failure since the deflections under fire can be large even under moderate temperatures while the structure may be largely undamaged. This is because damage is caused by mechanical strains and not thermal strains. Usmani and Rotter [37] proposed other criteria that could be used for assessing structural failure, which are the amount of non-recoverable plastic strains, the rupture of the reinforcement (measured by tensile mechanical strains), undesirable horizontal displacements of columns, and large deflections of beams near the compartment boundaries where breach of compartmentation can occur.

Rupture of reinforcement is considered to be a potential cause of failure since the reinforcement provides the tensile membrane action capacity of a slab. Typically, in design empirical restrictions are made based on the maximum temperature that the reinforcement reaches or the ultimate strain of the reinforcement. Izzudin *et al.* [38] critisised these simplistic criteria as they do not take into account the geometric configuration, bond characteristics, reinforcement ratio and steel stress-strain response. Clearly, more research is required to quantify reliable criteria that take into account all the physical parameters. In this work the maximum temperature reached in the reinforcement of a concrete slab was used just as a damage index for comparison between different fires in Chapter 5 similarly to previous work by Law *et al.* [39]. The plastic deformations were also monitored as an identification of damage as well as column horizontal displacements.

### 2.3.2 Material properties

Outside of thermal expansion that affects greatly the way that structures perform in fire, their behaviour is also influenced by their material properties (thermal

and mechanical) which are changing during heating and subsequent cooling in a fire. Only steel and concrete will be discussed here as this research studies the behaviour of composite buildings in fire. For other materials like timber and aluminium the reader can refer to standard textbooks [5]. These material characteristics were implemented in the finite element framework OpenSees following the Eurocode stipulations as presented in the next chapter.

#### 2.3.2.1 Steel

Historically most of the research conducted on the fire behaviour of materials was focused on steel and thus its well understood. This is because steel is widely considered to be a weaker material when heated and thus attracted most of the interest of researchers. A lot of experiments have been conducted in the past in order to characterise its thermal and mechanical properties which can be found in design codes such as the Eurocodes [40, 41]. The variation of the specific heat and thermal conductivity of steel with temperature, according to the Eurocodes, can be seen in Figures 2.5 and 2.6 respectively. Heat propagates relatively fast in steel sections due to its high thermal conductivity, and thus a uniform temperature profile is a common assumption used by researchers when examining the structural behaviour of steel members in fire [42]. The relationship provided for steel's specific heat in the Eurocodes takes into account the phase change in the material, which is represented by the spike seen in the curve at 750 ℃.

In addition, steel's mechanical properties such as its modulus of elasticity and compressive and tensile strength are degraded as temperatures increase but are usually assumed to be restored back to their original values during cooling. These

reduction factors can be found in the Eurocodes and are shown in Figures 2.7 and 2.8.

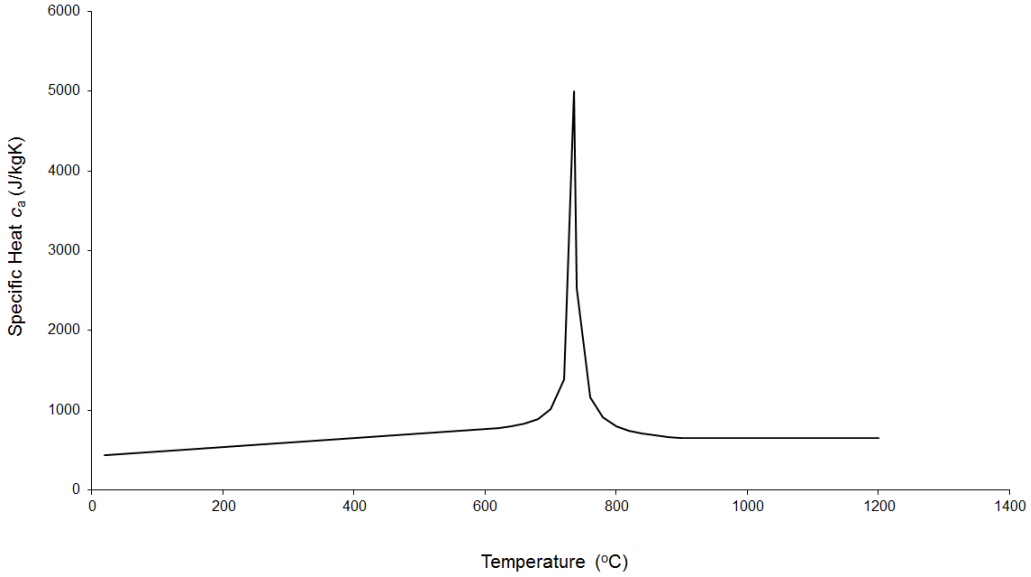


**Figure 2.5:** Specific heat of carbon steel

Thermal strains are provided as thermal elongations in the Eurocodes instead of defining the variation of steel's coefficient of thermal expansion with temperatures. The thermal strains are also typically assumed to be fully restored at ambient after cooling and thus only plastic strains will remain at this stage (if any). The thermal strains (or thermal elongations) given by Eurocode 3 [40] are as follows:

For $20^oC \leq T \leq 750^oC$

$$\epsilon_{thermal} = -2.416 * 10^{-4} + 1.2 * 10^{-5}T + 0.4 * 10^{-8}T^2 \tag{2.3}$$

For $750^oC \leq T \leq 860^oC$

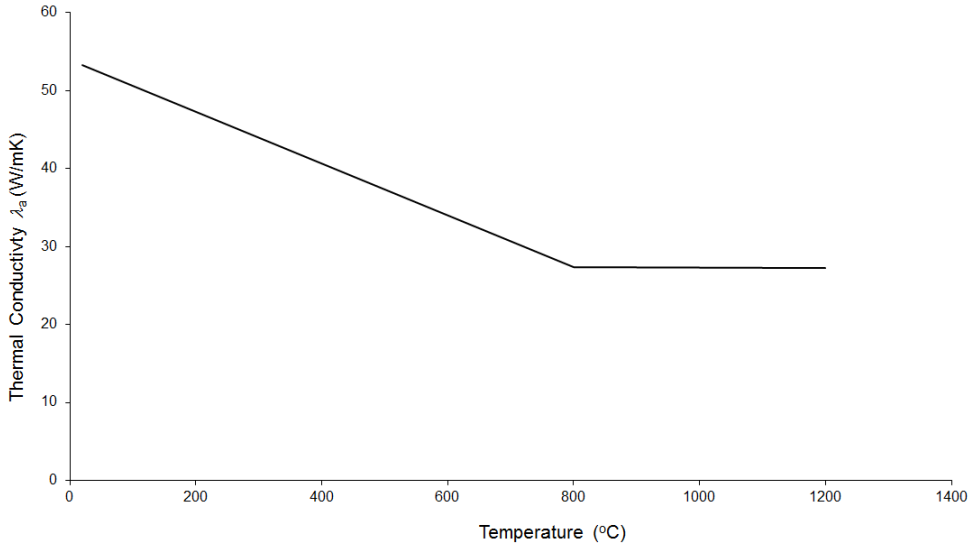


**Figure 2.6:** Thermal conductivity of carbon steel

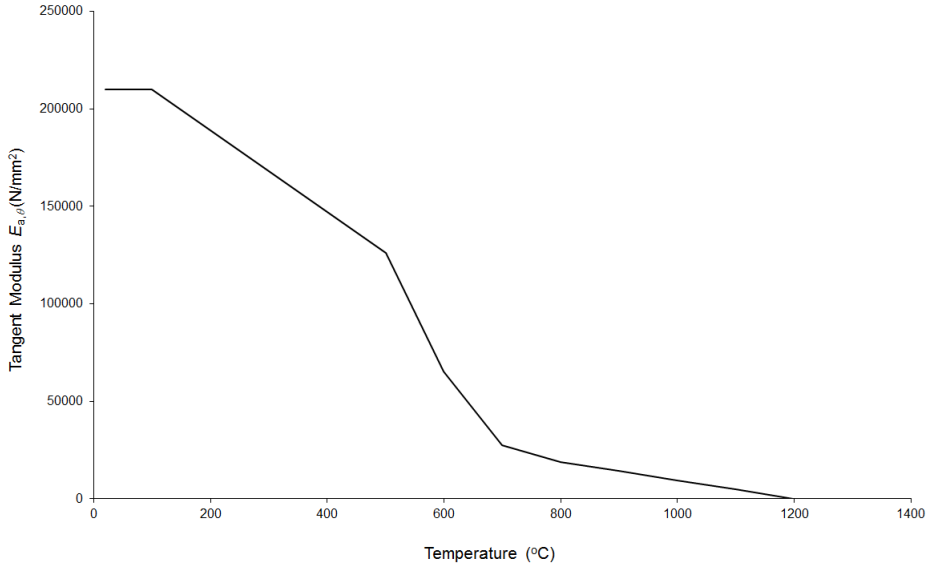


**Figure 2.7:** Tangent modulus of steel

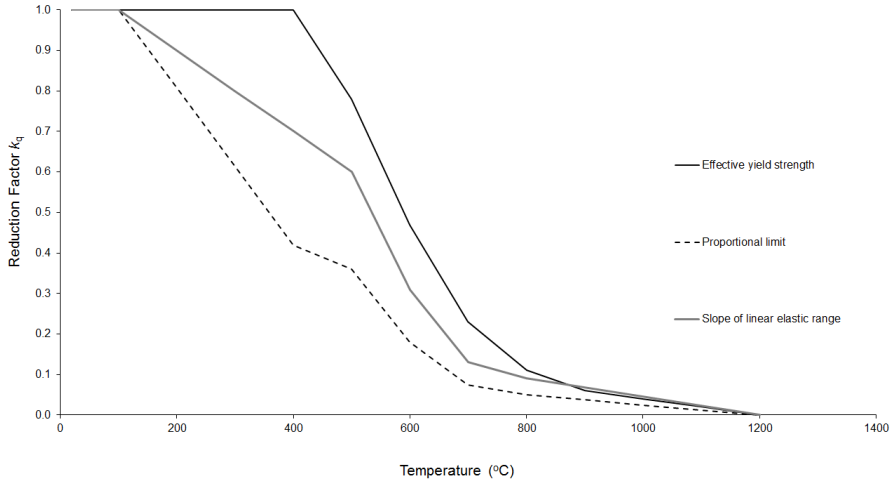


**Figure 2.8:** Reduction factors for steel

$$\epsilon_{thermal} = 1.1 * 10^{-2} \tag{2.4}$$

For $860^oC \leq T \leq 1200^oC$

$$\epsilon_{thermal} = -6.2 * 10^{-3} + 2 * 10^{-5} T \tag{2.5}$$

where $T$ is the temperature of the steel section.

Other codes use different reduction factors for the mechanical properties of steel (modulus and strength) and several other researchers have also proposed their own stress-strain relationships but these were not considered in the modelling carried out in this work. Relationships under multiaxial loading for steel have also been suggested [43].

#### 2.3.2.2 Concrete

Concrete is typically considered as a fire resistant construction material due to its low thermal conductivity and high specific heat. This assumption however is not always true as has been seen before. There are several cases where concrete structures (recently the Delft University building [44] and others [45]) experienced partial collapse, although this is rare. There have also been concerns in research for FRP-strengthened Reinforced Concrete (RC) [46, 47] and post-tensioned [48] structural members. Concrete has not been extensively investigated in the same manner as steel and there are still phenomena that are not fully understood such as spalling and cracking under fire. Concrete's thermal properties such as its thermal conductivity and specific heat are described in codes, and are presented in Figures 2.9 and 2.10 respectively, for normal and low weight concrete, based on Eurocode 2 [49]. It can be seen, that concrete has a lower thermal conductivity than steel, which leads to large temperature gradients even for thin concrete structural members. The strength of concrete under tension and compression is also degraded as for steel, but there are distinct differences. Concrete's compressive strength is much higher than its tensile strength. Eurocode [49] suggests that ignoring the tensile strength of concrete is a conservative assumption although this assumption has not been verified for concrete under high temperatures. Eurocode 2 [49] suggests values for the reduction factors of the tensile and compressive strength of concrete when temperatures increase and during return back to ambient. These values have been used in this work.

The thermal elongations used in this work were also taken from the Eurocodes. Eurocode 2 suggests different equations for normal weight concrete with siliceous or calcareous aggregates.

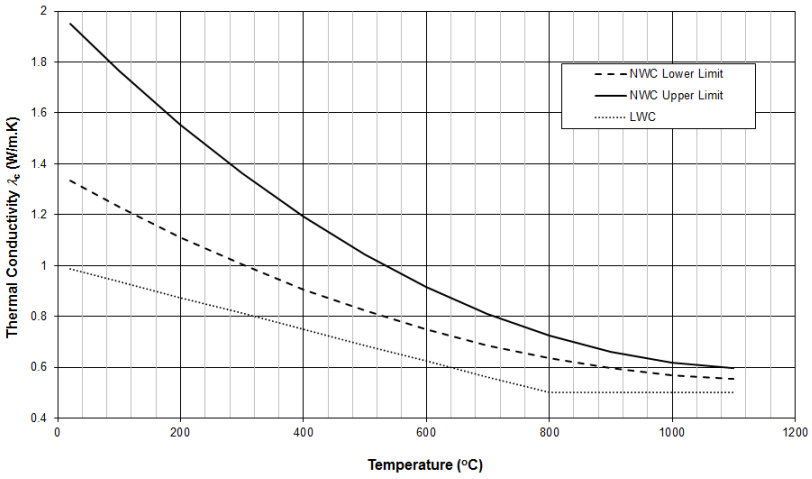


**Figure 2.9:** Thermal conductivity of concrete

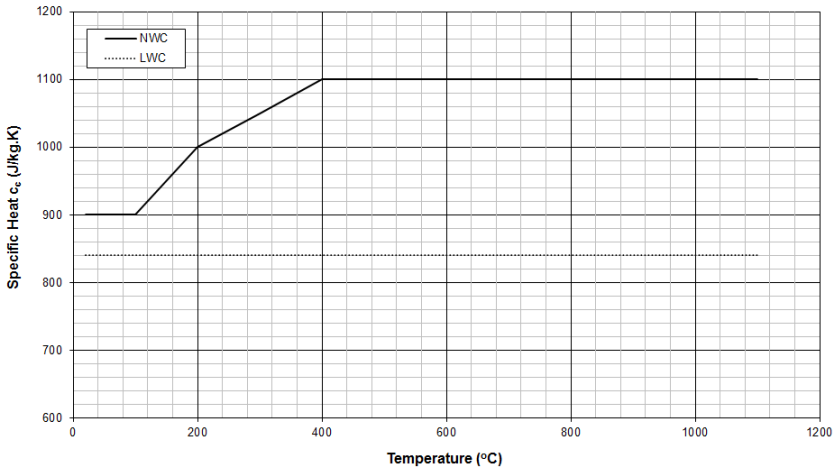


**Figure 2.10:** Specific heat of concrete

For concrete with siliceous aggregates the following equations are given;

For $20^oC \leq T \leq 700^oC$

$$\epsilon_{thermal} = -1.8 * 10^{-4} + 9 * 10^{-5}T + 2.3 * 10^{-11}T^3 \tag{2.6}$$

For $700^oC \leq T \leq 1200^oC$

$$\epsilon_{thermal} = 1.4 * 10^{-2} \tag{2.7}$$

where $T$ is the temperature of the concrete.

There is a lack of experimental data that could be used to establish a reliable stress strain curve of concrete in cooling [50, 51]. The compressive strength, strain corresponding to compressive strength and ultimate (crushing) strain of concrete do not recover during cooling. These properties were used in this work when cooling is considered according to $EN1994 - 1 - 2 : 2005$ [41]. The main hypothesis of EN 1994-1-2 is that in the stress strain relationship of concrete during the cooling phase of the fire, the concrete strain corresponding to the compressive strength is fixed during the whole cooling phase and equal to the value that was reached at the maximum temperature during the heating phase. Then based on the compressive strength and the corresponding strain, the elastic modulus can be calculated. Thermal strains during the cooling phase are typically assumed to be reversible. This is a commonly used assumption. However, this assumption has been questioned by previous researchers for temperatures over

$600^0C$ [52] due to material cracking. In this work this effect is not significant since the temperatures are not so high for concrete members.

The Eurocode reduction factors have been used for defining the failure surface in the multiaxial models that were developed in OpenSees although it should be mentioned that these properties are based on uniaxial testing and thus more research would be required to obtain robust concrete models under multiaxial loading at elevated temperatures since current material data is limited [53]. Moreover, transient creep is accounted for implicitly in Eurocode properties and hence any material unloading that take place will include the transient strain too. The implementation of transient creep as a separate strain component would also be required in more robust concrete material models.

## 2.4 Performance based design of tall buildings in fire

Structural fire resistance design is based on active and passive methods of fire protection and is usually applied in a prescriptive manner but increasingly performance based engineering approaches are being adopted, especially for large and complex projects. Fire in tall buildings presents a particularly unique challenge of ensuring safety of potentially very large numbers of occupants in the face of long emergency response times because of location (busy city centres) and building height. Furthermore, many previous tall building fires demonstrate that despite code compliant construction (designed to contain fires in the compartment of origin) fires often spread vertically and burn over multiple floors at the same

time. Tall buildings are often also complex and innovative in terms of structural form and contain spatial configurations involving large open spaces and high atria and column heights etc.

A performance based approach should include structural fire resistance as an integral part of the fire safety strategy since relying entirely on active protection measures presents many uncertainties, such as: in actual evacuation times or the non-activation of sprinklers due to malfunction (Parque Centrale, [54]); damage by earthquake (Northridge earthquake, [55]); or because the building is under construction (Mandarin hotel [4], large projects are sometimes under construction for years). NIST [56] suggests that tall buildings should be designed to resist the worst possible fires without taking sprinklers into account. By contrast the performance of passive protection measures, such as the inherent fire resistance of the structure, can be more reliably predicted and offers redundancy for robustness.

*Tall building features*

Tall buildings can have many different and unique forms that are dependent on many parameters such as architectural creativity, landscape, energy performance, environmental and cultural reasons, etc. However, there are common characteristics between the structural systems used which are typically categorised based on their effectiveness in resisting lateral loads, such as wind or earthquakes. These types are, moment resisting frame systems, braced frame and shear wall systems, core and outrigger systems, tubular systems (framed tubes, trussed tubes, bundled tubes) and hybrid systems [57]. Tall buildings are also typically categorised based on their use as office, hotel, residential or mixed use.

In this work the emphasis is given on a generic form of tall buildings with a core

in the centre of the building and perimeter columns that are connected to the core through composite floors made of steel beams (or trusses) and a concrete slab. This is the most popular form of construction for tall buildings. Cellular beams are also used often in design practice but were not investigated in this work. A typical collapse mechanism of such a system when on fire is the pulling in of the columns after large deflections develop in a floor which was experienced in the collapse of the WTC towers [58, 59, 60, 61] as seen in Figure 2.11. A similar collapse mechanism can also occur after a column is subjected to localised fires [62]. Bracing can also be used using either horizontal (hat truss) or vertical bracing. Recent research [62] has shown that horizontal bracing systems are less effective than vertical ones in reducing the pulling-in of columns when on fire.

### 2.4.1 Fires in tall buildings - lessons learnt

*Multifloor and travelling fires*

Previous high-rise buildings fires such as the ones in the WTC towers in New York, the 32 storey Windsor Tower in Spain (see Figure 2.12) [63], the Technical University of Delft and other fires, demonstrate that in high-rise structures fires can travel both horizontally and vertically, despite the commonly used design assumption of vertical and horizontal compartmentation.

Fires travel vertically in a tall building when vertical compartmentation is compromised. The most typical form of fire spread is upwards although in Windsor tower fire travelled vertically both upwards and downwards. Vertically travelling fires can occur when the perimeter fire barrier materials between the floor slab and curtains walls are compromised or the interior vertical ductwork is

ignited. External burning could also ignite combustibles in the upper floors by radiation heat transfer through glazing or by direct flame impingement through other openings. Moreover, external flaming is another way of vertical fire spread by igniting external insulation material.

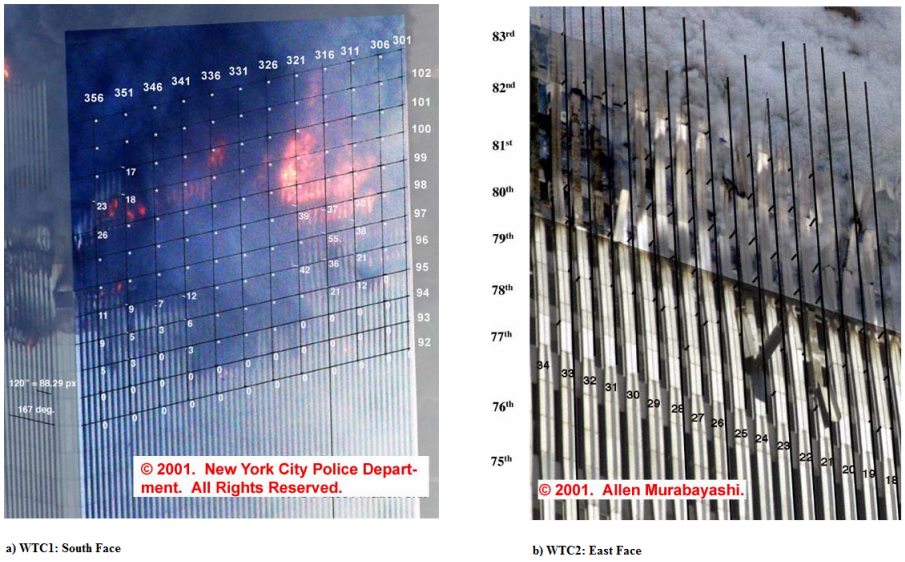


**Figure 2.11:** The pulling in of the collumns in the WTC towers

Traditional design of structures in fire assumes that the temperature is uniform inside a compartment and only one time temperature curve is used. This curve can either be a standard time temperature curve (BS 476 , ISO 834 , and ASTM E119) or a parametric time temperature curve as given in Eurocode 1 [11]. However, investigation of previous fires that occurred in tall buildings such as the WTC towers [64] (see Figure 2.13) or the Windsor Tower in Madrid demonstrate that fires travelled horizontally and were not uniform across the floor plate area. Thus it can be concluded that a uniform fire with a single time temperature curve would be an unrealistic assumption for open and large enclosures such as those seen in many tall buildings.

**Figure 2.12:** The Windsor Tower Fire, Madrid

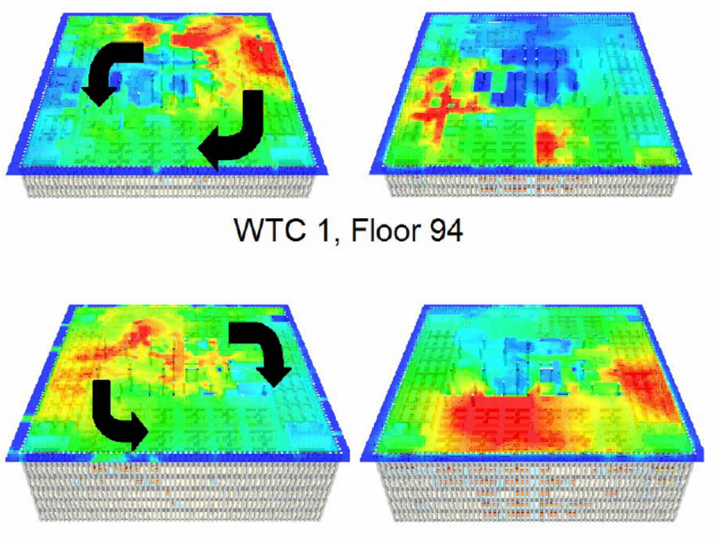


Figure 6–29. Direction of simulated fire movement on floors 94 and 97 of WTC 1.

**Figure 2.13:** Representation of travelling fires in the WTC towers

### 2.4.2 Design objectives and performance criteria

The main objectives of a performance based structural fire design are the following.

- Demonstration of safety

In a performance design context, safety can be demonstrated and is not assumed. This objective is of great importance, since recent failures (WTC complex, Windsor tower etc) have shown that for certain innovative structural layouts, prescriptive codes can be unsafe. An overview of such layouts have been recently reported by Flint *et al.* [65] for composite structures based on experience from real projects.

- Architectural freedom

Often architectural freedom (bare steel members, long spans etc) is constrained when trying to meet prescriptive fire safety requirements. Thus performance based fire engineering can help architects to achieve their designs by meeting the criteria of the codes.

- Economic savings to the client

Economic savings in a project are also always important. Significant savings can occur through the use of structural fire engineering since typically fire protection, especially for steel structures, is a big percentage of the overall construction cost, however this cannot be guaranteed as in some cases performance based

or engineered solutions maybe more expensive (e.g. depending upon specific performance objectives and the innovativeness and adventure in design).

- Property protection and business continuity

In tall buildings, that are often the hub of businesses, business continuity is important and losses due to business disruption can be many times higher than the cost of damage or repair of the structure itself. Hence, the fire design of such special structures needs to take into consideration this objective with proper consultation with the business owners and insurers. An example, although not a tall building, is the partial collapse of a bridge in Oakland in 2007 after a fire that was caused by the collision of a truck, as seen in Figure 2.14. Fortunately nobody died in this event and outside of the repair costs which were of the order of tens of million dollars, the economic losses due to business disruption that such a failure can have and the effect on everyday commuting to and from the heart of a city centre can be even more devastating. To be more specific, the bridge that collapsed was used by 75000 vehicles daily although this number raises to 280000 commuters every day if the fact that the accident occurred on a portion where three highways meet is considered, creating transportation problems to San Francisco for hundreds of thousands of people.

**Figure 2.14:** A bridge partially collapse after a fire

## 2.5 Knowledge gaps and significance of this research

This chapter presented a review of the current structures in fire context. The design fires used in structural fire engineering ands the structural behaviour and material properties under fire have been reviewed. The design objectives and performance criteria when designing structures against fire have also been discussed.

Several knowledge gaps have been identified in structural fire engineering research on the use of design fires for large enclosures. Most of the work conducted in previous research studies focused on assessing the structural behaviour of frames under fire using Eurocode's parametric or localised fires. Limited work has been conducted on the structural response of tall buildings under more realistic design fires, such as multifloor and travelling fires.

Building on previous work conducted at the University of Edinburgh, this

work examines the behaviour of tall buildings under multifloor and horizontally travelling fires.

# Chapter 3

# OpenSees for ambient and heated structures

## 3.1 Background

OpenSees stands for Open System For Earthquake Engineering Simulation and was developed at the Pacific Earthquake Engineering Research Center (PEER), University of California Berkeley (UCB), initially as a research project on object-oriented design of structural analysis software [66]. Currently, it is a finite element framework for simulating the performance of structural and geotechnical systems subjected to earthquakes. The framework is open-source and is written mainly in the C++ programming language following the object-oriented paradigm. Being a framework and not software implies that OpenSees is a collection of software components for building applications in a specific domain [66]. Due to

these attributes OpenSees has became a community tool and thus it has been continuously developed and has been used by many people globally [67].

Arguably, one of OpenSees' biggest advantages is its object-oriented architecture [68] since object-oriented design is focused on modelling objects (i.e. concepts) rather than just data, with each object having its own attributes and functions. This form of programming design permits the management of complex problems and allows for easier reusability and extensibility of the code [69]. This is in contrast to procedural programming (FORTRAN etc) where there is either just a list of instructions, or functions, that are based on not well defined or loose concepts that make it difficult for complex codes to be extended by a person other than the original programmer. All these strengths of object-oriented design make it a very suitable structural analysis software for use and continuous development by a virtual community [70].

OpenSees is also open-source, free for anyone interested to download, use and modify. This is extremely important compared to traditional programs where, even though it is often possible for researchers to add their own code, such as new materials or elements, the rest of the code remains a black box. Moreover, any bugs in open-source codes are easier to be traced and research ideas can be assessed or exchanged with other parties.

There are several software for modelling 'structures in fire' scenarios. These software can be generally categorised into two categories; *(i)* general Finite Element packages (such as ABAQUS [71] or ANSYS [72]) and *(ii)* specialist structural fire engineering software (ADAPTIC [73], VULCAN [74], SAFIR [75]) developed by university departments actively involved in this research field. Both categories of software have their advantages and disadvantages. The software

of the former category have the advantage of containing a large number of elements and materials which are widely validated, good graphics for pre- and post-processing and service support when required, yet their cost can be very high. Specialist programs are cheaper but they lack generality and versatility and suffer from a high level of dependency on a few individuals for maintenance, support and development.

In this work, it was decided to take advantage of OpenSees' powerful attributes and develop new structural fire modelling capabilities in this framework. It is believed that this development can be the base for a community owned research code which can be continuously under development by researchers collaborating freely across geographical boundaries. Hence the platform could be more easily maintained and managed and its components can be reused by future users and developers. Further work is also underway to link this version of OpenSees with the CFD code FireFOAM which is part of OpenFOAM [76], an open-source code capable of simulating fires. This combined effort will then be able to model all the phenomena associated with fire (CFD analysis, Heat Transfer and Structural analysis) in a common framework which is not possible at the moment in other codes and will be at the disposal of researchers and practitioners to use or modify freely.

## 3.2 Overview of OpenSees framework

A summary of the framework architecture along with its modelling capabilities are presented below. The basic classes of OpenSees are described for creating a finite element model. As regards modelling the emphasis is placed on beam-column

elements as they constitute a major component both in the software development and the modelling work carried out during this project.

### 3.2.1 Framework architecture

The object-oriented characteristics of OpenSees render it a uniquely useful tool for structural analysis. Most of the classes in OpenSees are written in C++ but there are also legacy FORTRAN code and external numerical libraries written in C or FORTRAN (such as Lapack, Petsc, Mumps and others) [77, 66]. The architecture of OpenSees is based on objects, making it modular, extensible and flexible. The framework contains **abstract** and **concrete** classes. An **abstract** class is the class which provides an interface and most or all of its methods (a method is code that is member of a class that acts on the data) can be implemented by its subclasses. These methods are called **abstract** methods. When a class implements every method defined in its interface, then it is called a **concrete** class. Typically developers, who want to extend the OpenSees platform, can provide new **concrete** classes that become subclasses of existing **abstract** classes.

**Domain** is the most basic class in OpenSees. A **Domain** object aggregates **DomainComponent** objects which are **Node**, **Element**, **SP_Constraint**, **MP_Constraint** and **LoadPattern** of a finite element model as seen in Figure 3.1. The **ModelBuilder** object builds the **Domain** information based on the input decided by the user each time. The **Analysis** object advances the **Domain** to a new state based on the user's selected type of **Analysis** and **Load** objects.

The diagram shown in Figure 3.1 adopts the unified modelling language (UML)

[78]. UML is typically used for describing the relationship between classes in object oriented software. The description of each relationship between the classes can be seen in Figure 3.2

One of the most basic abstractions of the OpenSees framework and every finite element code is the **Element** class. The element class provides the necessary abstractions for determining the resisting force of an element based on the displacements of the nodes. It can be seen that the element class also uses instances of the material class in order to compute the constitutive relationship of a finite element. The diamond symbol represents aggregation. This use of object composition makes it possible for users to combine different components.

There are other objects that facilitate the necessary methodologies for performing nonlinear analysis as seen in Figure 3.1. For example, the **Integrator** object is responsible for providing information for solving the system of equation. This object determines the predictor step, specifies the tangent matrix and residual vector at any iteration and determines the corrector step based on every displacement increment [77, 66]. The **Integrator** object is selected based on the demands and type of analysis. Typically **LoadControl** is used in static analysis and **Newmark** in dynamic analysis. The **SolutionAlgorithm** object determines the technique that will be used in order to solve the non-linear equation, for example **NewtonRaphson**. The **CHandler** object handles how the **SP_Contraint** objects and **MP_Contraint** objects are enforced, such as the **Lagrange** and **Penalty** objects.

The **Element**, **Material**, **ElementalLoad** and **LoadPattern** classes are of interest to this work, since new subclasses were provided for these classes in order

to facilitate *structures in fire* modelling. More information about these additions will be given later.

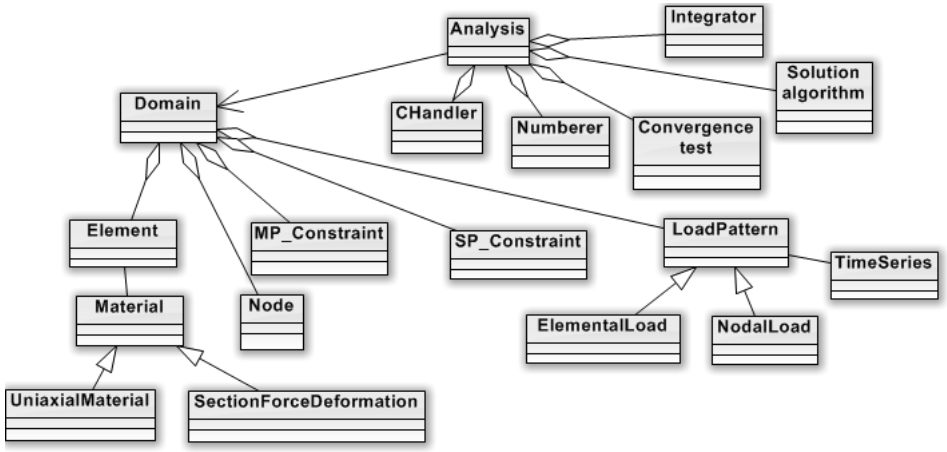


**Figure 3.1:** OpenSees class architecture

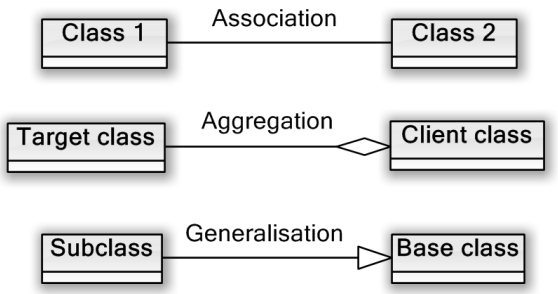


**Figure 3.2:** Description of relationships between classes

The interface between the user and the framework is provided through a Tcl nterpreter [79]. Tcl is a fully programmable string-based scripting language that is very efficient for handling very big models. The option of providing a main function is also possible but from the authors experience this can realistically be restricted to small models only or for benchmarking developed code.

### 3.2.2 Capabilities

OpenSees incorporates a big library of elements and materials that is continuously under development and expansion by researchers globally that become part of the official version, after all the appropriate testing is conducted. The most widely used elements are its beam-column elements. These elements were extended to develop structural fire modelling capabilities and are used in this work.

Opensees currently supports both distributed plasticity and concentrated plasticity based Euler-Bernoulli beam-column elements. Moreover, the distributed plasticity beam-column elements can be split into the typical displacement-based (**DispBeamColumn**) and force-based beam-column elements (**ForceBeamColumn**). The former are based on the stiffness method while the latter on the flexibility method. In the displacement-based element the strain field is approximated by means of appropriate interpolation methods from the nodal displacements. These elements ensure that compatibility of deformations will be satisfied but the force equilibrium is satisfied when sufficient number of elements per member are used. Hence, a dense mesh will be required where significant inelastic deformations are expected. Contrary to the displacement-based element, in the force-based element the section forces are calculated based on the nodal forces by interpolation in order to reach equilibrium [80]. Compatibility of deformations is satisfied by integrating the section deformations in order to obtain the element deformations and nodal displacements.

These displacement- and force-based two-noded elements have three degrees of freedom in two dimensions and six degrees of freedom per node in three dimensions [81] as seen in Figure 3.3. The integration in order to derive the stress strain

relationship can be performed through several schemes but the default one is Gauss-Lobatto quadrature in order to capture the inelastic behaviour of an element by monitoring the strain field on several sections along the element (see Figure 3.3, [80, 82]). Typically five integration points have been shown to be appropriate. The number of integration points affects the assumed plastic hinge length and localisation effects can arise when this number is not the optimum one [83]. These effects can occur easier in force-based elements. Employing materials with hardening response instead of perfectly plastic materials can help avoid these problems based on the author's experience. A denser mesh also helps. These elements are typically used along with co-rotational transformation in which the rigid body modes of the element are separated from its deformations by attaching a reference coordinate system to the element as it deforms [84, 85]. This theory allows the separation of the nonlinear geometric response of an element from its nonlinear material response [84].

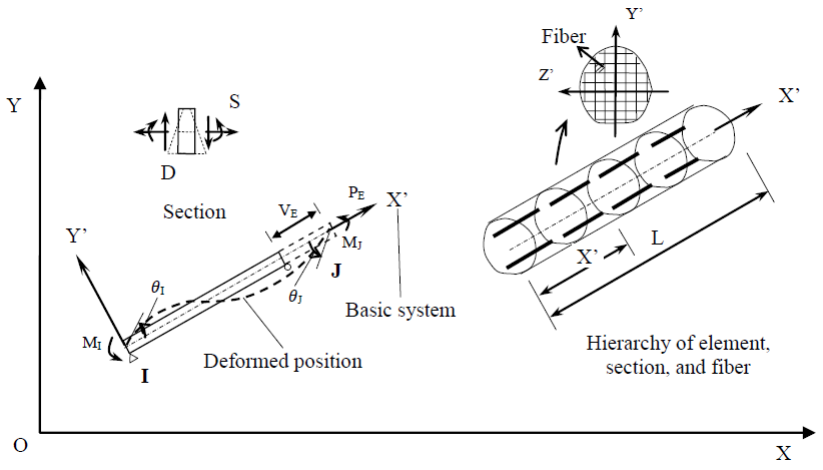


**Figure 3.3:** Basic and global coordinate system

There are also shell elements in OpenSees. In the ambient versions of OpenSees, there is a geometrically linear **ShellMITC4** element object, which uses a bilinear isoparametric formulation in combination with a modified shear interpolation [86],

and more recently the nonlinear **ShellNL** element has been introduced in version 2.3.2, which is a Lagrangian nine-noded shell element [87].

## 3.3 Using OpenSees for structures in fire

The work carried out concerning OpenSees and structural fire engineering can be categorised into software development and modelling parts.

### 3.3.1 Software development

The development of OpenSees with fire capabilities took advantage of the benefits of its object-oriented architecture and hence the new classes that were developed for modelling structures in fire required minimal changes to the original code. The developed code for modelling beam-columns consisted of a new thermal edition of the nonlinear displacement based element both in 2D and in 3D (**Dispbeamcolumn2dthermal**, **Dispbeamcolumn3dthermal**), new thermal editions of classes for defining the fiber section representation (**FiberSection2dthermal**, **FiberSection3dthermal**, **FiberSectionGJthermal**), new thermal editions of uniaxial material classes (**Steel01Thermal**, **Steel02Thermal**, **Concrete02Thermal**), thermal load elemental classes for 2D and 3D beams(**Beam2DThermalAction**,**Beam3DThermalAction**) and a fire load pattern class (**FireLoadPattern**). A diagram showing all the developed classes can be seen in Figure 3.4 using the Unified Modelling Language (UML) [78].

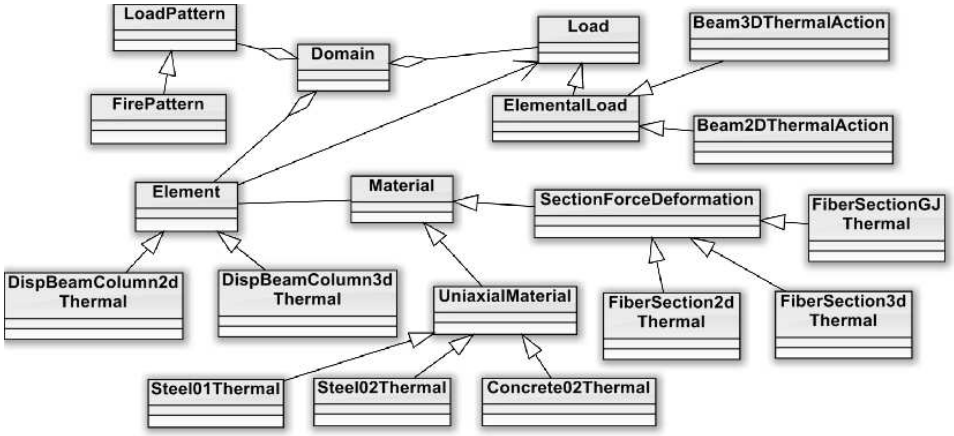


**Figure 3.4:** Diagram of the fire related classes for beam-column elements

The interface for the **DispBeamColumn2DThermal** element class developed can be seen in Figure 3.5. The interface for **DispBeamColumn3DThermal** element is similar. These classes are modified versions of the original OpenSees classes. Some methods for output and sensitivity are omited for clarity. It can be seen that a method was added to make structural fire analysis possible, *addLoad(ElementalLoad *theLoad, const Vector &loadFactors)*. This method, examines if a thermal load is defined on the element, and then determines the section thermal response (forces and moments). This method follows the philosophy of the existing method, *addLoad(ElementalLoad *theLoad, double loadFactor)*, however for fire situations when **FireLoadPattern** is called instead of a typical **LoadPattern**, then multiple temperature (or loadfactor) - time relationships exist which could not be passed using the original method that only passes one value as only one loadfactor per element exists under ambient temperature. For generality the method allows also only one loadfactor to be used when an element is heated uniformly, as can be seen in Appendix A. In the early versions of the modified OpenSees [88] this method was not included

and thus all the elements were assumed to be heated with the same loadfactor-time relationship even when they were heated non-uniformly. This limitation was tackled in later work by introducing the **FireLoadPattern** class [89].

```
class DispBeamColumn2dThermal : public Element
{
  public:
    DispBeamColumn2dThermal(int tag, int nd1, int nd2,
          int numSections, SectionForceDeformation **s,
          BeamIntegration &bi, CrdTransf &coordTransf,
          double rho = 0.0);
    DispBeamColumn2dThermal();
    ~DispBeamColumn2dThermal();

    const char *getClassType(void) const {return "
        DispBeamColumn2dThermal";};

    int getNumExternalNodes(void) const;
    const ID &getExternalNodes(void);
    Node **getNodePtrs(void);

    int getNumDOF(void);
    void setDomain(Domain *theDomain);

    // public methods to set the state of the element
    int commitState(void);
    int revertToLastCommit(void);
    int revertToStart(void);

    // public methods to obtain stiffness, mass, damping and
        residual information
    int update(void);
    const Matrix &getTangentStiff(void);
    const Matrix &getInitialStiff(void);
    const Matrix &getMass(void);

    void zeroLoad();
    int addLoad(ElementalLoad *theLoad, double loadFactor);
    int addLoad(ElementalLoad *theLoad, const Vector &loadFactors);

    int addInertiaLoadToUnbalance(const Vector &accel);

    const Vector &getResistingForce(void);
    const Vector &getResistingForceIncInertia(void);
```

**Figure 3.5:** Interface for **DispBeamColumn2DThermal** element class

The interface for the **FiberSection2dThermal** material class developed can be

seen in Figure 3.6. The interface for **FiberSection3dThermal** and **FiberSectionGJThermal** is similar. The difference between **FiberSection3dThermal** and **FiberSectionGJThermal** is that **FiberSectionGJThermal** includes torsion in its section definition while **FiberSection3dThermal** does not, as in the original OpenSees classes. In the ambient version of OpenSees, **FiberSection3dThermal** can be assigned torsion by combining its response with another torsion assigned elastic section using a **SectionAggregator** object, but this procedure is not currently implemented for thermal applications. It can be seen that the method *const Vector &getTemperatureStress(const Vector &tData)* has been introduced. This method distributes the temperatures to each fiber according to the user input and determines the section response.

The interface for the **Steel01Thermal** material class developed can be seen in Figure 3.7. The interface for **Steel02Thermal** and **Concrete02Thermal** is similar. These classes are modified versions of the original OpenSees **Steel01**, **Steel02** and **Concrete02** classes. Some methods for output and sensitivity are omited for clarity. It can be seen that the methods, *setTrialStrain(double strain, double FiberTemperature, double strainRate)*, *getElongTangent(double, double&, double&, double)* and *getThermalElongation(void)*, have been added to incorporate structural fire analyses. The method, *getElongTangent(double, double&, double&, double)*, for determing the current thermal elongation and thermal tangent can be seen in section A.2.1 in the Appendix. It should be noted that in this method the maximum temperature that each fiber reaches is also passed. This was done in order to consider cooling of materials such as concrete where the stress strain relationship is affected by the maximum temperature reached in a fire. This can be seen in the code for the method *getElongTangent(double, double&, double&, double)* in **Concrete02Thermal** in

```
class FiberSection2dThermal : public SectionForceDeformation
{
  public:
    FiberSection2dThermal();
    FiberSection2dThermal(int tag, int numFibers, Fiber **fibers);
    FiberSection2dThermal(int tag, int numFibers, UniaxialMaterial
        **mats,
         SectionIntegration &si);
    ~FiberSection2dThermal();

    const char *getClassType(void) const {return "
        FiberSection2dThermal";};
    int    setTrialSectionDeformation(const Vector &deforms, const
        Vector&); //PK changed 18 to 27
    const Vector &getSectionDeformation(void);

    const Vector &getStressResultant(void);
    const Matrix &getSectionTangent(void);
    const Matrix &getInitialTangent(void);
    const Vector &getTemperatureStress(const Vector &tData);


    int    commitState(void);
    int    revertToLastCommit(void);
    int    revertToStart(void);

    SectionForceDeformation *getCopy(void);
    const ID &getType (void);
    int getOrder (void) const;

    int sendSelf(int cTag, Channel &theChannel);
    int recvSelf(int cTag, Channel &theChannel,
     FEM_ObjectBroker &theBroker);
    void Print(OPS_Stream &s, int flag = 0);

    Response *setResponse(const char **argv, int argc,
        OPS_Stream &s);
    int getResponse(int responseID, Information &info);

    int addFiber(Fiber &theFiber);
```

**Figure 3.6:** Interface for **FiberSection2dThermal** section class

Section A.2.2 in Appendix where the characteristics are modified according to Eurocode. This addition was not included in earlier thermal versions [88] as cooling was not considered.

The interface for the **FireLoadPattern** class developed can be seen in Figure 3.8.

```
public:
    Steel01Thermal(int tag, double fy, double E0, double b,
        double a1 = STEEL_01_DEFAULT_A1, double a2 =
            STEEL_01_DEFAULT_A2,
        double a3 = STEEL_01_DEFAULT_A3, double a4 =
            STEEL_01_DEFAULT_A4);
    Steel01Thermal();
    ~Steel01Thermal();

    const char *getClassType(void) const {return "Steel01Thermal";};


    double getThermalElongation(void); //***JZ
    double getElongTangent(double, double&, double&, double);//***JZ
         //PK add to include max temp

    int setTrialStrain(double strain, double strainRate =0);
    int setTrialStrain(double strain, double FiberTemperature,
        double strainRate); //***JZ

    int setTrial (double strain, double &stress, double &tangent,
        double strainRate = 0.0);
    double getStrain(void);
    double getStress(void);
    double getTangent(void);
    double getInitialTangent(void) {return E0;};

    int commitState(void);
    int revertToLastCommit(void);
    int revertToStart(void);

    UniaxialMaterial *getCopy(void);

    int sendSelf(int commitTag, Channel &theChannel);
    int recvSelf(int commitTag, Channel &theChannel,
     FEM_ObjectBroker &theBroker);
```

**Figure 3.7:** Interface for **Steel01Thermal** material class

It can be seen that one method, *void setFireTimeSeries(TimeSeries *theSeries1, TimeSeries *theSeries2, TimeSeries *theSeries3, TimeSeries *theSeries4, TimeSeries *theSeries5, TimeSeries *theSeries6, TimeSeries *theSeries7, TimeSeries *theSeries8, TimeSeries *theSeries9);*, has been added to incoporate structural

fire analyses. This method defines nine **TimeSeries** objects, representing different temperature-time histories for each point along the section of an element, in order to be passed as data to the **Element** object. It is considered that nine temperature curves are considered to be appropriate for most cases, based on a comparison against other software capabilities (in ABAQUS for example, up to five points can be provided for beam elements) and previous modelling validation against the cardington tests [29]. The **FireLoadPattern** object is used in association to an **ElementalLoad** object that defines the thermal conditions of an element. For beam-column elements, these objects are **Beam2DThermalAction** in 2D and similarly **Beam3DThermalAction** in 3D. The interface of **Beam2DThermalAction** class can be seen in Figure 3.9. When these objects are constructed, up to nine temperatures and nine locations in the cross-section are stored in a **Vector** object which is passed into the appropriate **Element** class when asked for.

```
1 class FireLoadPattern : public LoadPattern
2 {
3   public:
4     FireLoadPattern(int tag);
5     ~FireLoadPattern();
6     FireLoadPattern(int tag, int classTag);
7
8     void applyLoad(double time);
9
10    bool addSP_Constraint(SP_Constraint *);
11    bool addNodalLoad(NodalLoad *);
12
13    void setFireTimeSeries(TimeSeries *theSeries1, TimeSeries *
          theSeries2,
14          TimeSeries *theSeries3, TimeSeries *theSeries4, TimeSeries
              *theSeries5,
15          TimeSeries *theSeries6, TimeSeries *theSeries7, TimeSeries
              *theSeries8, TimeSeries *theSeries9);
```

**Figure 3.8:** Interface for **FireLoadPattern** class

```
public:
  // Constructors based on 9, 5 or 2 temperature points
  // t-temperature; locY-coordinate through the depth of section
  Beam2dThermalAction(int tag,
          double t1, double locY1, double t2, double locY2,
          double t3, double locY3, double t4, double locY4,
          double t5, double locY5, double t6, double locY6,
          double t7, double locY7, double t8, double locY8,
          double t9, double locY9,
          int theElementTag);

  Beam2dThermalAction(int tag,
          double t1, double locY1, double t2, double locY2,
          double t3, double locY3, double t4, double locY4,
          double t5, double locY5, int theElementTag);

  Beam2dThermalAction(int tag,
          double t1, double locY1, double t2, double locY2,
          int theElementTag);

  Beam2dThermalAction();

  ~Beam2dThermalAction();
```

**Figure 3.9:** Interface for **Beam2DThermalAction** class

New classes were also added for modelling slabs under fire, a nonlinear shell element was developed based on the linear **ShellMITC4** element, the **ShellMITC4GeoNonlinear** element was developed by adopting a Total Lagrangian formulation [90]. Modified thermal editions have also been developed of the *DruckerPrager* multi-dimensional material class [90] which has its drawbacks but can model concrete under elevated temperatures. The changes for these classes were very similar to those described for the beam-column elements and thus are not reproduced here.

## 3.3.2 Modelling

### 3.3.2.1 Materials

Three different materials have been developed for modelling structures in fire. These are **Steel01Thermal**, **Steel02Thermal** and **Concrete02Thermal**.

### 3.3.2.2 Elements

*Section representation*

The definition of a fiber section has to accurately describe the section properties of a beam-column element. In OpenSees individual fibers or circular and rectangular patches that generate fibers can be defined. For two dimensional problems, the fibers only in one local axis of the section are considered and hence both individual fibers or patches can be utilised. For three dimensional conditions, the section definition has to consider both local y and z axis and hence the utilisation of patches is more suitable. For three dimensional problems, torsion for the section has to be defined as well. Uniform temperature is assumed for each fiber according to the location of the centre of the fiber. That implies that in order to represent high temperature gradients, a minimum appropriate number of fibers must be defined.

*Meshing*

Typically several displacement based elements have to be used when modelling beam-clolumns in fire in order to account for the member $P - \delta$ effects.

#### 3.3.2.3 Fire load definition

*Fire Pattern*

Thermal loads have distinctively different characteristics than typical static loads when considering their implementation in a finite element framework. This is because, unlike static loads, thermal loads do not have a single value through the depth of a section in order to define a single load - time relationship for the particular element. Temperature gradients occur over at least one direction of a structural element, especially in structural members of low thermal conductivity like concrete. Thus the thermal load definition for these members has to incorporate multiple temperature - time relationship curves for each element. For this reason a fire pattern command was developed in order to accurately define these temperature gradients. Up to nine temperature points and corresponding locations along any direction (one at a time) of a section can be defined.

*Heat Transfer mapping*

Heat transfer mapping is also an alternative to the tcl definition of fire loads using **FireLoadPattern** object, especially when considering complex spatially varying temperatures like those found in localised fires. This capability is still under development, and was not used during the research of this thesis. Fire definition was solely done using the **FireLoadPattern** object.

#### 3.3.2.4 Solution algorithms

*Structural Instabilities*

Instability or buckling of a structure happens when it experiences a sudden change in its geometry during compressive forces or moments and thus loses its ability to resist to the loads applied. In the case of fire related problems, the procedure involves two step by step events. First the mechanical load is applied and remains constant and then the temperature is increased. If the structure loses its stability and fails then the temperature at which this failure occurs is the critical temperature of the structure (or the time is the critical time). Structures buckle when the load deflection path undergoes bifurcation or limit points. These critical points arise when the global stiffness matrix of the structure becomes singular ($detKs = 0$). For simple determinate structures under fire the temperature at which any element fails is considered the critical temperature for the whole structure while for redundant structures local failure does not imply global failure which may be able to continue to carry the loads, without the contribution from the failed member. This is because redundant structures can find different load paths by which to support additional load when its local strength is reached at a single location [91]. Critical Limit points usually are sometimes followed by nonlinear instability regions in which snap-through or snap-back occurs and in which the equilibrium path goes from one stable point to a new stable point after a large displacement has occurred. During this snap buckling the tangent stiffness of the structure which is represented by the slope in the equilibrium path becomes zero. When this phenomenon occurs many nonlinear solvers encounter convergence problems.

*Path following methods for structures in fire*

The buckling response of a structure is described by a load-deformation diagram, also known as equilibrium path because all its points correspond to equilibrium

states. In nonlinear static analysis the following methods are used to trace the equilibrium path. The load control method is the most common method of integration employed in structural fire analysis. Its efficiency in dealing with fire problems has been shown in many studies. During that procedure the thermal load in increased and when the equilibrium conditions are satisfied the displacement of the structure is found. The main disadvantage of this method is that it cannot go beyond limit points. Displacement control applies incremental displacements and performs well for snapthrough problems but often it is not possible to trace snap-back and is only helpful if a characteristic displacement is chosen which is often not efficient for the analysis of large structures in fire containing thousands of degrees of freedom. The merits of this method are applicable mainly in the earthquake engineering field. Arc length method is also an efficient numerical method that is used widely for the stability analysis of structures under ambient temperature. It has been shown to handle very well both snap through and snap back problems. However, this method is also not applicable for structural fire analysis where the mechanical load is assumed to remain constant when the thermal load is applied to the structure. Very few researchers [92] have used this method in the past for structural fire problems, for isolated elements with limited application to big models.

Due to the limitations discussed above and also due to the strength of OpenSees in dynamic analysis, a dynamic approach was employed in this work to examine the stability of structures under fire loading. It should be emphasised that the dynamic procedure is applied not because fire is necessarily a dynamic phenomenon rather as a numerical tool to go beyond limit points and account for temporary dynamic motion which is not present during the whole duration of a fire. Such a procedure has previously been implemented in the structural

fire software SAFIR [93] and has also been incorporated in an explicit way in the VULCAN analysis software for modelling the collapse of portal frames in fire [94].

The dynamic force equilibrium equation [95] is shown below,

$$F(t) = Mu''(t) + Cu'(t) + Ku(t) \tag{3.1}$$

Where $F(t)$ is the external force, $Mu''(t)$ is the inertia force, $Cu'(t)$ is the damping force and $Ku(t)$ is the internal force due to deformation

The numerical scheme selected for the dynamic analysis is an implicit solution. The reason for selecting implicit over explicit analysis solution scheme is because an implicit analysis solves the system of equations for each increment and performs Newton-Raphson iterations until it reaches convergence while explicit analysis does not attempt to reach a converged solution for each timestep. For that reason an explicit analysis typically uses many more timesteps than an implicit one. Franssen and Gens [93] have suggested that numerical damping is accurate enough for most "structures in fire" applications since there are no highly dynamic effects present despite fire's transient nature. They proposed increasing the Newmark "$\beta$" and "$\gamma$" parameters when using the Newmark integrator. A similar procedure is followed in this thesis by adding numerical damping when conducting dynamic analyses of structures in fire. This has been achieved in OpenSees either by using the Newmark integrator with the values suggested (0.8 and 0.45) by Franssen and Gens [93] or by adopting a Hilber Hughes Taylor (HHT) [96] integrator with an appropriate factor to account for numerical damping (0.7 in this thesis). It is widely considered that HHT is a better option since it can be unconditionally stable while achieving second order accuracy [96].

Furthermore, as part of the dynamic stress analysis, a representation of the mass of the system has to be defined. For the cases that are examined in this work the lumped mass matrix method is preferred due to its computational simplicity and the small storage requirements. In this method the diagonal terms of the matrix are given the concentrated or lumped mass that was assigned at every node and more specifically to its associated degree of freedom. All the other off-diagonal terms are zero.

### 3.3.3 Verification and validation

A series of verification and validation studies have been performed at the University of Edinburgh to confirm the capability of OpenSees on modelling the thermal and mechanical response of structures in fire. This section will present the findings on some of the mechanical related verification and validation studies. The full extent of these validation and verification studies is not reproduced here. In addition, Jiang [97] details the thermal related verification and validation studies of OpenSees's developed heat transfer capabilities.

#### 3.3.3.1 Rubert and Schaumann's steel frame tests

This section presents the validation of OpenSees against the experimental tests on steel frames conducted by Rubert and Schaumann [98] in Germany. The same validation exercise as well as other validation and verification studies of the developed OpenSees code, carried out at the University of Edinburgh, can be found in [88, 99] and from other independent researchers in [100].

Rubert and Schaumann present a series of investigations carried out on steel frame assemblies made up from rolled sections (IPE80 I-shaped steel). The experimental setup as well the displacements that were monitored for the braced two-bar frame (EHR3 test) and two-bay portal frame (ZSR1 test) are shown in Figure 3.10 and Figure 3.11 respectively. For the EHR3 frame, all the members were uniformly heated while for the ZSR1 frame only one bay was subjected to a uniform temperature rise. For the computational model in OpenSees, a bilinear material representation was considered (**Steel01Thermal**) with the yield stresses and modulus of elasticity being 382MPa and 210000MPa at ambient temperature for EHR3 frame and 355MPa and 210000MPa for ZSR1 frame respectively.

The comparison between the experimental displacements and the numerical results from OpenSees is shown in Figure 3.12 and Figure 3.13 for the EHR3 and ZSR1 tests respectively. It can be seen that there is good agreement between the displacements from the experiments and those predicted by OpenSees. There are some differences which could be attributed to the modelling assumptions used.

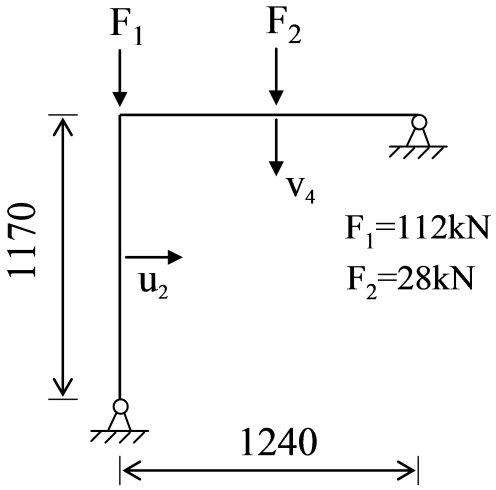


**Figure 3.10:** Experimental setup for EHR3 frame test

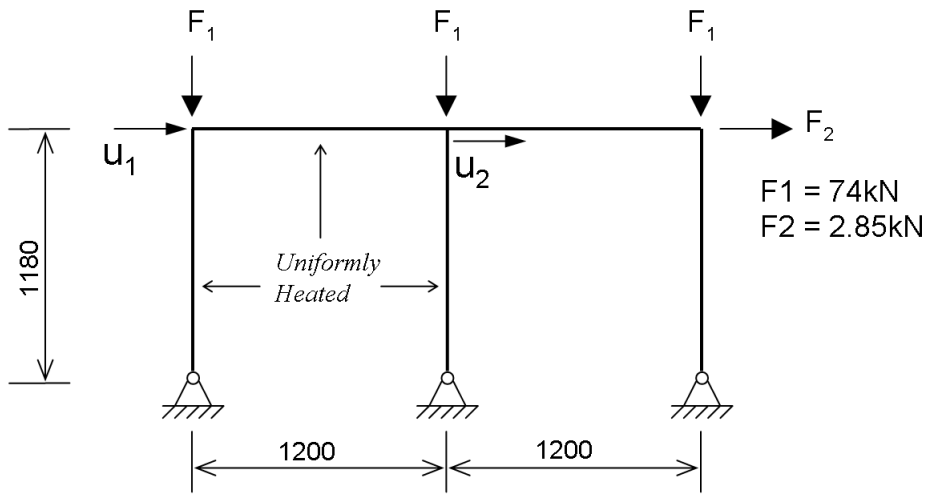


**Figure 3.11:** Experimental setup for ZSR1 frame test

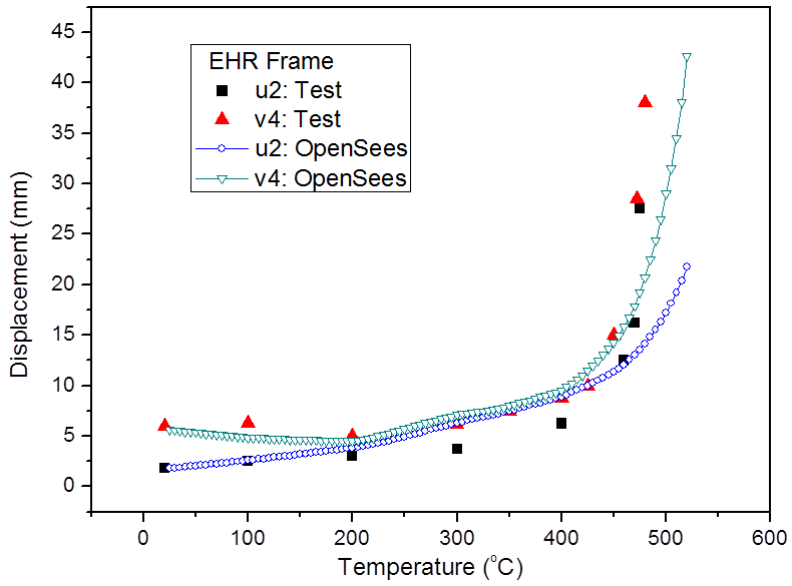


**Figure 3.12:** Comparison between OpenSees and experimental results for EHR3 frame test

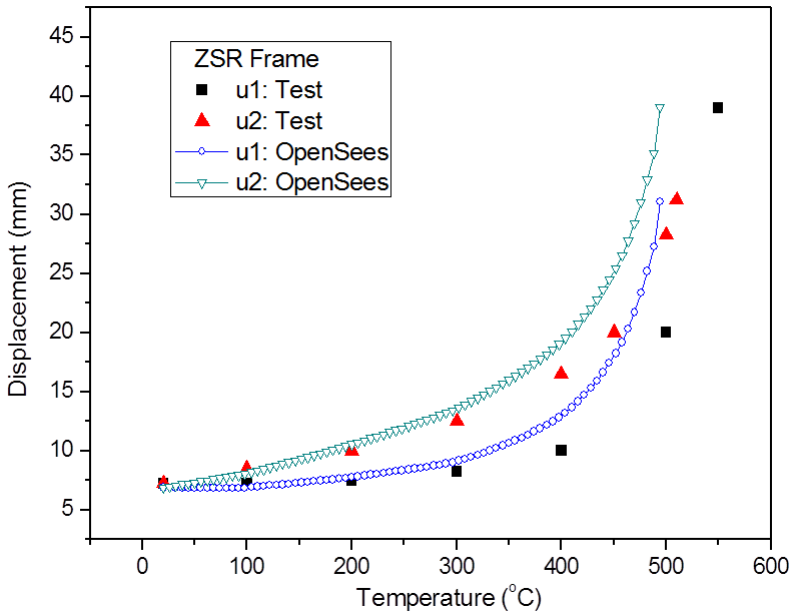


**Figure 3.13:** Comparison between OpenSees and experimental results for ZSR1 frame test

#### 3.3.3.2 Beam subjected to uniform temperature rise

The verification of OpenSees thermal capabilities against a commercial software (such as LS-DYNA [101] ) is examined in this section.

In LS-DYNA the Hughes-Liu beam element formulation can only be used for fire purposes. This element uses a single integration point along the element length for monitoring plasticity. For the steel section an MAT_STEEL_EC3 material can be adopted which represents a elliptic relationship and is compared against the bi-linear **Steel01Thermal** and elliptic Giuffre-Menegotto-Pinto **Steel02Thermal** materials in OpenSees. It should be noted, that unlike **Steel01Thermal** and **Steel02Thermal** materials in OpenSees that adopt only the yield and strain reduction factors according to EC3, MAT_STEEL_EC3 material in LS-DYNA

follows the exact stress-strain relationship provided in Eurocode 3 and hence the radius of the elliptic stress-strain curve varies with temperature.

*Simply supported beam*

This benchmark examines a simply supported beam subjected to uniform temperature rise of 700 ℃. The aim of this benchmark is to examine whether OpenSees can capture thermally induced expansion of structural members when heated. The beam section dimensions used in Chapter 6 are also used here. Figure 3.15 shows that there is an excellent agreement between the different materials in OpenSees and LS-DYNA.

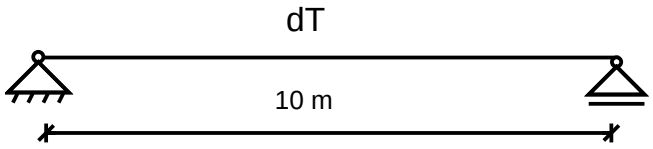


**Figure 3.14:** Simply supported beam

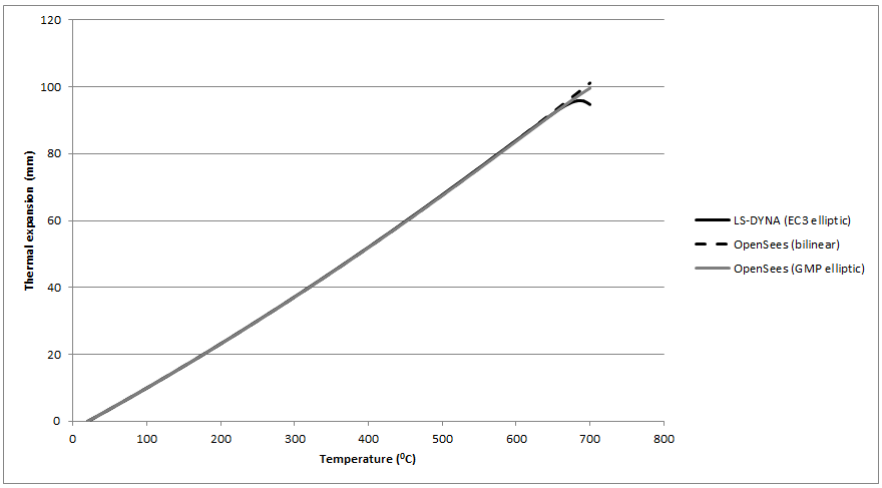


**Figure 3.15:** Horizontal displacement for the simply supported beam

*Pinned beam*

A comparison between the numerical prediction of OpenSees and a commercial software (LS-DYNA) on modelling a pinned beam subjected to a uniform temperature rise of 700 ℃is also presented. This modelling benchmark was selected as it demonstrates that OpenSees is able to capture the thermal stresses and subsequent deformations that are generated by restrained thermal expansion during a fire. Figure 3.17 shows that there is a good agreement between the different materials in OpenSees and LS-DYNA. The slight differences can be attributed to the differences in the stress-strain relationships of the materials. The oscillations that are appearing in the explicit dynamic LS-DYNA model are caused by the application of the gravity loads over a period of one second. Instead an implicit static analysis is used here for OpenSees.

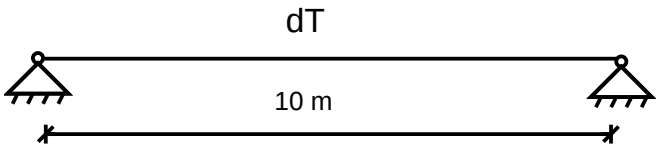


**Figure 3.16:** Pinned beam

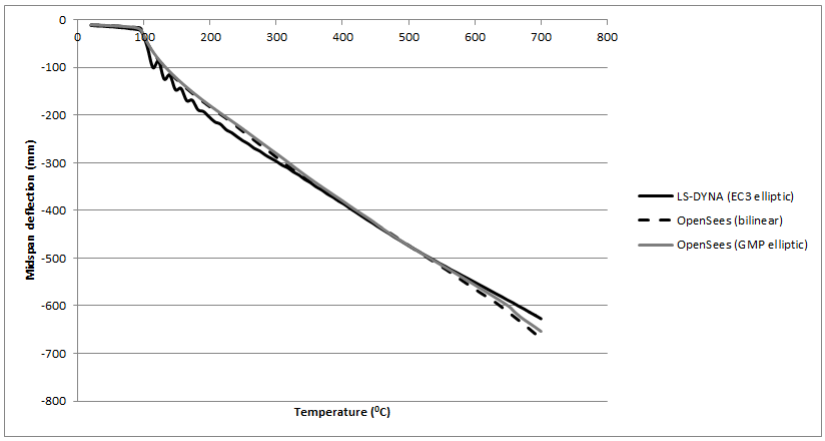


**Figure 3.17:** Midspan deflection for the pinned beam

## 3.4 Conclusion

This chapter presented the object-oriented framework of OpenSees as well as its extension with structural fire capabilities. A list of the classes developed was given and a description of each class followed. More specifically, new element, material, section, pattern and load classes have been introduced. The modelling capabilities were discussed, with an emphasis on OpenSees' beam-column elements, which are its most widely used elements under ambient temperature. The procedures required for modelling structures in fire are also presented with emphasis on dynamic analysis for following the postbuckling or post-peak load response of members. Some verification and validation studies of the developed code are also presented. In the next Chapters the developed code in OpenSees is used for modelling tall buildings under different fire scenarios such as multifloor and travelling fires.

# Chapter 4

# Collapse of tall buildings under multifloor fires

## 4.1 Introduction

The collapse of the World Trade Center buildings in a terrorist attack shocked the world because of the sheer magnitude of life loss and the grave implications of this event on the future of global peace and security. It also shocked structural engineers and architects as these were the first large modern steel frame buildings to collapse where fire could be described as the key contributing factor (impact damage did not cause collapse). Hence questions naturally arose on the stability of tall steel frame buildings in fire which needed to be addressed in order to properly explain and understand the cause of these collapses. These questions have assumed much greater urgency as the collapse of the WTC towers ironically coincided with the beginning of a decade of a tremendous surge in the building

of more and more super-tall buildings around the globe complemented by great innovation in the design of the super tall structures [102]. The engineers and architects seem to have shaken off their initial shock seeking comfort in the implausibility of the recurrence of a similar event and the security measures taken by the aviation industry [103]. The role that the fire had on these events, and thus the potential impact on other super-tall buildings, has thus been relegated to a lower level of importance [102].

Forensic investigation on the collapse of WTC towers was performed by the Federal Emergency Management Agency [104] and subsequently more comprehensively by the National Institute for Standards and Technology [64]. Other smaller scale independent research studies were carried out by Quintiere *et al.* [105], Usmani *et al.* [58], Kodur [106], Usmani [59] and Flint *et al.* [60]. The FEMA report and Quintiere et al studied the large deflections that were developed in the composite floor during the fire but did not present a clearly defined collapse mechanism. Usmani *et al.* and the NIST report identified that the instability that triggered the collapse was not from the aircraft damage or connection failure but from the interactions between the fire and the structure. NIST focused on reproducing the specific sequence of events and attempted to carry out a coupled analysis as far as possible, as advocated recently by Baum [107]. In contrast to this, Usmani et al concentrated on the vulnerabilities of the particular structural form, not including the aircraft damage but concentrating on the fire-structure interactions for a large range of parameterised temperature evolutions, in terms of growth rate, magnitude and spread. In both sets of studies a consistent global collapse mechanism where the perimeter columns were pulled in was found. NIST demonstrated that this sequence of events was in accordance with the photographic evidence.

The effect of perimeter columns in the structural behaviour in fire has been investigated in the past both experimentally and computationally. Ali and O'Connor [108] investigated experimentally the structural fire performance of columns under different rotational constraints. Franssen [92] compared the effect of the interaction of a column as part of a frame and as a single element. He used the arc length procedure in order to follow the postbuckling response of columns in fire. Huang *et al.* [109] examined numerically the internal forces, stresses and strains developed in columns under axial and moment loads and a uniform temperature profile. Results indicated that moments become important when the columns are not rotationally restrained. Shepherd and Burgess [110] also investigated the buckling and postbuckling behaviour of columns in fire including the snap through and snap back phases. They pointed out that robustness is essential in order for load redistribution to take place and for avoiding progressive collapse. Previous research conducted by Quiel and Garlock [111] compared the performance between 2D plane and 3D analysis for high rise buildings under fire. Their results indicated that a 2D plane analysis can adequately predict the interaction between the perimeter column and the floor slab for the specific type of buildings examined.

This study will examine the collapse mechanism of WTC type structural layouts in fire by expanding further the concepts that were presented by Usmani *et al.* [58] based on the same assumptions. The parametric treatment of fire, representing it as predefined temperature vs. time curves, is akin to a design approach and not a forensic treatment. Therefore, this study does not address the time to failure or any pre-existing damage and focuses on understanding the failure mechanism. Hence, the purpose of this study is not to compare against the actual collapse behaviour that these structures experienced which was greatly influenced by the

airplane impact. This allows the study of the particular structural form to be free from forensic aspects [112] and with a defined objective of understanding the behaviour of these structures to derive lessons that will improve future designs. This study will also examine further the two generic collapse mechanisms (the strong floor and the weak floor mechanisms) for tall buildings in the event of fire based on previous work by Usmani *et al.* [61] in order to draw useful lessons from this major structural engineering failure.

## 4.2 WTC Collapse

### 4.2.1 Structural layout

The two towers of the WTC encompassing 110 stories above ground were almost identical. They were built using a unique structural system exploiting the tube concept of Dr Fazlur Khan [113] to resist the immense wind loads on very tall buildings, coupled with an ultra-light truss floor system, all optimised for rapid construction. The details of the structural system including splices and connections and individual member dimensions are available in the publications by FEMA [104] and NIST [64]. The model presented in this chapter has also been used by Usmani *et al.* [58]. A two-dimensional sub-structure representing a 12 storey slice of the tower along the longest span floor area is modelled, assuming the core to be rigid. More specifically floors 90 to 101 are represented in the model which include the floors that were on fire. The typical dimensions of structural members included in the model are shown in Figure 4.1 (FEMA, [104]). As shown in Figure 4.1, the composite truss floor system is assumed to be rigidly restrained

against translation against the rigid core but is free to rotate (thus a pinned connection was used at the right end). The column to floor connection is also a pinned connection, constraining the translation degrees of freedom of the floor nodes to be equal to those of the column nodes but keep rotations independent.

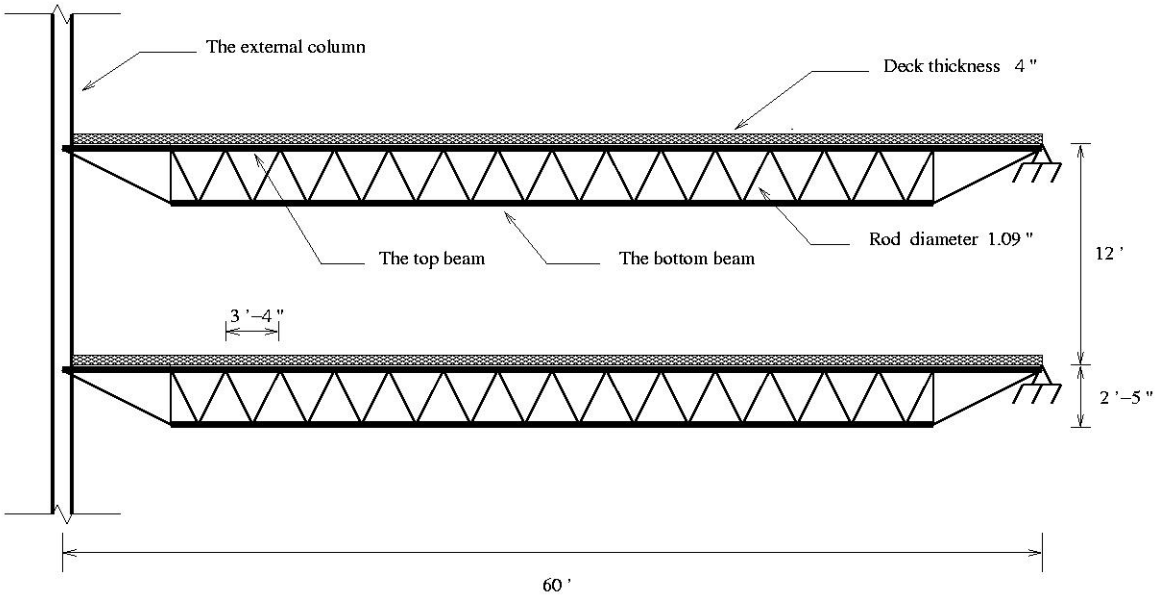


**Figure 4.1:** WTC towers typical structural layout

The actual composite floors had a span of 60ft ( 18.29m) (in the longer span direction) with a concrete deck thickness of 4inches ( 101mm) and a truss depth of 29inches ( 737mm). The truss' top and bottom chords were made from back to back angles of an equivalent area of 1.5 x 1.5 inches ( 38x38mm) and the diagonals had a diameter of 1.09inches ( 28mm). The storey height was 12ft (3.6m) and the columns were 350mm square hollow sections with varying plate thickness along the height of the column, which at the height considered here was 6mm. The truss' diagonals had a spacing of 40inches (1.016m) generally through the span, with the end diagonals being 13.33ft (4.063m) long. The composite floor was modelled using a span of 18m, with diagonals spaced at 1m and the end diagonal

was assumed to be 2m long. The truss was assumed to have a depth of 740mm in the finite element model.

### 4.2.2 Finite element modelling

#### 4.2.2.1 OpenSees

The current finite element model (Figure 4.2) was constructed using the open-source and object-oriented structural engineering software framework OpenSees [77, 66]. OpenSees is effectively a library of advanced computational tools for the nonlinear analysis of structures. The OpenSees framework is being extended at the University of Edinburgh by adding classes that introduce into OpenSees the capability of performing analyses of structures in fire including both heat transfer and thermo-mechanical analysis [88]. This work aims to enable the analyst to perform state of the art nonlinear analysis of structures under different situations (fire or earthquake) or multi-hazard (fire after earthquake) in a single numerical tool. The work so far includes truss and two and three dimensional beam column elements with temperature dependent nonlinear uniaxial materials based on the thermo-mechanical properties for steel and concrete published in the Eurocodes (EN1992 and EN1993).

OpenSees was chosen to carry out these studies so that the results from the newly developed code could be compared to previous research carried out with ABAQUS and hence help validate the code developments. Once all the new developments are validated and tested on a number of different operating systems, they will be offered to be included in a future general release of OpenSees (by PEER and UC

Berkeley) so that any interested engineer or researcher can examine and criticise this work and use the software freely for research purposes.

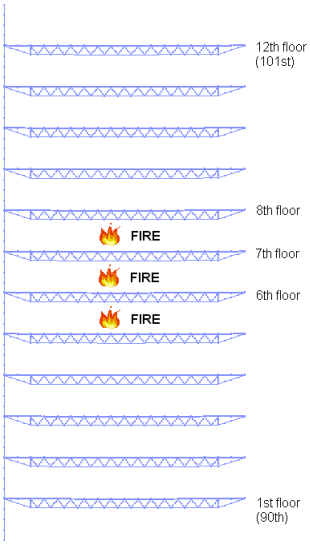


**Figure 4.2:** OpenSees finite element model of the WTC towers

#### 4.2.2.2 Meshing

All the structural members (columns, slab and truss) were modelled using the two-dimensional two-node dispBeamColumn2DThermal elements. These elements are modified versions of the original dispBeamColumn2D elements available in OpenSees that account for fire induced internal forces. DispBeamColumn2D elements are formulated using the finite element method and adopt a distributed (or spread of) plasticity concept which requires the user to select a number of integration points (or control sections) [82, 85, 114]. Five integration points were used for this study. Each control section usually represents a pre determined fiberSection. According to the fiberSection approach a cross-section is discretized (e.g., unilateral discretization, radial discretization) into a number of fibers where each fiber has a prescribed uniaxial stress-strain relationship. The nonlinear

geometry under large displacements (for example, as present in beams during a fire) can be incorporated by using a co-rotational formulation which transforms the coordinates to the global system. A sufficient number of these elements must be used in order to capture the nonlinear behaviour of the members (including p-delta type effects caused by restrained thermal expansion). At least four elements were used for each truss diagonal, bottom chord and top chord based on the sensitivity studies carried out by the author. This allowed the model to adequately capture the buckling of the compression diagonals and other members susceptible to buckling under heating induced restrained thermal expansion.

A uniform load of 5kN/m was applied to the floors. This value corresponds to the permanent and variable loads of the structure and was taken from NIST report [64]. Columns were subjected to a point load of 360kN representing the load transfered from storeys above. This value was calculated taking into account 40% of the load transfered from the uniform load (permanent and variable) acting on the nine floors above this twelve storey model.

#### 4.2.2.3 Composite action

The composite slab is modelled using separate beam-column elements for the top chord and the slab. In order to model the composite action between the concrete slab and the top chord of the steel truss, rigidLink constraints were used for the corresponding translations and rotation of the nodes. rigidLink is a multi freedom constraint which ties the degrees of freedom of a slave node to follow that of a master node. In this model the case of bond slip is not taken into account and the slab is assumed to act in full composite action with the top chord for the whole duration of the analysis. Therefore failure of shear connectors

cannot be modelled [115]. Shear connector failures typically begin at the ends of the composite member and therefore may not have a significant global impact however this issue is not addressed in this work.

#### 4.2.2.4 Materials

Several fire resistance tests [116, 117, 118, 119] of structural members have shown that high temperature causes material degradation so the reduction of material properties like Young's modulus and Yield Stress have to be accounted for by utilizing appropriate constitutive relationships. Hence, new uniaxial elastic plastic material models have been developed by modifying appropriately the existing ones under the OpenSees framework that take into account the material degradation under elevated temperatures, the steel bilinear material model (**Steel01Thermal**), the steel elliptic material model (**Steel02Thermal**), and concrete material model (**Concrete02Thermal**). The material properties are not exactly known and varied along the height of the structure so typical properties were used. For the steel members (column, truss members) a yield strength of $300N/mm^2$ and modulus of elasticity of $210GPa$ were assumed. The concrete slab was assumed to have a compressive strength of $30N/mm^2$ and a tensile strength of 5% of its compressive strength. The steel reinforcement was assumed to have yield strength of $475N/mm^2$.

#### 4.2.2.5 Numerical algorithm

Quasi-static integration methods like load control have significant limitations in dealing with local or global instabilities that commonly occur in modelling

structures subjected to fire (because of the stresses generated by restraining thermal deformations). For this reason an implicit dynamic procedure has been used in this work to trace post-buckling response of members and overcome instability points. The numerical scheme selected for the dynamic analysis is an implicit solution with a Hilber-Hughes-Taylor integrator with alpha=0.7 to add numerical damping to the model [96].

### 4.2.3 Fire modelling

Due to the aircraft impact on the structure and the fuel that caused ignition on the furniture, it can be assumed that multiple floor fires were developed at the same time in the tower [106]. For this work the fire is assumed to be simultaneous and on floors 5, 6 and 7 of the finite element model. A generalised exponential curve [58] is chosen to represent the time-temperature relationship and is given by Eq. 4.1

$$T(t) = T_0 + (T_{max} - T_0)(1 - e^{-at}) \tag{4.1}$$

Where $T_{max}$ is the maximum temperature (800 ℃in this study), $T_0$ is the ambient temperature (20 ℃), $a$ is a rate of heating parameter (0.005) and $t$ is the time (3600s). This fire curve is very general and it is not argued that it represents the fire that was seen in the case of the WTC towers; nevertheless, the range of temperatures covered is consistent with the fire modelling conducted by NIST [64]. As this paper is examining the collapse mechanism and not trying to reproduce the failure time, a parametric approach to the fire is reasonable. Since the fire

occurs on floors 5 to 7 (corresponding to floors 94 to 96 of the towers), the members affected are the composite trusses on floors 6 to 8 and the columns supporting them. Steel sections are assumed to be heated uniformly in contrast to concrete sections where thermal gradients appear. The columns are assumed to be protected and hence heated to a maximum temperature of 400 ℃while the steel truss is assumed to be unprotected and at the same temperature with the fire, being heated to a maximum temperature of 800 ℃. For the temperature distribution in the concrete slab, a 1D heat transfer analysis was performed. These time temperature curves can be seen in Figure 4.3 based on the relationship provided in Equation 4.1.

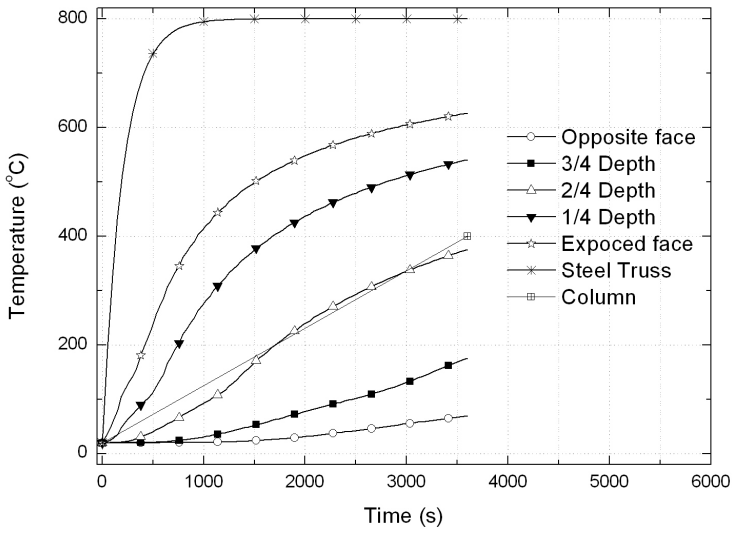


**Figure 4.3:** Temperature distribution in structural members

Due to the fact that the interface between the thermo-mechanical analysis part of OpenSees and the heat transfer part is still under development, the temperature evolution in the structural members from the fire was not assigned automatically.

### 4.2.4 Results

#### 4.2.4.1 Global response

The global behaviour of the structure can be seen from Figure 4.4 showing the deformed shape of the model. It can be seen that collapse occurs with the columns being pulled inside because of the large deflections in the floor. The horizontal displacement of the columns of the fire-affected floors is plotted in Figure 4.5. At an early stage of the fire the composite floors expand and the column is pushed outward by approximately 50 mm at about 150 seconds which corresponds to a fire temperature of 430 ℃. After this point the column is suddenly pulled in but stabilises and continues to displace inwards until the structure becomes irreversibly unstable at 250 seconds (fire temperature of 580 ℃). It is also of interest to note that when collapse occurs the column is almost at ambient temperature. Figure 4.6 illustrates the vertical displacement of the columns for floors 5 to 9 also showing collapse at 250 seconds. It should be noted that at that time (250 seconds), the column is still under almost ambient conditions (assumed to be protected), which exlains why there is no upward movement (due to thermal expansion) of the column.

Horizontal reactions at the floor connection to the stiff core show the change in membrane forces over temperature. Figure 4.7 illustrates that the middle fire floor is in tension initially but snaps into compression before failure occurs and then goes into tension again at the initiation of collapse. The top and bottom fire floors along with floors 4 and 10 experience compression until initiation of failure when they snap into tension. In contrast floors 5 and 9 are in tension and snap into compression at this point.

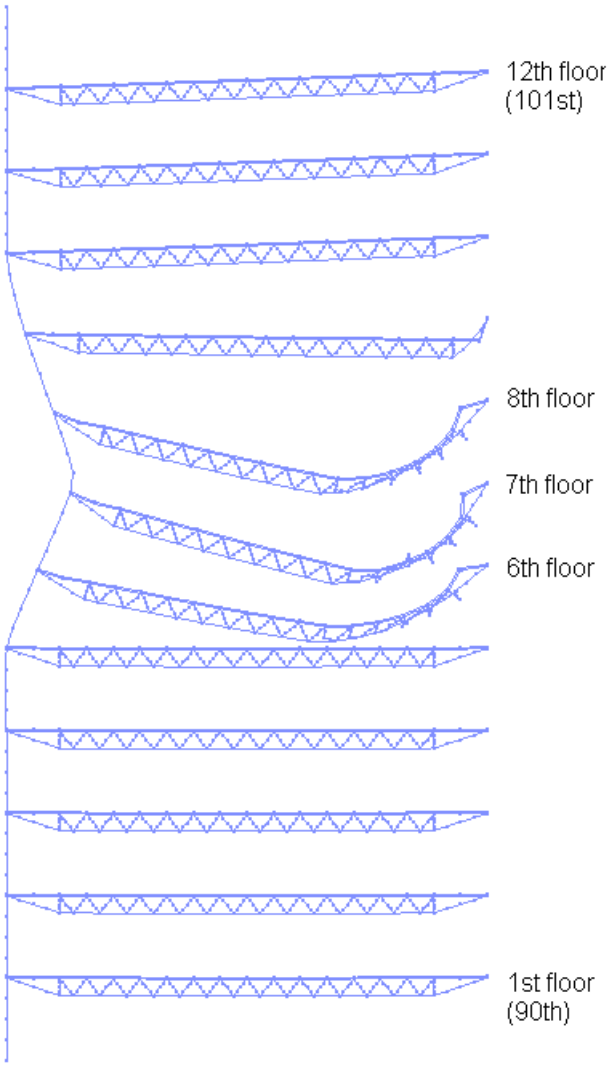


**Figure 4.4:** Deformed shape of the WTC Tower model

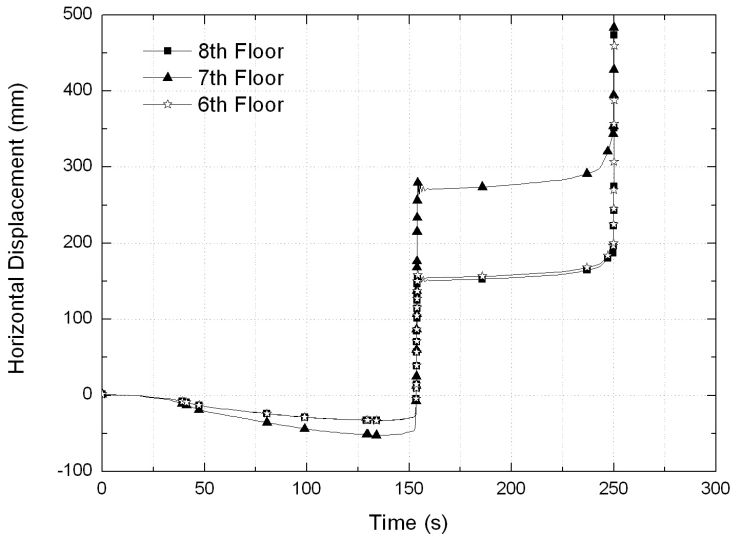


**Figure 4.5:** Horizontal displacement of floor-column joint nodes

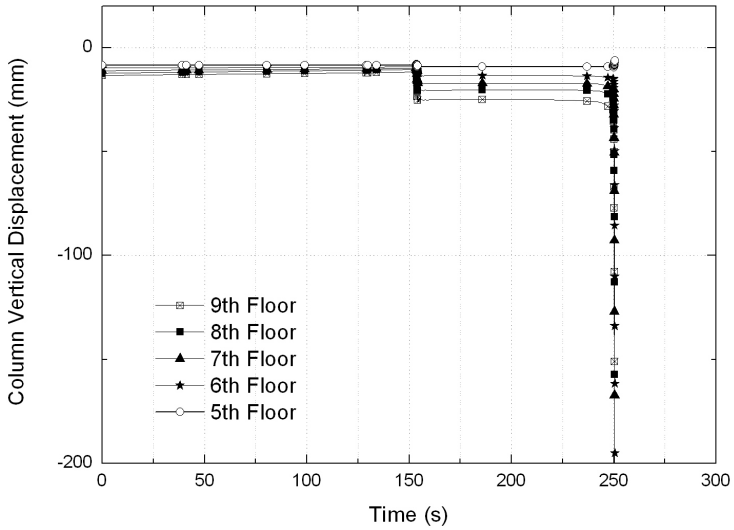


**Figure 4.6:** Vertical displacement of floor-column joint nodes

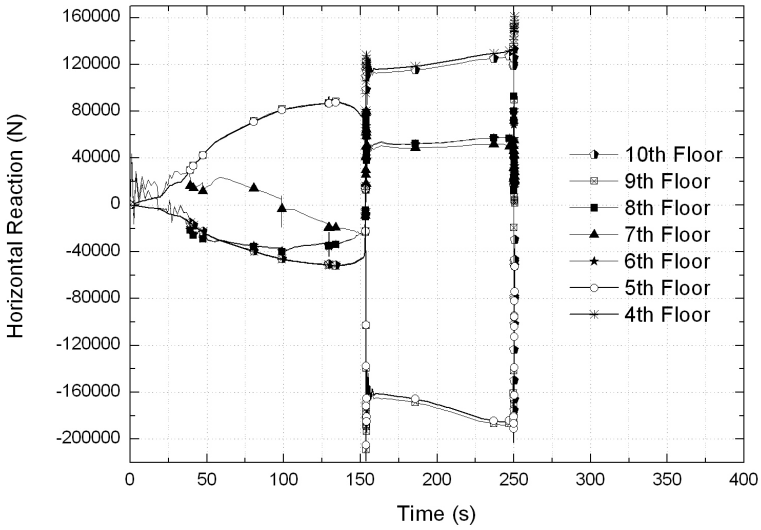


**Figure 4.7:** Membrane forces in the floors

Figure 4.8 plots the section moments in the column at the floor-column joint node. It can be seen that at around 150 seconds, the section plastic moment capacity is reached which initiates strong floor collapse. Figure 4.9 shows the column plastic rotation for floors 5, 7 and 9. The calculation of plastic rotation in OpenSees is performed by deducting the yield or recoverable rotation from the maximum absolute total rotation. This graph clearly shows that a plastic hinge mechanism has been formed.

#### 4.2.4.2 Truss response

In Figure 4.10 the plot of midspan deflection of the floors versus time is shown indicating the same pattern of behaviour as in the previous two figures. The large displacements, internal forces and material degradation cause the truss diagonals to buckle, particularly members located near the support to the stiff core. These

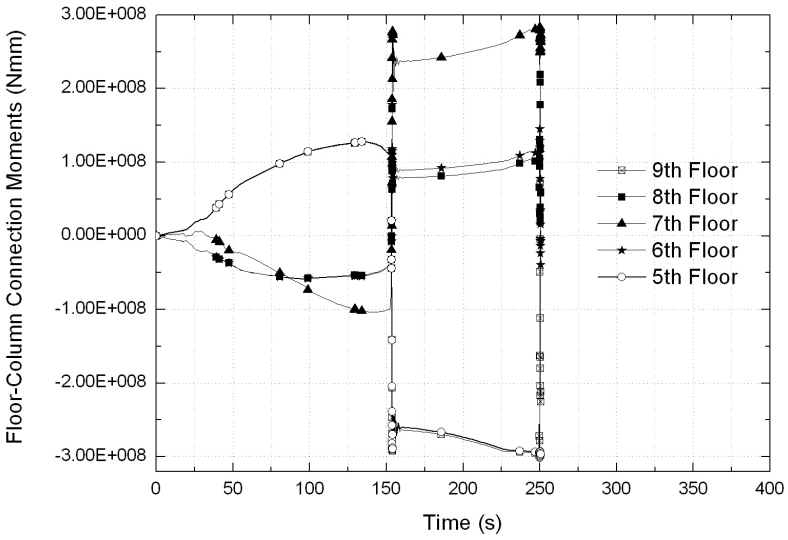


**Figure 4.8:** Column section moments at floor-column joint nodes

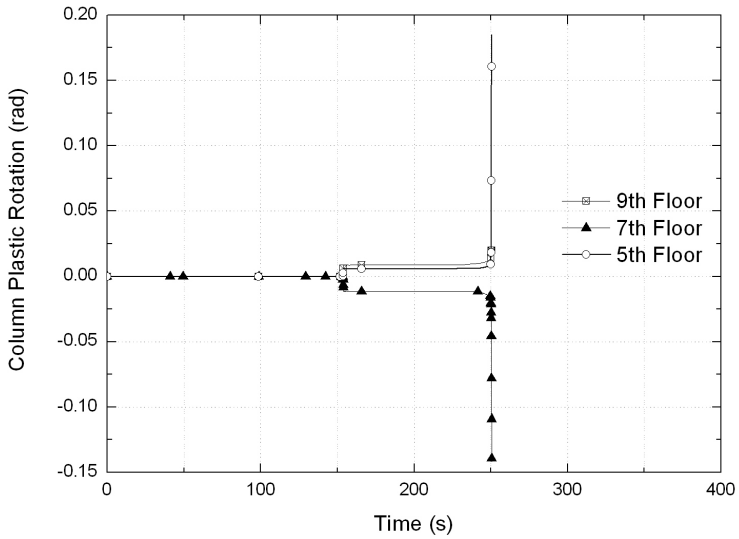


**Figure 4.9:** Column plastic rotations at floor-column joint nodes

members experience relatively larger forces arising from the restrained thermal expansion of the floor.

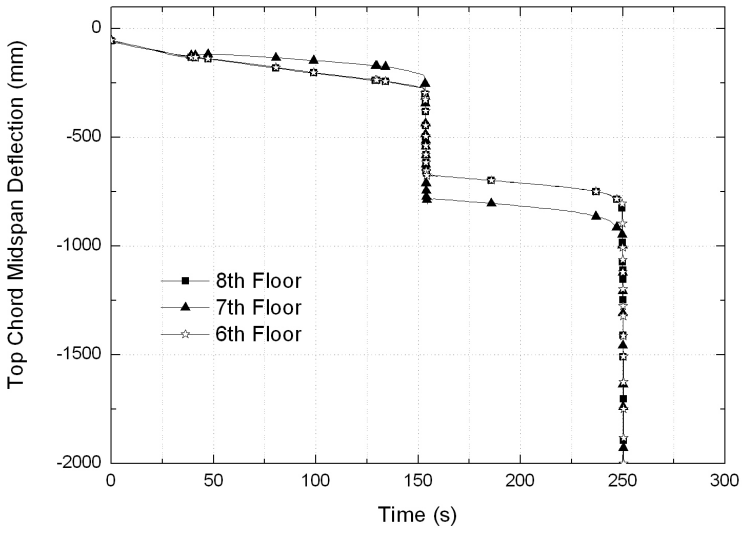


**Figure 4.10:** Midspan deflection of the floors

The axial forces in some critical members of the top chord at the 7th floor are shown in Figure 4.11 where members are numbered from the left to the right (so member 2 is near the column and member 15 is near the rigid core) as shown in Figure 4.1. The top chord is in compression as the temperature increases until the first instability at 150s and remains in compression for most its length during collapse. In contrast Figure 4.12 indicates that all the bottom chord members (numbered from left to right) were in tension for the whole duration of the fire until collapse but initiation and ultimate collapse are still indicated by sudden changes in magnitude. Figure 4.13 also displays axial forces in the inner truss diagonals (numbered from left to right) including the right end inclined and vertical members for the 7th floor of the model. The highest loaded compression diagonals are as expected the outer most compression diagonals (2nd and the

27th). As in the other figures the initiation and ultimate collapse are reflected in internal load redistributions in Figure 4.13 as well.

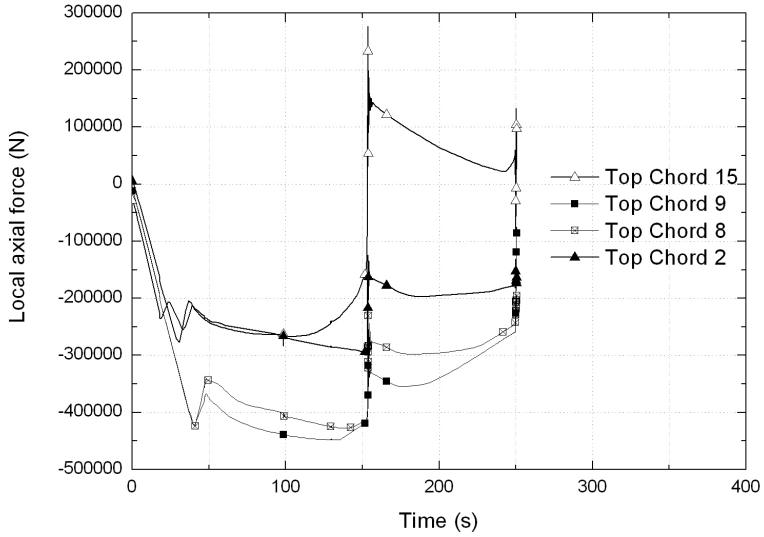


**Figure 4.11:** Top Chord axial forces for the 7th floor

## 4.3 Weak and strong floor collapse mechanisms

Previous research by Usmani *et al.* [61] has investigated the behaviour of tall buildings in fire with similar structural form to the WTC towers but with more generic sections for columns and beams instead of tubular columns and trusses. Their research has shown that the same collapse mechanisms are possible. Furthermore, two distinctive collapse mechanisms can be identified, namely the "weak floor" and "strong floor" mechanisms. The analysis presented here will reproduce these mechanisms and establish criteria that lead to one or the other based on a parametric study. For the analyses performed in this work the building will be assumed to have a fixed beam-column connection at the column end.

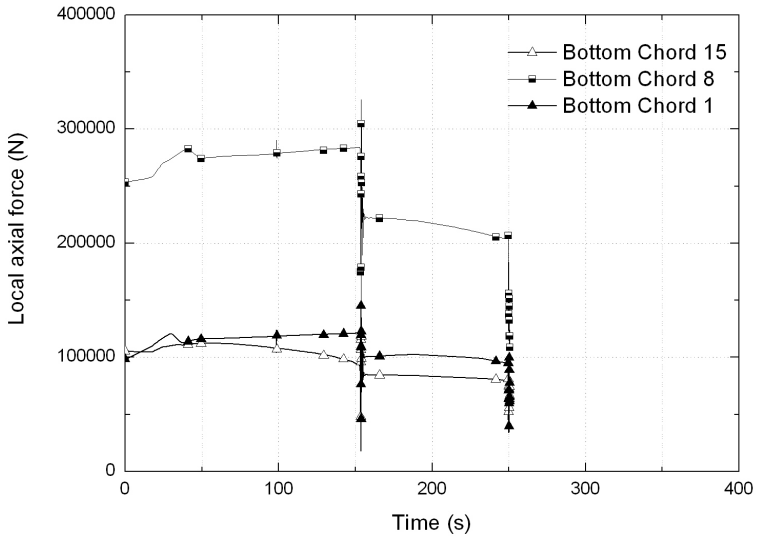


**Figure 4.12:** Bottom Chord axial forces for the 7th floor

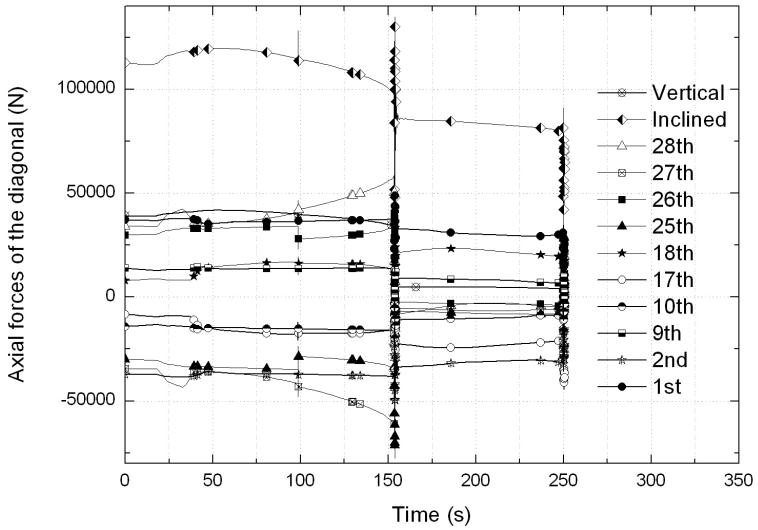


**Figure 4.13:** Axial forces in the diagonals for the 7th floor

This assumption, unlike in the WTC Towers shown previously, implies that both translation are rotation of the beam and column nodes are constrained to be the same. But as for the WTC Towers model the possibility of connection failure is not taken into account. At the rigid core end the steel beam and the slab (forming the composite floor) are both pinned to a rigid lateral restraint. This connection also simulates a fixed-end connection for the composite floor.

The structural model used is similar to the one used earlier except for universal beam and concrete slab composite floors and universal columns (instead of tubular columns and composite truss floors).

Previous research identified the two distinctive mechanisms but clear criteria governing the collapse mechanism type were not established. These criteria are based on the behaviour of the "bottom pivot" floor (the floor immediately below the lowest fire floor), which in this paper is the 5th floor. If the bottom pivot floor reaches its plastic moment capacity at midspan (from P-delta moments induced because of having to provide a reaction to the "pull in" forces at the fire floors, see Figure 4.14(a)), a hinge is formed (see Figure 4.14(a)) in the floor and the weak floor mechanism is initiated. The bending failure spreads to the lower adjacent floor and then further downwards (with potentially a similar failure spreading upwards from the top pivot floor) leading to a progressive disproportionate collapse of the structure. If the bottom pivot floor is able to sustain the increasing bending moments, the column connecting the pivot floor may reach its plastic moment capacity first (as indicated by the hinge shown in Figure 4.14(b)) at a section near the floor-column connection which then initiates the strong floor failure. A three hinge mechanism forms with two further hinges in upper floors. The key distinction between the two collapse mechanisms is the

initiation. In the weak floor mechanism collapse initiates due to bending failure of the bottom pivot floor itself, while in the strong floor mechanism collapse initiates due to combined compression and bending failure of the column adjacent to the bottom pivot floor. Figure 4.14 shows deformed shapes for weak and strong floor collapse under a three floor fire scenario (fire affected floors are floors 6 to 8) in a model of a typical tall steel frame composite structure as described above.

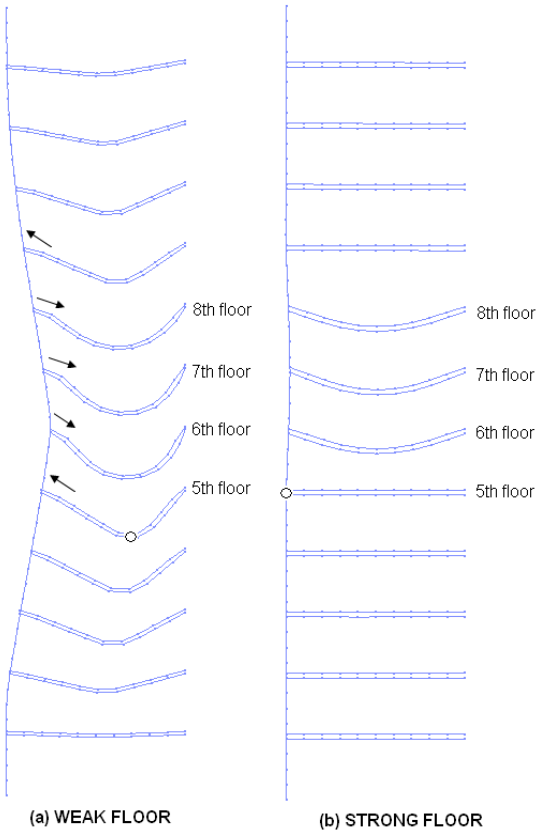


(a) Weak floor (b) Strong floor

**Figure 4.14:** Through-depth temperature profile for the slab at different locations

### 4.3.1 Strong floor collapse

Figure 4.15 shows the horizontal displacements of the column at the level of the fire floors (with negative direction denoting outward movement and positive denoting inward movement). Figure 4.16 shows the midspan deflections at the fire floors and Figure 4.17 the horizontal reaction force at the rigid end restraints at the right. These reactions represent the membrane forces in the floors. It can be seen that initially the bottom and top fire floors are in compression (negative sign) and then snap into tension (positive sign) when failure initiates. On the other hand, the pivot floors, 5 and 9 are in tension and when failure begins they snap into compression. Floor 7 is in tension when the floors are expanding but then goes into compression when the pull in process starts and finally goes into tension again when failure occurs.

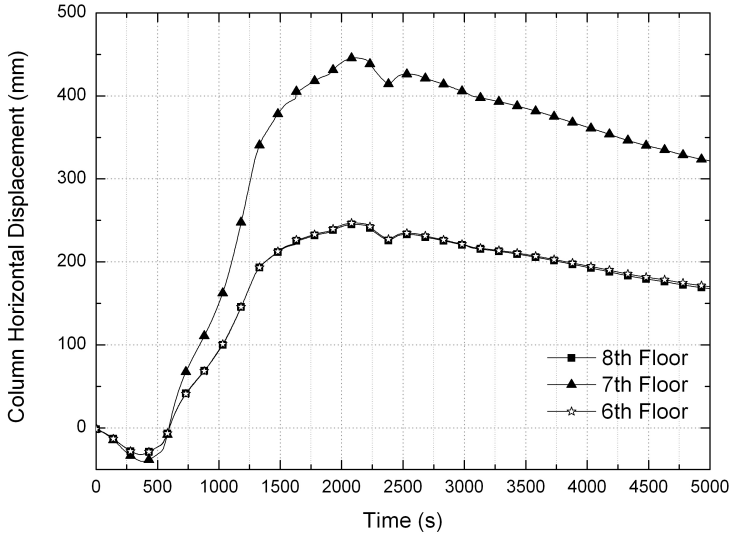


**Figure 4.15:** Column horizontal displacement for strong floor collapse

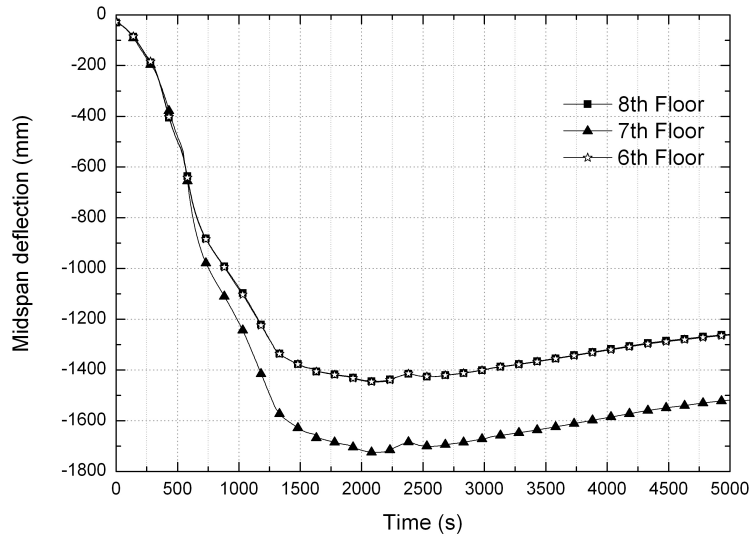


**Figure 4.16:** Midspan deflection for strong floor collapse

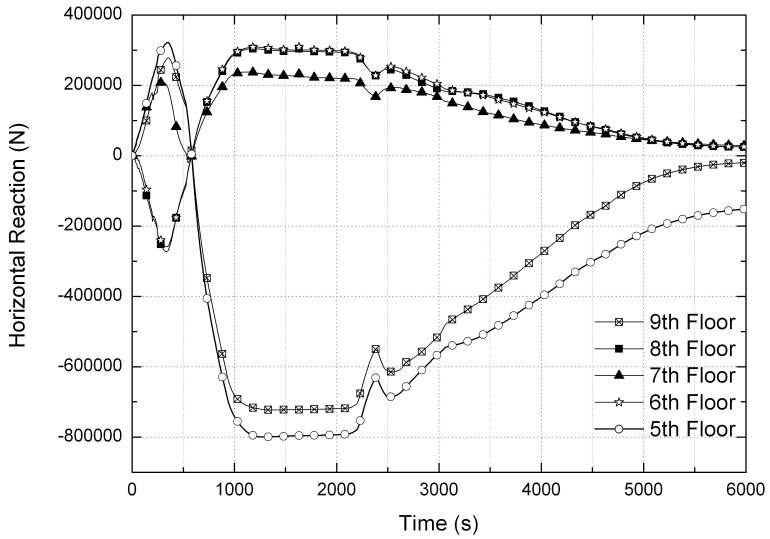


**Figure 4.17:** Membrane forces for strong floor collapse

### 4.3.2 Weak floor collapse

Weak floor collapse, if possible, will occur at an earlier time for the same column than the strong floor collapse. This is initiated at the bottom pivot floor if it cannot sustain the additional moment demand from the $P - \delta$ moments induced by the "pull in" forces at the fire floors. Furthermore, weak floors expand much less than strong floors before the "pull in" phase starts (as shown in Figure 4.18.

Figure 4.19 clearly shows that the bottom and top pivot floors suddenly experience significant deflections after the fire floor deflections reach between 700 to 800 mm, which is indicative of bending failure in the pivot floors. It can be seen in Figure 4.19 that the 5th floor (or the bottom pivot floor) of the structure also deflects when the collapse occurs. This indicates bending failure of the bottom pivot floor which does not occur in strong floor collapse and hence is a main distinguishing characteristic of weak floor collapse. Figure 4.20 shows the variation of membrane forces at the connection of the floors to the stiff core. Here the behaviour is similar to the strong floor mechanism. It can be seen that initially floors 6 and 8 are in compression and later snap into tension while floors 5, 7 and 9 are initially in tension and then snap into compression.

## 4.4 Parametric study of the effect of bending stiffness on collapse type

The analyses performed previously have identified that both types of collapse mechanisms are in bending, either in the floors or in the column. It could therefore

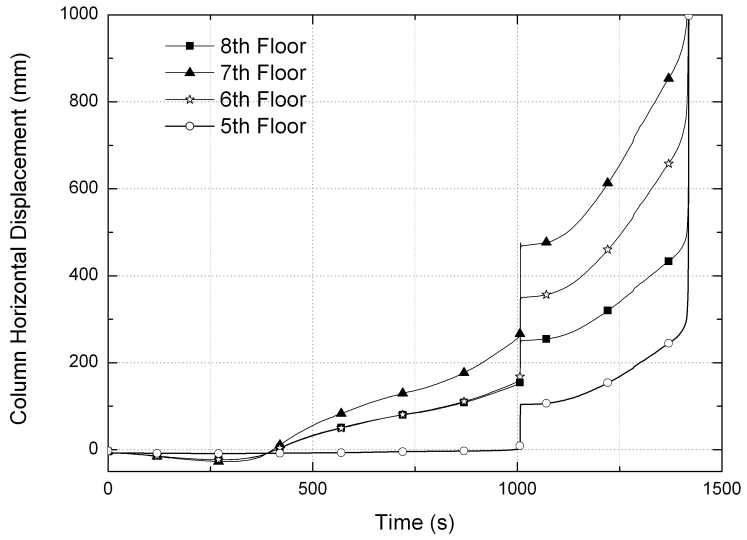


**Figure 4.18:** Column horizontal displacement for weak floor collapse

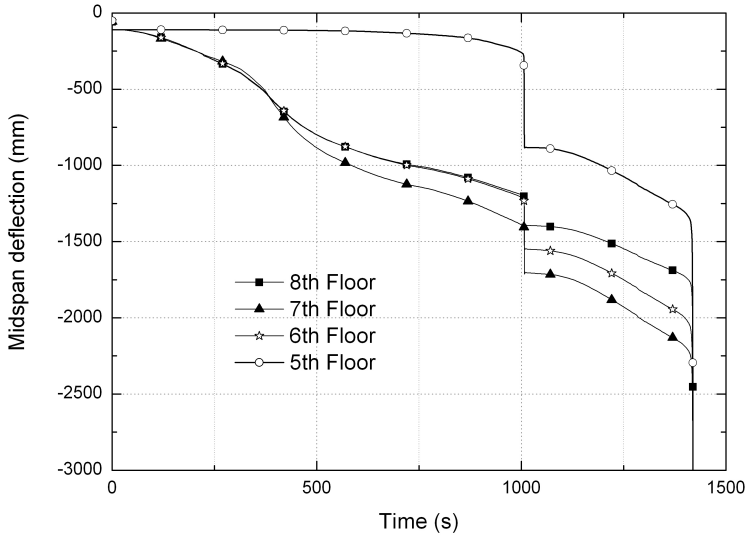


**Figure 4.19:** Midspan deflection for weak floor collapse

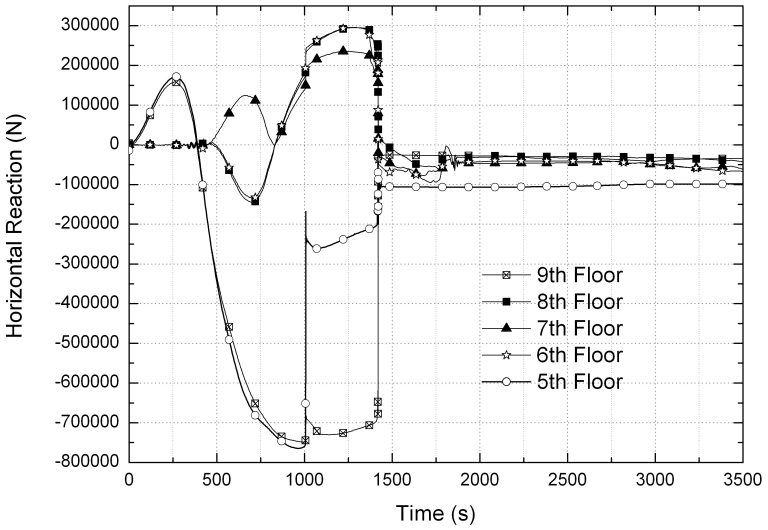


**Figure 4.20:** Membrane forces for weak floor collapse

be illuminating to examine the effect of different floor and column bending stiffness combinations. It is also clear that the number of floors on fire will also be a significant factor in what type of failure mechanism occurs. When a greater number of floors are subjected to fire, the bottom pivot floor will need to carry greater moments because of the larger forces required to anchor the sagging fire floors in tensile membrane action.

In order to investigate the effect of the ratio of bending stiffness between the column and floors, a number of analyses were performed keeping constant the height of the column (4m), the length of the floor (10m) and the concrete slab depth (100mm) and its width (6m) but varying the steel sections.

The ratio is defined as seen in Eq. 4.2 ,

$$\frac{S_{column}}{S_{floor}} = \frac{E_c I_c / L_c}{E_f I_f / L_f} \tag{4.2}$$

These quantities are calculated using the transformed area method for the floors as they are composite members. A wide range of different scenarios were considered for this paper. An indicative illustration is shown in Table 4.1

| UC/UB | 533x210x92 | 406x178x74 | 356x171x51 | 305x165x46 | 305x127x37 |
|---|---|---|---|---|---|
| 3 Floor Fire | | | | | |
| 356x406x235 | Strong floor | Strong floor | Strong floor | Strong floor | Weak floor |
| 356x368x153 | Strong floor | Strong floor | Strong floor | Strong floor | Weak floor |
| 305x305x158 | Strong floor | Strong floor | Strong floor | Strong floor | Weak floor |
| 4 Floor Fire | | | | | |
| 356x406x235 | Strong floor | Strong floor | Strong floor | Weak floor | Weak floor |
| 356x368x153 | Strong floor | Strong floor | Strong floor | Weak floor | Weak floor |
| 305x305x158 | Strong floor | Strong floor | Strong floor | Weak floor | Weak floor |
| 5 Floor Fire | | | | | |
| 356x406x235 | Strong floor | Strong floor | Weak floor | Weak floor | Weak floor |
| 356x368x153 | Strong floor | Strong floor | Strong floor | Weak floor | Weak floor |
| 305x305x158 | Strong floor | Strong floor | Strong floor | Weak floor | Weak floor |

**Table 4.1:** Collapse types for different scenarios

The analyses performed revealed that the collapse mechanism type depended on the bending stiffness ratio and the number of floors subjected to fire, as illustrated in Figure 4.21. The hatched area in the Figure shows a fuzzy region where either type of failure can occur. This sort of a diagram would allow a very quick check to determine what sort of failure could be expected for a particular building under

multiple floor fires keeping in mind that the possibility of failure of connections or shear connectors is not taken into account. This is useful information in case a weak floor collapse is indicated. Strengthening of the floors and conversion to a strong floor collapse would considerably extend the tenability of the structure and hence the time available for egress and intervention. In earthquake engineering strong columns and weak beams are preferred which seems to contradict the recommendation given here. This however is non-issue, because for strong floor collapse in fire, the higher stiffness of the floor is required at midspan (where a hinge should be avoided). In earthquake engineering the relevant floor stiffness relative to the column is that at the ends where a hinge may be allowed to be formed instead of in the column to ensure ductile behaviour.

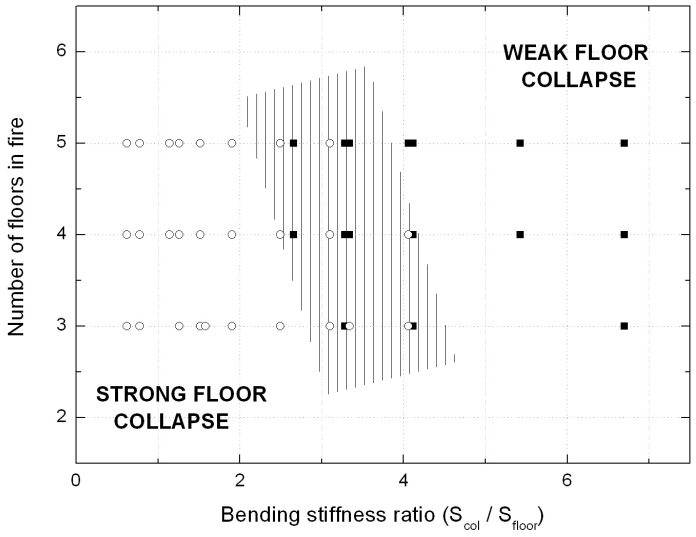


**Figure 4.21:** Collapse type envelope for different ratios

The results of the parametric studies performed in this chapter illustrate that the most probable type of failure is the strong floor collapse. The weak floor collapse has been seen to occur under certain cases too. For the three and four

floors fire scenarios the weak floor failure occurred for beams that were outside the serviceability limit state criterion of composite slabs as given by Eurocode 4 ($span/300$), but for the five floor scenario the serviceability limit state was satisfied. However, it should be noted that for the three and four fire floor scenarios, the possibility of weak floor collapse should be checked as variable bending stiffness or length along the floors or imperfections could produce different results. More research is required to investigate these mechanisms on other structural forms especially very long span floors made using trusses or cellular beams.

## 4.5 Collapse mechanisms under vertically travelling fires

### 4.5.1 Introduction

The collapses of the WTC complex buildings in 9/11 as well as other partial collapses like the ones of the Windsor Tower in Madrid and of the Technical University of Delft building posed new questions on the stability of tall buildings in fire. These accidents have shown that local or global collapse is possible in multifloor fires. Tall building collapse under multifloor fires has thus attracted the interest of researchers at the University of Edinburgh for more than a decade [58, 59, 61, 60, 89] since this is not an unusual scenario despite being usually ignored in practice. However first example of such a scenario in UK was introduced recently in the 200m high Heron Tower in London by ARUP's fire consultants considering the case of a simultaneous three floor fire [120]. Other researchers

have also examined the collapse of structures in case of other type of fires such as localised ones. Recently, Fang *et al.* [121] proposed a robustness assessment design framework that was involving a temperature-dependent approach (TDA) and a temperature-independent approach (TIA) for composite structures subjected to localised fires. Sun *et al.* [122] recently also presented a procedure that has been implemented into the VULCAN software in order to perform progressive collapse analysis of steel structures in fire.

In most of the previous work all floors were assumed to be heated simultaneously although in reality fires travel from one floor to another. Previous research considering vertical travelling fires is very limited. Recently, Roben *et al.* [123] examined the behaviour of structures during a vertically travelling fire scenario, however their member selection was based on the assumption that a global collapse will not occur and all the members will cool down to ambient. Their research indicated that possible connection failure may take place because of cyclic column movements. As the phenomenon of vertical fire spread in high-rise buildings is complex and out of the scope of this work, a simple time delay is used to simulate the beginning of heating on each successive floor. It is expected that this approach will be adequate to study the key structural effects of vertically travelling fires. The mechanisms of fire spread from one floor to another are however discussed and a range of time delays are considered for the parametric studies.

### 4.5.2 Fire and heat transfer modelling

Multifloor floor fires in high-rise buildings can be associated with a variety of factors. Generally speaking, there are three possible mechanisms that enable fire

to travel from one floor to an adjacent floor [124]. It can travel upwards by compromising the perimeter fire barrier materials between the floor slab and curtains walls, or by igniting the interior vertical ductwork through floors. Secondly, external burning, which is associated with most fully developed compartment fires, could ignite combustibles in the upper floors by radiation heat transfer through glazing or by direct flame impingement through other openings. Finally, external flaming could also ignite external insulation material which could then involve many floors on fire even more rapidly, as witnessed in the 28 storey high building in Shanghai. Modelling the actual process of vertical fire spread can be complicated by a number of factors, such as the geometry of the facade, the shape of the opening [4] , the fire resistance of the glazing, the ambient atmosphere and the type of occupancy. However, the problem can be simplified for structural fire analysis by recognizing that post-flashover fires can develop at different time intervals for different floors. Therefore, a simple yet important parameter, time delay ($\Delta t_{delay}$), has been introduced to study the structural performances in vertical travelling fires [61]. In this work, it is assumed that the fire travels upward progressively from one floor to the other, with vertical projection of the external flame not exceeding the most adjacent upper floor. The fire load and ventilation condition for each of the floors are identical. A constant time delay $\Delta t_{delay}$ is assigned to each floor once post-flashover fire has developed in its adjacent downward floor, with

$$\Delta t_{delay} = \Delta t_{Ignition} + \Delta t_{pre-flashover} \tag{4.3}$$

where $\Delta t_{Ignition}$ is the time interval between the time of flashover in the floor

below and $\Delta t_{pre-flashover}$ the time of ignition at the current floor and is the time taken from ignition to flashover at the current floor.

The time sequence of fire development at different floors is indicated in Figure 4.22. It is assumed that the post-flashover fire starts at the initial time $t_0$ at the $i^{th}$ floor. The first component of $\Delta t_{delay}$, $\Delta t_{ignition}$ , is associated with the fire spread from one floor to the other, and can vary greatly with these factors discussed at the beginning of this section. The values of $\Delta t_{ignition}$ are varied from 500 to 900s in the current work. The second component $\Delta t_{pre-flashover}$ is associated with the occurrence of flashover in compartment fires. Flashover can be interpreted as a case of thermal instability within the fire compartment which is dependant on the ventilation conditions and the thermal properties of the compartment boundaries [4]. It was however suggested that it is difficult to predict the time to flashover due to the dependency on random variations of some factors during the very early stage of compartment fires [4]. Reported values of time to flashover ($\Delta t_{pre-flashover}$) vary from 100 to 1600s [4, 125]. Therefore, $\Delta t_{delay}$ is selected here in the range of 600 to 2500s for the purpose of parametric studies. Shorter time delays correspond to faster travelling fires while longer ones for slower travelling fires.

The post-flashover fires for each floor are represented by parametric fires as given in EC1 [11]. The fire load density is 420.0 MJ/m$^2$ for typical office buildings according to [40]. The compartment has a floor area of 240 m$^2$ and an opening factor of 0.07. The lining material is assumed to be light weight concrete, corresponding to the thermal inertia of 1159 J/m$^2$s$^{0.5}$K. It is also assumed that the fire growth rate is medium which gives the shortest possible duration of

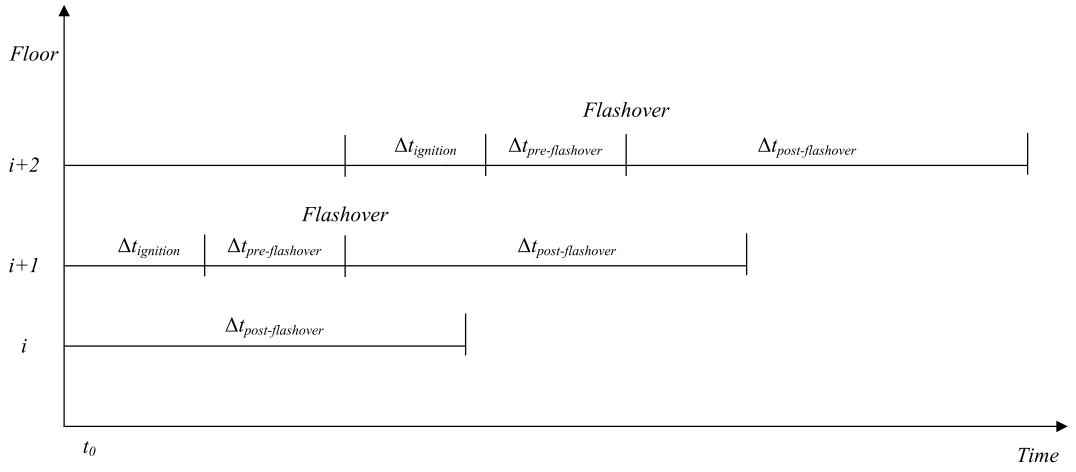


**Figure 4.22:** Time sequence of the development of fires on multi-floors

heating phase $t_{lim} = 20$ min according to EC1 [11]. By applying these values, the temperature-time curve is obtained as shown in Figure 4.23.

In the current work, the steel beams are unprotected contrary to columns. This is a conservative assumption but akin to a worst case design approach or deliberate omission of beam fire protection as part of a performance-based engineering approach [126]. This could also imply possible previous damage that occurred during an explosion or earthquake, that are usual phenomena preceding a fire, or that the structure is still under construction. Two dimensional heat transfer analyses are performed for the composite sections using the fire imposed boundary conditions specified earlier. The recently developed fire and heat transfer modules in OpenSees are used for the temperature predictions [88]. The temperature-dependent thermal properties of the concrete (with moisture content of 1.5%) and the slab are specified according to [40]. The top surface of the concrete slab is assumed to be exposed to ambient at 20 degrees. The convection coefficient and the emissivity are 25 kW/m$^2$ and 0.7 respectively. A contour plot of temperature

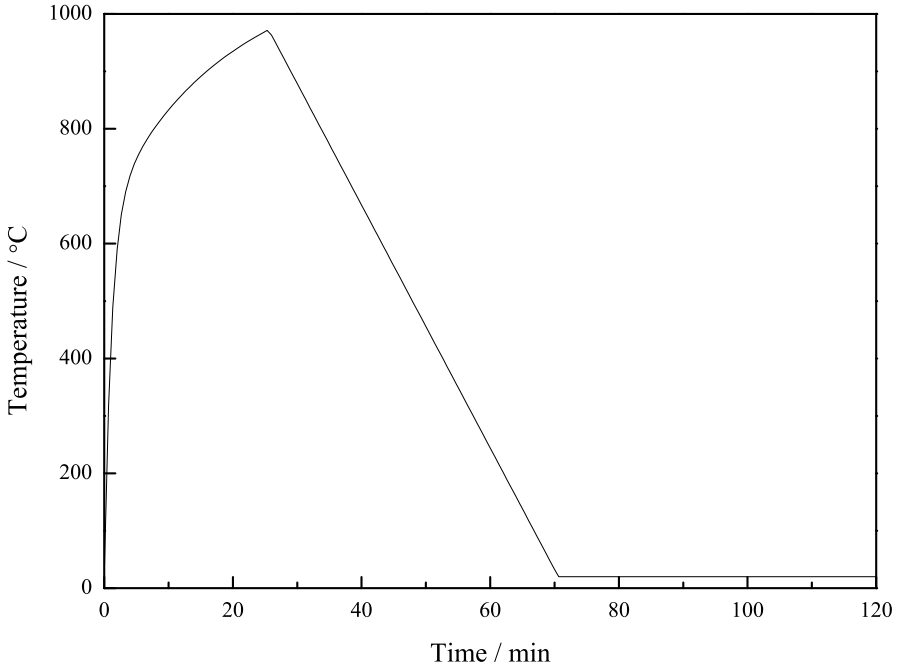


**Figure 4.23:** Temperatures for the parametric fire

distribution at 1000s in the composite section is shown in Figure 4.24. The temperature distribution in the beam is relatively uniform except for the values in the top flange which are around 200 degrees lower than those at other locations due to heat sink effect of the adjacent concrete slab. Large temperature gradients are developed through the depth of the concrete slab owing to its low heat conductivity.

The column is assumed to be fully protected with 2 cm sprayed-on mineral fibre. One side of the section is exposed to ambient at 20 degrees, while the other three sides are exposed to the fire environment. Thermal properties of the protection material are 300 kg/m$^3$ for density, 0.12 W/mK for heat conductivity, 1200 J/kg K for specific heat [127]. The convection coefficient is 25 kW/m$^2$ and the emissivity is 0.7. As shown in Figure 4.25, the temperature rise in the column is no greater than 400 degrees until 2000s when the fire temperature reaches its peak values. For

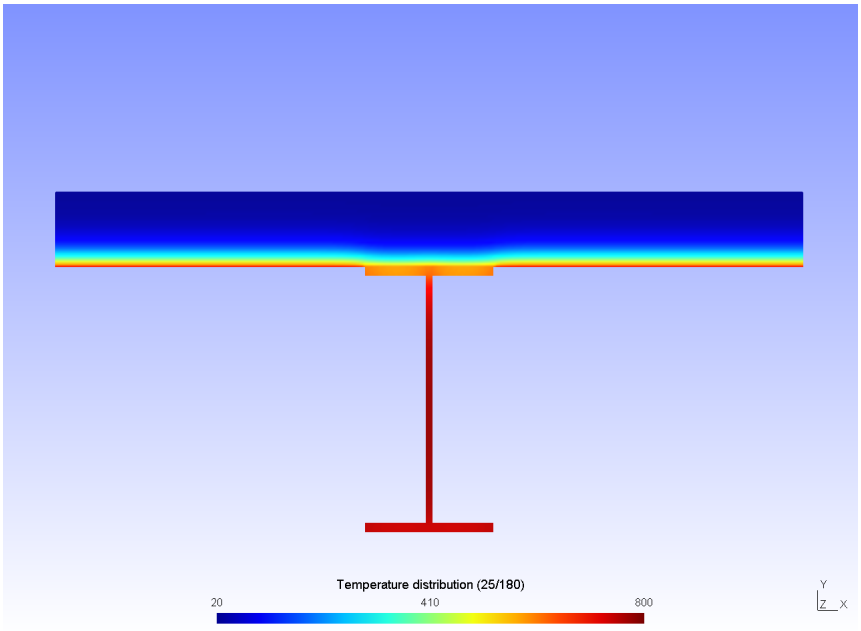


**Figure 4.24:** Temperature in the composite section at 1000s

simplicity, the columns were considered to be heated uniformly in the subsequent structural modelling based on the results of the heat transfer analysis.

### 4.5.3 Modelling results

#### 4.5.3.1 Strong floor

Figures 4.26 to 4.28 plot the column horizontal displacements over time for the 6th, 7th and 8th floors respectively (i.e. the heated floors). The comparison for all the cases demonstrates that as the time delay of the travelling fires increases the maximum positive column horizontal displacement decreases. Moreover the displacements increase substantially only when all the three floors are on fire. It can also be noticed that the maximum negative displacement (thermal expansion phase) for the 6th floor, which is the first to heat, is similar for all

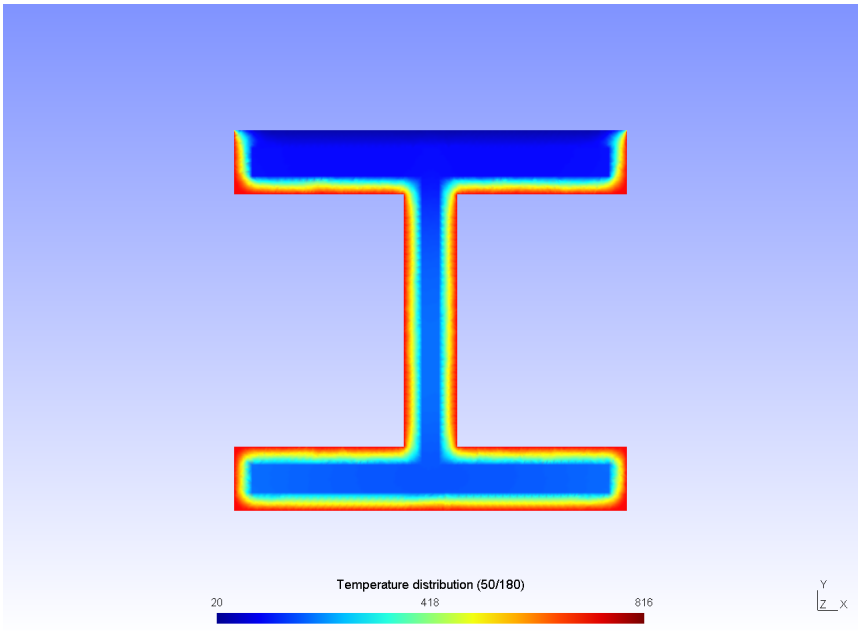


**Figure 4.25:** Temperature in the protected column section at 2000s

cases independent of the time delay opposite to the 7th and 8th floors which heat later and the maximum displacement reached is similar for the travelling fires but less compared to the simultaneous ones. As expected, the time that these floors expand also increases as the time delay is increasing. Figure 4.29 plots the midspan deflection of the 7th floor (middle fire floor). It can be seen that as the travelling speed decreases, the maximum midspan deflection obtained decreases too (from approximately L/5 for dt=0, to L/9 for dt=2500). The rate of deflections decrease becomes smoother as the time delay of the travelling fires increases. Figures 4.30 and 4.31 plot the variation of membranes forces in the 7th and 8th floor for different travelling rates. It can be seen that as the time delay of travelling fires increases the maximum tensile force also increases. The maximum compressive forces are also much higher than those in the simultaneous case. It should however be mentioned that the variation of both the maximum tensile and compressive forces is not large between the travelling fires.

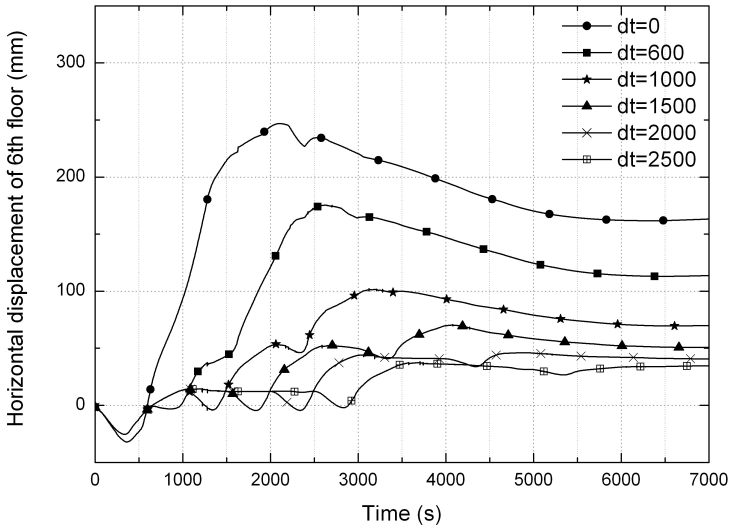


**Figure 4.26:** Horizontal displacement of the sixth floor

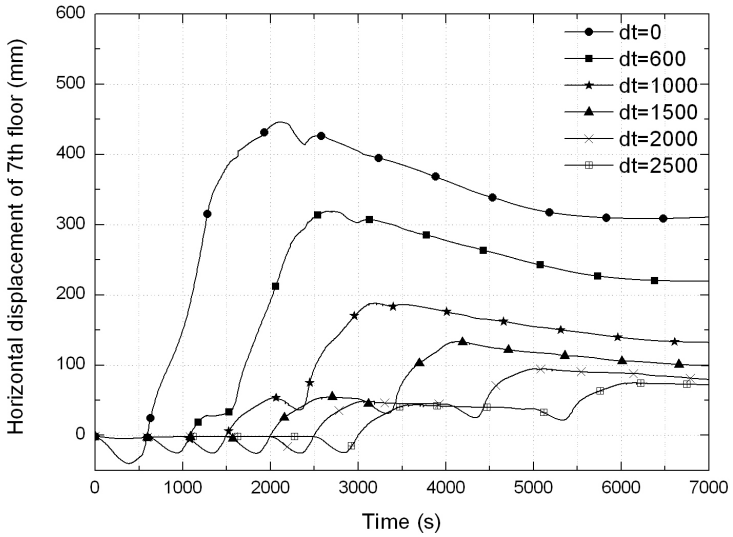


**Figure 4.27:** Horizontal displacement of the seventh floor

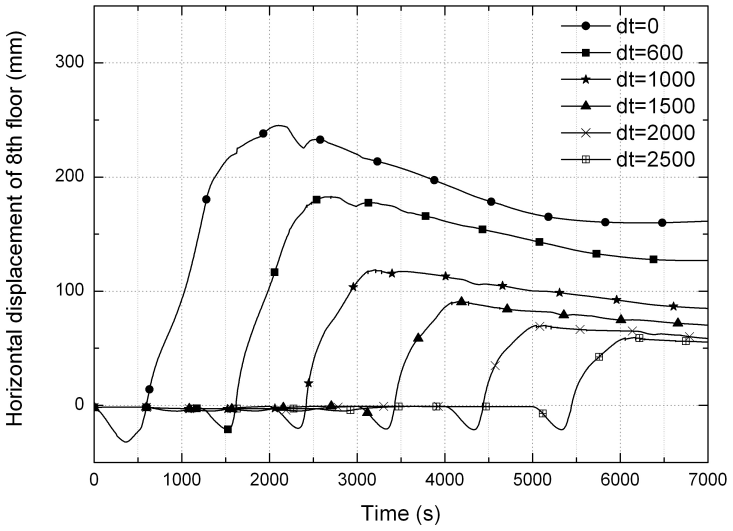


**Figure 4.28:** Horizontal displacement of the eighth floor

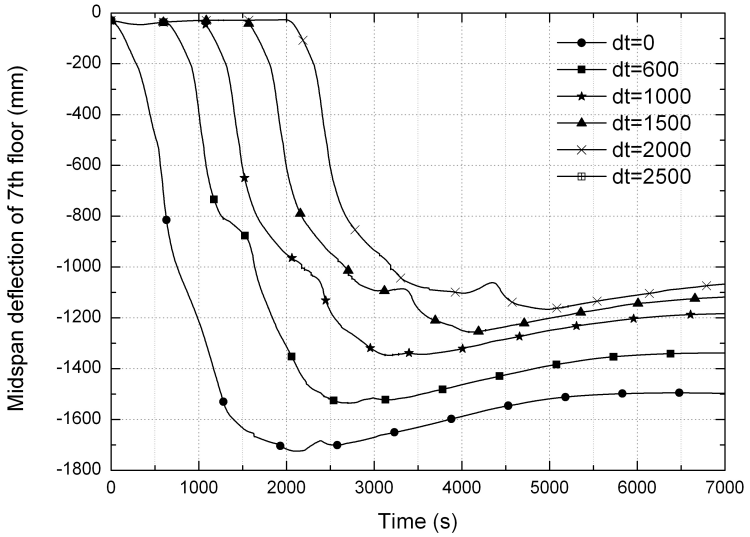


**Figure 4.29:** Midspan deflection of the seventh floor

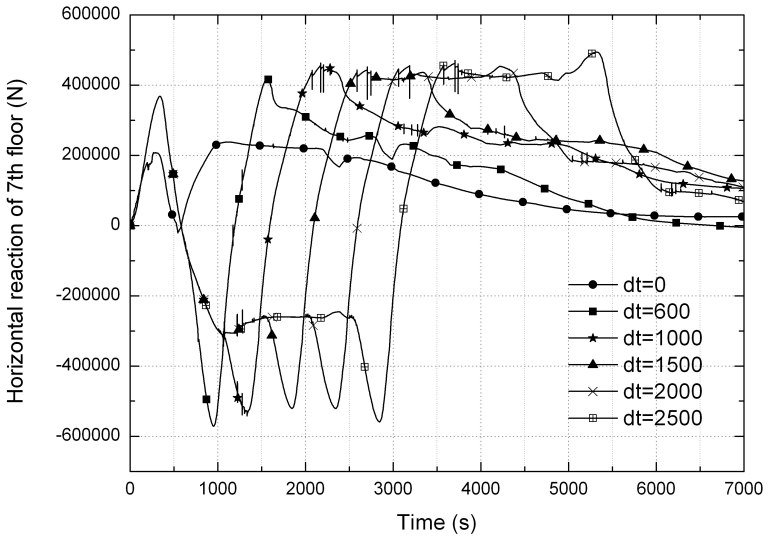


**Figure 4.30:** Membrane forces of the seventh floor

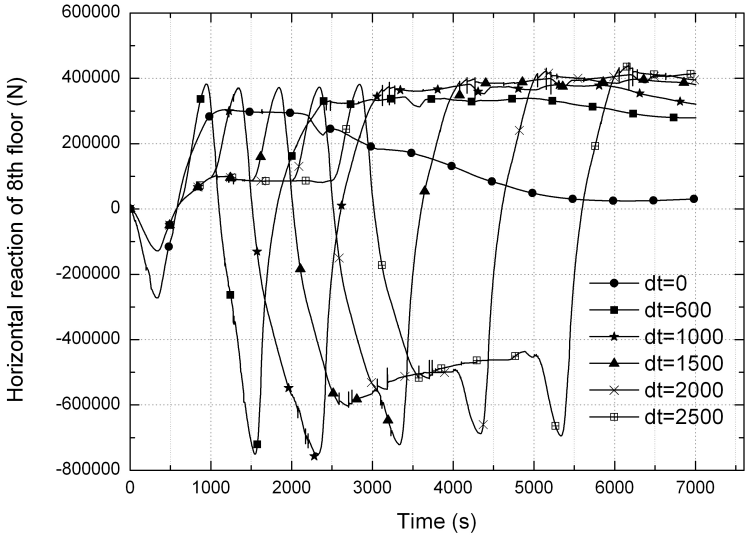


**Figure 4.31:** Membrane forces of the eighth floor

#### 4.5.3.2 Weak floor

Figure 4.32 plots the midspan deflection of the 5th floor for a weak floor collapse mechanism. It can be seen that for rapid rates of spread (600, 800) the floor fails while for slower rates of spread the floors does not fail and hence weak floor collapse does not occur but strong floor collapse could. Through the parametric studies it was seen that there are other cases that weak floor collapse could still occur irrespectively of the time of spread used. Figures 4.33 to 4.35 plot the horizontal displacements of the column for the 6th to 8th floor respectively and demonstrate that the column pulls in less as the travelling speed decreases. Figures 4.36 and 4.37 plot the membranes forces of the 7th and 8th floor for different travelling rates for the weak floor case. The observed differences in terms of maximum tensile force reached are similar to the strong floor case in that as dt (i.e. time delay) increases the maximum tensile force also increases.

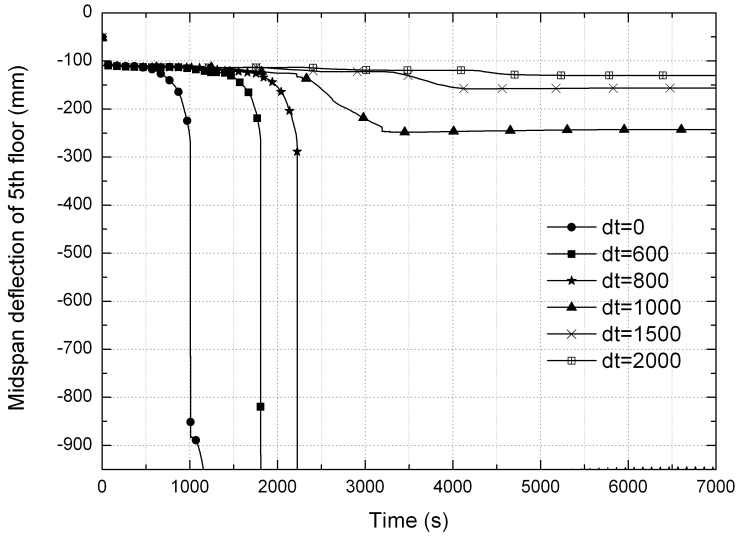


**Figure 4.32:** Midspan deflection of the fifth floor

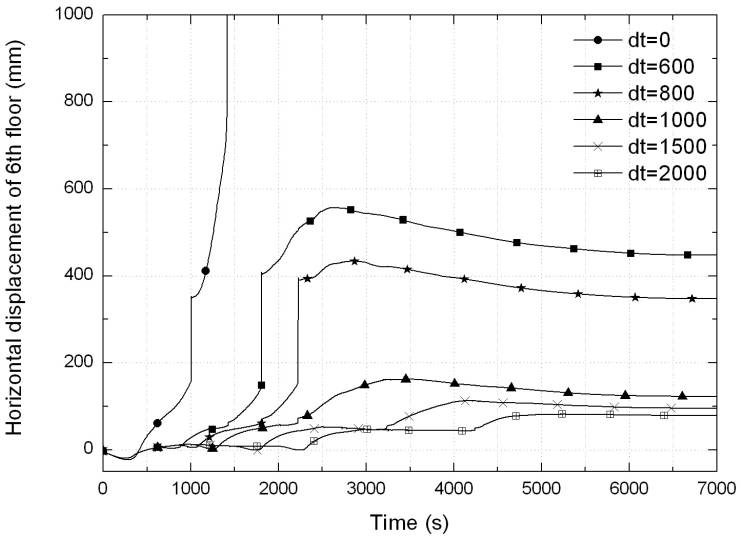


**Figure 4.33:** Horizontal displacement of the sixth floor

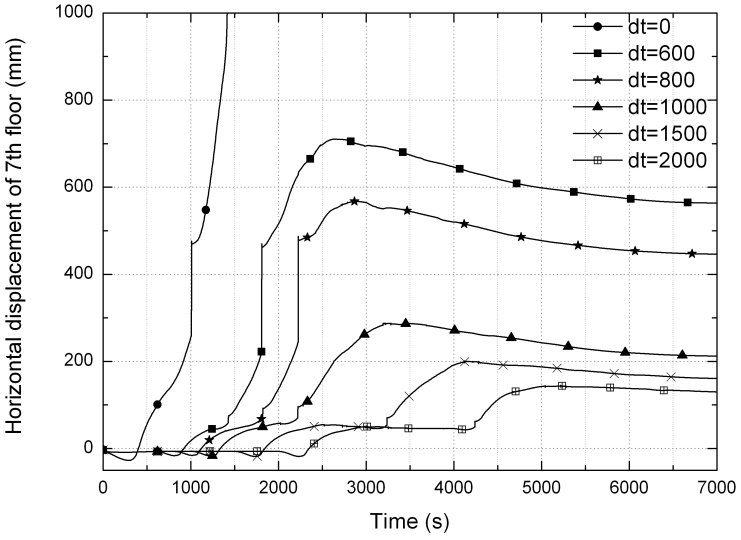


**Figure 4.34:** Horizontal displacement of the seventh floor

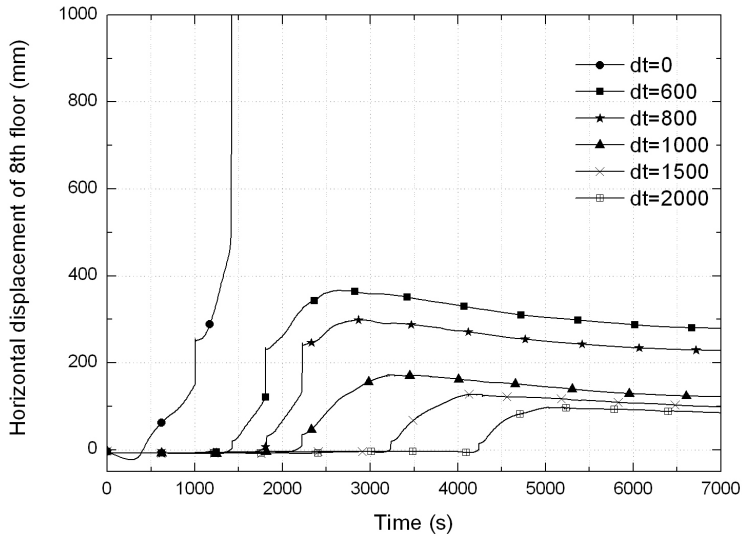


**Figure 4.35:** Horizontal displacement of the eighth floor

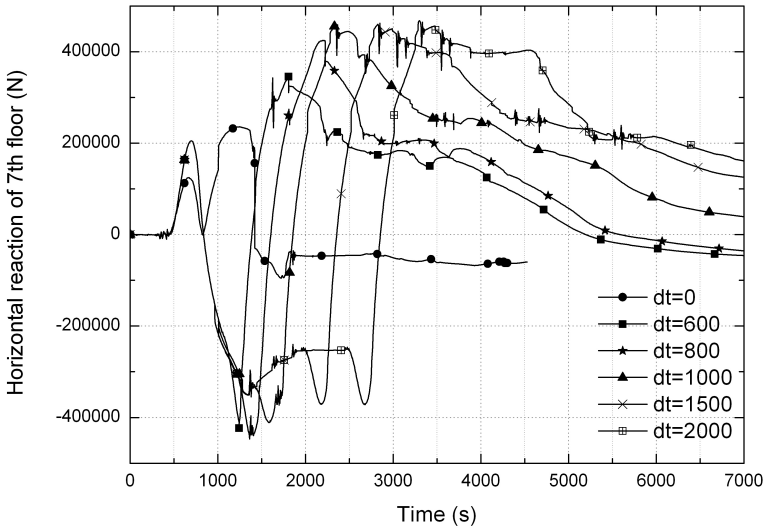


**Figure 4.36:** Membrane forces of the seventh floor

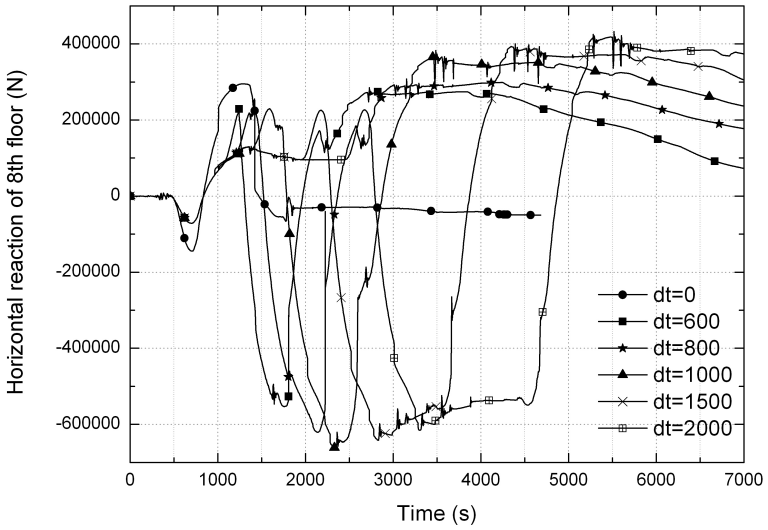


**Figure 4.37:** Membrane forces of the eighth floor

### 4.5.4 Application of vertical traveling fires to the WTC towers

It would be interesting to examine the effect of travelling fires on an actual tall building that collapsed due to fire such as the WTC towers. Even after a decade since this event it seems that there are still lessons to be learned from this high profile failure. This section will discuss whether simultaneous fires assumed in previous studies were conservative and how the tower may have responded under vertically travelling fires.

#### 4.5.4.1 Modelling results

The WTC towers were modelled under a three floor travelling fire, varying the rate of travel to investigate this phenomenon in the context of a real failure. A range

of values were used, similar to the earlier study on more generic tall buildings. The deformed shape for the 3-floor simultaneous fire scenario is demonstrated in Figure 4.39. Similarly the deformed shapes for a travelling speed of 1000 and 2500 can be seen on Figures 4.40 and 4.41. Figures 4.42-4.44 plot the horizontal displacement of the 6th, 7th and 8th floors. It can be seen that instability occurs in all possible scenarios with varying travelling speeds examined. A clear difference in the expansion phase can be seen between the simultaneous and the travelling fire cases. For all the travelling fire cases the expansion is very small. For all the travelling fire cases, global instability is seen when a 3rd floor starts to heat too (i.e. the 8th floor in this work). Figures 4.45 and 4.46 also plot the axial forces on the first and last element of the top chord of the truss system. The figures indicate that the members experience increased tension as the travelling time delay increases but also compression which for the travelling fires cases is significantly higher that the simultaneous one. The results of the study denote that the WTC towers will show similar collapse behaviour even for slow travelling fires and that the same collapse mechanism shown in previous research still applies. This denotes that vertical compartmentation could probably delay but not avoid collapse if 3 floor fire scenario occurred and also suggests that the WTC towers had a structural form that was particularly vulnerable to fire that could not be assessed outside of a performance based framework.

## 4.6 Discussion and conclusions

A summary of the main points that came out from this work are the following.

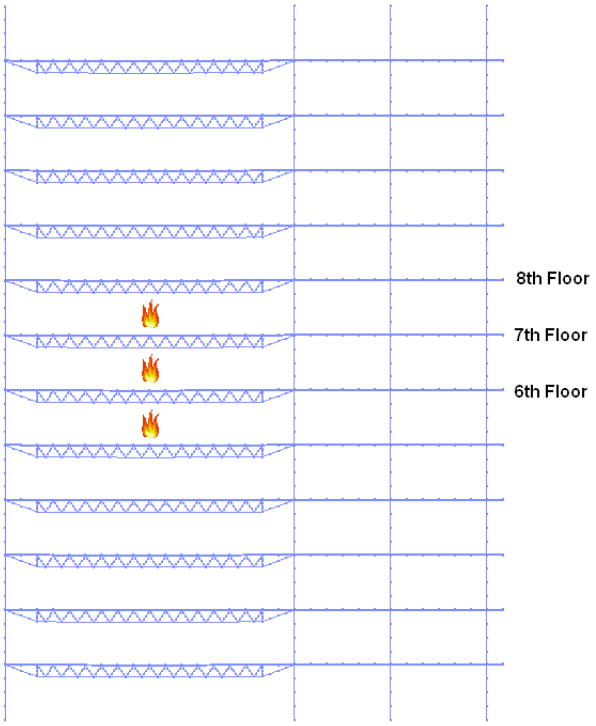


**Figure 4.38:** Finite element model of the WTC Towers

### 4.6.1 Collapse of tall buildings

The analysis presented in this Chapter has examined the response of the WTC towers in fire and explored various collapse scenarios indicated from previous work. The column "pull in" that triggers the instability of the structure and may lead to collapse has been explained. The global behaviour of the structure as well as the local behaviour of the truss has been examined.

In order to understand tall building collapse in fire, a simpler and more typical steel frame composite structure was modelled. The two different types of collapse mechanisms, weak floor and strong floor failure, have been confirmed and clear distinctions have been drawn in terms of their initiation at specific locations in the structure.

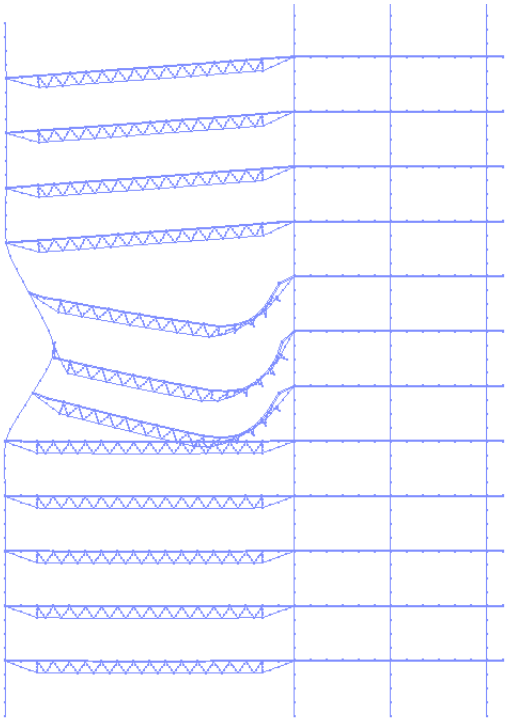

**Figure 4.39:** Deformed shape for simultaneous fires

Parametric studies were performed in order to evaluate the conditions at which one or the other type of collapse occurs. This has led to a simple design and assessment criterion of column-floor stiffness ratio against the number of floors on fire. The results of these studies have also shown that the most common type of collapse mechanism is the strong floor collapse, however weak floor collapse becomes more likely with more floors on fire. The knowledge of these mechanisms is of practical use if stakeholders wish to extend the tenability of a tall building structure in a major fire.

Finally, this work also showed the capability of OpenSees to perform progressive collapse analysis under fire since the same global collapse mechanisms seen in previous work [58, 59, 60, 61] have been reproduced without any significant difference. A primary reason for OpenSees being advantageous for this parametric

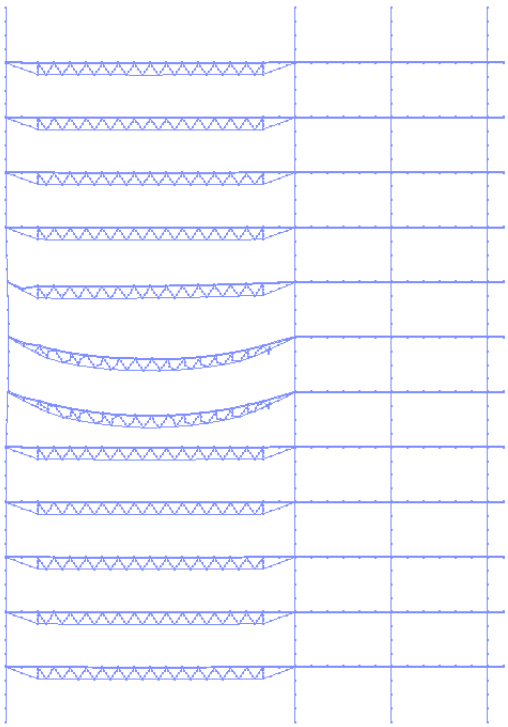

**Figure 4.40:** Deformed shape for travelling fires with a 1000sec rate

study compared to a commercial software such as ABAQUS is that it is more computationally efficient. Its computational efficiency arises primary from its well-written object-oriented architecture and relatively low overhead compared to commercial codes. It would however be easy to perform the same kind of analysis with commercial codes as well. Differences were only seen in failure times after the pulling-in process was initiated for the generic tall buildings but these resulted from the time scaling that was used in previous research (from 3600s to 3.6s) that underestimated the dynamic effects [61].

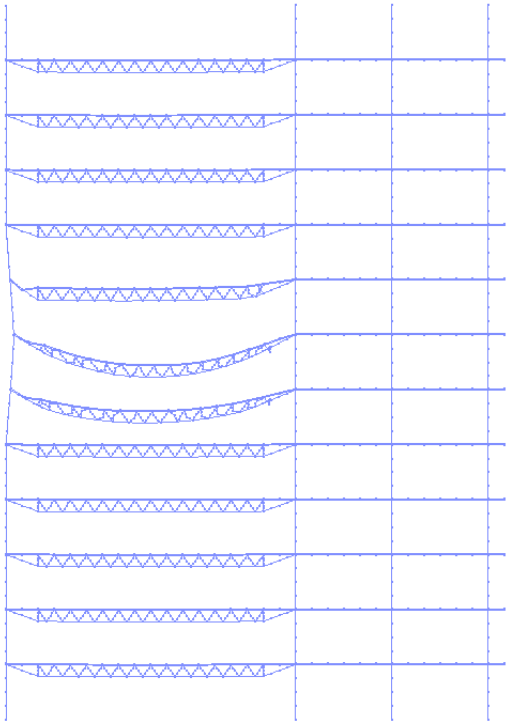

**Figure 4.41:** Deformed shape for travelling fires with a 2500sec rate

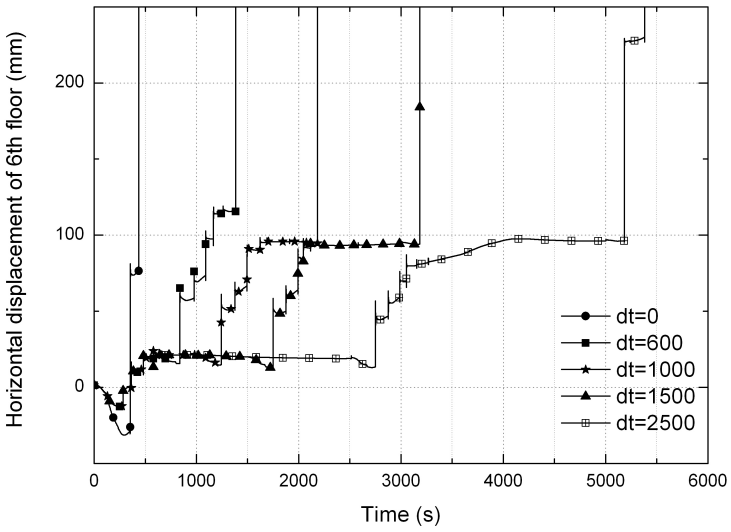


**Figure 4.42:** Horizontal displacement of the sixth floor

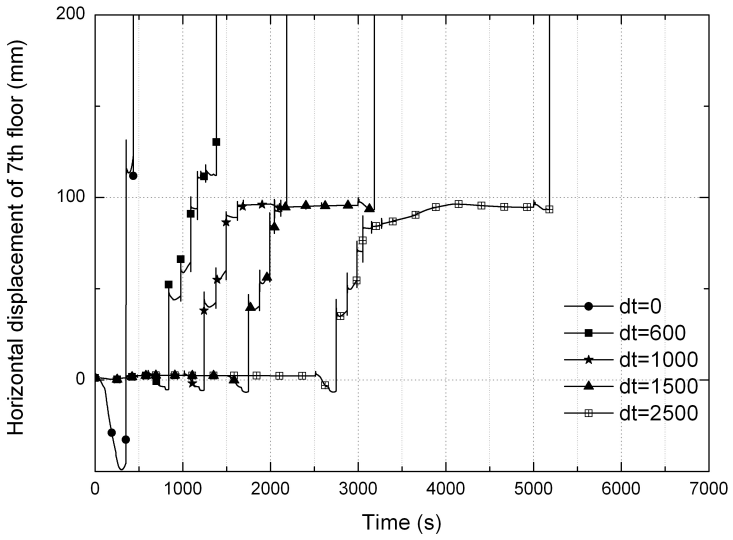


**Figure 4.43:** Horizontal displacement of the seventh floor

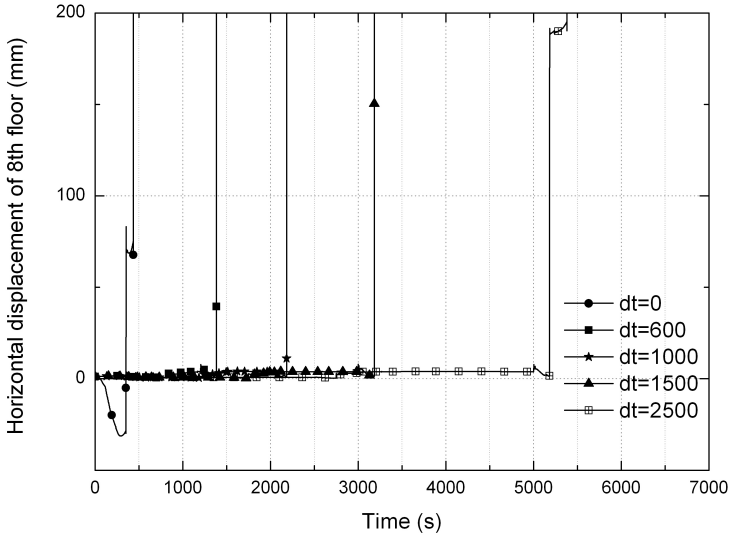


**Figure 4.44:** Horizontal displacement of the eighth floor

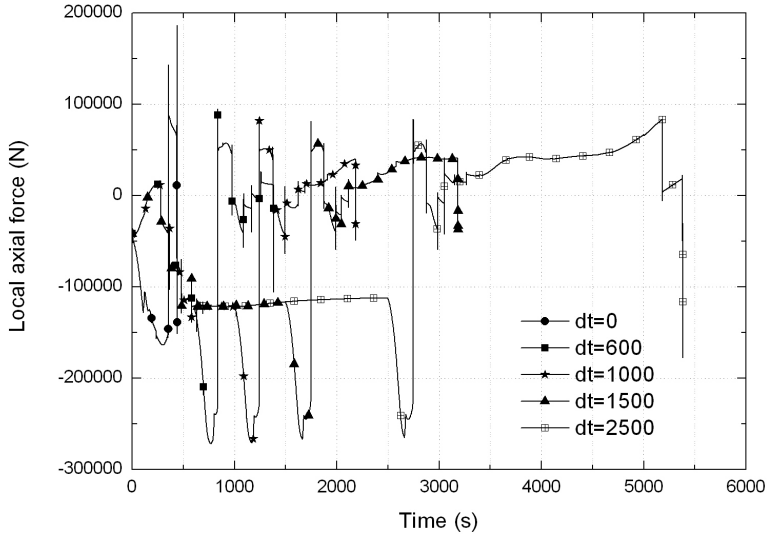


**Figure 4.45:** Local axial force of first element in top chord of the seventh floor

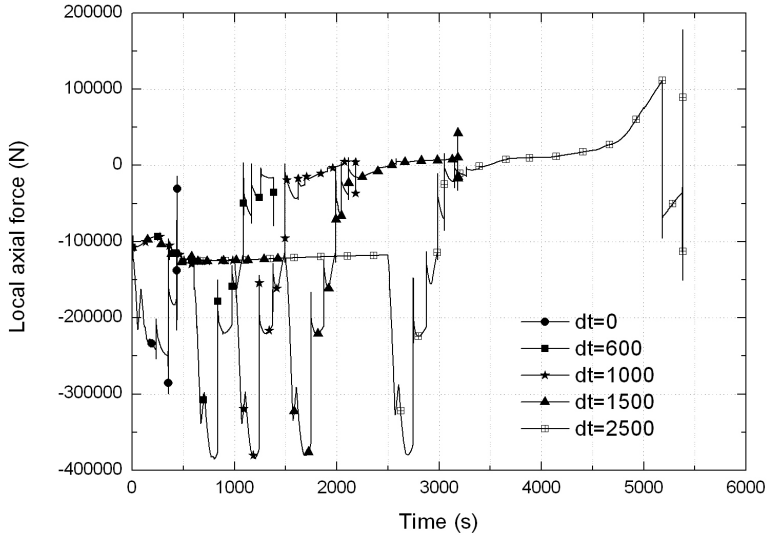


**Figure 4.46:** Local axial force of last element in top chord of the seventh floor

### 4.6.2 Vertically travelling fires

Multifloor fires can cause collapse, and designers will need to include this scenario when designing tall buildings in fire, but there is no guidance on the number of floors in fire and the travelling rate of the fires between the floors. This work investigated the effects of vertically travelling fires on the collapse mechanism of tall buildings with the aim of providing guidance to designers when using multiple floor fire scenarios as part of their design. The results of the study demonstrate that travelling fires have beneficial impact in terms of the global structural response of composite tall buildings in comparison to simultaneous fires. This is because the steel members of the composite frame have time to cool down and thus regain strength and stiffness. This suggests that a simultaneous multiple floor fire could provide an upper bound scenario when designing composite tall buildings against fire induced collapse. This will be of interest to designers wishing to investigate the performance of tall building in a multiple floor fire since it is practically impossible to predict the actual time (or rate) needed for a fire to travel vertically since it depends on many factors as discussed in Section 4.5.2. Contrary to the beneficial effect of the travelling fires in terms of the global structural response, it was noticed that significantly higher tensile forces were also present in the floors compared to the case of simultaneous multiple floor fires. This was also observed in the study of Roben *et al.* [123] and can result in possible connection failure in case the connections do not have the adequate tensile capacity to withstand these higher tensile forces. Although more research is needed on this issue, it was observed that the variation in the maximum tensile force reached for the different travelling rates is small. This is important information for designers, as it is difficult to consider all possible travelling rates.

The results of this study also highlighted the importance of vertical fire compartmentation on the behaviour and possible collapse of tall buildings. Restricting fire from travelling to another floor would decrease substantially the possibility of collapse (since the collapse mechanisms discussed are less likely to occur in single floor fires). However, it is recognised that this cannot be achieved easily in practise and hence the use of thermally-resistant window assemblies and horizontal projections [124] should reduce the speed of vertical spread reducing the risk of collapse or at least delaying it in order for evacuation and emergency response to occur safely. Simultaneous multiple floor fires can be considered as a simpler and conservative upper bound scenario for design again collapse in multiple floor fires. However, a scenario where a slow travelling fire should also be examined to ensure that the tensile capacity of connections is not underestimated. More research will be required for defining an appropriate travelling rate. In this work, the detailed vertical fire spread process was not explicitly addressed, instead a time delay was used as a lumped parameter to study the consequence of vertically travelling fires. Fires travelling horizontally across the floor are also not included. The models presented in this work were based on the assumption that post-flashover fires developed for each floor and a uniform temperature distribution is assumed in the whole compartment. It is recognised that this may not be valid for structures of very large floor areas or long column heights (characteristics that are common in modern infrastructure) where in reality fire is not burning uniformly and simultaneously on each floor. Further research in applying a horizontally travelling methodology to tall buildings is presented in the next chapter.

# Chapter 5

# Thermal and structural behaviour of a composite tall building under horizontally travelling fires

## 5.1 Introduction

Most of the studies in the past have used codified design fires (such as the standard fires and parametric fires) for modeling the response of structures in fire. Almost all these design fires attempt to simulate the effects of post-flashover fires and inherently assume spatially uniform fire temperatures within the compartment [4, 11]. However, recent work has shown that even in post-flashover fires, the distributions of fire temperatures in relatively small compartments is not

uniform [20]. Furthermore, fire accidents have shown that in larger spaces, fires tend to travel rather than burn uniformly and simultaneously [24]. These observations have drawn the attention of researchers who have questioned on the application of conventional design fires on modern structures with large spaces [128, 129]. However, perhaps due to lack of proper understanding of travelling fires, conventional temperature-time curves are still used, and an artificial time-delay has been introduced in order to study the effects on structural performances. For example, Ellobody *et al.* [130] used the parametric curves to represent the travelling fires in a large compartment which was divided into a number of zones and each zone was subjected to a parametric fire curve at different time intervals.

To address this problem and meet the need of structural fire design for modern structures, Rein and Stern-Gottfried [128, 24, 16] have developed a novel methodology which represents travelling fires more realistically by including key aspects of fire dynamics in large enclosures. This methodology has undergone a number of iterations over its development. The major merit of this methodology over conventional post-flashover fire models is to horizontally divide the whole fire environment into two regions, i.e. "near field" and "far field", which generates spatially non-uniform and transient temperature curves for the whole floor. Different approaches can be adopted to calculate the fire generated thermal environment in these two regions including CFD calculations. However, using CFD approach for large building can be computationally restrictive and expensive [128]. Therefore, Stern-Gottfried *et al* [24, 14] adopted an empirical correlation to calculate the far-field temperatures which has the advantage of rapid resolution of the thermal environment with sufficient accuracy for engineering applications. This methodology has been applied to study the structural responses of a concrete structure,

where the results showed that conventional design fires may not be considered conservative when compared to some travelling fire scenarios [24, 39].

The travelling fire methodology developed by Rein and Stern-Gottfried [16] works best for performance-based structural fire design of modern buildings which are beyond the validity of conventional design codes. However, this would normally require detailed thermal and structural modeling in order to quantify the actual response of structures to fire, which naturally requires robust and easy to use structural simulation software. There are many commercial finite element packages (such as ABAQUS, ANSYS, DIANA etc.) that offer excellent capabilities for most routine modeling activity in research and in the commercial and consulting organizations. These codes can however be restrictive for a field that is growing at a rapid pace (as the field of structures and fire is, with increasing interest and development in both research and industry). Furthermore, the licensing costs can be prohibitive for researchers who have limited resources despite academic discounts.

For the above reasons, this work has chosen OpenSees software framework to develop "structures in fire" analysis capability that could be used by researchers all around the world at no cost [88]. The OpenSees framework was initially developed at UC Berkeley as an open source community code for simulating the response of framed structures to earthquakes [66]. It has been recently extended at the University of Edinburgh by adding new software modules and modifying existing codes. New capabilities include heat transfer modeling in structural members with fire imposed boundary conditions, and thermal-mechanical modeling using both beam and shell elements with temperatures calculated by the heat transfer module [88].

The latest developed travelling fire methodology [16] has been implemented in the OpenSees framework, which is then used to investigate both the thermal and structural responses of a generic composite structure subjected to a range of horizontally travelling fires. Composite structures made of concrete slabs and steel beams are a popular form of tall building construction preferred by architects and engineers because they optimize the use of materials and enable rapid construction. However, the effects of travelling fires on the performance of this type of construction have not been examined in detail before. A study examining the response of horizontally travelling fires on the response of a concrete structure in fire has been performed in [39]. The results demonstrated that travelling fires of medium fire sizes produced a more conservative estimate of the structural response compared to parametric fires. However, the results of this study are limited to concrete structures of the particular layout examined in [39]. Further investigation will be carried out in this work to examine whether these conclusions are applicable to a composite structure too. Lamont *et al.* [131] studied the response of a small composite frame under "short hot" and "long cool" parametric fires. The authors concluded that the most detrimental fire was the "short hot" fire as large deflections were developed in very short time although the "long cool" fire resulted in higher displacements for some elements but much later in terms of time. These findings were challenged by the results in [126] where the authors examined the behaviour under "short hot" and "long cool" fires of an eleven story building. The results showed that there was no failure when they considered a "short hot" fire but a "runaway" failure was seen for a part of the structure involving 10 m beams under a "long cool" fire. Until further research is carried out, these studies suggest that the worst case scenario for each structure

can not be a priori defined and that it depends on the structural materials and layouts used.

## 5.2 The travelling fire methodology

In the travelling fire methodology, the fuel is normally assumed to be uniformly distributed across the whole floor plate with a fire load density $q_f$ (MJ/m$^2$). Assuming the fire burns with an area of $A_f$ (m$^2$) and a constant heat release rate per unit area $\dot{Q}''$ (kW/m$^2$), this corresponds to a power $\dot{Q}$ (kW) for this particular size of fire. Each fire area would have a constant burning time , which is given by [16, 24]

$$t_b = \frac{q_f}{Q''} \tag{5.1}$$

The floor area where the fire has traveled across is deemed to be burnt out. Note that $t_b$ is a characteristic burning time of the near field, and is determined by fuel load density and the properties of the fuel but independent of fire sizes.

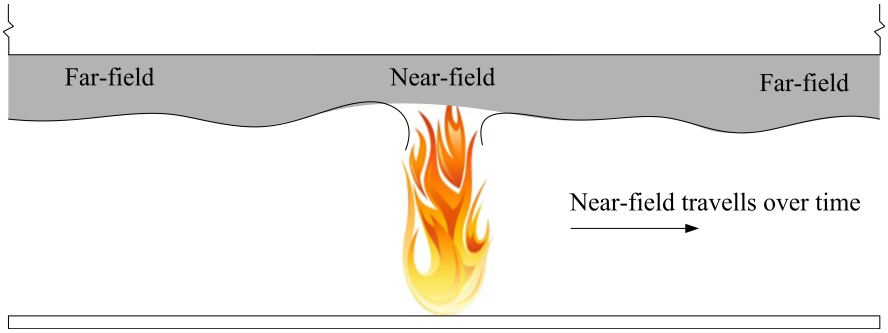


**Figure 5.1:** Illustration of a travelling fire with near field and far fields

As the fire travels across the floor, the thermal environment can be divided into

two horizontal regions, namely, "near field" and "far field", with reference to the fire source at any time interval (as illustrated in Figure 5.1) [24]. The near field is the burning region of the fire, and a constant representative temperature may be assumed [24, 128, 39]. The far-field is the region remote from the burning area where the structure is mainly heated by hot smoke moving away from the fire source. The fire temperature of the far field may be approximately determined by the empirical Alpert correlation [24, 39, 132, 23]

$$T_{max} - T_{\infty} = \frac{5.38(\dot{Q}/r)^{2/3}}{H} \tag{5.2}$$

where $T_{max}$ is the maximum temperature in the ceiling jet, $T_{\infty}$ is the ambient temperature, $\dot{Q}$ is the heat release rate of the fire, $r$ is the distance from the fire center, $H$ is the floor height.

The use of Alpert's correlation has been shown to be conservative and adequate by comparing the calculated ceiling jet temperatures with CFD modeling results [16]. Good agreement between the results was found which justifies using this simple empirical correlation to predict the far-field temperatures. Eq. (5.2) produces a monotonically decaying temperature distribution along the distance away from the fire. One constraint should be noted that this correlation is only applicable to unconfined ceiling jet and no accumulated smoke layer should be present [23]. Therefore, possible structural members such as beams under the ceiling should not have a depth which could violate the validity of this correlation.

As a result of the travelling nature of fire, any location above the fire floor would experience sequentially the initial far-field heating, the near-field heating, the posterior far-field heating, and the cooling to the ambient (20 ℃), where gas temperatures during the first and third phase are determined by Eq. 5.2. The

arrival time of the near-field is dependent on both the travelling speed and the distance from the fire origin. Therefore, the travelling fire methodology produces spatially and temporally varying heating conditions across the floor, which can not be naturally addressed by conventional design fires such as the parametric fire curves as given in EC 1 [11]. Figure 5.2 shows a typical temperature curve at any arbitrary location above the floor.

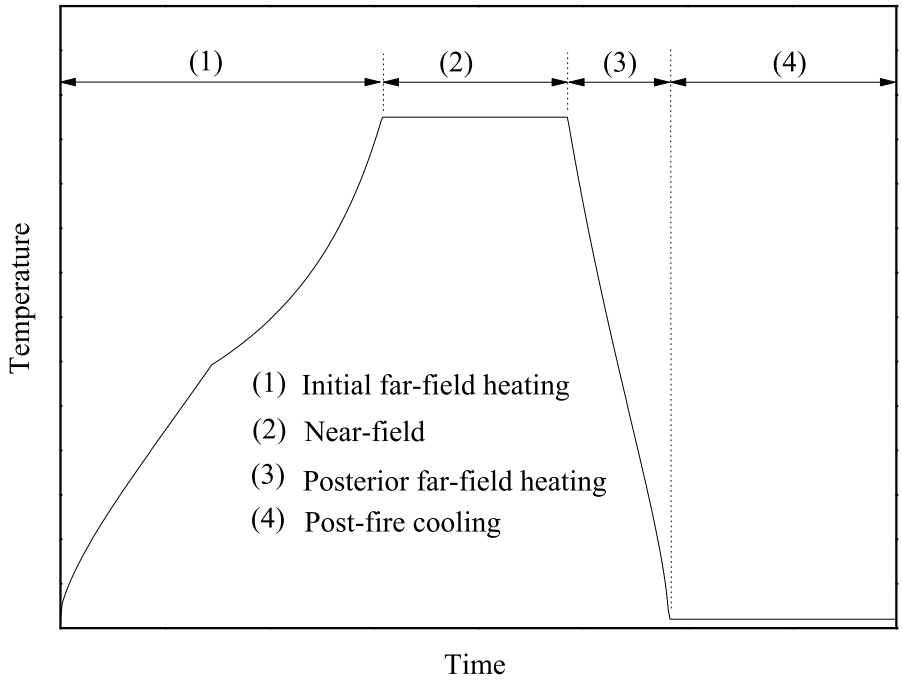


**Figure 5.2:** Near-field and far-field exposure at an arbitrary location above the floor

## 5.3 Case study of a composite structure

### 5.3.1 The structure

The structural layout examined in this work is a generic modern tall building with a floor height of 4 m. The typical floor plan is shown in Figure 5.3, which

could possibly produce fire propagation similar in form to that of the WTC towers [64]. The dimensions of the beams are selected according to preliminary design criteria. These are UB 533×210×122 for the girders, UB406×140×39 for the primary beams and UB356×171×51 for the secondary beams. The floor area $A_{total}$ is 1152 m$^2$, with a core of 192 m$^2$. The presence of core is important to structural behavior and should be taken into account when performing structural analysis. However, it is a reasonable approximation to neglect the core when calculating the fire temperatures [24].

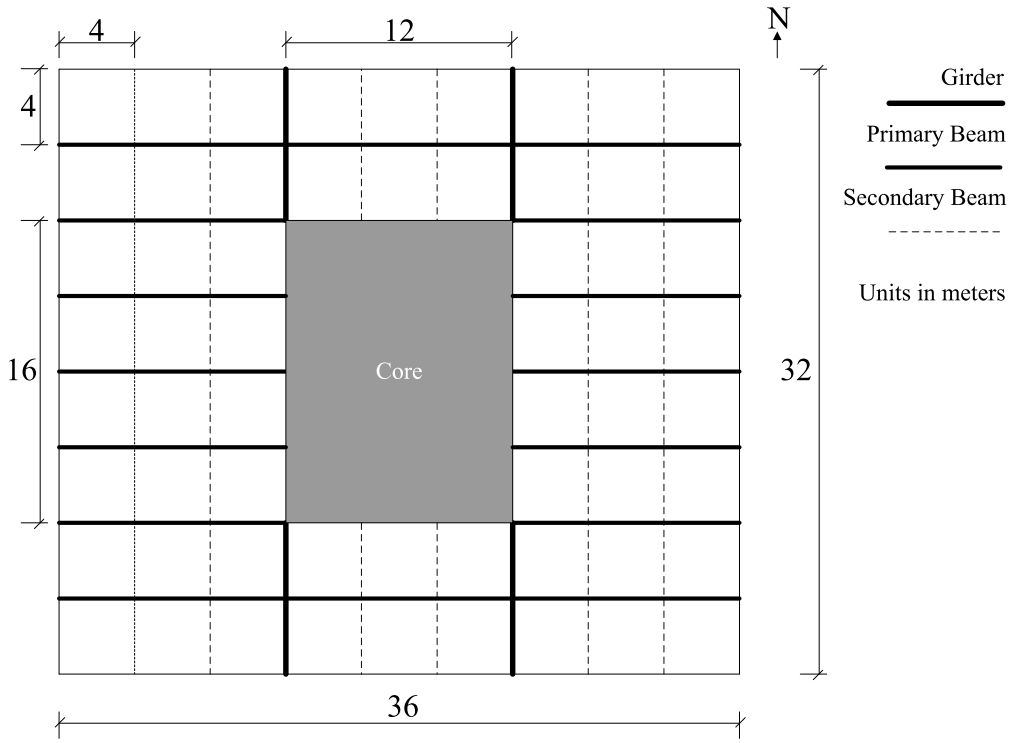


**Figure 5.3:** Schematic plan view of the structure

### 5.3.2 The travelling fire scenarios

The building is assumed to be used for office purpose and the fuel is uniformly distributed on the floor plate with a characteristic fire load density of 420 MJ/m$^2$

as given in [64]. Mass burning rate of typical office fuels are reported in the range of 20∼40 g/m$^2$s [133], which suggests that the heat release rate per unit area would range from 320 to 640 kW/m$^2$ if we assume a typical heat of combustion of 16 kJ/g for cellulose fuels [4]. An average value of 480 kW/m$^2$ is taken in this work. It is assumed that the fire travels in a linear path from the west to the east of the floor and extends over the whole width of the building, which is similar to the treatment used in [24, 39]. The initial length of the fire is $L_0 = 0.1$ m, and then it maintains a constant length $L_f$ (near-field) once the fire has grown to the specified size $A_f$,

$$L_f = \frac{A_f}{W} \tag{5.3}$$

Larger fires would travel faster than smaller ones, and the travelling speed $s$ (m/s) is characterized by [16]

$$s = \frac{L_f}{t_b} \tag{5.4}$$

For a linearly travelling firesuch as the one examined in this work, the total burning time may be calculated by the following equation [24]

$$t_{total} = t_b(\frac{L - L_0}{L_f} + 1) \tag{5.5}$$

The size of fire is a major variable in the travelling fire methodology, which balances the far field temperature and the total burning time [24, 128, 39]. In this work, the fires are varied from 4% to 50% of the floor area. Other parameters associated with the fire size are summarized in Table 5.1.

It should be noted that in this work, the main input from the travelling fire model

**Table 5.1:** Summary of the travelling fire scenarios

| $A_f$(m$^2$) | Fire size | $L_f$(m)(Eq. (5.3)) | $\dot{Q}$(MW) | $t_{total}$(min)(Eq. (5.5)) | $s$(m/min)(Eq.(5.4)) |
|---|---|---|---|---|---|
| 48 | 4% | 1.5 | 23 | 364.0 | 0.1 |
| 96 | 8% | 3 | 46 | 189.3 | 0.2 |
| 192 | 17% | 6 | 92 | 102.0 | 0.4 |
| 288 | 25% | 9 | 138 | 72.8 | 0.6 |
| 384 | 33% | 12 | 184 | 58.3 | 0.8 |
| 480 | 42% | 15 | 230 | 49.5 | 1.0 |
| 576 | 50% | 18 | 276 | 43.7 | 1.2 |

is the temporal and spatial varying gas temperature $T_f$. The fire imposed heat fluxes are then calculated, by summing the convective and radiative heat fluxes, using the following formula,

$$q = q_c + q_r \tag{5.6}$$

Where, the convective and radiative heat fluxes, can be simply calculated respectively as shown below,

$$q_c = h_c(T_f - T_s) \tag{5.7}$$

$$q_r = \epsilon\sigma(T_f^4 - T_s^4) \tag{5.8}$$

Where, $T_s$ in the above equations represents the surface temperature of the solid phase. It is clear that as the gas temperature $T_f$ is time and location dependent,

the subsequent heat flux $q$ is also not a constant value but temporarily and spatially varying.

The temperature distribution in the composite floor (on top of the ceiling of the fire compartment) along the longest direction will be examined, as the structure along this direction is more susceptible to stability issues in case of a fire. Figure 5.4 shows a linear travelling fire and four locations (A, B, C, D) for temperature analysis across the floor. The schematic of the composite section and corresponding temperature locations on the section are also indicated in Figure 5.5.

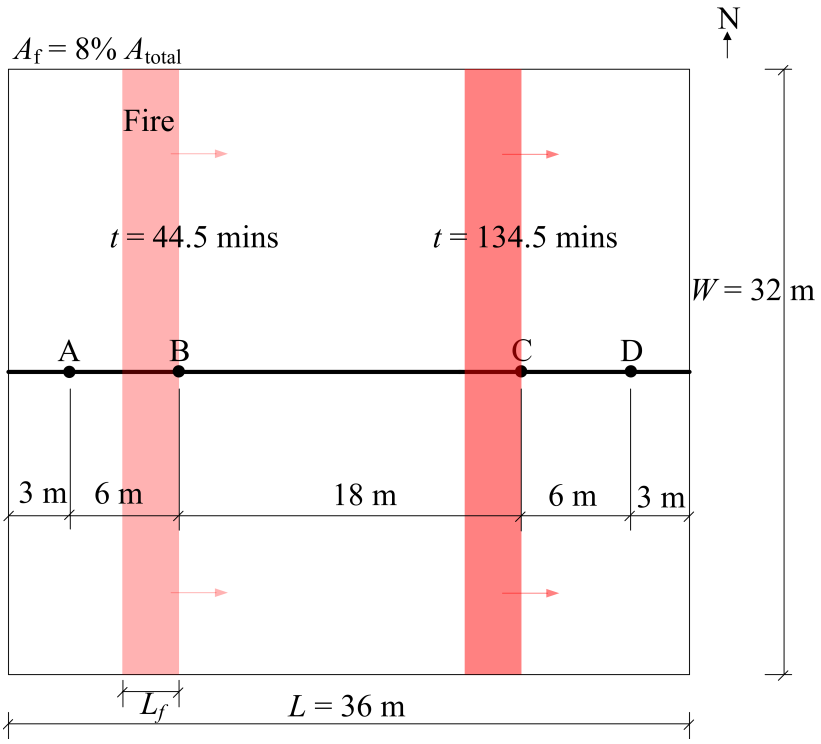


**Figure 5.4:** Schematic of the linearly travelling fire across the floor plate

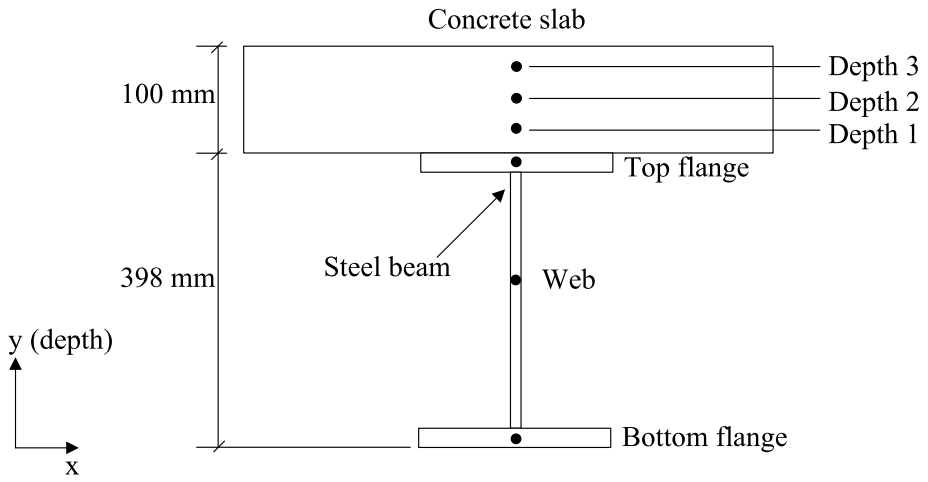


**Figure 5.5:** Dimensions of the the composite section and temperature locations

### 5.3.3 Fire and heat transfer modelling in OpenSees

The recently developed fire and heat transfer modules in OpenSees [88, 97] are used in this work to calculate the transient temperature rise in the composite structure. As a result of the travelling fires, the heat transfer in the composite floor could have a fully three dimensional character; however, we have chosen to ignore heat conduction along the direction of fire propagation to simplify the problem and reduce the computational expense. Furthermore, the rate of heat conduction along that direction would be much slower than the fire travelling speed [16]. Hence two dimensional heat transfer analyses are carried out for separate sections at the locations (A, B, C, D) specified in Figure 5.4. This approach is justified by Franssen *et al.* [134], who showed that even if a steel member is subject to highly localized heating conditions, a series of separate two dimensional heat transfer analyses represent fully three dimensional heat transfer analyses with adequate accuracy.

A 0.9 mm thick metal deck between the steel beam and the concrete slab

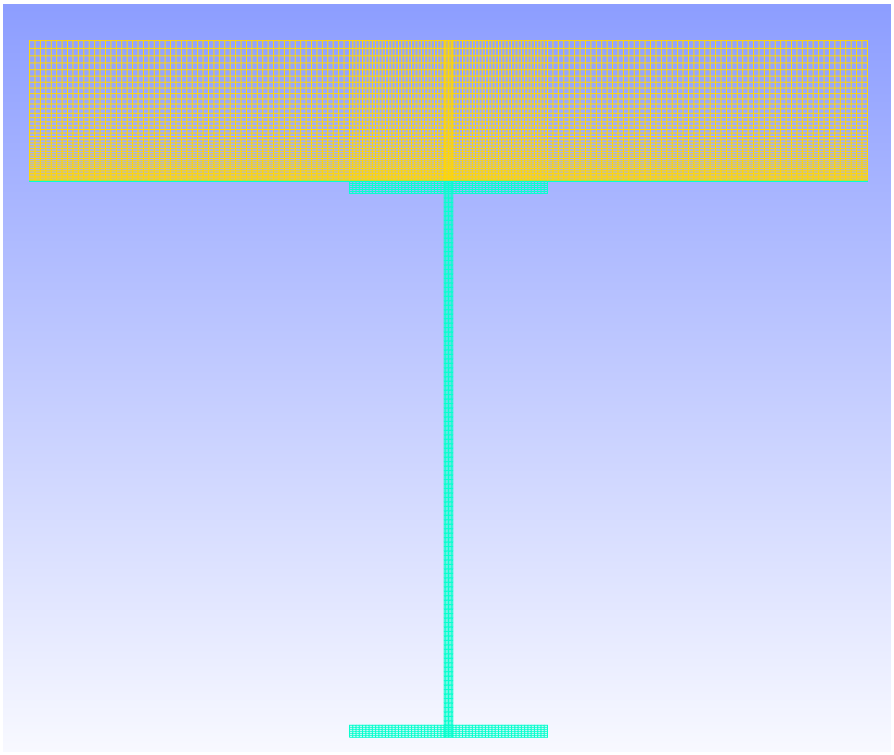

**Figure 5.6:** Finite element model of the the composite section

is included in the finite element model. The temperature-dependent material properties of concrete (with a moisture level of 1.5%) and steel are taken from [41] and [135] respectively. The top of the concrete slab is assumed to be exposed to ambient environment of 20 ℃. The bottom surface of the slab and three sides of the beam are exposed to the thermal environment generated by the travelling fires. The convection coefficients for fire-exposed surfaces and unexposed surfaces are taken as 25 kW/m$^2$ and 4 kW/m$^2$ respectively [11]. An emissivity of 0.7 is specified for both the concrete and steel according to [41]. The finite element model of the composite section is shown in Figure 5.6. Radiative attenuation in the I-section cavities is not considered here as the aspect ratio of the cavity is relatively low (0.18) for the steel member examined, which suggests that the geometric attenuation of radiative heat fluxes at the inner surfaces is not

prominent [136] and the uniform thermal exposure for all the section surfaces may be considered as a reasonable approximation.

### 5.3.4 Structural fire modelling in OpenSees

A two dimensional substructure is modeled that represents a generic 12 storey slice of the building along the longest span (12m) floor area. The core of a generic building is assumed to be rigid. By including appropriate number of floor below and above the fire floor ensures that the stiffness of the surrounding structure is accurately modeled. It is recognised that although a two-dimensional representation does not take into account the load redistribution effects however previous research that compared two and three dimensional models in [137, 111] has demonstrated that a two dimensional model can accurately predict the performance of a perimeter column-floor interaction system in fire. Especially in the context of travelling fire methodology, a much more inexpensive two dimensional model can efficiently provide a first overview of structural behaviour of a building under different travelling fires that maybe otherwise be much more expensive to conduct using three dimensional models. After the two dimensional model, a three dimensional grillage model is also examined and the two models are compared. In the grillage model, the load redistribution effects are considered, however the concrete slab is still considered in a simplistic manner by treating it as a series of beam-column elements. The grillage model is discussed in more detail in Chapter 6. All the structural members of the building (column, slabs and beams) were modeled using the two-node displacement based and distributed plasticity **dispBeamColumn2DThermal** or **dispBeamColumn3DThermal**elements. Plasticity for these elements was chosen to be monitored in five locations along the

length of the element and using a fiber section approach along the depth of each element. An appropriate number of elements has been used to take into account the p-delta effects while a co-rotational transformation is used to incorporate the large displacements developed. The composite action of the floor between the steel beam and the concrete slab is achieved by modelling them with separate series of elements that are connected with multipoint rigid link constraints that tie the corresponding degrees of freedom (translations and rotation). At the rigid core end the steel beam and the slab (forming the composite floor) are both pinned to a rigid lateral restraint. This connection also simulates a fixed-end connection for the composite floor. A fixed connection is also assumed for the floor-column connection. This assumption implies that translations and rotations of the beam and column at the node joining the two members are constrained to be identical. It should be noted that connection or reinforcement failure is not taken into account in the current work. In addition, spalling of the concrete slab is also not considered.

For the steel columns and beams a yield strength of 300 N/mm$^2$ and modulus of elasticity of 210 GPa were used. The concrete slab was assumed to have a compressive strength of 30 N/mm$^2$ and a tensile strength of 5% of its compressive strength adopting a modified Kent and Park model [138] as its material constitutive model. The steel reinforcement was assumed to have yield strength of 475 N/mm$^2$. The temperature dependence of material properties for steel and concrete in OpenSees are based on Eurocodes [40, 41]. During the cooling stage of a fire, steel is assumed to regain its stiffness and strength, while the compressive strength, strain corresponding to compressive strength and ultimate (crushing) strain of concrete do not recover during cooling and were varied according to [41].

Thermal strains are generally assumed to be reversible. An implicit dynamic procedure is used in this work to overcome numerical instabilities caused due to the high restraint to thermally induced displacements. For the case of travelling fires, big numerical instabilities are present due to highly localised temperatures and steep heating curves compared to parametric fires or exponential fire curves [137]. The numerical scheme selected for the dynamic analysis is an implicit solution with a Hilber-Hughes-Taylor integrator with $\alpha = 0.7$ to add numerical damping to the model [96].

## 5.4 Results and discussions

When examining composite members in fire, it should be noted that the thermal response affects significantly the structural response. Significant information on the structural behaviour under thermal effects was gained based on the Cardington tests over the previous years [139]. Composite floors are designed for flexure but also carry loads through compressive and tensile membrane action. During the heating phase, the composite section experiences a mean temperature rise which leads to overall compression in a laterally restrained member. It also experiences a thermal gradient over the depth of the section which leads to a uniform hogging moment along the length of a rotationally restrained member (which is usually the case, at least at low temperatures). The hogging moment also causes compression forces in the bottom flange of the steel beam. Further research by Lamont *et al.* [131] has investigated the behaviour of composite members under a "short-hot" and a "long-cool" fire scenarios. Their research has shown that in a "short-hot" fire the composite section experiences higher thermal gradients and in the case of a "long-cool" fire the composite section

has a higher mean temperature. When exposed to high temperatures concrete experiences creep and loses its load bearing capacity, and steel reinforcement at 550 ℃ loses almost 50% of its strength and 30% of its elastic stiffness [41]. That is why concrete slabs are required to have an appropriate cover to the steel reinforcement. Law *et al.* [39] suggested that the peak temperature at the rebar location could be used as a criterion to measure the structural performance. The thermal and structural responses of the composite structure subjected to different travelling fire scenarios will be further discussed in detail in the following sections.

This work was collaborative and hence, both the thermal and structural responses were examined for the generic structure examined here. More information on the thermal response of the structure can be found in [97], but the basic information is also included here. This works focuses more on the structural response of the structure.

### 5.4.1 Thermal response

#### 5.4.1.1 Temperature rise

Typical fire temperatures and the temperature histories through the depth of the beam and concrete slabs are shown in Figure 5.7 for four locations across the floor, which is shown for a fire with small size (8% of the total floor area). It is clear that the heating condition is strongly non-uniform across the floor in travelling fires. It is interesting to note that the fire curves are symmetric for the geometrically symmetric locations (A and D, B and C). This is because the far field temperature is a function of relative distance to the fire center as given in

Eq. (5.2). Note, according to the "equal area hypothesis" [4], the fire severity at location A (96 mins) and location D (186 mins) would be the same due to identical areas under the two fire curves (above a reference temperature of 300 ℃). However, temperatures in the beam at location D (186 mins) are up to 77% higher than the corresponding values at location A (96 mins), while temperatures in the slab (depth 3) at location A (96 mins) are up to 102% higher than those at location D (186 mins). Similar results are also found for other travelling fire scenarios in this work. This clearly goes against the traditional measure of fire severity in terms of the "equal area" concept which links fire severity to the area under the temperature-time curve [4].

The peak temperatures at the bottom flange and centre of the web reach the near field temperature (1150 ℃) in all the cases, although peak values for the top flange are slightly lower. Therefore, the time taken to reach a critical temperature seems to be a more meaningful parameter for the investigation here, as unprotected steel members may fail rapidly in fires [4]. The critical temperature is taken as 550 ℃ as this value is often used as a simple failure criterion for steel members [4]. As shown in Figure 5.8, it takes shorter time for the beam to reach the critical temperature when exposed to larger fires. This is expected as larger fires travel faster and lead to earlier arrival of the near-field heating. It takes slightly longer for the top flange to reach 550 ℃ due to the heat sink effect of the concrete slab. As pointed out in [16], the time to reach a specified temperature depends not only on fire sizes but also the distance relative to the fire origin. Location A has the shortest distance to the initial fire location and it is the earliest to experience the near field heating. Therefore, the steel beam there suffers the most detrimental heating conditions compared to other locations, which reaches 550 ℃ within 2.5 mins for the 42% fire size, corresponding to a heating rate of 220

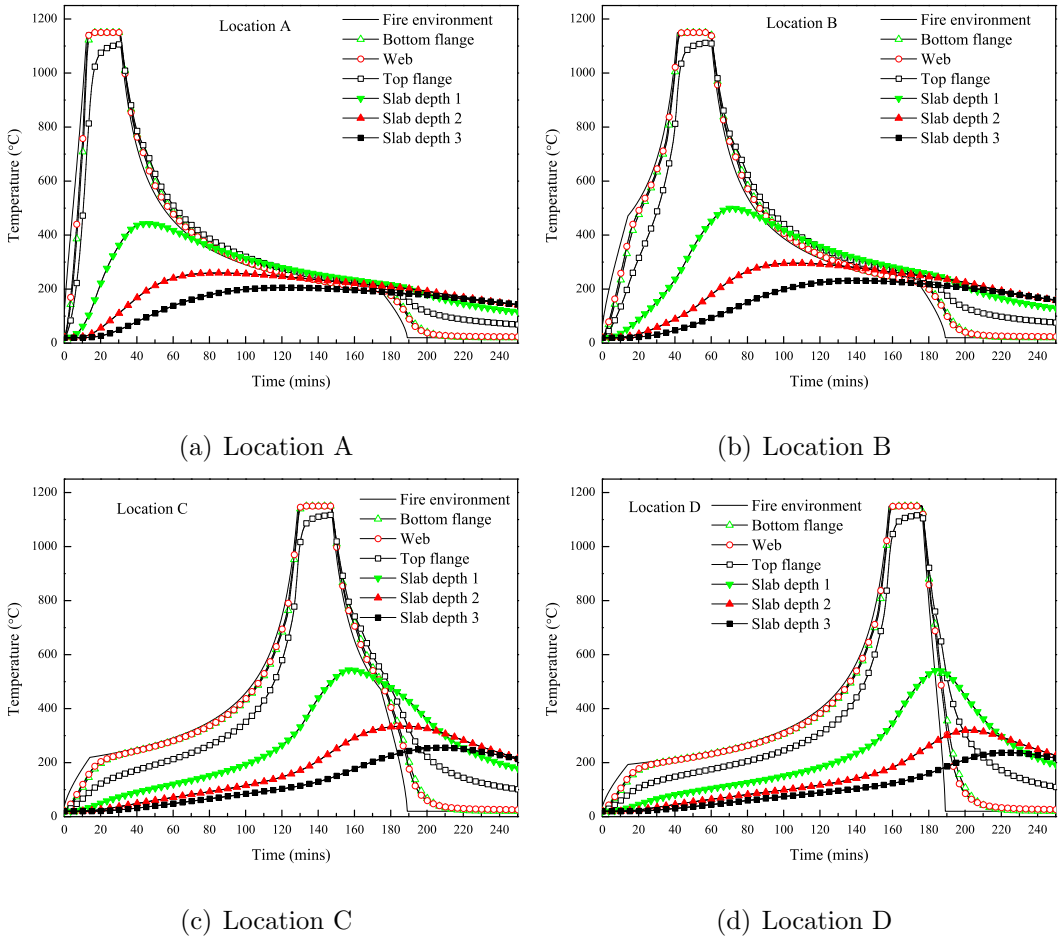


(a) Location A (b) Location B

(c) Location C (d) Location D

**Figure 5.7:** Temperature rise in the composite section subjected to travelling fire (8% of the floor area) at different locations

℃/min. However, it should be noted that global structural fire performance is not simply determined by local critical temperatures, and mechanical interactions between structural members need to be considered as well.

Figure 5.9 shows the variations of peak temperatures in the concrete slab. As shown in the figure, smaller fires such as 4% and 8% fire sizes produce the highest temperatures at every location. This is due to the fact that smaller fires produce lower far-field temperature but burns for much longer time. As given in Table 5.1, the total burning time for the 4% fire is about 7 times as that for the 42%

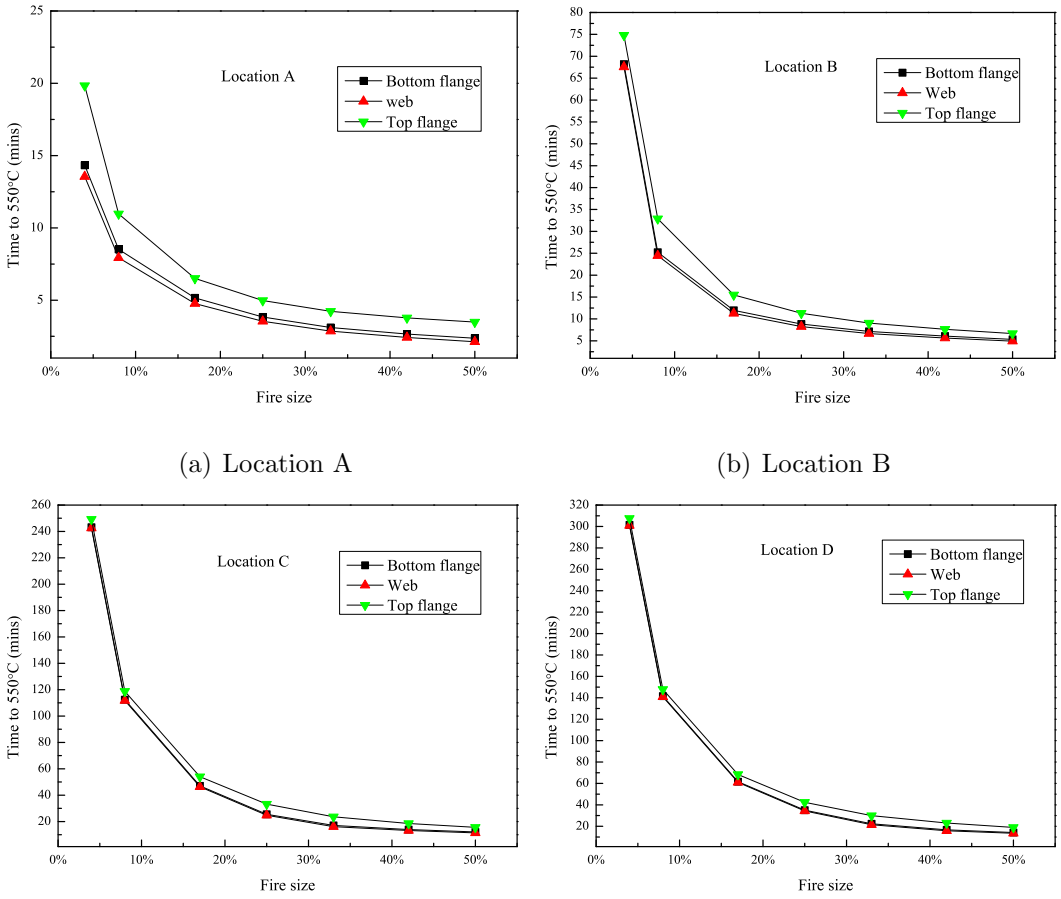


(a) Location A (b) Location B

(c) Location C (d) Location D

**Figure 5.8:** Time taken to reach reference temperature (550 °C) different locations

fire. Plus concrete has very low thermal conductivity, which means more heat would penetrate through the concrete slab subjected to smaller travelling fires. Similar results are also found by Law *et al.* [39], who suggested that smaller fires (10%∼20%) represent an optimum heating balance between far-field temperature and far-field heating duration. Therefore, in light of peak temperature reached in the concrete slab, 4% fires would be the most onerous in the current case study. It is also noted that peak values increase with the distance away from fire origin, as temperatures in Figure 5.9(c) and 5.9(d) are generally higher than the corresponding values in Figure 5.9(a) and 5.9(b), which was also seen in previous

studies for concrete structures [24, 39]. Similar to what we discussed above, this is because that further locations experience a relatively long period of far-field heating prior to the arrival of near-field as shown in Figure 5.7.

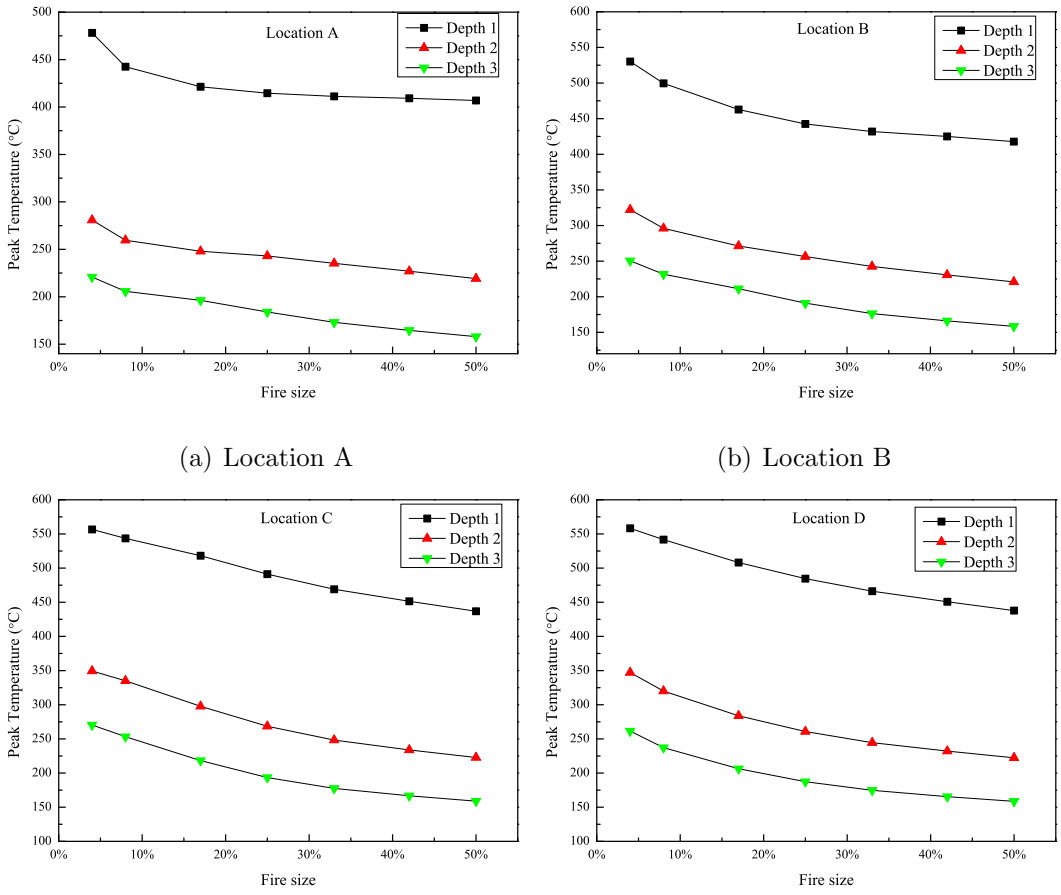


(a) Location A

(b) Location B

(c) Location C

(d) Location D

**Figure 5.9:** Peak temperature in the concrete slab at different locations

#### 5.4.1.2 Through-depth thermal gradient

As mentioned at the beginning of this section, thermal gradient through the depth of the composite floor plays an important role in determining the structural behavior of composite structures. This section examines the effect of travelling

fires on the thermal gradients in composite sections at different locations across the floor plate.

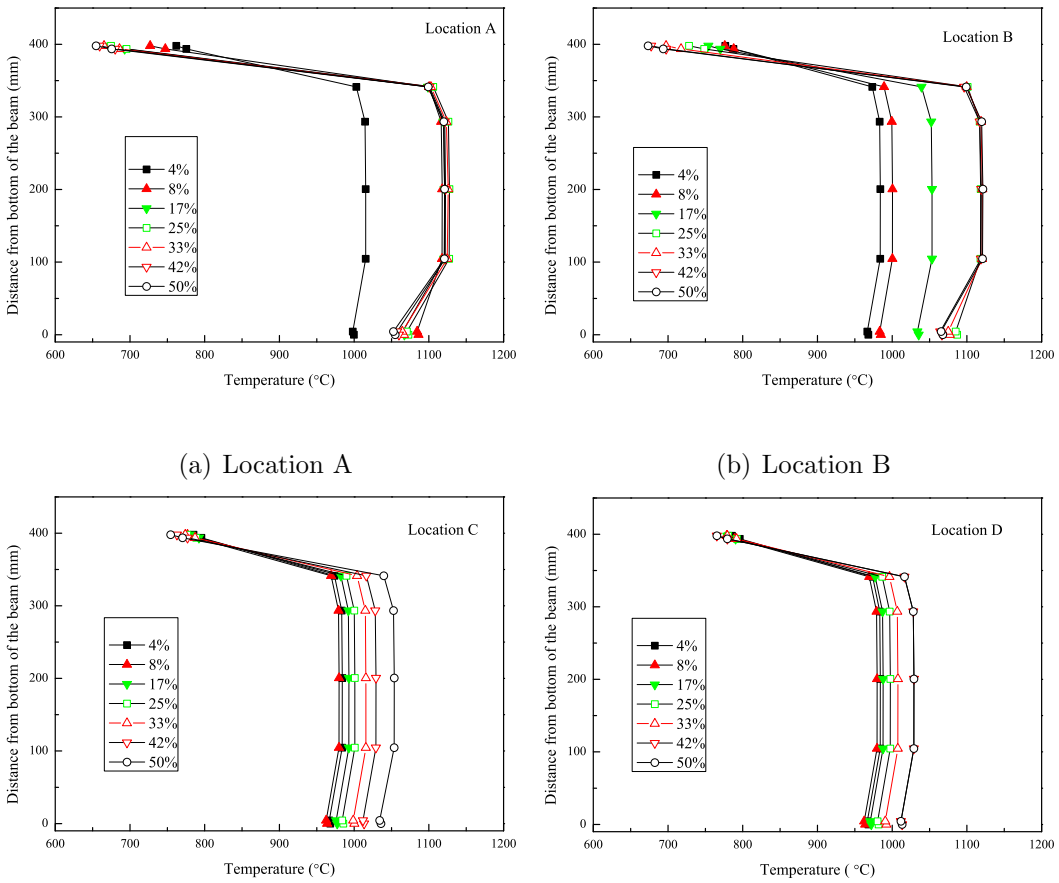


(a) Location A (b) Location B

(c) Location C (d) Location D

**Figure 5.10:** Through-depth temperature profile for the beam at different locations

Figure 5.10 shows the through-depth temperature profiles in the steel section at the four locations, where the gradients can be easily identified. Temperature profile in the section should be transient, and each single profile curve in these figures represents the maximum through-depth thermal gradient in the course of temperature development in the beam section under a specific fire scenario. It is noted that the temperature does not strictly follow a linear distribution across the

whole section depth. Temperatures in the bottom flange and most part of web are relatively close, although with values in the web slightly higher. This is because that the web is normally slightly thinner than the flanges. Large gradients are observed between upper region of the web and the top flange. This is due to the heat sink effect of the concrete slab which has an appreciable effect on the thermal gradient in the beam section, with temperatures in the top flange up to 400 ℃ lower than those in the web. These through-depth temperature profiles indicate that using a uniform temperature distribution or a uniform thermal gradient for the whole beam section may not be realistic. Incorporating this thermal gradient can have significant influence in modeling steel beams in fire [140]. Figure 5.10 also shows that larger fires (25∼50%) produce greater thermal gradient than smaller fires at all of the four locations (more obvious at location A and B). This is because larger fires generate higher far-field temperatures and travel faster across the floor plate. Besides, they have shorter burning durations and thereby structural members are subjected to more intense heating within shorter time. The results are similar to those found in the study of effects of "long-cool" and "short-hot" parametric fires [131], where "short-hot" fires burn out quicker and produces larger thermal gradient through the section depth. It is also noted that the gradients generally decrease with the distance from the fire origin, which makes sense as beams at further locations experience longer and less rapid initial far-field heating.

Figure 5.11 shows the temperature profiles (selected according to maximum overall through-depth gradients) in the concrete slab at different locations across the floor. Unlike those for the steel beam, much steeper gradients are found within shallower regions of the slab, while smaller gradients are found in deeper regions. The through-depth temperature profiles are smoother and demonstrate much

stronger non-linear behaviour compared to those for the steel beam. Temperature gradients seem to be insensitive to the fire sizes at location (A) close to the initial fire origin. At locations further away from the fire origin (B,C,D), fire size has some effects on the thermal gradients indeed, i.e. smaller fire sizes tends to produce smaller gradients but higher temperatures particularly in shallower regions which should be again attributed to the longer initial far-field heating from smaller fires. These spatial variations in temperature profiles seem to be more realistic but can not be obtained by conventional post-flashover fire models which assume uniformly heating throughout the whole compartment.

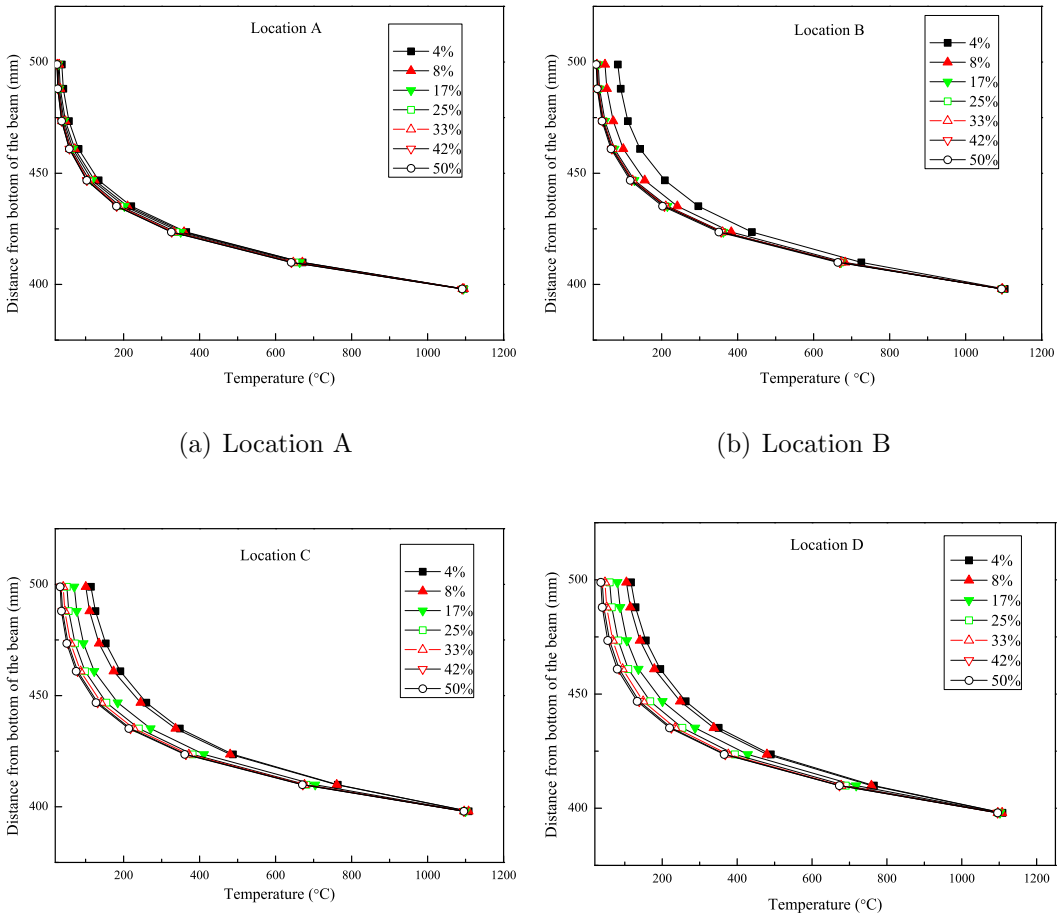


(a) Location A

(b) Location B

(c) Location C

(d) Location D

**Figure 5.11:** Through-depth temperature profile for the slab at different locations

It should be noted that the largest contribution to the thermal gradient in a composite section comes from the difference in mean temperatures between in the steel beam and concrete slab. In terms of its structural effect it can be an order of magnitude larger than the gradients within the beam or the slab on their own.

### 5.4.2 Structural response

It will be interesting to examine the structural response of the structure under different travelling fire sizes as well as to compare them with the parametric fires. Two parametric fires are also considered with the same fire load density as given in Section 5.3.2, but with different ventilation conditions (opening factor 0.0264 $m^{0.5}$ and 0.186 $m^{0.5}$ for the "long-cool" and "short-hot" fires respectively). In all the metrics examined for the building in this work, the structure did not show any sudden collapse bahaviour. So the most onerous scenario that could lead to failure can not be identified for this case study.

#### 5.4.2.1 Results from 2D model

*Global behaviour*

The global structural behaviour under different fire sizes can be seen in Figure 5.12(a) and 5.12(b) for sizes 4% and 50% respectively. The different characteristics of different sizes of travelling fires as well as parametric fires will be discussed. The deflections of the floor at the midspan as well as locations at 3 m (1/4 of the span) and 9 m (3/4 of the span) are shown in Figures 5.13 - 5.15 respectively.

The figures show that the travelling fires examined in this work produced higher deflections at all locations for all the sizes compared to the parametric fires. Concerning the different sizes of travelling fires, it is seen that the smaller fire sizes result in higher maximum deflection ( 2500mm) but at a later time especially as the distance from the fire origin becomes larger (e.g. 3/4 of the span). It is interesting to note also that as the fire sizes become larger (over 25%) the results begin to converge for all the locations. In addition for all locations the "short hot" parametric fire results in higher maximum deflections and faster than the long cool parametric fire. It should be highlighted that deflections are reported here as a structural dimension and does not imply that higher deflections as those seen in case of the travelling fires ( L/5) will lead to failure of the structure. It is wide practice to assume a L/20 deflection limit criterion which is based on furnace tests however this criterion does not imply collapse [126]. Previous research in Cardington demonstrated that composite structures were able to sustain large deflections by using tensile membrane action to carry the loads, although a breach of horizontal compartmentation can occur [126], and that deflections are associated with thermal strains and not with mechanical strains thus do not necessarily imply damage [28, 91].

Figure 5.16 plots the longitudinal displacement at the floor column connection at the fire floor. It can be seen that for all travelling fire sizes as well as parametric fires that the floors initially expand pushing the column outwards (negative direction) and then with the large deflections developing in the floor, the column pulls back inside (positive direction). The parametric fires cause the floor to expand to the same order of magnitude, about 25 mm, compared to the travelling fires at about 15 mm. The parametric fires also cause larger pull back compared to the travelling fires with the "long cool" fire achieving the highest

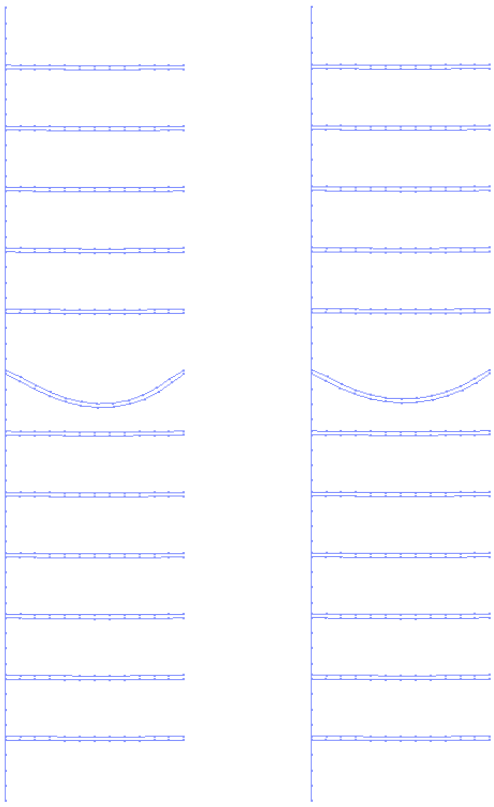

(a) fire size 4% (b) fire size 50%

**Figure 5.12:** Deformed shape under travelling fires of different sizes

value, although much later than other fire scenarios. It should also be noted that the travelling fires reach a similar maximum inward displacement as the "short hot" fire, with the larger fire sizes achieving it earlier than the "short hot" fire. Stability of the column is ensured for all the cases as there is no sudden change.

*Local response*

It would be interesting also to examine the horizontal reactions at the floor connection to the stiff core which represent the variation of the membranes forces during the fire. Figure 5.17 shows the membranes forces of the floor as well as the forces of steel and concrete alone respectively. It can be seen that for both

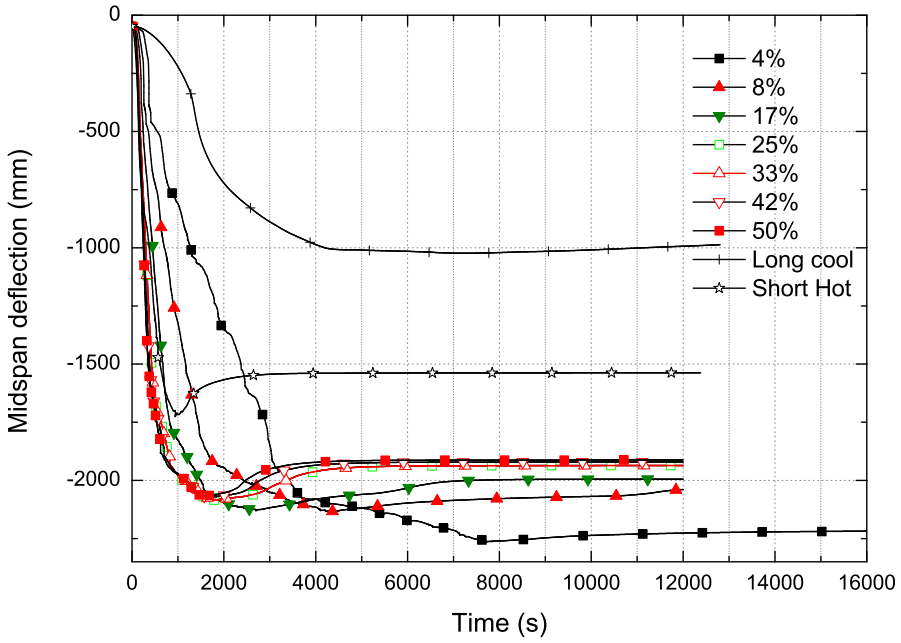


**Figure 5.13:** Deflection at midspan of the composite floor

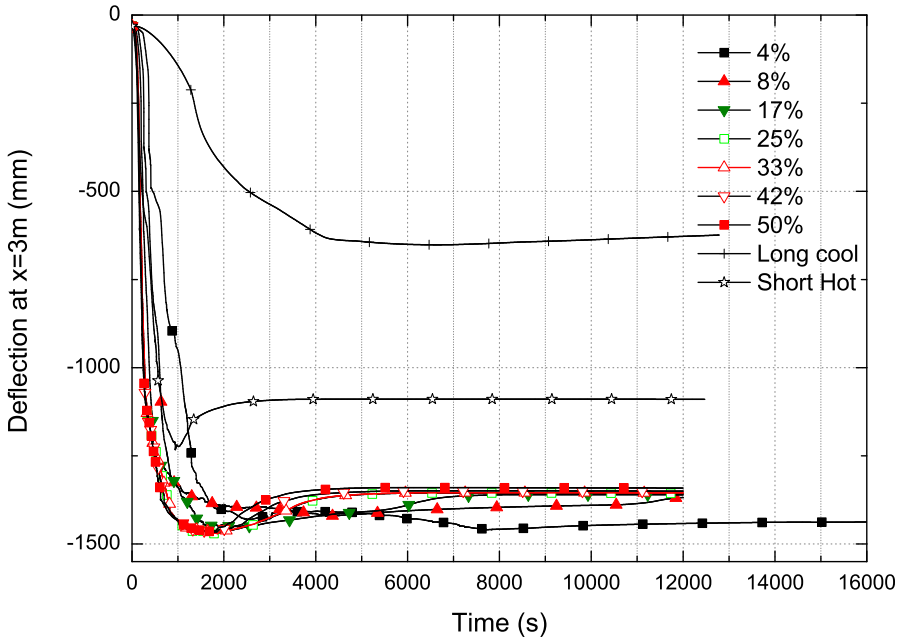


**Figure 5.14:** Deflection at 1/4 of the span of the composite floor

the travelling and parametric fires, the floor is initially in compression and then snaps into tension. The maximum compressive force reached is similar for both

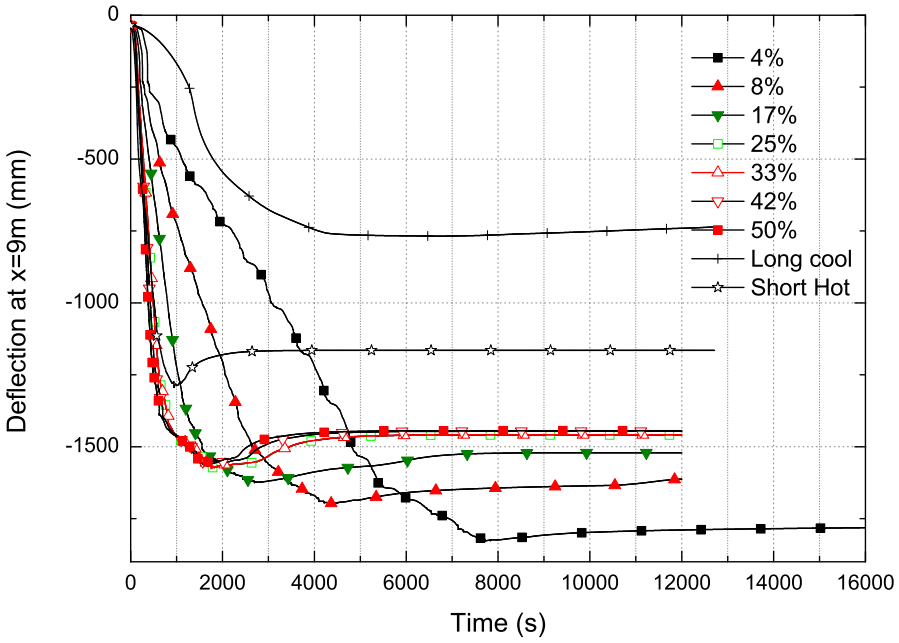


**Figure 5.15:** Deflection at 3/4 of the span of the composite floor

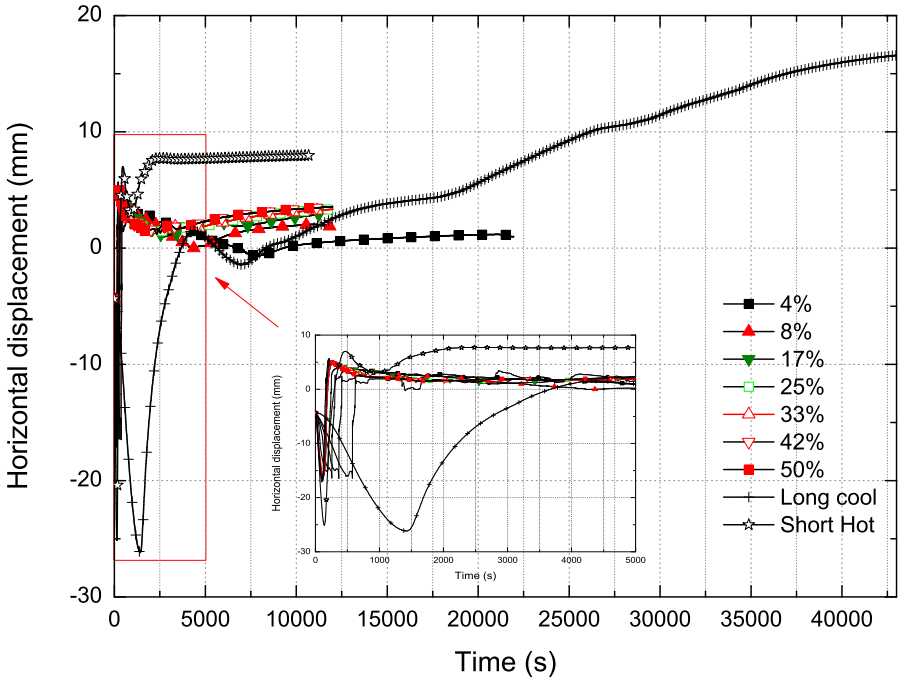


**Figure 5.16:** Horizontal displacement of the composite floor

the parametric fires and travelling fire scenarios with those of the parametric fires being higher. This was expected as in the case of a uniform fire, yielding will take place simultaneously along the length of the steel beam as well as development of plastic strains during simultaneous cooling that cause large tensile forces as the steel beam is regaining its strength [28]. Larger fire sizes lead to quicker transition to tension as well as higher maximum tensile force reached. The "long cool" parametric fire also achieves higher tensile force after 22000 seconds. The axial forces in steel as shown in Figure 5.18 play a major role in the composite response in relation to concrete (Figure 5.19). This is expected as the composite floor is predominantly in tension and since concrete is weak in tension the forces are carried by the reinforcement and the steel beam. It should be mentioned here that reinforcement failure which would be critical in such a scenario is not accounted in the current model as it is outside the scope of the current research work however designers should take this possibility into account.

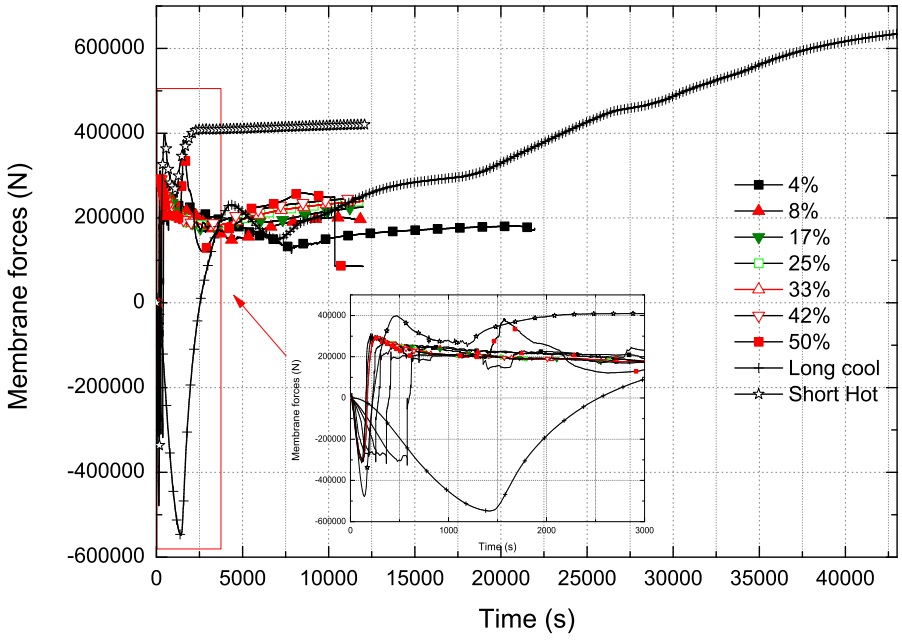


**Figure 5.17:** Membrane forces of the composite floor

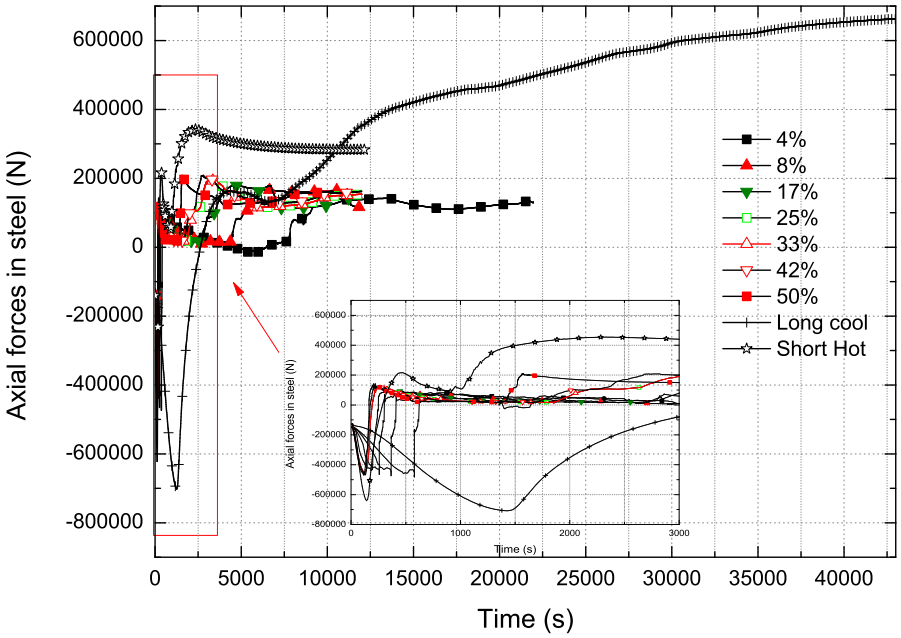


**Figure 5.18:** Axial forces in the steel beam

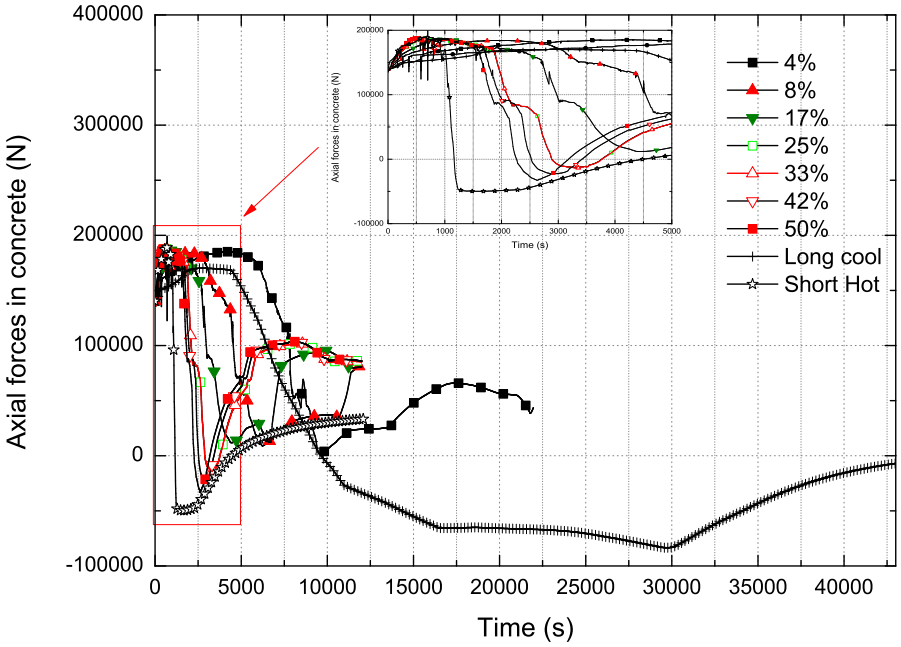


**Figure 5.19:** Axial forces in the concrete slab

Figures 5.20 to 5.22 plot the horizontal displacements at 3 m (1/4 of the span), 6 m (midspan) and 9 m (3/4 of the span). It can be seen that the different travelling

fire sizes show different characteristics along the length of the floor. There is significant horizontal cyclic displacements for the travelling fire scenarios which increase contrary to the fire sizes and that are not seen under parametric fires especially for the locations at midspan and at 3/4 of the span. For the first location (1/4 span), the 4% fire size reaches the biggest maximum positive horizontal displacement while the higher fire sizes reach the biggest maximum negative horizontal displacement. For the other two locations, there is mainly positive horizontal displacement, and smaller fire sizes reach the maximum horizontal displacement.

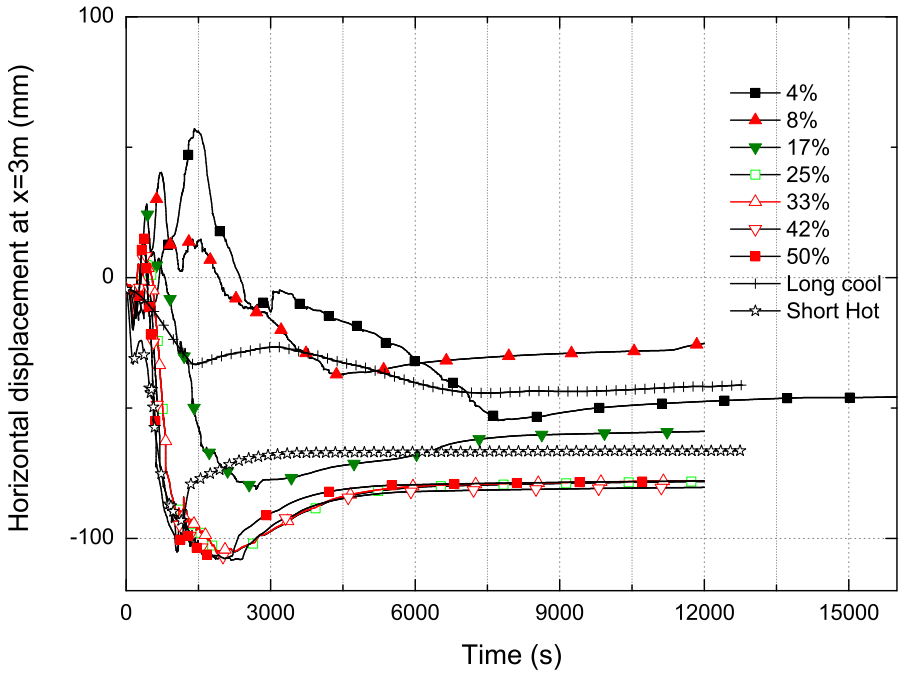


**Figure 5.20:** Horizontal displacement at 1/4 of the span

Due to the fact that a distributed plasticity approach is used in this study and thus each element has five fiber sections along its length with each fiber having its own stress strain relationship history, the plastic deformation of the elements is a more flexible qualitative measure or indicator of damage. The plastic deformation

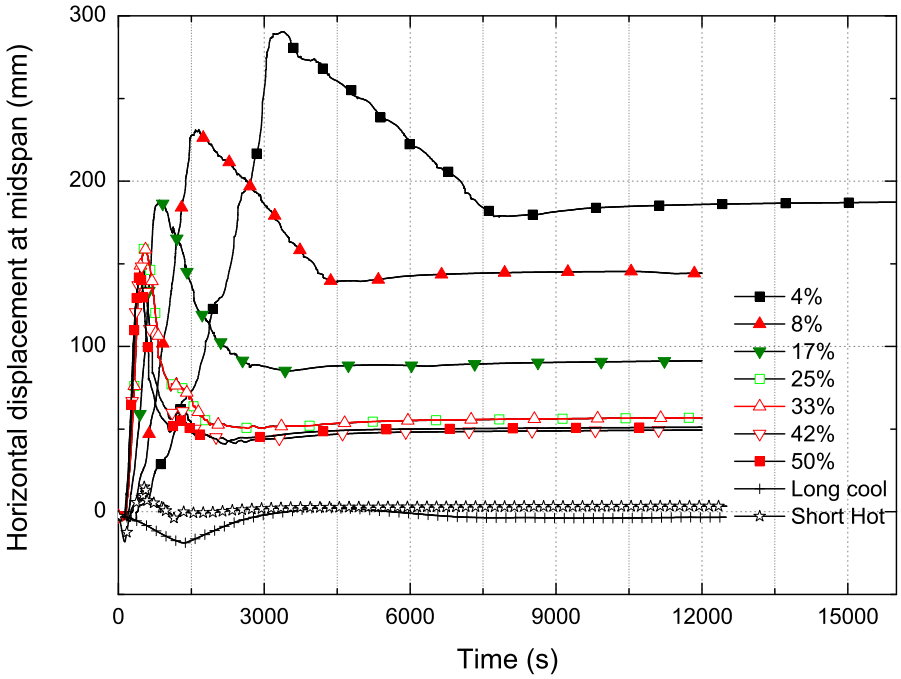


**Figure 5.21:** Horizontal displacement at midspan

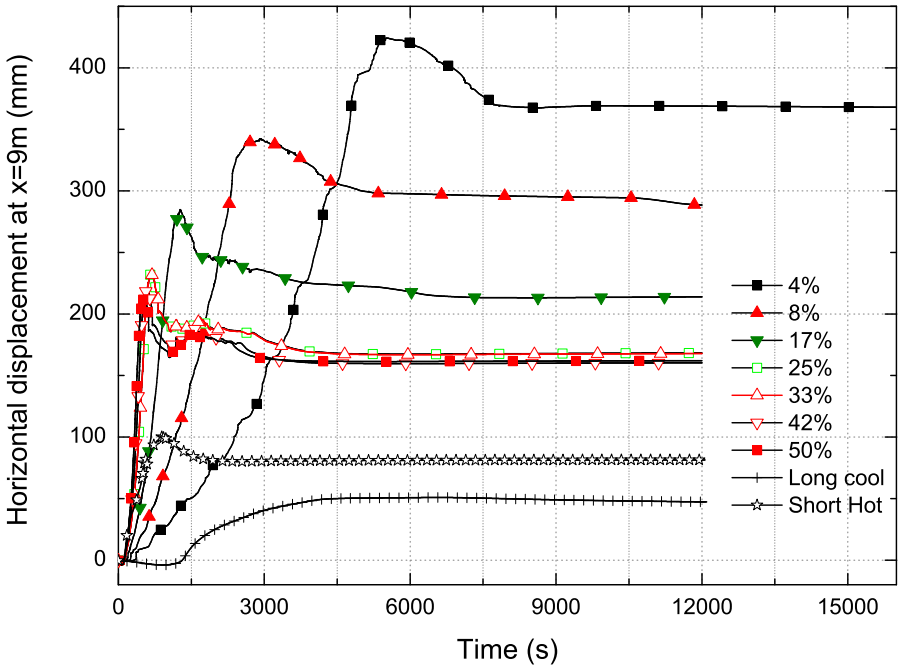


**Figure 5.22:** Horizontal displacement at 3/4 of the span

of the steel beam at locations 1/4 , midspan and 3/4 is plotted in Figures 5.23-5.25 respectively. The plastic deformation presented here follows Eurocode material definition and thus includes creep implicitly. This assumption has been challenged as an explicit inclusion of creep may give a more accurate presentation. However, creep is a type of plastic deformation and it is outside the scope of this research to study this matter in depth. The emphasis is on the differences between certain locations according to the different fires.

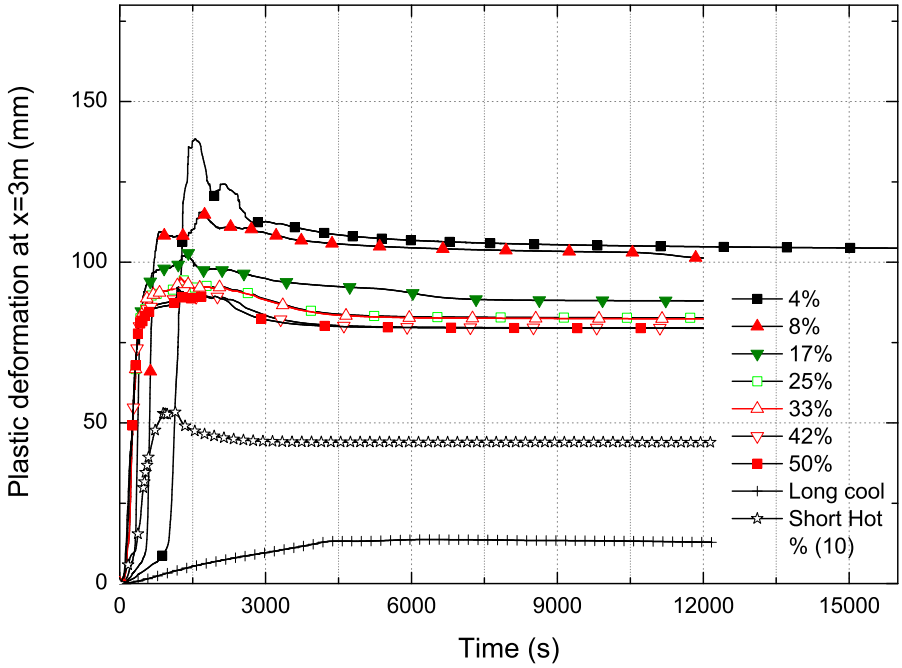


**Figure 5.23:** Plastic deformation of the steel beam at 1/4 of the span

It can be seen that severe plastic deformation occurs along the length of the floor. The plastic deformation is not uniform as it was seen when plotting horizontal displacements. However, contrary to the horizontal displacements, the most onerous plastic deformation here occurs at the place of fire origin (on the left side). This is more firmly seen for the smaller travelling sizes. This is explained because as fire travels the elements subjected to near-field heating yield and also

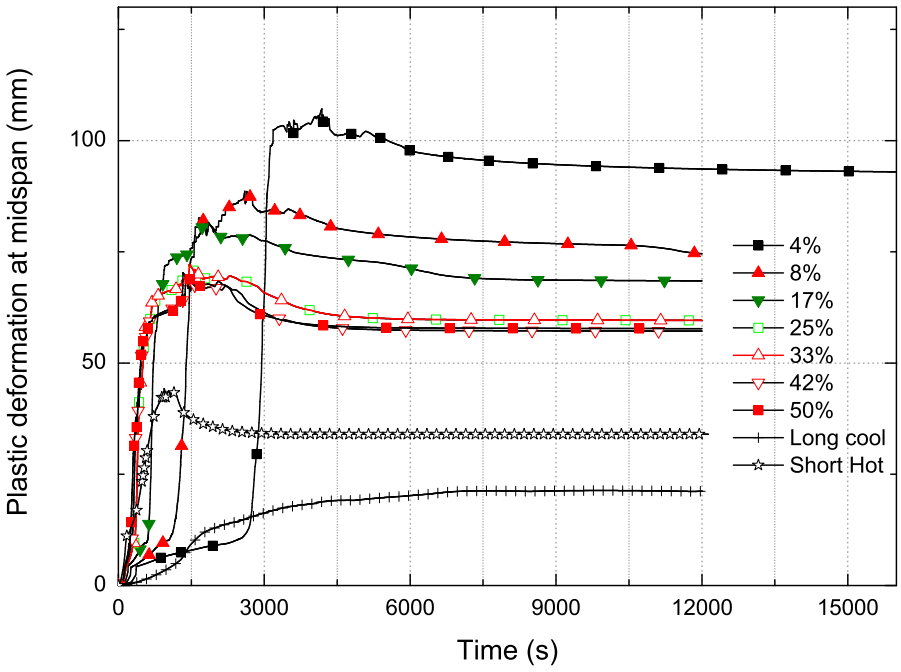


**Figure 5.24:** Plastic deformation of the steel beam at midspan

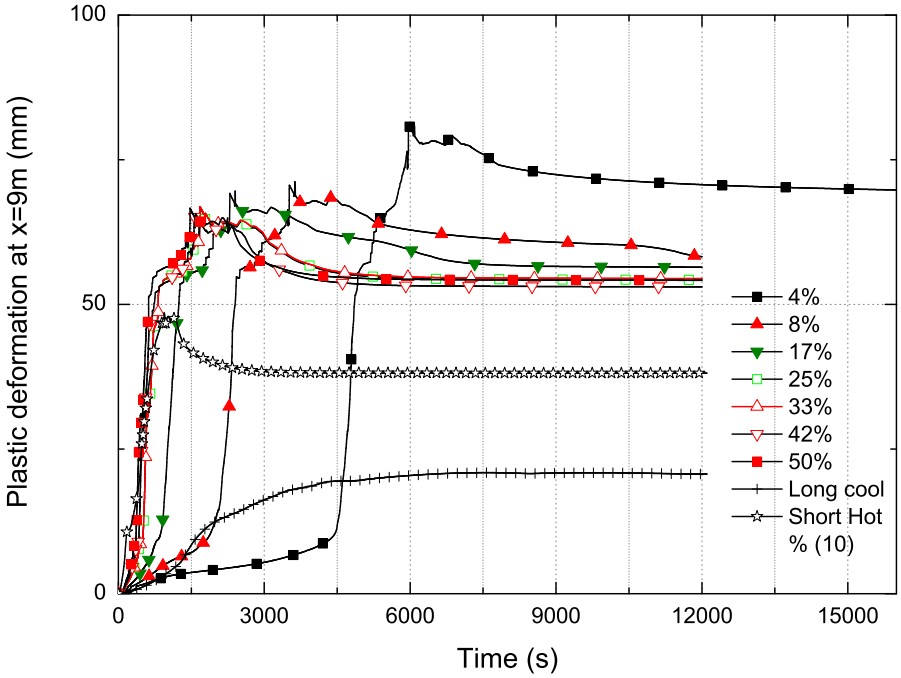


**Figure 5.25:** Plastic deformation of the steel beam at 3/4 of the span

expand against their neighboring elements on the right that are just subjected to less intense far-field heating. This process generates even higher stresses for the near field elements especially for travelling fires of smaller sizes that it takes longer time for neighboring elements to reach similar temperatures.

Moreover, previous research during Cardington experiments [28] illustrated that deflections depend on the total strains and arise from thermal expansion strains. Thus high deflections commonly seen in fire were not strictly associated with mechanical strains and thus damage to the structures. The results demonstrate that these findings do not hold for non-uniform travelling fires when comparing different sizes between them, however for the same fire size the less deflected size on the left has higher plastic deformation than the more deflected right part of the floor.

These analyses can also provide guidance in the context of local failure and repair after a fire, although this work is not getting into detail on this aspect. This information is also useful to insurers that are interested in performance-based criteria when determining possible damage levels in fire in order to quantify insurance premiums. Further research will be required to examine these behaviors in other structural layouts such as trusses where possible buckling of a diagonal may take place or cellular beams.

#### 5.4.2.2 Results from 3D model

Based on the results obtained from the two-dimensional model shown before, it was decided that a selection of representative fire sizes can be adequate in representing the majority of possible scenarios. These were selected to be a small

fire size of 4%, a medium fire size of 25% and a large fire size of 50%. The fire size is a major component in the travelling fire methodology. The properties for these fire sizes can be seen in Table 5.2.

| $A_f$(m$^2$) | Fire size | $L_f$(m)(Eq. (5.3)) | $\dot{Q}$(MW) | $t_{total}$(min)(Eq. (5.5)) | $s$(m/min)(Eq.(5.4)) |
|---|---|---|---|---|---|
| 48 | 4% | 1.5 | 23 | 364.0 | 0.1 |
| 288 | 25% | 9 | 138 | 72.8 | 0.6 |
| 576 | 50% | 18 | 276 | 43.7 | 1.2 |

**Table 5.2:** Selected travelling fire scenarios

The results produced from the grillage model can be seen in Figures 5.26 to 5.31.

Figure 5.26 compares the midspan deflection for the travelling sizes examined against the parametric fires. It can be seen that the travelling fires produces higher deflections than the parametric fires. It should be kept in mind though that the maximum temperature reached in travelling fires was higher (1150 ℃). The maximum deflection reached was similar for all travelling fire scenarions, but for the smaller fire size the time it was reached was later. Compared to the two-dimensional model, smaller maximum deflections are observed but the trends are the same.

The horizontal displacements at the column level can be seen in Figure 5.27. It is observed that for the parametric fires, the fire floor expands and the columns pull-in more more than for the travelling fires. The column horizontal displacements are very similar to those of the two-dimensional model.

The behaviour of the horizontal displacements at the columns shows the same trend, as expected, with the floor membrane forces plotted in 5.28. The

parametric fires produce larger maximum compressive and tensile forces compared to the travelling fires.

Figures 5.29, 5.30, and 5.31 plot the plastic deformations for the different fire scenarios at 1/4 of the span, midspan and 3/4 of the span respectively. These plastic deformations can be considered as a damage indicator for the steel beam. The results suggest, similarly to those of the two-dimensional study (Figures 5.23 to 5.25), that travelling fires produce larger plastic deformations in the steel beam compared to the parametric fires. In these Figures there are also some differences observed with those of the two-dimensional model. More specifically, in the two-dimensional model the smaller fire size (4%) produced the largest plastic deformation along the whole beam, while in the three-dimensional model the smaller fire size (4%) procuces the most onerous response near the column which is also the fire origin while the medium fire size (25%) produces the most onerous response in the midspan and at 3/4 of the span. Moreover, the maximum plastic deformations of the three-dimensional models are lower that those of the two-dimensional model for all the fire scenarios.

The two-dimensional study predicted edequately the trends of the structural behaviour when compared to the grillage model. The prediction of the column horizontal displacements and forces were almost identical (with the 3D model resulting in marginaly higher displacements than the 2D model) to that of the grillage model although the deflections were larger. Moreover, the two-dimensional model showed that the smaller fire sizes had greater plastic deformation all along the floor, while the grillage model showed that this is only the case for the some part of the floor (near the columns) while other locations did not have big variation in maximum plastic deformations achieved for different fire sizes with the

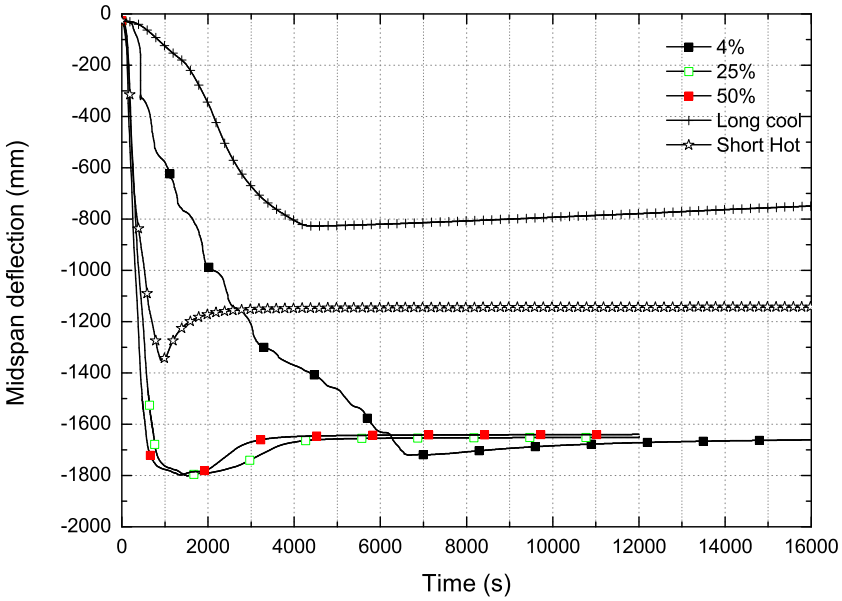


**Figure 5.26:** Midspan deflection of the fire floor

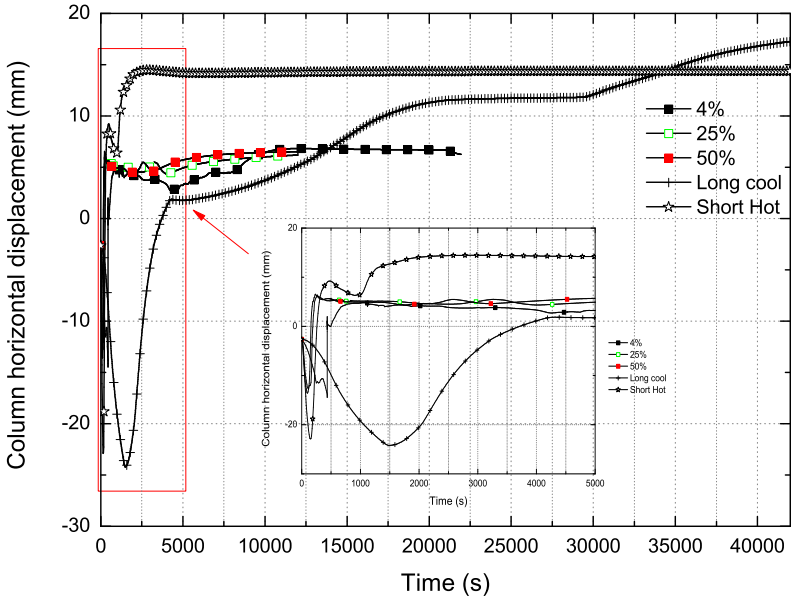


**Figure 5.27:** Horizontal displacement of the 4th floor

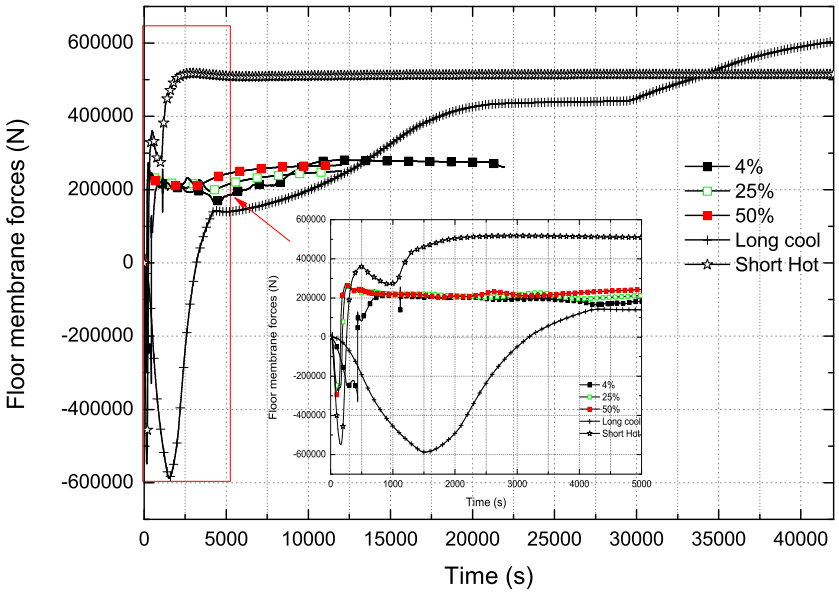


**Figure 5.28:** Membrane forces of the 4th floor

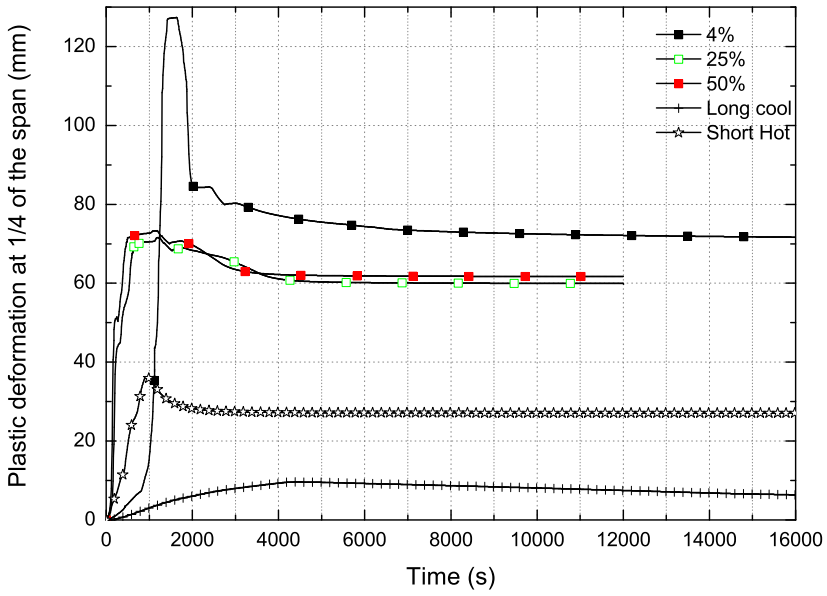


**Figure 5.29:** Plastic deformation at 1/4 span of the 4th floor

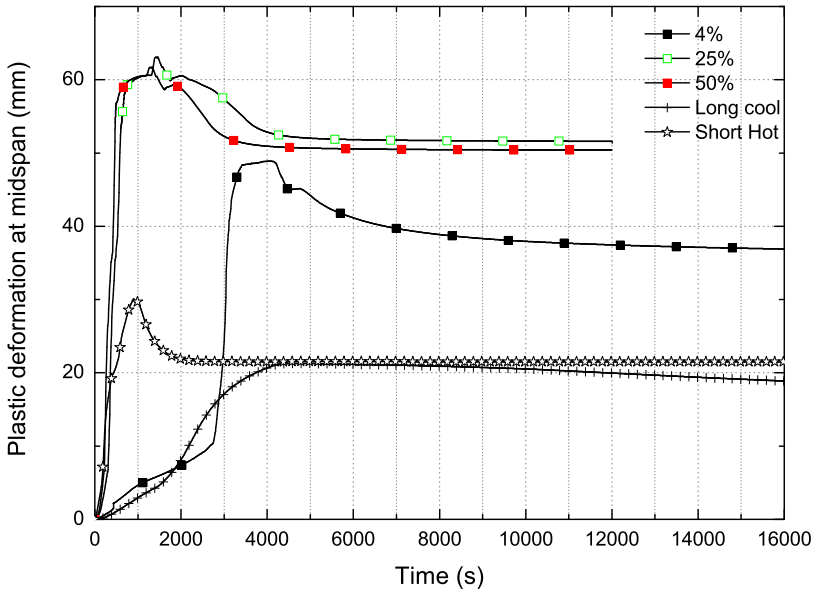


**Figure 5.30:** Plastic deformation at midspan of the 4th floor

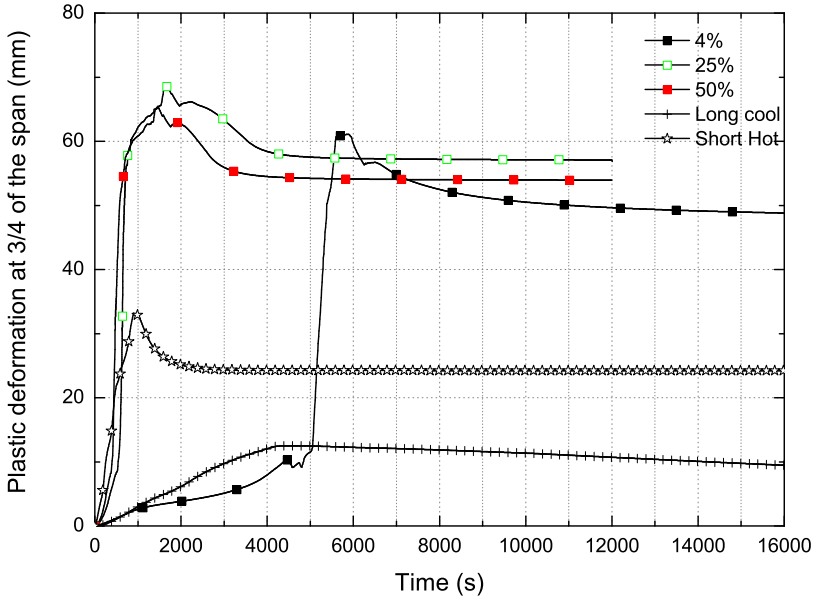


**Figure 5.31:** Plastic deformation at 3/4 of the 4th floor

medium fire size having the largest. However, both models showed that the plastic deformations under travelling fires were larger than parametric fires.

## 5.5 Conclusions

The travelling fire methodology for structural fire design has been implemented in the OpenSees software framework. A case study has been carried out to examine both the thermal and structural responses of a composite structure in travelling fires. This case study examines a generic tall building which represents the typical characteristics found in modern construction.

The following are some of the major findings from the thermal analysis: (1) Traditional thinking of fire severity in light of "equal area" concept seems to be invalid for travelling fires. Fire temperature curves at symmetric locations were supposed to have identical fire severity according to the "equal area hypothesis" but lead to temperature differences of up to 102% at these locations in the composite floor. (2) Travelling fires of larger sizes lead to lower times to reach critical steel temperature. (3) Travelling fires of smaller sizes (and hence of longer burning times) produce higher peak temperatures in the concrete slab. (4) Thermal gradients are created in the upper regions of the beam due to the presence of neighboring concrete slab, and larger fires produce higher thermal gradients. (5) Large through-depth thermal gradients are observed in concrete slab. Smaller fire sizes tend to produce smaller gradients but higher temperatures at locations further away from the fire origin.

For the structural response of the building examined in this work, a two-dimensional and a three-dimensional grillage model were used. For both models travelling fires produced larger midspan deflections than the parametric fires. For the two-dimensional model travelling fires of smaller sizes produced the most onerous responses (in terms of deflection), although later in time while for the three-dimensional model a similar maximum midspan deflection was reached for all fire sizes. However, it should be noted that deflection is not the only criterion as it does not necessarily imply failure of the structure. The membrane forces in the floor were also monitored for all the cases. The composite floor was initially in compression and then snapped into tension where steel was taking most of the axial forces for the rest of the time. The results showed that the parametric fires resulted in higher compressive and tensile forces compared to the travelling fire scenarios. Larger cyclic horizontal displacements were also seen for the travelling cases that were not seen in the uniform parametric fires. Moreover, larger plastic deformations were observed for the travelling fires compared to the homogeneous parametric fires that could be an indicator of greater damage. In the two dimensional model larger plastic deformations were observed for the smaller sizes all along the floor while in the three dimensional model this was observed for the locations near the column with the other locations to have small variation in plastic deformation with higher sizes having more. This also implied that deflections may not always be an accurate representation of damage as seen during the Cardington tests [28].

The results of this study challenge the usual assumption that uniform post-flashover fires are always more conservative. Travelling fires which are non-homogeneous fires are seen to produce different structural behaviour which could not be predicted using uniformly burning fire models. Consequently,

taking into account that homogeneous fire models like the parametric fires are unrealistic in large compartments, designers should examine the response of open plan tall buildings using a travelling fire methodology to address any potential vulnerabilities that may arise. Hence designers of complex and innovative structures are advised to perform a parametric analysis by varying the fire sizes and ensure robustness for each scenario according to the predicted behaviour. This approach is similar to that in earthquake engineering where near field and far field earthquakes have different characteristics in terms of resulting structural performance and any of them can be more onerous depending on the structure type. It should be mentioned here that this study concentrated on a structural form of a conventional and generic tall building. It would be interesting also to examine the effect of travelling fires in different and larger structural layouts where they could potentially have an even bigger influence.

# Chapter 6

# Effect of multifloor horizontally travelling fires

## 6.1 Background

There is an increasing demand on the use of performance based structural fire engineering by architects and engineers for the design of innovative complex and large structures for ensuring structural safety and optimising fire protection of structures. However, in order for performance based structural fire engineering to be used in practise effectively, *realistic* fire conditions must be taken into account. In the unlikely scenario that sprinklers malfunction in a tall building, previous fire disasters have shown that fire will travel *horizontally* across the floor plate and also *vertically* to other floors than the floor of origin. However despite this fact, currently there is no research study to the authors' knowledge looking at the behaviour of a structure under a combined horizontally and vertically travelling

fire scenario. This chapter will provide an understanding of the structural behaviour of a generic composite tall building under such a scenario.

## 6.2 Travelling fires

The description of the horizontally travelling fire methodology was given in detail in Chapters 2 and 5 and thus there is no need in reproducing it here in detail. The horizontally traveling fire methodology produces spatially and temporally varying heating conditions across the floor plate. As the fire travels across the floor, the thermal environment can be divided into two horizontal regions, namely, "near field" and "far field", with reference to the fire source at any time interval [24].

Modelling of the actual process of vertical fire spread can be complicated by a number of factors, such as the geometry of the facade, material properties of wall insulations, the shape of openings [4] , the fire resistance of the glazing, the ambient atmosphere and the type of occupancy. Previous work (Chapter 4) has simplified the problem for structural fire analysis by recognising that post-flashover fires can develop at different time intervals for different floors, thus a simple parameter, time delay ($\Delta t_{delay}$), has been introduced. Similarly, this approach is followed here for the consideration of the combined effects of both vertically and horizontally travelling fires on the structural response. Two typical limiting values are used, i.e. 300s and 3600s, that cover a possible range of vertical fire spread time from one floor to its upper adjacent neighbour. The lower bound of $\Delta t_{delay}$ corresponds to rapid fire spread along vertical directions while longer one for slower fire spread. The spread rate may be affected by the material properties and thickness of the wall linings or insulation layers. Detailed

discussions on these are not considered here as the focus is on global structural behaviour and the use of a time delay to represent vertical fire spread suffices for this purpose. Note in this work vertical fire spread is considered only along the west wall of the structure in order to avoid the otherwise over complexity being involved. The vertical travelling spread and horizontal travelling spread can be significantly different and they have no direct correlations as the types of fuel along the wall and across the floor can differ considerably.

The number of floors on fire is also a critical uncertainty when considering a structure under multifloor fires. In this work, a three floor fire scenario is assumed in all cases. This is consistent to previous work carried out by [61, 137, 89] that considered three floor fire scenarios and demonstrated that possible collapse may arise when three plastic hinges develop in a column due to the pull-in of the floor developing a mechanism. Assuming a three fire floors scenario, makes it possible to compare all the possible combinations against this collapse criterion, which does not imply by any means that these plastic hinges develop only when three floors are on fire, but can develop with more or less floors on fire too as seen in Usmani *et al.* [58] where several scenarios involving different floors on fire were considered for the WTC towers and demonstrated the same mechanism.

## 6.3 Structural modelling

In this chapter a three dimensional *grillage model* has been employed in order to understand the structural behaviour under vertically and horizontally travelling fires. Since rigid restraints do not exist, extra floors other than the fire floors have been added to the model to represent the stiffness of the surrounding structure

better. A representation of *seven* stories is selected for this study with appropriate boundary conditions to simulate a section through the height of a tall building. The layout of the building examined is regular and thus a suitable representation of the floors and columns was used to create the model. Columns are assumed to have the same cross section through the whole height for the seven storeys modelled here. Table 6.1 displays the dimensions of the structural members that were used in this parametric study. Figure 6.1 also demonstrates a section of the composite floor across its longitudinal direction.

| *Member* | *Depth(mm)* | *Breadth(mm)* | *Flange(mm)* | *Web(mm)* |
|---|---|---|---|---|
| Column | 381 | 394.8 | 30.2 | 18.4 |
| Primary beams | 398 | 141.8 | 8.6 | 6.4 |
| Secondary beams | 398 | 141.8 | 8.6 | 6.4 |

**Table 6.1:** Structural dimensions of the steel members

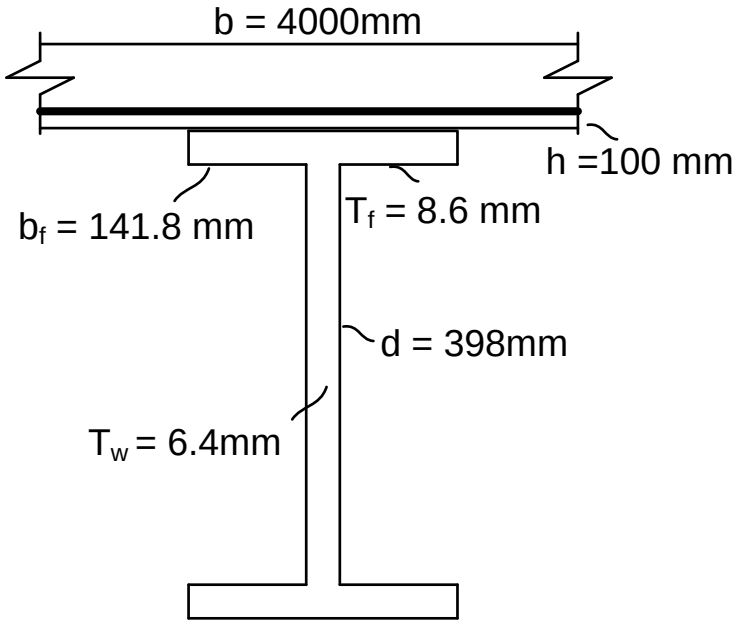


**Figure 6.1:** Composite slab in the longitudinal direction

### 6.3.1 Grillage model

A *grillage* model is a three dimensional structural model where all the structural members are represented using *beam-column* elements. The developed displacement-based beam-column elements discussed in Chapter 3 are used in this work. These kind of models have been used in the past for modelling the Cardington experiments at the University of Edinburgh [141, 91] and Imperial College [142, 143, 31] and have been found to predict the overall structural behaviour of a composite floor in fire well although they cannot capture the actual interaction between the membrane forces and bending, and in-plane shear stiffness of the slab cannot be modelled [144, 145]. Grillage models have been used in the past in order to assess the progressive collapse of composite tall buildings after sudden column loss [146, 147]. In this chapter such a grillage model is employed, since the structure that is examined is generic and thus trends are more important than the actual response [31]. A grillage model also provides a computationally efficient method of capturing the overall trends of global structural behaviour under horizontally and vertically travelling fires. A schematic of the grillage model as used can be seen in Figure 6.2 while the OpenSees finite element model can be seen in Figure 6.3 and the same model is shown in plan view in Figure 6.4.

### 6.3.2 Boundary conditions

The seven storey model used here is assumed to represent a slice of a *generic composite* tall building, hence appropriate *boundary conditions* have to be defined. For the columns, at the top and at the bottom of the model half of the column

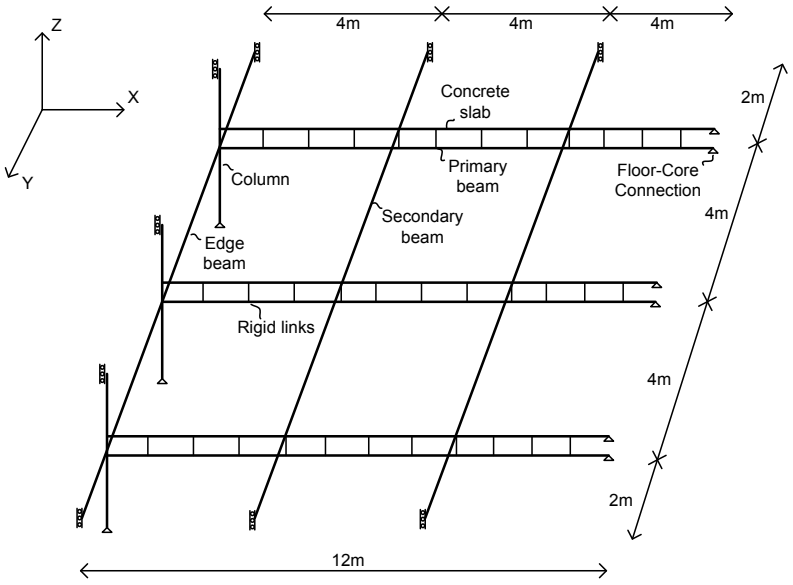


**Figure 6.2:** Schematic of grillage model for one floor

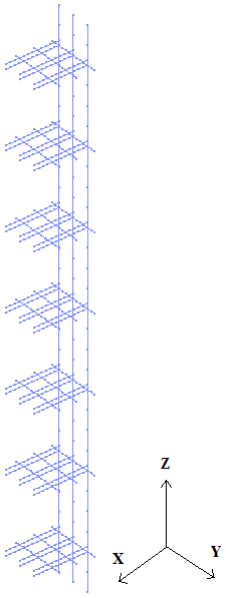


**Figure 6.3:** Grillage finite element model in OpenSees

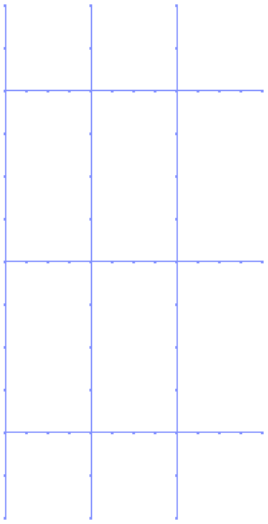

**Figure 6.4:** Finite element model representation in plan

is modelled due to symmetry, thus at the column top all translational degrees of freedom are assumed to be free as well as the rotational degree of freedom along Z axis, and similarly for the bottom of the column but the degree of freedom along the height (Z axis) is constrained. This can be seen graphically in Figure 6.5(a) for the top of the column. The axis follow the same pattern as in Figure 6.2.

At the end of the secondary beams, again due to symmetry, half of the end secondary beams is modelled, thus the end conditions are representing the midspan of the secondary beams. This implies that the nodes at these locations are allowed to displace horizontally and vertically (perpendicular to the floor plane) as well as rotate along the Y axis. This is again illustrated graphically in Figure 6.5(b).

The connection of the composite floor to the core is assumed to be a fixed connection since the concrete core is assumed to be totally rigid, not allowing any translations or rotations. Hence, possible connection failure at the core (or at

any other location) is not taken into account explicitly as it is outside the scope of the current work but this should be considered in a performance based design, if considered important.

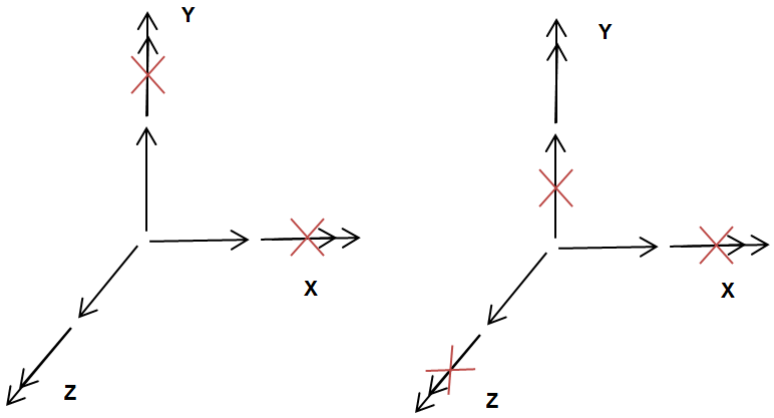


(a) At the top of the column (b) For the secondary beams

**Figure 6.5:** Representation of the boundary conditions of the model

### 6.3.3 Element connectivety

Where structural members or degrees of freedom (dofs) are connected they can be modelled using multi-point constraints. These multi-point constraints in OpenSees can be assigned using a *rigidlink* or an *equaldof* command. The *equaldof* command makes all of the degrees of freedom specified by the user to be exactly equal between the master and slave node (the constraint matrix has only diagonal terms of value equal to one), while the *rigidlink* command is in fact representing the presence of a very stiff element by adding also off diagonal terms that take into account the distance between the two nodes. In OpenSees a nodal degree of freedom can have multiple slave degrees of freedom but there can be only one master degree of freedom or node. For this work, the primary steel beams have

been considered to be the master nodes for the multi-point constraints in all cases when tying their dofs with those of the concrete slab, secondary steel beams, edge steel beam and steel columns.

### 6.3.4 Materials

For both models, the beams and columns are assigned the developed *Steel01Thermal* material which is representing a bilinear stress-strain relationship with a yield stress of 300 N/mm$^2$ and a modulus of 210 GPa. The reinforced concrete slab was assigned with the uniaxial material *Concrete02Thermal* adopting a modified Kent and Park model [138] with a compressive strength of 20 N/mm$^2$ and reinforcement using the *Steel01Thermal* material with a yield stress of 475 N/mm$^2$ and a modulus of 210 GPa.

### 6.3.5 Mechanical loads

A gravity loading of 6kN/m$^2$ is assumed for the slab, representing both the dead and live load. A value representing load transferred from storeys above the modelled floors was also specified at the vertical degree of freedom at the top of the columns.

### 6.3.6 Analysis procedure

The analysis procedure is the same to the one described in Chapters 4 and 5. A dynamic analysis is performed as a second load step after the gravity analysis.

All the output presented in this work is plotted against time, which is real time in this case since a transient analysis is performed and not temperature which is often the control parameter when static analysis is performed.

## 6.4 Parametric study with multiple floor fires

The structural behaviour of a generic composite building under a single floor horizontally travelling fire was examined in the previous Chapter. The results of the study demonstrated that there was greater damage in case of travelling fires, especially for smaller fire sizes. Travelling fires also reached higher maximum temperatures, however the membrane forces in the composite floor were lower for the travelling fire scenarios compared to the parametric fires. This suggests that although greater damage can be caused to the composite floor, this will not necessarily lead to the types of collapse mechanisms discussed in this thesis in Chapter 4. Thus, it is of interest to examine, whether the parametric fires that produce the highest membrane forces in the floor are also the most severe fires against a collapse scenario involving multiple floors on fire. In order to investigate the effect of the combined scenario of horizontally and vertically travelling fires, a parametric study is performed. The following horizontally and vertically travelling fire scenarios have been considered (as seen in Table 6.2). These represent a series of different representative scenarios.

| Scenario | Description |
|---|---|
| 1 | Three floors simultaneously heated with 4% floor area burning |
| 2 | Three floors simultaneously heated with 25% floor area burning |
| 3 | Three floors simultaneously heated with 50% floor area burning |
| 4 | Three floors (rapid time delay) heated with 4% floor area burning |
| 5 | Three floors (rapid time delay) heated with 25% floor area burning |
| 6 | Three floors (rapid time delay) heated with 50% floor area burning |
| 7 | Three floors (slow time delay) heated with 4% burning area |
| 8 | Three floors (slow time delay) heated with 25% burning area |
| 9 | Three floors (slow time delay) heated with 50% burning area |
| 10 | Three floors simultaneously heated with a short hot fire |
| 11 | Three floors simultaneously heated with a long cool fire |

**Table 6.2:** Scenarios for horizontally and vertically travelling fires

### 6.4.1 Simultaneous scenarios

An indicative deformed shape for the 50% fire size can be seen in Figure 6.6. The results of the parametric study for the simultaneous fires can be seen in Figures 6.7 to 6.12. Figure 6.7 plots the midspan deflection of the middle fire floor for all the scenarios. The deflection pattern is similar to that seen previously for the single floor fire in the previous Chapter. The same pattern is also observed in the midspan deflections of the top fire floor in Figure 6.8.

The horizontal displacements at the columns at the middle fire floor level and top fire floor level (which presents a similar response as the bottom fire floor due to symmetry since this is a simultaneous scenario) are plotted in Figures 6.9 and 6.10 respectively. The pattern is similar in both floors. It can be observed

that the parametric fires cause greater thermally induced deformations than the travelling fires. After the pull-in of the column, the *short-hot* parametric fire produces the most demanding response (by resulting in larger column horizontal displacements) and the *long-cool* parametric fire the least demanding response with travelling fires in the middle. Between the travelling fire sizes the variations are not large, but for larger fire sizes, the maximum horizontal displacement is reached quicker.

The membrane forces in the floors are plotted in Figures 6.11 and 6.12 for the 4th and 5th floor respectively. These membrane forces can be obtained by summing the reaction forces of the steel beam and concrete slab at their connection with the rigid core. It is observed that the "short hot" fire produces the largest compressive and tensile forces. The travelling fires produce similar response for all the sizes. The larger sizes reach their maximum tensile force earlier than the smaller ones. The "long cool" fire produces lower tensile forces than the travelling fires.

### 6.4.2 Rapid vertically travelling scenarios

Figures 6.13 to 6.19 demonstrate the findings for the scenarios involving rapidly travelling fires with an inter-floor time delay of 300s. Figures 6.13, 6.14 and 6.15 plot the horizontal displacements at the floor-column connection for the bottom, middle and top floor respectively. The behaviour for all fire sizes is comparable but the middle floor pulls-in more as expected. Compared to the simultaneous scenario presented earlier, it can be seen that the short inter-floor time delay does not influence significantly the maximum displacements reached although these are

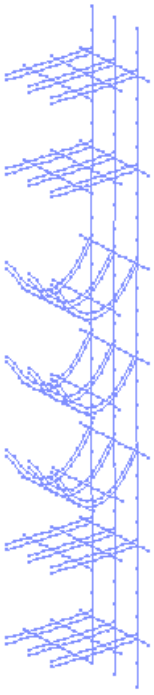

**Figure 6.6:** Deformed shape for the 50% fire size

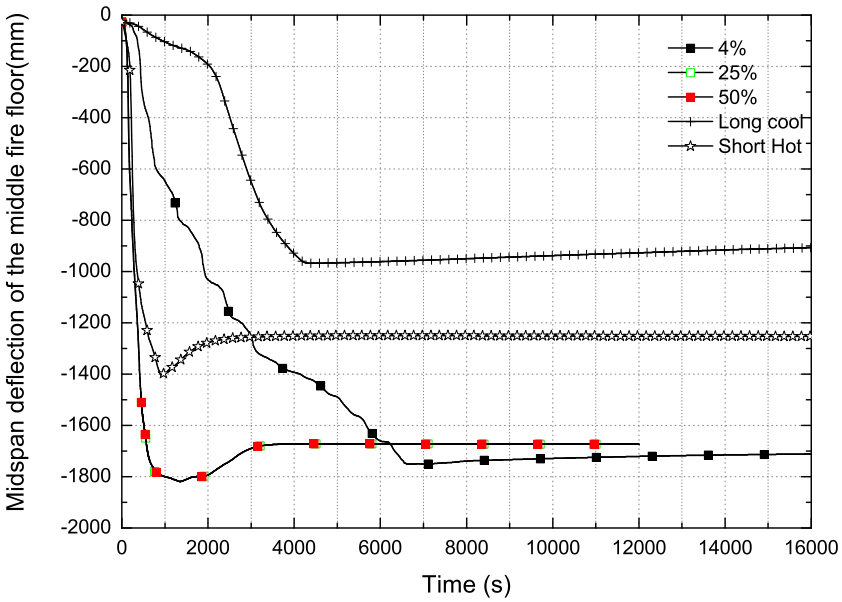


**Figure 6.7:** Midspan deflection of the middle fire floor

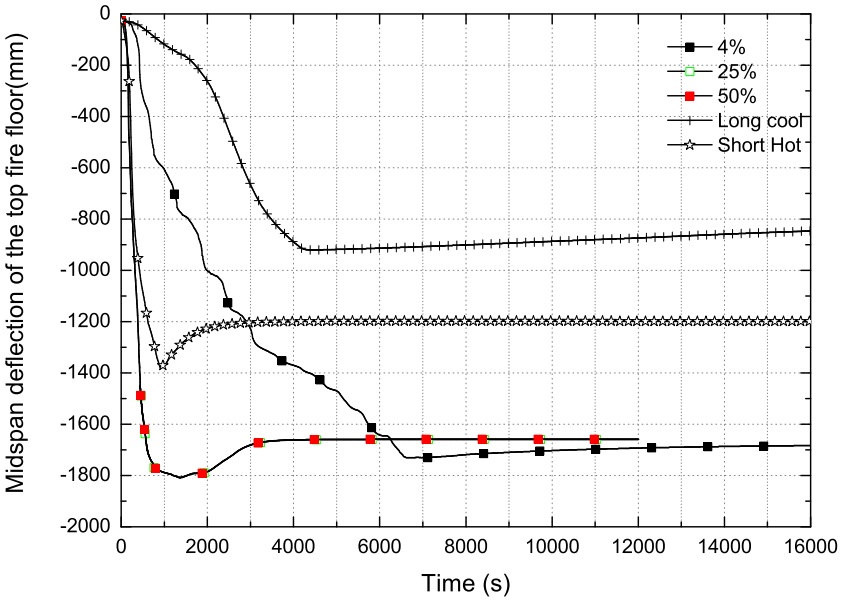


**Figure 6.8:** Midspan deflection of the top fire floor

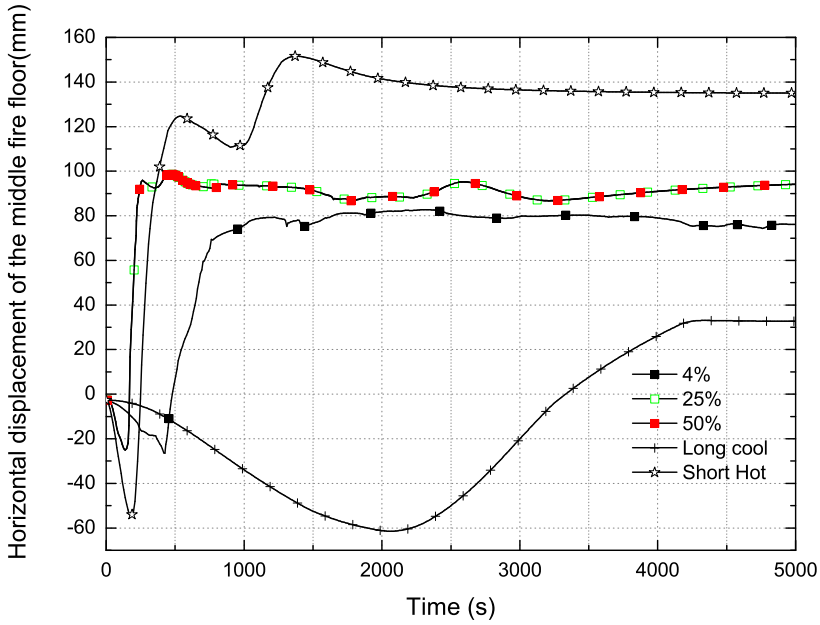


**Figure 6.9:** Horizontal displacement of the middle fire floor

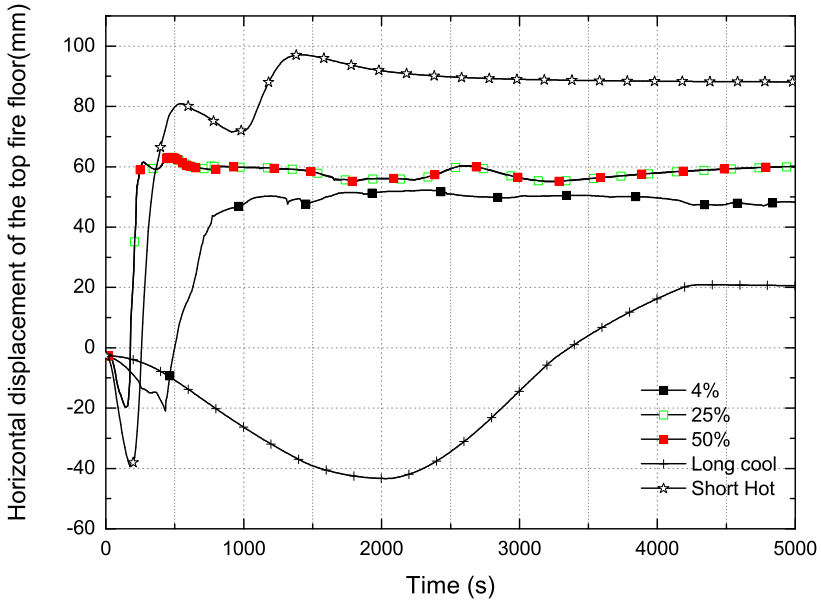


**Figure 6.10:** Horizontal displacement of the top fire floor

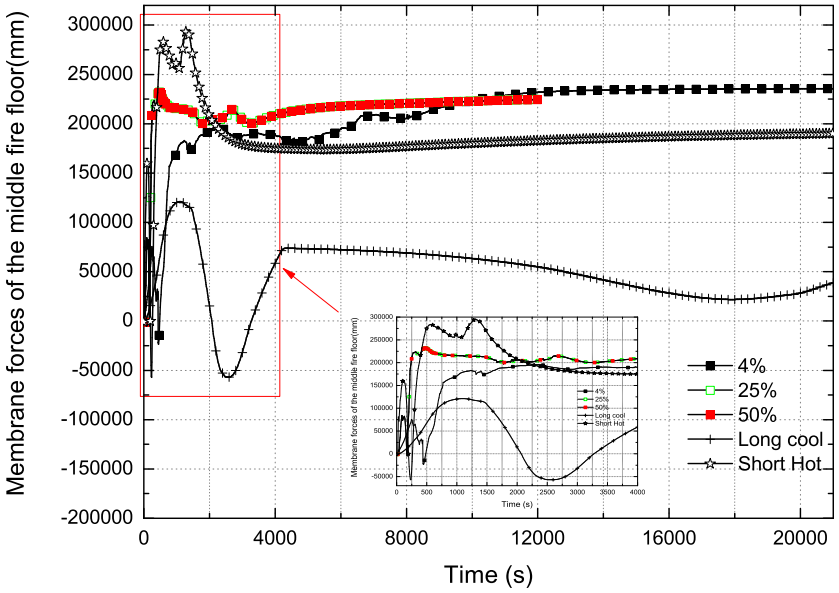


**Figure 6.11:** Membrane forces in the middle fire floor

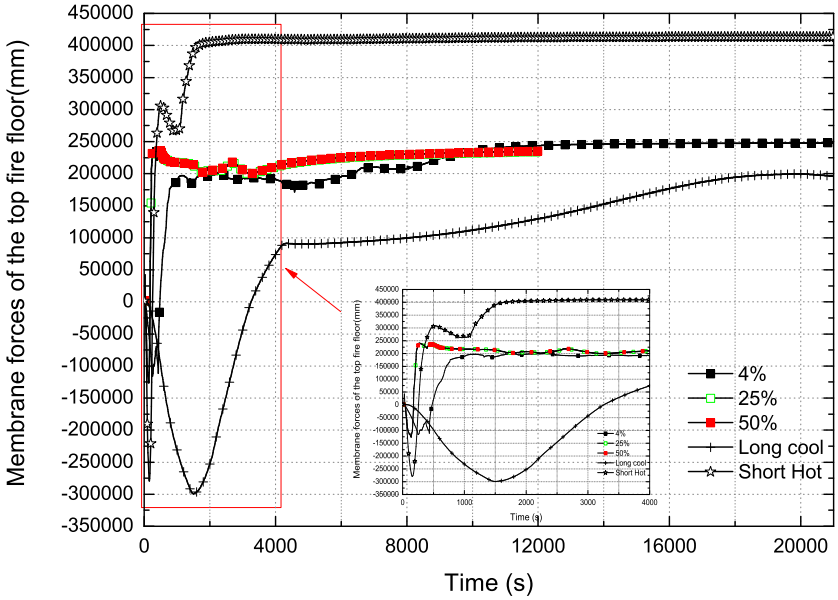


**Figure 6.12:** Membrane forces in the top fire floor

delayed. However, cyclic displacement patterns are observed even for this small time delay, which are not seen for the simultaneous scenarios.

Figure 6.16 plots the midspan deflection of the middle floor. It is observed that the maximum deflections reached in all cases occur with a time delay but are not affected. It should be noted that even this time delay is only present for the larger fires. This is expected as travelling fires are not uniform in the floor and thus there is no simultaneous regain of strength during cooling. On the contrary, several parts of the floor are cooling while others are heating, and this phenomenon is more notable in smaller fires that require more time to travel through the whole floor plate.

Figures 6.17, 6.18 and 6.19 plot the membrane forces for the bottom, middle and top floor respectively. The pattern is similar to that of the horizontal

displacements and is similar to the case of simultaneous fires although more cyclic. It should be noted that for the middle and top fire floor, higher compressive forces appear compared to the simultaneous case but the tensile forces do not change significantly. This is in contrast to the case of parametric fires as seen in Chapter 4, that even a short time delay of 600s caused higher tensile forces on the middle and top fire floors.

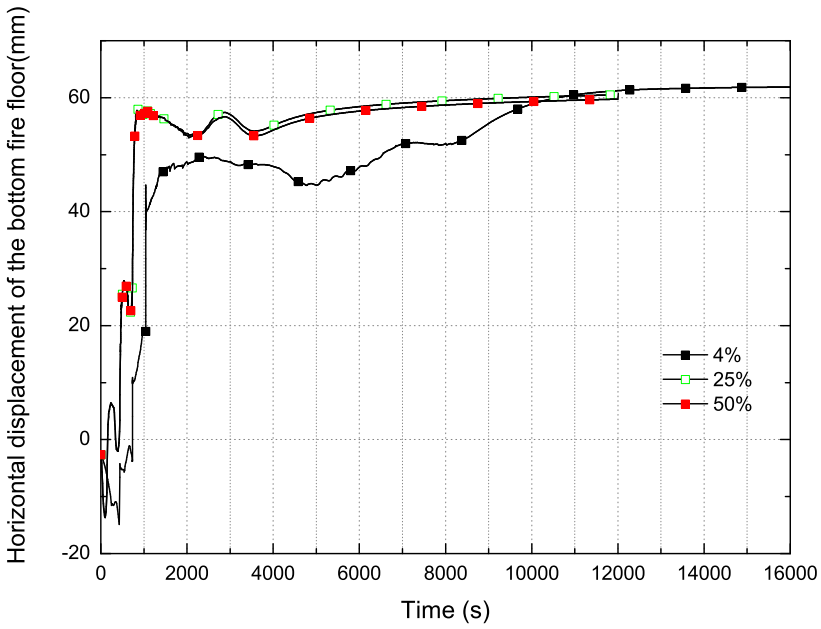


**Figure 6.13:** Horizontal displacement of the bottom fire floor for short inter-floor time delay

### 6.4.3 Slow vertically travelling scenarios

Figures 6.20 to 6.26 demonstrate the findings for the scenarios involving slow vertically travelling fires with an inter-floor time delay of 3600s. The horizontal displacements of the bottom, middle and top fire floor can be seen in Figures

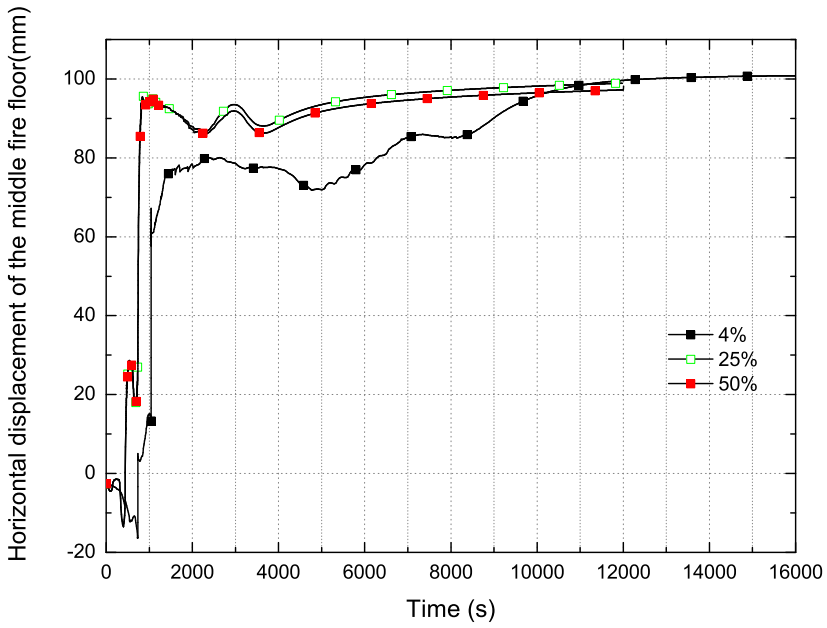


**Figure 6.14:** Horizontal displacement of the middle fire floor for short inter-floor time delay

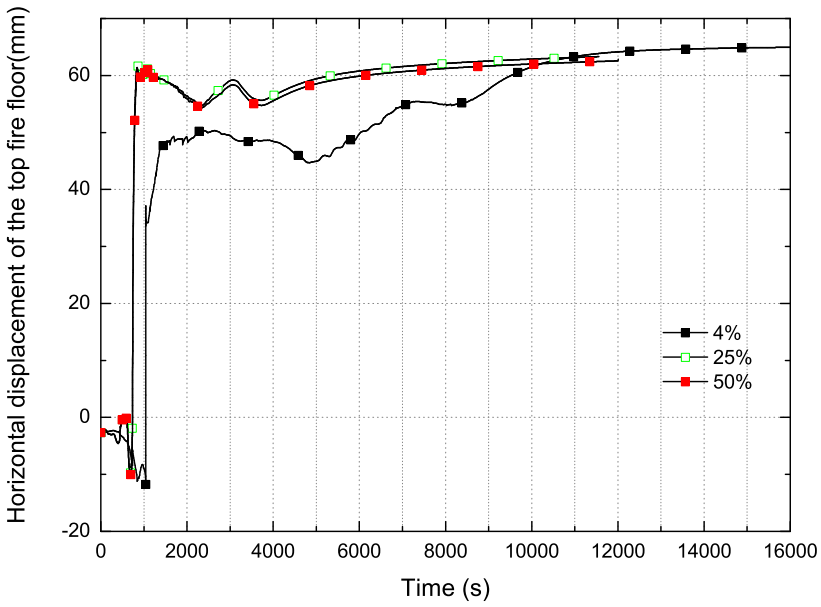


**Figure 6.15:** Horizontal displacement of the top fire floor for short inter-floor time delay

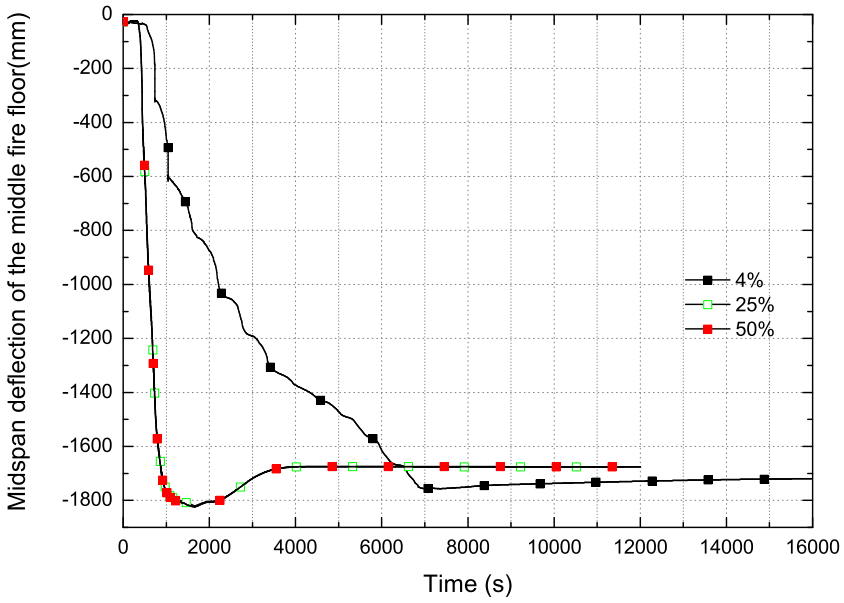


**Figure 6.16:** Midspan deflection of the middle fire floor for short inter-floor time delay

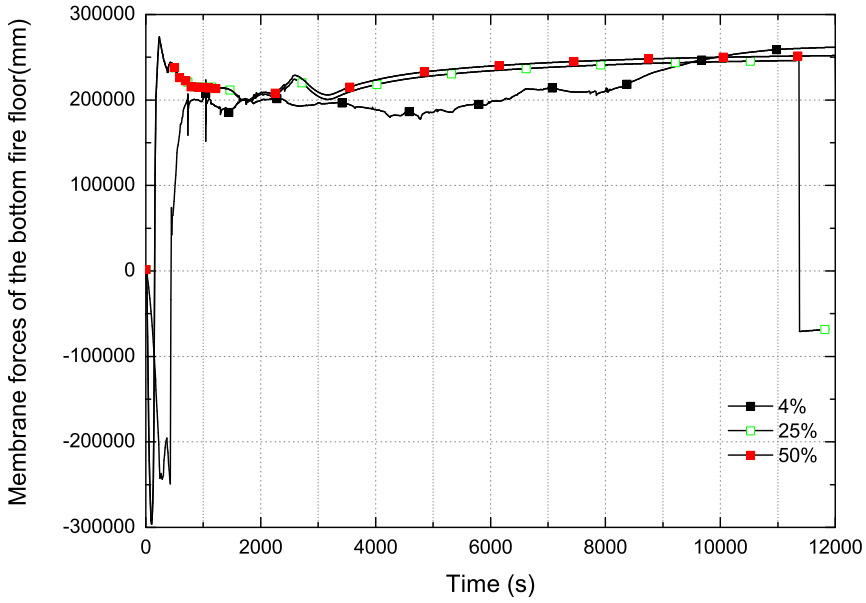


**Figure 6.17:** Membrane forces in the bottom fire floor for short inter-floor time delay

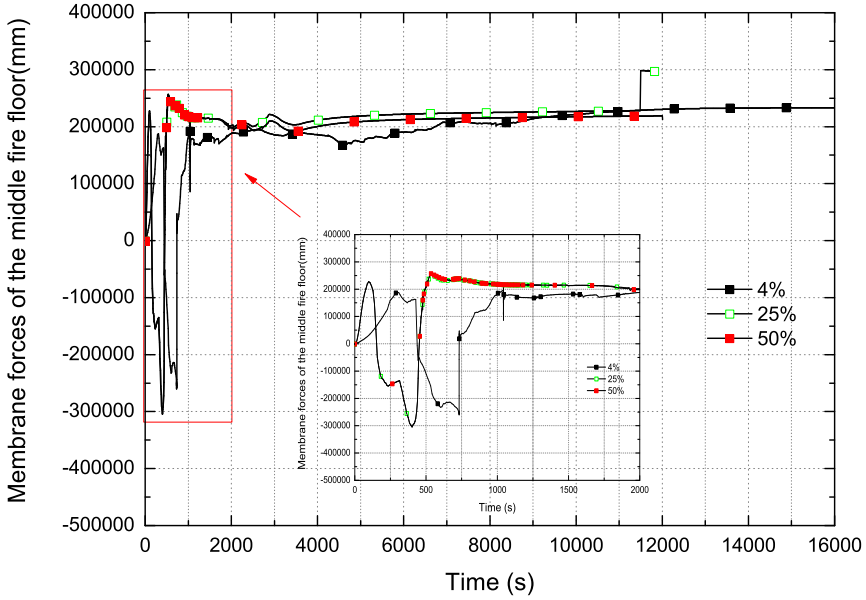


**Figure 6.18:** Membrane forces in the middle fire floor for short inter-floor time delay

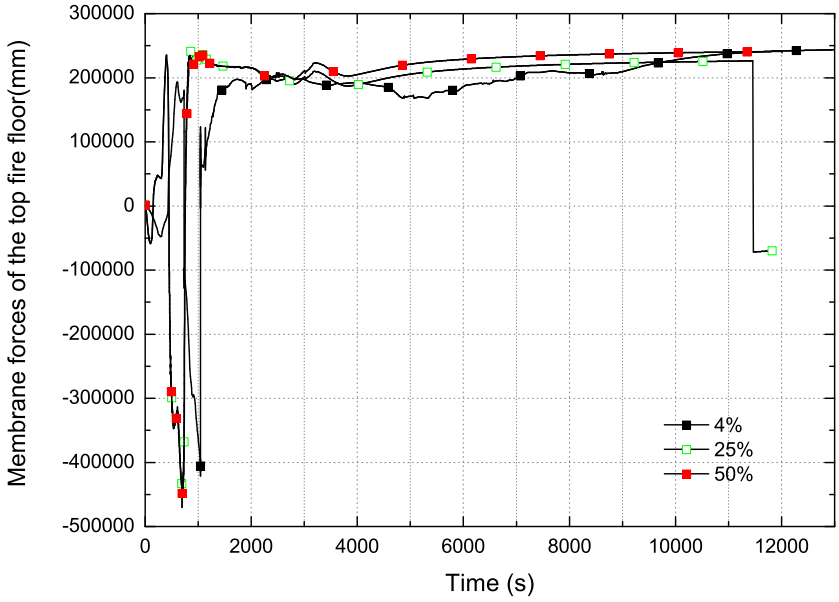


**Figure 6.19:** Membrane forces in the top fire floor for short inter-floor time delay

6.20 to 6.22 respectively. It can be seen that the pattern of displacements is different from the simultaneous and rapid travelling scenarios but is similar for all fire sizes. Large cyclic movements are observed when a new floor starts to heat (that is after 3600s for the middle floor and 7200s for the top floor). These cyclic displacements are larger than those seen for the rapid travelling fires. Outside of this difference in the displacement pattern, it is also interesting to note that for the larger fire sizes the maximum displacements reached in all floors are reduced compared to the simultaneous and travelling scenarios. Notably, the maximum displacement reached in the middle floor was reduced from around 100mm for the simultaneous and rapid travelling scenarios to around 65mm here and from around 60mm to approximately 40mm for the other two floors. The maximum displacement reached in the case of the smallest fire size (4%), although achieved much later is not affected by this large time delay for all the fire floors and thus produced the most demanding response. The maximum displacement reached during the initial expansion phase is not affected significantly by the inter-floor time delay.

The maximum midspan deflection although reached later in time for the middle floor is also not affected significantly by the time delay as seen in Figure 6.23.

Figures 6.24 to 6.26 plot the membrane forces for the bottom to top fire floor respectively. It can be seen that overall the maximum compressive and tensile forces are similar to those reached in the rapid travelling fires, although these are reached in later time and the pattern of forces is more cyclic.

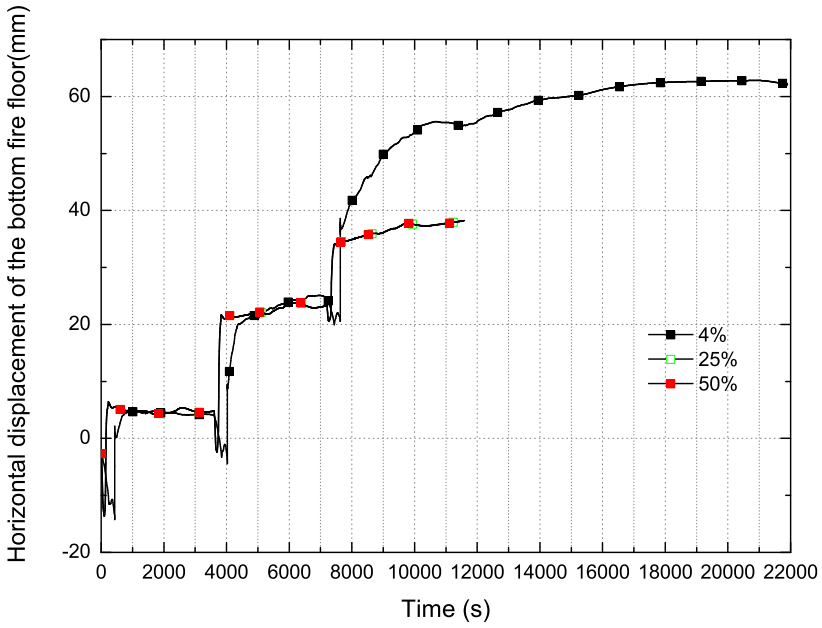


**Figure 6.20:** Horizontal displacement of the bottom fire floor for large inter-floor time delay

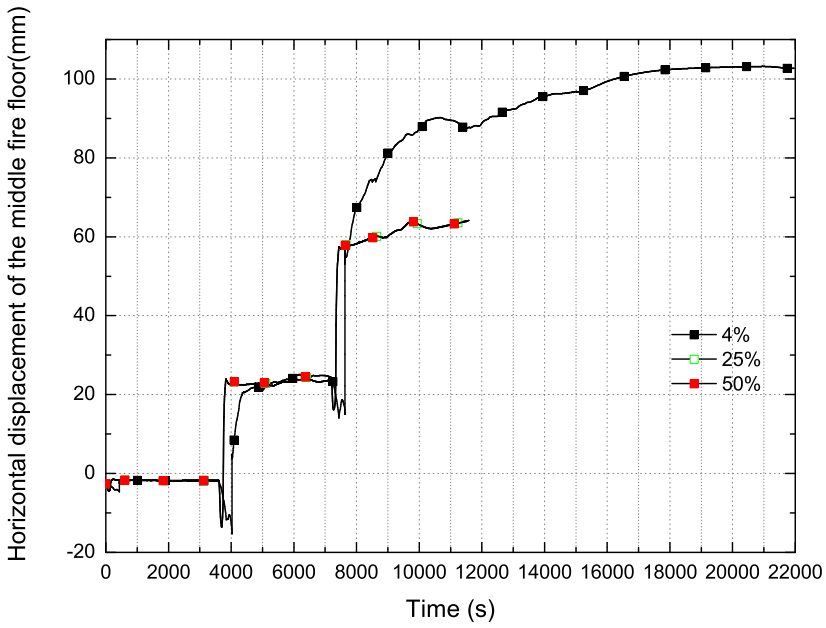


**Figure 6.21:** Horizontal displacement of the middle fire floor for large inter-floor time delay

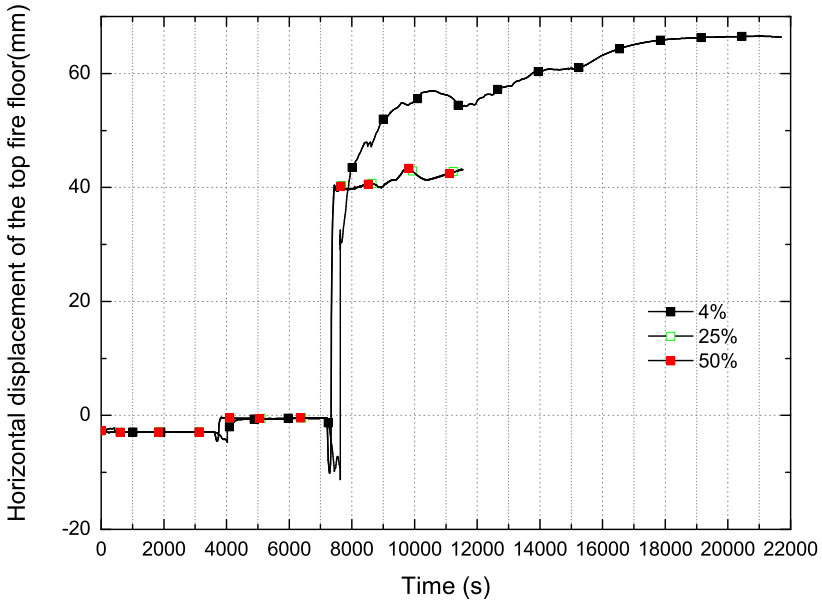


**Figure 6.22:** Horizontal displacement of the top fire floor for large inter-floor time delay

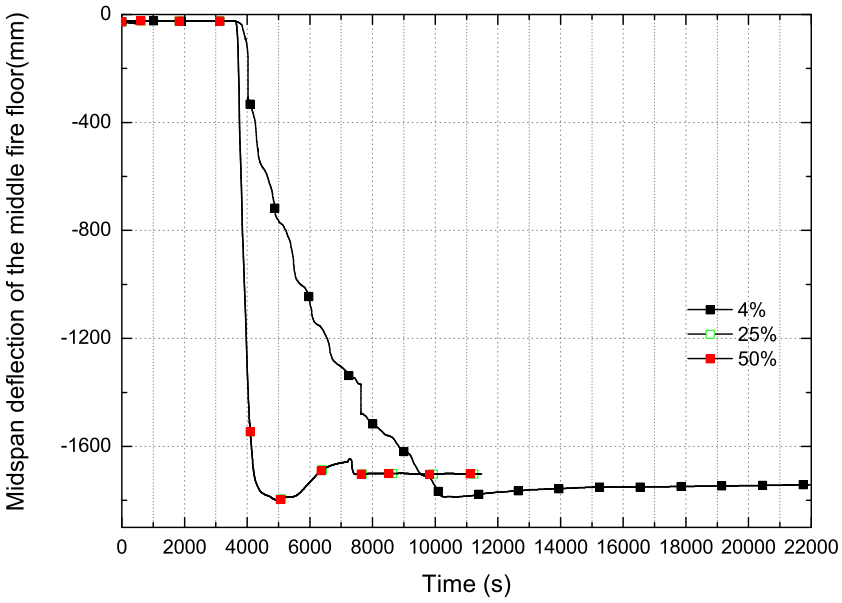


**Figure 6.23:** Midspan deflection of the middle fire floor for large inter-floor time delay

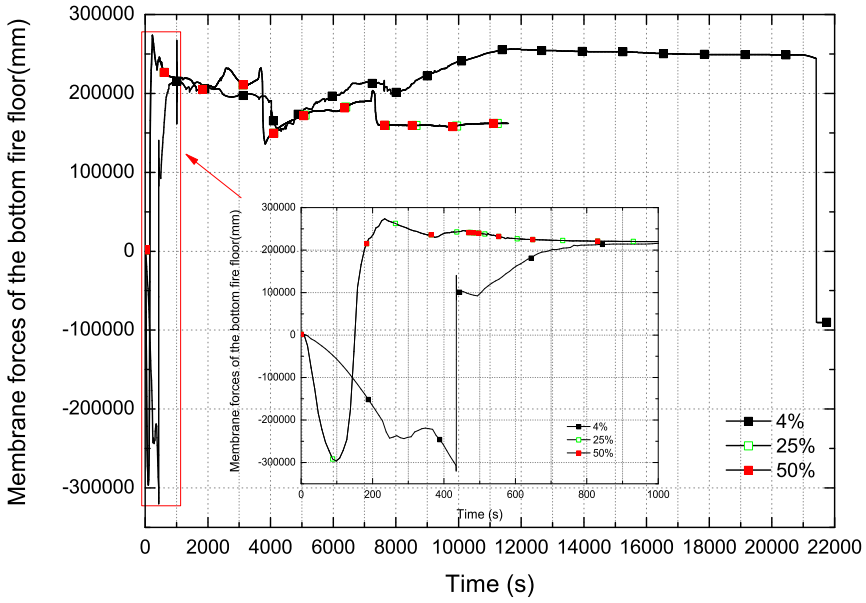


**Figure 6.24:** Membrane forces in the bottom fire floor for large inter-floor time delay

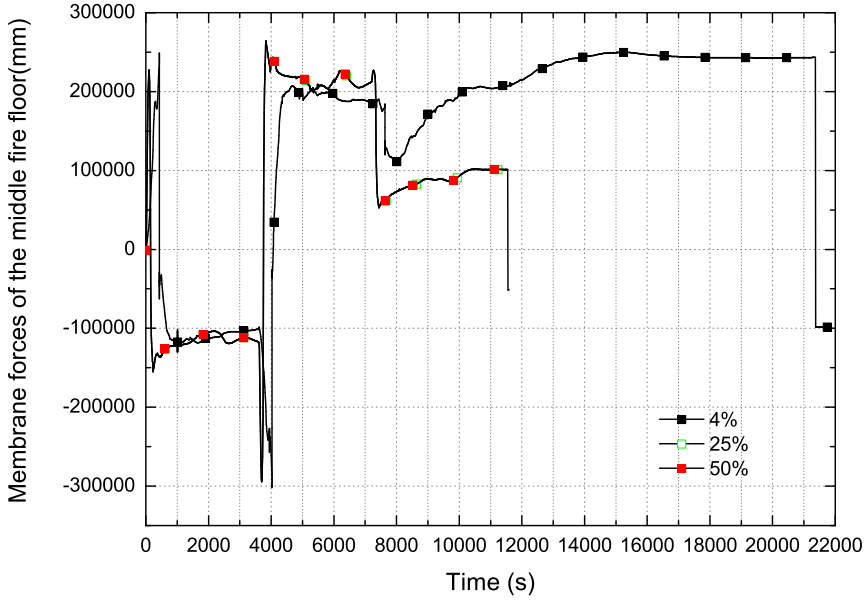


**Figure 6.25:** Membrane forces in the middle fire floor for large inter-floor time delay

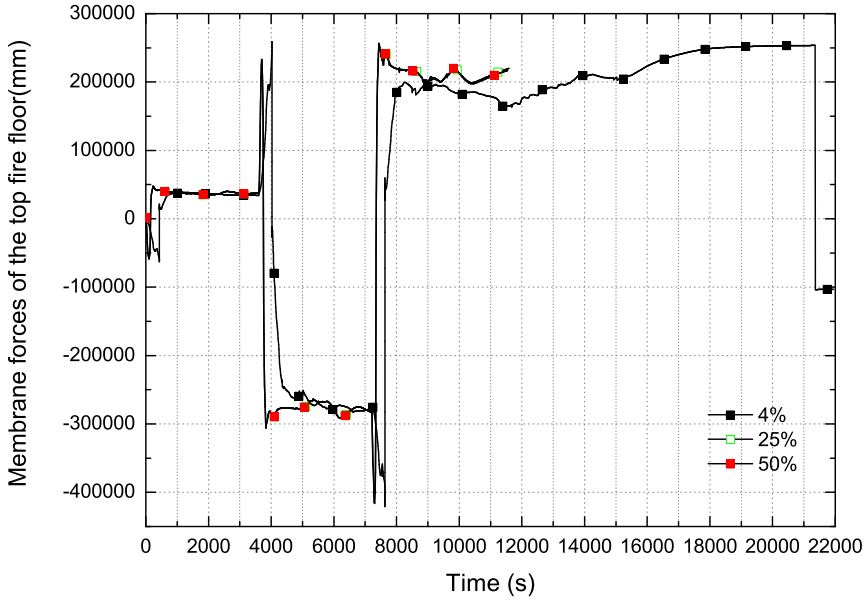


**Figure 6.26:** Membrane forces in the top fire floor for large inter-floor time delay

## 6.5 Conclusions

Travelling fires provide a much more realistic thermal environment for large enclosures typically found in tall buildings. The effect of a combined scenario of both horizontally and vertically fires is examined. Moreover, the effect of multifloor travelling fires is compared against multifloor parametric fires.

The parametric study demonstrated that, for the particular case studied, uniform fires may be more demanding in terms of potential for collapse. It is shown that although travelling fires may cause higher damage to the floor itself, the *short-hot* parametric fire induces higher membrane forces along the floor which pulls the column inside more than the travelling fires. This suggests that in long floors where uniform heating is less likely, the time of failure predicted by parametric fires covering multiple floors will be conservative. A performance based methodology involving a family of fire sizes can provide a more realistic definition of the thermal environment and thus ensure safety for all the scenarios considered.

The findings from the study demonstrated also that for vertically and horizontally travelling fires, small inter-floor time delays did not affect significantly the observed behaviour of the building and thus in performance based design, a simultaneous initiation of fires on multiple floors can be a lower bound (in terms of time) or upper bound scenario (in terms of collapse potential). For the slow travelling fires, large cyclic displacement patterns were observed. The overall structural behaviour is though less conservative for the large fire sizes since less maximum displacements appear. On the contrary, for the smaller size the maximum displacement is not affected by the large time delay although this is

reached later. Thus the small fire size is the most demanding scenario in terms of maximum horizontal displacements (and thus potential collapse) for large inter-floor time delays. On the contrary, the most demanding scenario cannot be easily defined for the simultaneous and rapid travelling fires between all sizes. For both rapid and slow travelling fires, a similar increase in maximum compressive membrane forces was observed compared to simultaneous fires but the maximum tensile forces were similar for all cases. This is not in accordance with previous findings with post-flashover fires e.g. Chapter 4, where both the tensile and compressive forces increased, although similarly, in vertically travelling scenarios.

It should be kept in mind that the results of this study can be considered to be applicable to structures of the particular structural form considered here. Further research is required to investigate the effects that these fires could have on other structural layouts where other phenomena may appear. In a performance based context, the behaviour of each structure has to be separately addressed.

# Chapter 7

# Summary and Future Research

This Chapter will provide an overview of the work carried out during this PhD research and highlight the originality and significance of the work as well as its limitations and its implication for practice. Possible areas of future research will also be discussed.

## 7.1 Summary

This thesis fits into the broader context of performance based structural fire engineering and involved two core themes, the software development of OpenSees and modelling of tall buildings in fire using OpenSees. In this work a review of the current structure in fire context was initially carried out and the object-oriented and open-source finite element framework OpenSees was presented along with its extension with structural fire modelling capabilities. All the new classes that were developed were then used to examine the collapse mechanisms of generic tall

buildings under multiple floor fires based on the lessons learnt from the collapse of the WTC towers. The effect of vertically travelling fires has also been studied. This research on tall buildings has been continued by examining the thermal and as structural response of tall buildings under horizontally travelling fires, overcoming the typical assumption of uniform fires. This work was extended by modelling the combined scenario of horizontally and vertically travelling fires and examining the potential demand for collapse. A critical review of the main points that can been drawn from the studies carried out for this thesis will be given in the next sections.

### 7.1.1 An open-source platform for structural fire analysis

The finite element framework OpenSees was presented and the merits of its object-oriented architecture (flexibility, modularity and reusability)and open-source code (community tool, no "black box" and free) were highlighted. The software development of OpenSees with structural fire modelling capabilities was also discussed. New beam-column elements were developed based on the existing classes that can take into account the thermaly-induced stresses (**DispBeamColumn2DThermal** and **DispBeamColumn3DThermal**). In addition, new **fiberSection** classes were also developed based on the exisitng ones. These classes map the temperature based on their location for each fiber and determine their thermal stresses. New materials have also been developed that their stress-strain relationship is based on the Eurocode suggestions. New classes were also developed for applying the thermal loads into the elements as well as a new **Pattern** class that can incorporate up to nine different temperature-time curves along the section of an element. The procedures for modelling structures

in fire were also presented with emphasis on an implicit dynamic analysis for overcoming local instabilities. This work demonstrated that using this procedure makes it possible to follow the global failure of structures in fire, since the analyses performed on the collapse of tall buildings in multiple floor fires were able to converge and produce similar results with those in previous work [61]. This thesis also demonstrated that OpenSees is a flexible platform for performing advanced structural fire analysis methods by integrating fire, heat transfer and structural models by applying a horizontally travelling methodology for the characterisation of the thermal environment of large enclosures.

### 7.1.2 Collapse of tall buildings under multifloor fires

This research has examined the collapse of the WTC towers under multiple floor fires, similarly to previous work [58, 60], in order to draw useful lessons on the collapse of tall buildings in fire. The column "pull in" that triggered the instability of the towers and lead to their collapse has been discussed. In addition, the local behaviour of the WTC Towers' truss system has been examined as well as the buckling of the diagonals due to the restrained thermal expansion of the floor. Since this research was focused on understanding the collapse mechanisms of tall buildings in fire, a generic composite steel and concrete structure was modelled. Using this model, the two different collapse mechanisms that were observed before [61], weak floor and strong floor failure, have been confirmed and discussed in more depth. Moreover, clear distinctions have been described on when on or the other collapse mechanism occurs in terms of their initiation at specific locations in the structure. A series of parametric studies were performed in order to examine the probability of each collapse mechanism and the conditions that affect which

mechanism occurs. These parametric studies demonstrated that the collapse mechanism type depended on the column-floor bending stiffness ratio and the number of floors on fire. The results of these parametric studies have also shown that the most probable collapse mechanism type is strong floor failure, like the one seen for the WTC Towers. The weak floor collapse has occurred mainly for floors that were outside the serviceability limit state criterion, however it can become more likely with more floors on fire. The understanding of these mechanisms can assist in extending the tenability of a tall building structure in multiple floor fires. The effect of vertically traveling fires on the collapse of tall buildings has also been studied and has been compared to the simultaneous multiple floor fires considered before. The parametric study performed demonstrated that vertical compartmentation of fire is very important in securing structural integrity of tall buildings and allowing time for the safe evacuation of people. Simultaneous multiple floor fires have been found to be more severe than vertically travelling fires in terms of global structural behaviour. The study suggested that a strong floor collapse is less probable for slower travelling fires and a weak floor collapse in a simultaneous or rapidly travelling fire may become strong floor collapse for a slow travelling fire. Therefore, it can be argued that a suitable number of floors simultaneously burning can be used as a conservative upper bound scenario by designers. Although simultaneous multiple floor fires produced the most onerous response in terms of global behaviour, it was observed that vertically travelling fires produce higher tensile axial forces in the floors and thus the potential of connection failure is increased. Therefore, the tensile capacity of connections has to be strengthened to be adequate to withstand the thermally induced forces. Suggested values for travelling times cannot be defined as these

depend on multiple parameters specific to a building or structure, and thus cannot be generally applicable.

### 7.1.3 Tall buildings and travelling fires

Although the work that was described previously considered the effect of vertically travelling fires, the fire in each floor was assumed to be uniform. However, in large floor areas, fires travel across the floor plate. Hence, the travelling fire methodology developed recently [24] has been implemented and compared against the more typically used parametric fires. As a case study, a similar structural layout was used with longer spans compared to previous work that involved uniform fires, representing typical characteristics of modern construction. The thermal and structural response were examined under a horizontally travelling fire in a single floor. The results of the thermal analyses demonstrated that measuring fire severity using the "equal area" hypothesis is invalid for travelling fires. Large temperature differences were observed between different locations of the composite floor that were supposed to have an equal fire severity according to the "equal area" concept. The findings from the thermal analyses also showed that travelling fires of larger sizes can lead to lower times to reach critical temperature while travelling fires of smaller sizes produce higher peak temperatures in the concrete slab. In addition, it was observed that thermal gradients develop in the upper part of the steel beam due to the contact with the concrete slab, with larger fire sizes producing higher thermal gradients. Moreover, large through-depth thermal gradients were seen in the concrete slab. The gradients are smaller for smaller fire sizes but higher maximum temperatures are observed especially for locations further away from the fire origin.

A parametric study has been performed for the structural modelling, comparing the response of different fire sizes with the typically used short hot and long cool parametric fires. Both a two-dimensional and a three-dimensional grillage model were used. All the travelling fires produced higher midspan deflections than the parametric fires. It should be kept in mind that travelling fires reached higher maximum temperatures than the parametric fires. Moreover, smaller fire sizes produced larger maximum deflections but later in time although this effect was more evident in the two-dimensional modelling. However, it should be mentioned that high deflections alone are not leading necessarily to failure. In terms of the membrane forces in the composite floor, the analyses showed that the floor was initially in compression and then snapped into tension during the pull-in process of the column. Parametric fires resulted in higher maximum compressive and tensile forces compared to the traveling fire scenarios. Moreover, large cyclic horizontal displacements were observed for the travelling fires that were not observed for the parametric fires. Larger plastic deformations were also observed for the travelling fires compared to the parametric fires which suggests that the damage is higher on the floor. In the two dimensional model larger plastic deformations and thus greater damage were observed for the smaller sizes for all the locations along the floor while in the three dimensional model larger plastic deformations were observed for the locations near the column while the other locations had small variation in plastic deformations with bigger sizes producing larger plastic deformations. Thus the three-dimensional model presented a more complex response than the one seen in the two-dimensional model, however the smaller fire size can still be considered the most demanding scenario as it causes greater damage near the columns. This is in contrast to previous findings by Law

*et al.* for a concrete building where the medium size burning areas (e.g. 25%) were identified as the most demanding scenario for the structure.

The findings from the performed parametric studies, challenge the usual assumption that uniform fires are the worst case design fires. On the contrary, non-uniform fires such as travelling fires produced different structural behaviour which could not be considered otherwise for uniform fires. Hence, it is suggested that travelling fires can provide a much more realistic thermal environment for large enclosures such as those found in tall buildings where parametric fires are outside their range of applicability. Thus designers can perform a parametric study by varying the fire sizes in order to address different possible scenarios and ensure robustness for each scenario.

It is of interest to note that travelling fires have been found to predict lower maximum compressive and tensile forces compared to the parametric fires although travelling fires reached higher maximum temperatures. Thus although greater damage was observed in the composite floor for the travelling fires, this suggests that these higher thermally induced forces seen in parametric fires can lead to collapse situations similar to those described before. Thus this research compared a simultaneous multifloor scenario involving parametric fires with a simultaneous multifloor scenario involving horizontally travelling fires. The findings from the study demonstrated that parametric fires cause greater thermally induced deformations with the short hot parametric fire producing the most demanding response after the pull-in of the columns. In addition the short hot fire produces the largest maximum compressive and tensile forces. In contrast the long cool fire produces lower tensile forces than the travelling fires. The results of this study suggest that for long span floors such as those found typically in tall buildings

where uniform heating is less likely, parametric fires will provide a conservative estimate on the failure of a building under multiple floor fires.

In the work described before a simultaneous three floor horizontally travelling scenario was considered. Hence, it is of interest to examine the effect that vertically travelling fires would have in such a scenario compared to the simultaneous fires. For the purposes of this work, a rapid and a slow vertically travelling rate have been considered in order to cover different possible scenarios (depending on the geometry of the opening, the thermal properties of the glazing, etc). The results of this parametric study showed that a rapid vertically travelling fire presented similar behaviour to that of the simultaneous scenario. Thus a simultaneous burning of fires on multiple floors can be considered, when a horizontal travelling fire methodology is employed, as a lower bound in terms of time. For the slow vertically travelling fires, large cyclic displacement patterns were observed that were not seen for the rapid vertically travelling and simultaneous scenarios. The overall structural behaviour under this scenario is less onerous since smaller maximum displacements appear for the large fire sizes (25% and 50%) while for the small fire size (4%) the maximum inward displacement is not affected by the large inter-floor time delay but this is reached later. Thus the small fire size can be clearly considered the most demanding scenario for large inter-floor time delays, while the most demanding scenario cannot be easily defined for the simultaneous and rapid travelling fires that all the fires produce similar maximum displacements. For both rapid and slow travelling fires, a similar increase in maximum compressive membrane forces was seen when compared to simultaneous fires but the maximum tensile forces were similar for all cases. This is not in accordance with previous findings with parametric fires, as seen before when examining the effect of vertically travelling fires on the collapse of tall buildings, where both the

tensile and compressive forces increased, although similarly, in vertically travelling scenarios.

### 7.1.4 Discussion

*Significance*

A major outcome of this work is the development of OpenSees platform with structural fire modelling capabilities [88]. As discussed in Chapter 3, both general finite element software and specialist structural fire engineering software have each their advantages and disadvantages. OpenSees can not be easily categorised in one of these two categories. Being an open-source and highly modular software due to its object-oriented architecture, it pocesses advantages from both categories described earlier. All these attributes can be found in limited software, capable of modelling structures in fire. Hence, the software development in this work brings the potential of a community owned research code that allows researchers within the fire community and other disciplines to collaborate freely across geographical boundaries. Examples of such communities in the fire safety field are the Fire Dynamics Simulator (FDS) and OpenFoam communities. In this work it was also demonstrated that OpenSees can be a flexible platform for integrating fire, heat transfer and structural models. Once, further integration takes place with FireFoam, the combined framework can advance the state of research since very few work exists today on integrating CFD and finite element software.

There are also outcomes from this work regarding the collapse of tall buildings in multiple floor fires that could inform further research in this area. In fact despite some very notable partial or total collapses in the past and the fact that most tall

building fires have involved many floors, there is very little research carried out, on the effects of multiple floor fires on tall buildings. This research examined the collapse mechanisms of tall buildings under simultaneous multiple floor fires and vertically travelling fires and thus provides a better understanding for achieving resilient future construction. One major conclusion that can be drawn from this work is that multiple floor fires should be considered as part of a performance based design for tall buildings. This can also be achieved by the means of simple calculations if detailed finite element models are considered too expensive for a particular project or time is restricted.

Previous tall building fires have demonstrated that fire travels horizontally across the floor plate and vertically to other floors. The use of realistic fire conditions is very important in a performance based framework, since design is based on predicted performance. However, most of the research carried out assumes that fire is uniform along the floor of a building and there is limited research that has used these travelling fires. This research employed horizontally and vertically travelling fires separately and in combined scenarios and examined their effect on thermal and structural response of a tall building in order to address this challenge.

*Limitations*

There are also several limitations in this research work. Firstly, this thesis focuses on a particullar form of construction (composite steel-concrete tall buildings with a rigid core), and does not examine the influence that other structural layouts such as cellular beams or long span trusses or even other materials (such as concrete or timber buildings) could have on the overall structural behaviour. It is possible that other phenomena may be encountered, hence the results cannot

be a priori treated as generally applicable to all structural forms and more research would be required. Nevertheless, this type of structural form is very popular in modern tall building construction. Moreover, there are limitations on the vertically and horizontally travelling fire scenarios considered in this work. For the vertically travelling fires, only exterior fire spread was considered with fire travelling upwards progressively from one floor to the other. This is the most typical mechanism of fire spread in tall buildings but other less typical fire scenarios can also occur such as interior fire spread, downwards travel or simultaneous upward and downwards travel (such as in Windsor tower). For the horizontally travelling fires, the limitation of this study was in the fact that it considered only linearly travelling fires with the origin of the fire being near the columns. There are other forms of travel such as corner or ring (inwards and outwards) fires [24]. Although the linearly travelling fire can be considered less realistic for nearly rectangular floor plans, it can help understand the fundamental structural behaviour of a floor under various travelling fire scenarios by varying the fire sizes. As regards the previously mentioned types of travelling fires, there are limitations in the current travelling fire methodology (such as the far-field definition) that makes them less easily applicable to tall buildings with rigid cores. These limitations were not considered in previous work by removing the rigid core in the heat transfer analyses [24]. The use of CFD could resolve these issues, but a predetermined path would still be required, and the analyses would be computationally intensive [97].

*Implication for practice*

The advantages of the OpenSees' software development with structural fire capabilities are not restricted to research purposes. Although admittedly, an

open-source platform is more useful to researchers willing to introduce new ideas, it is also a community tool for exchanging ideas. Practicing structural fire engineers can get advantage of this community platform in order to keep up to date with structural fire research and implement research findings into their own work.

After the 9/11 events there is considerable demand by owners, insurers and regulatory authorities on ensuring safety of tall buildings under potential hazards such as explosions or fires. A recent example is the structural fire design of Heron Tower in London where a simultaneous three floor fire scenario was considered for demonstrating the safety of the structure in accordance to the criteria set by the developers. Despite this, there is limited work on the response of tall buildings under multifloor fires, and hence little guidance is given to the practising structural fire engineer. This work examined the collapse of tall buildings under multifloor fires and discussed possible collapse mechanisms that can occur. A direct consequence from this work for the insurance industry would be to consider whether a tall building has been assessed for its structural response in fire, when determining the insurance premium of the building. In addition, a vertically travelling fire methodology has been described and the assumption of simultaneous multifloor fires has been discussed.

The realistic representation of fire is also an important challenge that the industry faces. In practice, the uncertainty in design comes from selecting suitable and realistic fire conditions rather than from the detailed structural response which is very rarely examined. The travelling fire methodology [24] that is used in this thesis provides a realistic fire definition in large enclosures. This methodology already had its first application in practice on the design of Ludgate building

in London by Arup consultants as discussed recently by Law *et al.* [148]. For the composite tall building examined in this work, the thermal and structural response under travelling fires in single floor and in multiple floors have been examined which can provide insight into the design of similar structures in the future.

## 7.2 Future Research

Both the OpenSees framework as well as the travelling fire methodology that were employed in this work are on the cutting edge of fire research and thus there are several areas that are relatively unexplored and future research is needed in order to develop good modelling tools and gain better understanding of structural response in fire.

### 7.2.1 Further development of the OpenSees framework

In this work all of the time-temperature histories were assigned to the corresponding elements manually using the *tcl* interface of OpenSees (**FireLoadPattern**). Although this procedure worked well and is efficient for the cases examined, there are scenarios where it will not be appropriate. Such scenarios can be localised or corner travelling fires where there are simultaneously temperature gradients along the depth, width and length of an element. For such a scenario, an interface between the Heat Transfer and Structural Fire modelling part of OpenSees must be developed. This interface can map temperatures at any time from a file according

to the location of each fiber (**FiberSection** classes). This mapping can also include nonuniform temperature distribution along the element length. However, in such a situation, modification of linear axial interpolation will be required as this implies uniform axial strain along the element. Except from the HT interface, a new connection element is also the next logical step from this work in order to account for the realistic connection relationship which is semi-rigid as well the degradation of mechanical properties in the connection as temperature increases. This way possible connection failure can also be predicted. In OpenSees this could be realised through the use of a predefined tcl script containing the model of a series of parallel spring elements. Moreover, all the work carried out on this work has been run in a single processor. Multiple processors were only used when running multiple models at the same time. However, for big three dimensional models, this procedure will not be equally effective. Hence, the use of advanced parallel computing resources in OpenSees can be exploited in order to model these big models. Recently, Jeffers and Sotelino [149] have argued that force-based elements can be more computationally effective in modelling structures in fire, since fewer elements per any structural member would be required in an analysis. The analysis of structures in fire using OpenSees' force-based elements could also be examined.

### 7.2.2 Tall buildings and travelling fires

This research examined the response of a composite tall building under a linearly horizontally travelling fire. This was mainly because there are limitations in the current travelling fire methodology and hence further development of the methodology is required in order to make it more applicable to more complicated

structural layouts and to more realistic travelling paths such as the corner travelling fires. The use of experimental data such as those from the ESPRC funded project "Real Fires for the Safe Design of Tall Buildings" (ESPRC reference: EP/J001937/1) that are expected soon can help in that direction. After the methodology is further developed, the structural behaviour under more realistic fire conditions can be considered. Moreover, other structural layouts such as long span trusses or cellular beams could be examined under horizontally travelling fires where findings may be different or more critical that the behaviour seen for the building layout examined in this work. It should also be mentioned that the models that were used in this thesis did not take take into account any spalling for concrete members or creep for steel members. These phenomena can occur more often for horizontally travelling fires due to long far-field heating times of several hours, especially for smaller fire sizes, compared to the lower duration of more typical room fires. Further research can examine this aspect too. Long times of heating and cooling can also lead to connection failure which was not treated in this work. Finally, the methodology that was used is this work aimed at examining the behaviour of a particular structure under certain pre-defined fire conditions. However, it is recognised that in real life, fire conditions are not predefined but must be based on certain arguments and structures are designed based on the loads and limit states considered by the designers. Thus a probabilistic design framework that takes into account different rates of horizontal and vertical spread and their subsequent structural response has to be developed in order for such a methodology to be used in practise.

# References


[1] C. Buchanan, The economic impact of high density development and tall buildings in central business districts, British Property Federation.

[2] I. Charney, The politics of design: architecture, tall buildings and the skyline of central london, Area 39 (2) (2007) 195–205.

[3] J. Gales, C. Maluk, L. Bisby, Large-scale structural fire testing-how did we get here, where are we, and where are we going?, in: 15th International conference on experimental mechanics: Fire symposium, 2012.

[4] D. Drysdale, An introduction to fire dynamics, Wiley, 2011.

[5] A. Buchanan, Structural design for fire safety, Vol. 273, Wiley New York, 2001.

[6] P. Thomas, J. Heselden, Cib international cooperative programme of fully developed fires in single compartments: Comprehensive analysis of results, Tech. rep., Internal Note 374, Fire Research Station (1970).

[7] P. Thomas, A. Heselden, fully developed fires in single compartments, a co-operative research program of the conseil international du batiment (cib report no. 20), Tech. rep., Fire Research Note (1972).

[8] T. Harmathy, A new look at compartment fires, part i, Fire technology 8 (3) (1972) 196–217.

[9] T. Harmathy, A new look at compartment fires, part ii, Fire Technology 8 (4) (1972) 326–351.

[10] O. Pettersson, S. Magnusson, J. Thor, Fire engineering design of steel structures, Lund Institute of Technology, Division of Structural Mechanics and Concrete Construction, 1976.

[11] C.E.N., Eurocode 1: Actions on structurespart 1-2: General actionsactions on structures exposed to fire, Tech. rep. (1991).

[12] T. Harmathy, Some overlooked aspects of the severity of compartment fires, Fire Safety Journal 3 (4) (1981) 261–271.

[13] A. Majdalani, Fires in compartments in buildings, in: Presentation in Building Research Establishment, 2012.

[14] J. Stern-Gottfried, A. Law, G. Rein, M. Gillie, J. Torero, A performance based methodology using travelling fires for structural analysis, in: 8th International Conference on Performance-Based Codes and Fire Safety Design Methods, 2010.

[15] J. Stern-Gottfried, G. Rein, Travelling fires for structural design–Part I: Literature review, Fire Safety Journal 54 (2012) 74–85.

[16] J. Stern-Gottfried, G. Rein, Travelling fires for structural design-Part II: Design methodology, Fire Safety Journal 54 (2012) 96–112.

[17] V. Babrauskas, R. Williamson, Post-flashover compartment fires: Basis of a theoretical model, Fire and Materials 2 (2) (1978) 39–53.

[18] S. Magnusson, S. Thelandersson, Temperature-time curves of complete process of fire development: Theoretical study of wood fuel fires in enclosed spaces, Royal Swedish Academy of Engineering Sciences, 1970.

[19] S. Welch, A. Jowsey, S. Deeny, R. Morgan, J. Torero, Bre large compartment fire testscharacterising post-flashover fires for model validation, Fire Safety Journal 42 (8) (2007) 548–567.

[20] J. Stern-Gottfried, G. Rein, L. Bisby, J. Torero, Experimental review of the homogeneous temperature assumption in post-flashover compartment fires, Fire Safety Journal 45 (4) (2010) 249–261.

[21] Y. Hasemi, Y. Yokobashi, T. Wakamatsu, A. Ptchelintsev, Modelling of heating mechanism and thermal response of structural components exposed to localized fires: A new application of diffusion flame modelling to fire safety engineering, in: Thirteenth meeting of the UJNR panel on fire research and safety, 1996, pp. 237–247.

[22] J. Schleich, L. Cajot, M. Pierre, M. Brasseur, J. Franssen, D. Joyeux, L. Twilt, J. Van Oerle, G. Aurtenetxe, Development of design rules for steel structures subjected to natural fires in large compartments, Tech. Rep. EUR 18868 EN, European Communities (1999).

[23] R. Alpert, Ceiling jet flows, SFPE Handbook of Fire Protection Engineering 3 (1) (2002) 2–18.

[24] J. Stern-Gottfried, Travelling fires for structural design, Ph.D. thesis, The University of Edinburgh (2011).

[25] M. Law, A relationship between fire grading and building design and contents, Fire Research Station, 1971.

[26] O. Pettersson, The Connection Between a Real Fire Exposure and the Heating Conditions According to Standard Fire Resistance Tests: with Special Application to Steel Structures, Lund Institute of Technology, Division of Structural Mechanics and Concrete Construction, 1974.

[27] M. Law, Prediction of fire resistance, in: Joint Fire Research Organization Symposium, no. 5, 1973.

[28] A. Usmani, J. Rotter, S. Lamont, A. Sanad, M. Gillie, Fundamental principles of structural behaviour under thermal effects, Fire Safety Journal 36 (8) (2001) 721–744.

[29] A. Usmani, Application of fundamental structural mechanics principles in assessing the cardington restrained beam test, in: Structures in Fire Proceedings of the First International Workshop, 2002.

[30] A. Usmani, S. Lamont, Key events in the structural response of a composite steel frame structure in fire, Fire and materials 28 (2-4) (2004) 281–297.

[31] B. Izzuddin, D. Moore, Lessons from a full-scale fire test, Proceedings of the Institution of Civil Engineers. Structures and buildings 152 (4) (2002) 319–329.

[32] G. Newman, Structural fire engineering investigation of Broadgate phase 8 fire, Steel Construction Institute, 1991.

[33] M. Law, Some Selected Papers by Margaret Law: Engineering Fire Safety, Arup, 2002.

[34] D. Lange, Risk and performance based fire safety design of steel and composite structures, Ph.D. thesis, The University of Edinburgh (2009).

[35] G. Deierlein, S. Hamilton, Framework for structural fire engineering and design methods, in: NIST-SFPE Workshop for Development of a National R&D Roadmap for Structural Fire Safety Design and Retrofit of Structures: Proceedings, 2004, p. 75.

[36] S. Hamilton, Performance-based fire engineering for steel framed structures: A probabilistic methodology, Ph.D. thesis, Stanford University (2011).

[37] A. Usmani, M. Rotter, Failure of structures under fire, in: The steel in fire forum, 2001.

[38] B. Izzuddin, A. Elghazouli, Failure of lightly reinforced concrete members under fire. i: Analytical modeling, Journal of Structural Engineering 130 (1) (2003) 3–17.

[39] A. Law, J. Stern-Gottfried, M. Gillie, G. Rein, The influence of travelling fires on a concrete frame, Engineering Structures 33 (5) (2011) 1635–1642.

[40] C.E.N., Eurocode 3: Design of steel structures part 1-2: General rules-structural fire design, Tech. rep., EM 1993-1-2, Brussels, 2005.

[41] P. EN1994, 1-2. eurocode 4. design of composite steel and concrete structures. part 1.2. general rules. structural fire design (2005).

[42] H. Saab, D. Nethercot, Modelling steel frame behaviour under fire conditions, Engineering Structures 13 (4) (1991) 371–382.

[43] Y. Anderberg, Modelling steel behaviour, Fire Safety Journal 13 (1) (1988) 17–26.

[44] B. Meacham, M. Engelhardt, V. Kodur, Collection of data on fire and collapse, faculty of architecture building, delft university of technology, in:

National Science Foundation, CMMI, Research and Innovation Conference 2009, 2009, pp. 22–25.

[45] J. Beitel, N. Iwankiw, Historical survey of multistory building collapses due to fire, Fire Protection Engineering 27 (2005) 42.

[46] V. Kodur, L. Bisby, M. Green, Frp retrofitted concrete under fire conditions, Concrete international 28 (12) (2006) 37–44.

[47] V. Kodur, L. Bisby, M. Green, Experimental evaluation of the fire behaviour of insulated fibre-reinforced-polymer-strengthened reinforced concrete columns, Fire safety journal 41 (7) (2006) 547–557.

[48] J. Gales, L. Bisby, C. MacDougall, K. MacLean, Transient high-temperature stress relaxation of prestressing tendons in unbonded construction, Fire Safety Journal 44 (4) (2009) 570–579.

[49] C. CEN, Eurocode 2: Design of concrete structures part 1-2: General rules-structural fire design, Tech. rep., EM 1992-1-2, Brussels, 2004.

[50] G. Khoury, Effect of fire on concrete and concrete structures, Progress in Structural Engineering and Materials 2 (4) (2000) 429–447.

[51] I. Fletcher, S. Welch, J. Torero, R. Carvel, A. Usmani, Behaviour of concrete structures in fire, Thermal Science 11 (2) (2007) 37–52.

[52] U. Schneider, Concrete at high temperatures: a general review, Fire Safety Journal 13 (1) (1988) 55–68.

[53] A. Haksever, C. Ehm, Application of biaxial concrete data for bearing members under fire attack, Fire safety journal 12 (2) (1987) 109–119.

[54] J. Moncada, Fire Unchecked, NFPA Fire Journal, 2005.

[55] C. Scawthorn, A. Cowell, F. Borden, Fire-related aspects of the Northridge earthquake, National Institute of Standards and Technology, Building and Fire Research Laboratory, 1998.

[56] T. McAllister, R. Gann, J. Averill, J. Gross, W. Grosshandler, J. Lawson, K. McGrattan, H. Nelson, W. Pitts, K. Prasad, et al., Federal building and fire safety investigation of the world trade center disaster: Structural fire response and probable collapse sequence of world trade center building 7, NIST NCSTAR (2008) 1–9.

[57] B. Taranath, Steel, concrete, and composite design of tall buildings, McGraw-Hill New York, 1998.

[58] A. Usmani, Y. Chung, J. Torero, How did the wtc towers collapse: a new theory, Fire Safety Journal 38 (6) (2003) 501–533.

[59] A. Usmani, Stability of the world trade center twin towers structural frame in multiple floor fires, Journal of engineering mechanics 131 (2005) 654.

[60] G. Flint, A. Usmani, S. Lamont, B. Lane, J. Torero, Structural response of tall buildings to multiple floor fires, Journal of Structural Engineering 133 (2007) 1719.

[61] A. Usmani, C. Roben, A. Al-Remal, A very simple method for assessing tall building safety in major fires, International Journal of Steel Structures 9 (1) (2009) 17–28.

[62] R. Sun, Z. Huang, I. W. Burgess, The collapse behaviour of braced steel frames exposed to fire, Journal of Constructional Steel Research 72 (2012) 130–142.

[63] D. Parker, Madrid tower designer blames missing fire protection for collapse, New Civil Engineer, 2005.

[64] R. Gann, NIST NCSTAR 1: Final report of the National Construction Safety Team on the collapse of the World Trade Center Twin Towers, Federal Building and Fire Safety Investigation of the World Trade Center Disaster, National Institute of Standards and Technology (NIST), Gaithersburg, MD, 2005.

[65] G. Flint, S. Lamont, B. Lane, H. Sarrazin, L. Lim, D. Rini, C. Roben, Recent lessons learned in structural fire engineering for composite steel structures, Fire Technology (2013) 1–26.

[66] F. McKenna, Object-oriented finite element programming: frameworks for analysis, algorithms and parallel computing, Ph.D. thesis, University of California,Berkeley (1997).

[67] S. Mazzoni, F. McKenna, M. Scott, G. Fenves, et al., OpenSees command language manual, Pacific Earthquake Engineering Research (PEER) Center, 2005.

[68] M. Scott, G. Fenves, F. McKenna, F. Filippou, Software patterns for nonlinear beam-column models, Journal of structural engineering 134 (4) (2008) 562–571.

[69] B. Stroustrup, The C++ programming language, Addison-Wesley Longman Publishing Co., Inc., 1997.

[70] G. Fenves, Object-oriented programming for engineering software development, Engineering with computers 6 (1) (1990) 1–15.

[71] Hibbett, Karlsson, Sorensen, Hibbitt, ABAQUS/Standard: user's manual, Vol. 1, Hibbitt, Karlsson & Sorensen, 1998.

[72] P. Kohnke, ANSYS theory reference, Ansys, 1999.

[73] L. Song, B. Izzuddin, A. Elnashai, P. Dowling, An integrated adaptive environment for fire and explosion analysis of steel framespart i:: analytical models, Journal of Constructional Steel Research 53 (1) (2000) 63–85.

[74] J. Cai, I. Burgess, R. Plank, A generalised steel/reinforced concrete beam-column element model for fire conditions, Engineering Structures 25 (6) (2003) 817–833.

[75] J. Franssen, Safir: A thermal/structural program for modeling structures under fire, Engineering Journal-American Institute of Steel Construction Inc 42 (3).

[76] J. Wen, A. Heidari, V. Madhav Rao, S. Ferraris, V. Tam, Simulating flame propagation in obstructed channels with OpenFOAM, Centre for Fire and Explosion Studies, Faculty of Engineering, Kingston University, UK, 2010.

[77] F. McKenna, G. Fenves, M. Scott, OpenSees: Open system for earthquake engineering simulation, Pacific Earthquake Engineering Research Center. USA, 2002.

[78] G. Booch, J. Rumbaugh, I. Jacobson, The unified modeling language user guide, Pearson Education India, 1999.

[79] B. Welch, K. Jones, J. Hobbs, Practical programming in Tcl and Tk, Vol. 1, Prentice Hall PTR, 2003.

[80] F. Taucer, E. Spacone, F. Filippou, A fiber beam-column element for seismic response analysis of reinforced concrete structures, Vol. 91, Earthquake Engineering Research Center, College of Engineering, University of California, 1991.

[81] E. Spacone, F. Filippou, F. Taucer, Fibre beam-column model for non-linear analysis of r/c frames: Part i. formulation, Earthquake Engineering and Structural Dynamics 25 (7) (1996) 711–726.

[82] A. Neuenhofer, F. Filippou, Geometrically nonlinear flexibility-based frame finite element, Journal of Structural Engineering 124 (1998) 704.

[83] J. Coleman, E. Spacone, Localization issues in force-based frame elements, Journal of Structural Engineering 127 (11) (2001) 1257–1265.

[84] M. Crisfield, Nonlinear finite element analysis of solids and structures. Volume 1: Essentials, Wiley, New York, NY (United States), 1991.

[85] R. De Souza, Force-based finite element for large displacement inelastic analysis of frames, Ph.D. thesis, University of California,Berkeley (2000).

[86] E. Dvorkin, K. Bathe, A continuum mechanics based four-node shell element for general non-linear analysis, Engineering computations 1 (1) (1984) 77–88.

[87] O. Zienkiewicz, R. Taylor, The Finite Element Method: Solid Mechanics, Vol. 2, Butterworth-heinemann, 2000.

[88] A. Usmani, J. Zhang, J. Jiang, Y. Jiang, I. May, Using opensees for structures in fire, Journal of Structural Fire Engineering 3 (1) (2012) 57–70.

[89] P. Kotsovinos, A. Usmani, The world trade center 9/11 disaster and progressive collapse of tall buildings, Fire Technology (2013) 1–25.

[90] J. Jiang, Nonlinear thermomechanical analysis of structures using opensees.

[91] J. Rotter, A. Sanad, A. Usmani, M. Gillie, Structural performance of redundant structures under local fires, in: Proceedings of Interflam, Vol. 99, 1999, pp. 1069–1080.

[92] J. Franssen, Failure temperature of a system comprising a restrained column submitted to fire, Fire Safety Journal 34 (2) (2000) 191–207.

[93] J. Franssen, F. Gens, Dynamic analysis used to cope with partial and temporary failures, in: Proceedings of SiF'04: Third International Structures in Fire workshop, IRC, 2004.

[94] Y. Song, Z. Huang, I. Burgess, R. Plank, A new design method for industrial portal frames in fire, in: Proc. Structures in Fire Workshop, pp302, Vol. 312, 2008.

[95] A. K. Chopra, Dynamics of structures: Theory and applications to earthquake engineering, Vol. 2, Prentice Hall, 2001.

[96] H. Hilber, T. Hughes, R. Taylor, Improved numerical dissipation for time integration algorithms in structural dynamics, Earthquake Engineering & Structural Dynamics 5 (3) (1977) 283–292.

[97] Y. Jiang, Development and application of a thermal analysis framework in opensees for structures in fire, Ph.D. thesis, University of Edinburgh (2012).

[98] A. Rubert, P. Schaumann, Structural steel and plane frame assemblies under fire action, Fire Safety Journal 10 (3) (1986) 173–184.

[99] J. Jiang, L. Jiang, P. Kotsovinos, J. Zhang, A. Usmani, F. McKenna, G.-Q. Li, OpenSees Software Architecture for the Analysis of Structures in Fire, Journal of Computing in Civil Engineering, 2013.

[100] S. Selamet, Fire Performance of an Unprotected Composite Beam, Applications of structural fire engineering. Prague, 2013.

[101] J. Hallquist, et al., LS-DYNA keyword users manual, Livermore Software Technology Corporation, 2007.

[102] J. Torero, Challenging Attitudes on Codes and Safety, Council on Tall Buildings and Urban Habitat issue Journal (CTBUH), 2011.

[103] M. Lamster, Castles in the air, Scientific American 305 (3) (2011) 76–83.

[104] T. McAllister, G. Corley, U. S. F. Insurance, M. Administration, U. S. F. E. M. A. R. II., G. . O'Mara, World Trade Center Building performance study: Data collection, preliminary observations, and recommendations, Federal Emergency Management Agency, Federal Insurance and Mitigation Administration, 2002.

[105] J. Quintiere, M. Di Marzo, R. Becker, A suggested cause of the fire-induced collapse of the world trade towers, Fire Safety Journal 37 (7) (2002) 707–716.

[106] V. Kodur, Role of fire resistance issues in the collapse of the twin towers, in: Proceedings of the CIB-CTBUH International Conference on Tall Buildings, Vol. 8, 2003, p. 10.

[107] H. Baum, Simulating fire effects on complex building structures, Mechanics Research Communications 38 (1) (2011) 1–11.

[108] F. Ali, D. OConnor, Structural performance of rotationally restrained steel columns in fire, Fire Safety Journal 36 (7) (2001) 679–691.

[109] Z. Huang, K. Tan, S. Ting, Heating rate and boundary restraint effects on fire resistance of steel columns with creep, Engineering structures 28 (6) (2006) 805–817.

[110] P. G. Shepherd, I. Burgess, On the buckling of axially restrained steel columns in fire, Engineering Structures 33 (10) (2011) 2832–2838.

[111] S. Quiel, M. Garlock, Parameters for modeling a high-rise steel building frame subject to fire, Journal of Structural Fire Engineering 1 (2) (2010) 115–134.

[112] J. Torero, Fire-induced structural failure: the world trade center, new york, Proceedings of the ICE-Forensic Engineering 164 (2) 69–77.

[113] R. Weingardt, Engineering legends: great American civil engineers: 32 profiles of inspiration and achievement, American Society of Civil Engineers, 2005.

[114] E. Spacone, V. Ciampi, F. Filippou, Mixed formulation of nonlinear beam finite element, Computers & structures 58 (1) (1996) 71–83.

[115] E. Spacone, S. El-Tawil, Nonlinear analysis of steel-concrete composite structures: state of the art, Journal of Structural Engineering 130 (2) (2004) 159–168.

[116] Y. Anderberg, S. Thelandersson, Stress and deformation characteristics of concrete at high temperatures, Lund Institute of Technology. Division of Structural Mechanics and Concrete Construction, 1976.

[117] T. Harmathy, W. Stanzak, Elevated-temperature tensile and creep properties of some structural and prestressing steels, in: Fire Test Performance: A Symposium Presented at the Winter Meeting, American Society for Testing and Materials, Denver, Colo., 2-7 Feb. 1969, Vol. 464, ASTM International, 1970, p. 186.

[118] B. Kirby, R. Preston, High temperature properties of hot-rolled, structural steels for use in fire engineering design studies, Fire Safety Journal 13 (1) (1988) 27–37.

[119] G.-Q. Li, S.-C. Jiang, Y.-Z. Yin, K. Chen, M.-F. Li, Experimental studies on the properties of constructional steel at elevated temperatures, Journal of Structural Engineering 129 (12) (2003) 1717–1721.

[120] S. Deeny, Structural fire engineering in tall buildings, in: Presentation at the University of Edinburgh, 2011.

[121] C. Fang, B. Izzuddin, A. Elghazouli, D. Nethercot, Robustness of steel-composite building structures subject to localised fire, Fire Safety Journal 46 (6) (2011) 348–363.

[122] R. Sun, Z. Huang, I. Burgess, Progressive collapse analysis of steel structures under fire conditions, Engineering Structures 34 (2012) 400–413.

[123] C. Röben, M. Gillie, J. Torero, Structural behaviour during a vertically travelling fire, Journal of Constructional Steel Research 66 (2) (2010) 191–197.

[124] J. Quiter, Guidelines for designing fire safety in very tall buildings, Tech. rep., Society of Fire Protection Engineers (2012).

[125] C. Lai, M. Ho, T. Lin, Experimental investigations of fire spread and flashover time in office fires, Journal of Fire Sciences 28 (3) (2010) 279–302.

[126] S. Lamont, B. Lane, G. Flint, A. Usmani, Behavior of structures in fire and real design-a case study, Journal of fire protection engineering 16 (1) (2006) 5–35.

[127] J. Franssen, R. Zaharia, V. Kodur, Designing steel structures for fire safety, CRC Press, 2009.

[128] G. Rein, X. Zhang, P. Williams, B. Hume, A. Heise, A. Jowsey, B. Lane, J. Torero, Multi-story fire analysis for high-rise buildings, 11th Interflam, London, 2007.

[129] A. Law, J. Stern-Gottfried, M. Gillie, G. Rein, Structural engineering and fire dynamics: Advances at the interface and Buchanan's challenge, in: IAFSS 2011: 10th International Symposium on Fire Safety Science, 2011, pp. 1563–1576.

[130] E. Ellobody, C. Bailey, Structural performance of a post-tensioned concrete floor during horizontally travelling fires, Engineering Structures 33 (6) (2011) 1908–1917.

[131] S. Lamont, A. Usmani, M. Gillie, Behaviour of a small composite steel frame structure in a long-cool and a short-hot fire, Fire Safety Journal 39 (5) (2004) 327–357.

[132] R. Alpert, Calculation of response time of ceiling-mounted fire detectors, Fire Technology 8 (3) (1972) 181–195.

[133] J. Milke, V. Kodur, C. Marrioon, Appendix a: Overview of fire protection in buildings, in: World Trade Center Building Performance Study: Data collection, preliminary observations, and recommendations, Federal Emergency Management Agency, 2002, pp. A1–A28.

[134] J. Franssen, D. Pintea, J. Dotreppe, Considering the effects of localised fires in the numerical analysis of a building structure, Fire Safety Journal 42 (6) (2007) 473–481.

[135] T. Lie, et al., Structural fire protection, Vol. 78, American Society of Civil Engineers, 1992.

[136] Y. Jiang, G. Rein, S. Welch, A. Usmani, Modeling fire-induced radiative heat transfer in smoke-filled structural cavities, International Journal of Thermal Sciences.

[137] G. Flint, Fire induced collapse of tall buildings, Ph.D. thesis, The University of Edinburgh (2005).

[138] D. Kent, R. Park, Flexural members with confined concrete, Journal of the Structural Division 97 (7) (1971) 1969–1990.

[139] A. Usmani, Understanding the response of composite structures to fire, Engineering Journal, AISC 42 (2) (2005) 83.

[140] M. Garlock, S. Quiel, Plastic axial load and moment interaction curves for fire-exposed steel sections with thermal gradients, Journal of structural engineering 134 (6) (2008) 874–880.

[141] A. Sanad, J. Rotter, A. Usmani, M. O'Connor, Composite beams in large buildings under firenumerical modelling and structural behaviour, Fire Safety Journal 35 (3) (2000) 165–188.

[142] A. Elghazouli, B. Izzuddin, A. Richardson, Numerical modelling of the structural fire behaviour of composite buildings, Fire Safety Journal 35 (4) (2000) 279–297.

[143] A. Elghazouli, B. Izzuddin, Response of idealised composite beam–slab systems under fire conditions, Journal of Constructional Steel Research 56 (3) (2000) 199–224.

[144] M. Gillie, A. Usmani, J. Rotter, A structural analysis of the first cardington test, Journal of Constructional Steel Research 57 (6) (2001) 581–601.

[145] B. Izzuddin, X. Tao, A. Elghazouli, Realistic modeling of composite and reinforced concrete floor slabs under extreme loading. i: Analytical method, Journal of Structural Engineering 130 (12) (2004) 1972–1984.

[146] B. Izzuddin, A. Vlassis, A. Elghazouli, D. Nethercot, Progressive collapse of multi-storey buildings due to sudden column losspart i: Simplified assessment framework, Engineering Structures 30 (5) (2008) 1308–1318.

[147] A. Vlassis, B. Izzuddin, A. Elghazouli, D. Nethercot, Progressive collapse of multi-storey buildings due to sudden column losspart ii: Application, Engineering Structures 30 (5) (2008) 1424–1438.

[148] A. Law, N. Butterworth, J. Stern-Gottfried, Y. Wong, Structural fire design: Many components, one approach, in: The 1st International Conference on Performance Based and Life Cycle Structural Engineering, Hong Kong, 2012.

[149] A. E. Jeffers, E. D. Sotelino, Analysis of steel structures in fire with force-based frame elements, Journal of Structural Fire Engineering 3 (4) (2012) 287–300.

# Appendix A

# Overview of the methods developed for structural fire analysis

## A.1 Elements

### A.1.1 DispBeamColumn2DThermal

The following method is for adding the thermal loads in **DispBeamColumn2DThermal** class. The code is similar for **DispBeamColumn3DThermal**.

```
int
DispBeamColumn2dThermal::addLoad(ElementalLoad *theLoad, const
    Vector &factors)
{
  int type;
  const Vector &data = theLoad->getData(type, factors(0));
```

```
6   double L = crdTransf->getInitialLength();
7
8  //JZ 07/10
      ////////////////////////////////////////////////////////////
      start
9   if (type == LOAD_TAG_Beam2dThermalAction) {
10  //PK
11    //   Vector &factors = theLoad->getfactors();
12
13    double loadFactor = factors(0);
14    loadFactor2=factors(1);
15    loadFactor3=factors(2);
16    loadFactor4=factors(3);
17    loadFactor5=factors(4);
18    loadFactor6=factors(5);
19    loadFactor7=factors(6);
20    loadFactor8=factors(7);
21    loadFactor9=factors(8);
22
23    dataMix[0] = data(0)*loadFactor;
24    dataMix[2] = data(2)*loadFactor2;
25    dataMix[4] = data(4)*loadFactor3;
26    dataMix[6] = data(6)*loadFactor4;
27    dataMix[8] = data(8)*loadFactor5;
28    dataMix[10] = data(10)*loadFactor6;
29    dataMix[12] = data(12)*loadFactor7;
30    dataMix[14] = data(14)*loadFactor8;
31    dataMix[16] = data(16)*loadFactor9;
32
33    dataMix[1] = data(1);
34    dataMix[3] = data(3);
35    dataMix[5] = data(5);
36    dataMix[7] = data(7);
37    dataMix[9] = data(9);
38    dataMix[11] = data(11);
39    dataMix[13] = data(13);
40    dataMix[15] = data(15);
41    dataMix[17] = data(17);
42
43    //PK add the maximum temperatures to be passed along with the
         factor ones in the dataMix
44    //18-26
45    dataMix[18] = data(0);
46    dataMix[19] = data(2);
47    dataMix[20] = data(4);
48    dataMix[21] = data(6);
49    dataMix[22] = data(8);
50    dataMix[23] = data(10);
51    dataMix[24] = data(12);
52    dataMix[25] = data(14);
53    dataMix[26] = data(16);
54    //PK end of change
55
56    counterTemperature = 0;
57    q0Temperature[0] = 0.0;
58    q0Temperature[1] = 0.0;
```

```
59      q0Temperature[2] = 0.0;
60
61      double L = crdTransf->getInitialLength();
62      double oneOverL = 1.0/L;
63
64      //const Matrix &pts = quadRule.getIntegrPointCoords(numSections)
            ;
65      //const Vector &wts = quadRule.getIntegrPointWeights(numSections
            );
66      double xi[maxNumSections];
67      beamInt->getSectionLocations(numSections, L, xi);
68      double wt[maxNumSections];
69      beamInt->getSectionWeights(numSections, L, wt);
70
71      // Loop over the integration points
72      for (int i = 0; i < numSections; i++) {
73
74        int order = theSections[i]->getOrder();
75        const ID &code = theSections[i]->getType();
76
77        double xi6 = 6.0*xi[i];
78
79        // Get section stress resultant
80
81        // FMk const Vector &s = theSections[i]->getTemperatureStress(
              dataMix);
82        Vector dataMixV(dataMix, 27);
83        const Vector &s = theSections[i]->getTemperatureStress(
              dataMixV);
84
85        double si;
86        for (int j = 0; j < order; j++) {
87    si = s(j)*wt[i];
88    switch(code(j)) {
89    case SECTION_RESPONSE_P:
90      q0Temperature[0] += si; break;
91    case SECTION_RESPONSE_MZ:
92      q0Temperature[1] += (xi6-4.0)*si;
93      q0Temperature[2] += (xi6-2.0)*si; break;
94    default:
95      break;
96    }
97        }
98      }
99
100     q0[0] -= 0;
101     q0[1] -= 0;
102     q0[2] -= 0;
103   }
104
105   else {
106     opserr << "DispBeamColumn2dThermal::addLoad(Vector) -- load type
            " << theLoad->getClassType()
107       << "unknown for element with tag: " << this->getTag() << "\n";
108     return -1;
109   }
```

```
110
111   return 0;
112 }
```

## A.2 Materials

### A.2.1 Steel01Thermal

Method for determing elongation and tangent in **Steel01Thermal** material class. The method is similar for the all the developed **UniaxialMaterial** and **nDMaterial** classes.

```
1  double
2 Steel01Thermal::getElongTangent(double TempT, double &ET, double &
      Elong, double TempTmax) //PK add to include max temp
3 {
4   //JZ updated, from rebar to C steel
5
6   // EN 1992 pt 1-2-1. Class N hot rolled  reinforcing steel at
       elevated temperatures
7   if (TempT <= 80) {
8     fy = fyT;
9     E0 = E0T;
10
11    //b=TempT*0.00325/80;
12
13    fp = fyT;
14  }
15  else if (TempT <= 180) {
16    fy = fyT;
17    E0 = E0T*(1 - (TempT - 80)*0.1/100);
18
19    //b=0.00325+(TempT - 80)*0.00325/100;
20
21    fp = fyT*(1 - (TempT - 80)*(1-0.807)/100);
22
23  }
24  else if (TempT <= 280) {
25    fy = fyT;
26    E0 = E0T*(0.9 - (TempT - 180)*0.1/100);
27
28    //b=0.0065+(TempT - 180)*0.00325/100;
```

```
29
30      fp = fyT*(0.807 - (TempT - 180)*(0.807-0.613)/100);
31    }
32    else if (TempT <= 380) {
33      fy = fyT;
34      E0 = E0T*(0.8 - (TempT - 280)*0.1/100);
35
36      //b=0.00975+(TempT - 280)*0.00355/100;
37
38      fp = fyT*(0.613 - (TempT - 280)*(0.613 - 0.42)/100);
39    }
40    else if (TempT <= 480) {
41      fy = fyT*(1 - (TempT - 380)*0.22/100);
42      E0 = E0T*(0.7 - (TempT - 380)*0.1/100);
43
44      //b=0.0133+(TempT - 380)*0.0133/100;
45
46      fp = fyT*(0.42 - (TempT - 380)*(0.42 - 0.36)/100);
47    }
48    else if (TempT <= 580) {
49      fy = fyT*(0.78 - (TempT - 480)*0.31/100);
50      E0 = E0T*(0.6 - (TempT - 480)*0.29/100);
51
52      //b=0.0266+(TempT - 480)*0.0136/100;
53
54      fp = fyT*(0.36 - (TempT - 480)*(0.36 - 0.18)/100);
55    }
56    else if (TempT <= 680) {
57      fy = fyT*(0.47 - (TempT - 580)*0.24/100);
58      E0 = E0T*(0.31 - (TempT - 580)*0.18/100);
59
60      // b=0.0402-(TempT - 580)*0.0067/100;
61
62      fp = fyT*(0.18 - (TempT - 580)*(0.18 - 0.075)/100);
63    }
64    else if (TempT <= 780) {
65      fy = fyT*(0.23 - (TempT - 680)*0.12/100);
66      E0 = E0T*(0.13 - (TempT - 680)*0.04/100);
67
68      // b=0.0335-(TempT - 680)*0.0067/100;
69
70      fp = fyT*(0.075 - (TempT - 680)*(0.075 - 0.005)/100);
71    }
72    else if (TempT <= 880) {
73      fy = fyT*(0.11 - (TempT - 780)*0.05/100);
74      E0 = E0T*(0.09 - (TempT - 780)*0.02/100);
75
76      //   b=0.0268-(TempT - 780)*0.0067/100;
77
78      fp = fyT*(0.05 - (TempT - 780)*(0.05 - 0.0375)/100);
79    }
80    else if (TempT <= 980) {
81      fy = fyT*(0.06 - (TempT - 880)*0.02/100);
82      E0 = E0T*(0.0675 - (TempT - 880)*(0.00675 - 0.0045)/100);
83
84      //   b=0.0201-(TempT - 880)*0.0067/100;
```

```
85
86      fp = fyT*(0.0375 - (TempT - 880)*(0.0375 - 0.025)/100);
87    }
88    else if (TempT <= 1080) {
89      fy = fyT*(0.04 - (TempT - 980)*0.02/100);
90      E0 = E0T*(0.045 - (TempT - 980)*(0.0045 - 0.00225)/100);
91
92      // b=0.0134-(TempT - 980)*0.0067/100;
93
94      fp = fyT*(0.025 - (TempT - 980)*(0.025 - 0.0125)/100);
95    }
96    else if (TempT <= 1180) {
97      fy = fyT*(0.02 - (TempT - 1080)*0.02/100);
98      E0 = E0T*(0.0225 - (TempT - 1080)*0.0225/100);
99
100     //  b=0.0067-(TempT - 980)*0.0067/100;
101
102     fp = fyT*(0.0125 - (TempT - 1080)*0.0125/100);
103   }
104   else  {
105     opserr << "the temperature is invalid\n";
106   }
107
108   // caculation of thermal elongation of reinforcing steel. JZ
109 ///*
110   if (TempT <= 1) {
111       ThermalElongation = TempT * 1.2164e-5;
112     }
113   else if (TempT <= 730) {
114       ThermalElongation = -2.416e-4 + 1.2e-5 *(TempT+20) + 0.4e-8 *(
              TempT+20)*(TempT+20);
115   }
116   else if (TempT <= 840) {
117       ThermalElongation = 11e-3;
118   }
119   else if (TempT <= 1180) {
120       ThermalElongation = -6.2e-3 + 2e-5*TempT;
121   }
122   else {
123     opserr << "the temperature is invalid\n";
124   }
125
126  ET = E0;
127  Elong = ThermalElongation;
128  TemperautreC = TempT;
129
130  return 0;}
```

### A.2.2 Concrete02Thermal

Method for determing elongation and tangent in **Concrete02Thermal** material class.

```
1
2 double
3Concrete02Thermal::getElongTangent(double TempT, double& ET, double&
      Elong, double TempTmax) //PK add to include max temp
4{
5  //material properties with temperature
6  Temp = TempT;  //make up the 20 degree which is minus in the class
       of thermalfield
7  Tempmax = TempTmax; //PK add max temp for cooling
8  // The datas are from EN 1992 part 1-2-1
9  // Tensile strength at elevated temperature
10
11  if (Temp <= 80) {
12    ft = ftT;
13  }
14  else if (Temp <= 580) {
15    ft = (1.0 - 1.0*(Temp -80)/500)*ftT;
16    Ets = (1.0 - 1.0*(Temp -80)/500)*fcT * 1.5 / epsc0T;
17    //Ets = (1.0 - 1.0*(Temp -80)/500)*EtsT;
18  }
19  else {
20    ft = 1.0e-3;
21    Ets = 1.0e-3;
22    //ft = 0;
23    //Ets = 0;
24  }
25
26  // compression strength, at elevated temperature
27  //   strain at compression strength, at elevated temperature
28  //   ultimate (crushing) strain, at elevated temperature
29  if (Temp <= 0) {
30    fc = fcT;
31    epsc0 = -0.0025;
32    fcu = fcuT;
33    epscu = -0.02;
34    //Ets = EtsT;  jz what is there the statement?
35  }
36  else if (Temp <= 80) {
37    fc = fcT;
38    epsc0 = -(0.0025 + (0.004-0.0025)*(Temp - 0)/(80 - 0));
39    fcu = fcuT;
40    epscu = -(0.0200 + (0.0225-0.0200)*(Temp - 0)/(80 - 0));
41  }
42  else if (Temp <= 180) {
43      fc = fcT*(1 - (Temp - 80)*0.05/100);
44    epsc0 = -(0.0040 + (0.0055-0.0040)*(Temp - 80)/100);
45      fcu = fcuT*(1 - (Temp - 80)*0.05/100);
46    epscu = -(0.0225 + (0.0225-0.0200)*(Temp - 80)/100);
```

```
47  }
48  else if (Temp <= 280) {
49      fc = fcT*(0.95 - (Temp - 180)*0.1/100);
50    epsc0 = -(0.0055 + (0.0070-0.0055)*(Temp - 180)/100);
51    fcu = fcuT*(0.95 - (Temp - 180)*0.1/100);
52    epscu = -(0.0250 + 0.0025*(Temp - 180)/100);
53  }
54  else if (Temp <= 380) {
55      fc = fcT*(0.85 - (Temp - 280)*0.1/100);
56    epsc0 = -(0.0070 + (0.0100-0.0070)*(Temp - 280)/100);
57    fcu = fcuT*(0.85 - (Temp - 280)*0.1/100);
58    epscu = -(0.0275 + 0.0025*(Temp - 280)/100);
59  }
60  else if (Temp <= 480) {
61      fc = fcT*(0.75 - (Temp - 380)*0.15/100);
62    epsc0 = -(0.0100 + (0.0150-0.0100)*(Temp - 380)/100);
63    fcu = fcuT*(0.75 - (Temp - 380)*0.15/100);
64    epscu = -(0.03 + 0.0025*(Temp - 380)/100);
65  }
66  else if (Temp <= 580) {
67      fc = fcT*(0.60 - (Temp - 480)*0.15/100);
68    epsc0 = -(0.0150 + (0.0250-0.0150)*(Temp - 480)/100);
69    fcu = fcuT*(0.60 - (Temp - 480)*0.15/100);
70    epscu = -(0.0325 + 0.0025*(Temp - 480)/100);
71  }
72  else if (Temp <= 680) {
73      fc = fcT*(0.45 - (Temp - 580)*0.15/100);
74    epsc0 = -0.0250;
75    fcu = fcuT*(0.45 - (Temp - 580)*0.15/100);
76    epscu = -(0.035 + 0.0025*(Temp - 580)/100);
77  }
78  else if (Temp <= 780) {
79      fc = fcT*(0.30 - (Temp - 680)*0.15/100);
80    epsc0 = -0.0250;
81    fcu = fcuT*(0.30 - (Temp - 680)*0.15/100);
82    epscu = -(0.0375 + 0.0025*(Temp - 680)/100);
83  }
84  else if (Temp <= 880) {
85      fc = fcT*(0.15 - (Temp - 780)*0.07/100);
86    epsc0 = -0.0250;
87    fcu = fcuT*(0.15 - (Temp - 780)*0.07/100);
88    epscu = -(0.04 + 0.0025*(Temp - 780)/100);
89  }
90  else if (Temp <= 980) {
91      fc = fcT*(0.08 - (Temp - 880)*0.04/100);
92    epsc0 = -0.0250;
93    fcu = fcuT*(0.08 - (Temp - 880)*0.04/100);
94    epscu = -(0.0425 + 0.0025*(Temp - 880)/100);
95  }
96  else if (Temp <= 1080) {
97      fc = fcT*(0.04 - (Temp - 980)*0.03/100);
98    epsc0 = -0.0250;
99    fcu = fcuT*(0.04 - (Temp - 980)*0.03/100);
100   epscu = -(0.045 + 0.0025*(Temp - 980)/100);
101 }
102 else  {
```

```
103       opserr << "the temperature is invalid\n";
104   }
105 //jz assign a miner to the valuables
106 
107    // epsc0 = epsc0T*strainRatio;
108    // epscu = epscuT*strainRatio;
109 
110   // caculation of thermal elongation
111     if (Temp <= 1) {
112       ThermalElongation = (Temp - 0) * 9.213e-6;
113     }
114   else if (Temp <= 680) {
115       ThermalElongation = -1.8e-4 + 9e-6 *(Temp+20) + 2.3e-11 *(Temp
              +20)*(Temp+20)*(Temp+20);
116   }
117   else if (Temp <= 1180) {
118       ThermalElongation = 14e-3;
119   }
120   else {
121     opserr << "the temperature is invalid\n";
122   }
123 
124   ET = 1.5*fc/epsc0;
125   Elong = ThermalElongation;
126 
127   //For cooling to exist T must go to Tmax and then decrease
128 //if cooling the factor becomes 1
129  //if (Temp = Tempmax) {
130     //cooling=1;
131  // }
132 
133 ////PK COOLING PART FOR DESCENDING BRANCH OF A FIRE////
134   // If temperature is less that previous commited temp then we have
         cooling taking place
135   if (Temp < TempP) {
136 
137 //opserr << "cooling " << Temp << " " << TempP << endln;
138 
139   double kappa;
140   double fcmax; //compr strength at max temp
141   double fcumax; //ultimate compr strength at max temp
142   double fcamb; //compr strength at cooled ambient temp
143   double fcuamb; //ultimate compr strength at cooled ambient temp
144   double epsc0max; //strain at compression strength for the max temp
145   double epscumax; //ultimate strain at ultimate compression
         strength for the max temp
146   if (TempP == Tempmax) {
147     //opserr << "cooling ,T,TP,Tmax " << Temp << " " << TempP << " "
           << Tempmax <<endln;
148   }
149   // PK Determine residual compressive strength of concrete heated
         to the max temp and then having cooled down to ambient
150   // This will be the same for all the timesteps during the cooling
         phase
151   // PK 1st step is to determine Kc,Tempmax according to table in
         3.2.2 (EN1994-1-2:2005)
```

```
152
153   if (Tempmax < 0) {
154     opserr << "max temperature cannot be less than zero " << " " <<
          Tempmax <<endln;
155   }
156   else if (Tempmax <= 80) {
157     kappa = 1;
158     fcmax = fcT;
159     fcumax = fcuT;
160   }
161   else if (Tempmax <= 180) {
162     kappa = 1 - (Tempmax - 80)*0.05/100;
163     fcmax = fcT*(1 - (Tempmax - 80)*0.05/100);
164     fcumax = fcuT*(1 - (Tempmax - 80)*0.05/100);
165   }
166   else if (Tempmax <= 280) {
167     kappa = 0.95 - (Tempmax - 180)*0.1/100;
168     fcmax = fcT*(0.95 - (Tempmax - 180)*0.1/100);
169     fcumax = fcuT*(0.95 - (Tempmax - 180)*0.1/100);
170   }
171   else if (Tempmax <= 380) {
172     kappa = 0.85 - (Tempmax - 280)*0.1/100;
173     fcmax = fcT*(0.85 - (Tempmax - 280)*0.1/100);
174     fcumax = fcuT*(0.85 - (Tempmax - 280)*0.1/100);
175   }
176   else if (Tempmax <= 480) {
177     kappa = 0.75 - (Tempmax - 380)*0.15/100;
178     fcmax = fcT*(0.75 - (Tempmax - 380)*0.15/100);
179     fcumax = fcuT*(0.75 - (Tempmax - 380)*0.15/100);
180   }
181   else if (Tempmax <= 580) {
182     kappa = 0.60 - (Tempmax - 480)*0.15/100;
183     fcmax = fcT*(0.60 - (Tempmax - 480)*0.15/100);
184     fcumax = fcuT*(0.60 - (Tempmax - 480)*0.15/100);
185   }
186   else if (Tempmax <= 680) {
187     kappa = 0.45 - (Tempmax - 580)*0.15/100;
188     fcmax = fcT*(0.45 - (Tempmax - 580)*0.15/100);
189     fcumax = fcuT*(0.45 - (Tempmax - 580)*0.15/100);
190   }
191   else if (Tempmax <= 780) {
192     kappa = 0.30 - (Tempmax - 680)*0.15/100;
193     fcmax = fcT*(0.30 - (Tempmax - 680)*0.15/100);
194     fcumax = fcuT*(0.30 - (Tempmax - 680)*0.15/100);
195   }
196   else if (Tempmax <= 880) {
197     kappa = 0.15 - (Tempmax - 780)*0.07/100;
198     fcmax = fcT*(0.15 - (Tempmax - 780)*0.07/100);
199     fcumax = fcuT*(0.15 - (Tempmax - 780)*0.07/100);
200   }
201   else if (Tempmax <= 980) {
202     kappa = 0.08 - (Tempmax - 880)*0.04/100;
203     fcmax = fcT*(0.08 - (Tempmax - 880)*0.04/100);
204     fcumax = fcuT*(0.08 - (Tempmax - 880)*0.04/100);
205   }
206   else if (Tempmax <= 1080) {
```

```
207     kappa = 0.04 - (Tempmax - 980)*0.03/100;
208     fcmax = fcT*(0.04 - (Tempmax - 980)*0.03/100);
209     fcumax = fcuT*(0.04 - (Tempmax - 980)*0.03/100);
210   }
211   else  {
212     opserr << "the temperature is invalid\n";
213   }
214   // PK 2nd step is to determine compressice strength at ambient
        after cooling as shown in ANNEX C (EN1994-1-2:2005)
215   if (Tempmax < 0) {
216     opserr << "max temperature cannot be less than zero " << " " <<
          Tempmax <<endln;
217   }
218   else if (Tempmax <= 80) {
219     fcamb = kappa*fcT;
220     fcuamb = kappa*fcuT;
221   }
222   else if (Tempmax <= 280) {
223     fcamb=(1-(0.235*(Tempmax-80)/200))* fcT;
224     fcuamb=(1-(0.235*(Tempmax-80)/200))* fcuT;
225   }
226   else if (Tempmax <= 1080) {
227     fcamb = 0.9*kappa*fcT;
228     fcuamb = 0.9*kappa*fcuT;
229   }
230   else {
231     opserr << "the temperature is invalid\n";
232   }
233
234   // Calculation of current compressive strength
235   // linear interpolation between ambient and maximum compressive
        strength (after and before cooling)
236
237   fc = fcmax - ((fcmax-fcamb)*(Tempmax-Temp)/Tempmax);
238   fcu = fcumax - ((fcumax-fcuamb)*(Tempmax-Temp)/Tempmax);
239
240   // Calculation of epsc0 for Tempmax and then keep it the same for
        all next time steps
241   if (Tempmax < 0) {
242     opserr << "max temperature cannot be less than zero " << " " <<
          Tempmax <<endln;
243   }
244   else if (Tempmax <= 80) {
245     epsc0max = -(0.0025 + (0.004-0.0025)*(Tempmax - 0)/(80 - 0));
246     epscumax = -(0.0200 + (0.0225-0.0200)*(Tempmax - 0)/(80 - 0));
247   }
248   else if (Tempmax <= 180) {
249     epsc0max = -(0.0040 + (0.0055-0.0040)*(Tempmax - 80)/100);
250     epscumax = -(0.0225 + (0.0225-0.0200)*(Tempmax - 80)/100);
251   }
252   else if (Tempmax <= 280) {
253     epsc0max = -(0.0055 + (0.0070-0.0055)*(Tempmax - 180)/100);
254     epscumax = -(0.0250 + 0.0025*(Tempmax - 180)/100);
255   }
256   else if (Tempmax <= 380) {
257     epsc0max = -(0.0070 + (0.0100-0.0070)*(Tempmax - 280)/100);
```

```
258     epscumax = -(0.0275 + 0.0025*(Tempmax - 280)/100);
259   }
260   else if (Tempmax <= 480) {
261     epsc0max = -(0.0100 + (0.0150-0.0100)*(Tempmax - 380)/100);
262     epscumax = -(0.03 + 0.0025*(Tempmax - 380)/100);
263   }
264   else if (Tempmax <= 580) {
265     epsc0max = -(0.0150 + (0.0250-0.0150)*(Tempmax - 480)/100);
266     epscumax = -(0.0325 + 0.0025*(Tempmax - 480)/100);
267   }
268   else if (Tempmax <= 680) {
269     epsc0max = -0.0250;
270     epscumax = -(0.035 + 0.0025*(Tempmax - 580)/100);
271   }
272   else if (Tempmax <= 780) {
273     epsc0max = -0.0250;
274     epscumax = -(0.0375 + 0.0025*(Tempmax - 680)/100);
275   }
276   else if (Tempmax <= 880) {
277     epsc0max = -0.0250;
278     epscumax = -(0.04 + 0.0025*(Tempmax - 780)/100);
279   }
280   else if (Tempmax <= 980) {
281     epsc0max = -0.0250;
282     epscumax = -(0.0425 + 0.0025*(Tempmax - 880)/100);
283   }
284   else if (Tempmax <= 1080) {
285     epsc0max = -0.0250;
286     epscumax = -(0.045 + 0.0025*(Tempmax - 980)/100);
287   }
288   else  {
289     opserr << "the temperature is invalid\n";
290   }
291 
292   //make eps0 = eps0max
293 
294   epsc0 = epsc0max;
295 
296   // Calculating epscu
297   epscu = epsc0 + ((epscumax-epsc0max)*fc/fcmax);
298 
299   ft=0;
300 
301   }
302   return 0;
303 }
```

## A.3 Loads and LoadPattern

### A.3.1 Firepattern

Method for setting nine **TimeSeries** objects in the **Firepattern** class.

```
void
FireLoadPattern::setFireTimeSeries(TimeSeries *theTimeSeries1,
    TimeSeries *theTimeSeries2,
            TimeSeries *theTimeSeries3, TimeSeries *theTimeSeries4,
            TimeSeries *theTimeSeries5, TimeSeries *theTimeSeries6,
            TimeSeries *theTimeSeries7, TimeSeries *theTimeSeries8,
            TimeSeries *theTimeSeries9)
{
  // invoke the destructor on the old TimeSeries
  if (theSeries1 != 0)
    delete theSeries1;
  if (theSeries2 != 0)
    delete theSeries2;
  if (theSeries3 != 0)
    delete theSeries3;
  if (theSeries4 != 0)
    delete theSeries4;
  if (theSeries5 != 0)
    delete theSeries5;
  if (theSeries6 != 0)
    delete theSeries6;
  if (theSeries7 != 0)
    delete theSeries7;
  if (theSeries8 != 0)
    delete theSeries8;
  if (theSeries9 != 0)
    delete theSeries9;

  // set the pointer to the new series objects
  theSeries1 = theTimeSeries1;
  theSeries2 = theTimeSeries2;
  theSeries3 = theTimeSeries3;
  theSeries4 = theTimeSeries4;
  theSeries5 = theTimeSeries5;
  theSeries6 = theTimeSeries6;
  theSeries7 = theTimeSeries7;
  theSeries8 = theTimeSeries8;
  theSeries9 = theTimeSeries9;
}
```

### A.3.2 Beam2DThermalAction

Constructor for defining nine temperatures and locations in the **Beam2DThermalAction** class. The code is similar for the three dimensional beam and shell elements.

```
Beam2dThermalAction::Beam2dThermalAction(int tag,
            double t1, double locY1, double t2, double locY2,
            double t3, double locY3, double t4, double locY4,
            double t5, double locY5, double t6, double locY6,
            double t7, double locY7, double t8, double locY8,
            double t9, double locY9,
            int theElementTag)
  :ElementalLoad(tag, LOAD_TAG_Beam2dThermalAction, theElementTag),
   T1(t1),LocY1(locY1),T2(t2),LocY2(locY2),T3(t3),LocY3(locY3),T4(t4
       ),LocY4(locY4),
   T5(t5),LocY5(locY5),T6(t6),LocY6(locY6),T7(t7),LocY7(locY7),T8(t8
       ),LocY8(locY8),
   T9(t9),LocY9(locY9)
{

}
```